Investigating Biomarkers of Keloid Scarring

Zoe Drymoussi

2015

A thesis presented for the degree of Doctor of Philosophy

Centre for Cutaneous Research, Blizard Institute, Barts and The London School of Medicine and Dentistry, Queen Mary, University of London

Declaration

I, Zoe Drymoussi, declare that the work presented in this thesis is my own and has not been submitted in any form for another degree or diploma at any university or other institute of tertiary education. Information derived from the published or unpublished work of others has been acknowledged in the text and a list of references is given.

Zoe Drymoussi,
PhD Student

1st August 2015

Abstract

Keloids are fibroproliferative scars that form in response to abnormal healing processes. The extracellular matrix (ECM) remodelling of the dermis in the maturation phase of normal wound healing is insufficient in keloids, leading to excessive ECM proteins being deposited in the granulation tissue. Keloid scars are unique to humans, and show increased prevalence in darker skin types. Current treatments rarely lead to permanent regression, and despite decades of study, the key molecular processes responsible for keloid scarring are still largely elusive. The research presented in this thesis aims to investigate markers of keloid scars, and to examine the impact of both the dermis and epidermis in keloid pathogenesis.

Histological examination of the keloid scars showed a thickened epidermis and densely collagenous dermis, both of which demonstrated a higher level of cell proliferation and myofibroblast expression, as compared to normal skin. Differences between the central and marginal regions of the scars were also noted. Protein expression patterns of Matrix Metalloproteinases (MMPs) 1, 2, 13 and 14 were examined in formalin fixed paraffin embedded biopsies from the same keloids (n=10) and healthy skin (n=9). MMPs 2 and 14 showed a distinct pattern of protein expression across the central, marginal, and adjacent non-keloid regions of the scar. In the dermis, MMP2 and 14 were most evident at the leading edge, whereas the epidermis revealed a strong but variable pattern along all regions. This was in contrast to healthy skin, where expression in both epidermis and dermis was much lower overall, and showed a more uniform pattern across the tissue.

Gene expression levels of key ECM and adhesion molecules, as well as select target genes across 10 signal transduction pathways, were analysed through Real-Time qPCR in keloid scars and healthy control skin from unaffected individuals (n=5). MMPs 1, 13 and 14 gene expression levels were significantly increased by 52, 24, and 3-fold respectively in keloid, compared to normal tissue. SPP1 and SPARC were also upregulated by 29.6 and 9.2-fold respectively, in keloid tissue. Hedgehog and Wnt pathway target genes were significantly altered in keloid tissue, with WISP1 and VEGFA being overexpressed by 10 and 2-fold respectively, and BMP2 and BMP4 underexpressed by 5 and 3.7-fold respectively.

Eighteen of the most altered of these 168 genes were examined further in primary cultured fibroblasts (n=6) and keratinocytes (n=4), from both keloid and healthy control skin. Gene expression profiles appeared complementary between fibroblast and keratinocyte cell-types, either of which did not necessarily match the gene expression profiles demonstrated earlier in whole tissue. This might be due to the epidermal and dermal cells being in isolation from each other, and therefore 3D culture containing both cell-types would be more representative of the original tissue environment. SPP1 was the only gene that consistently showed significant over-

expression in whole tissue and primary keloid cells. Protein expression levels of SPP1 appeared increased in keloid tissue compared to normal skin, particularly in the basal epidermis and edge dermis of the keloid scars.

In summary, a high level of inter-patient variability was observed throughout all biomarker investigations, though the leading edge of all keloids consistently appeared to be the most active region. The consistent detection of changes in expression SPP1 indicates a potential role for osteogenic-linked signalling in the fibrotic nature of keloid scarring.

Table of Contents

List of Figures

List of Tables

Abbreviations

aSMA	alpha-smooth muscle actin
BPE	bovine pituitary extract
BDL	bile-duct ligation
CCl_4	carbon tetrachloride
CTGF	connective tissue growth factor
COMP	cartilage oligomeric matrix protein
DAB	3, 3'-diaminobenzidine
DC	dendritic cell
DKK	dickkopf homolog
DMEM	dulbecco's modified Eagle's medium
DMSO	Dimethyl sulfoxide
DNA	Deoxyribonucleic acid
cDNA	complimentary DNA
gDNA	genomic DNA
DSFP	Dermatofibrosarcoma protuberans
ECM	extracellular matrix
EGF	epidermal growth factor
EGFR	epithelial growth factor receptor
ELISA	enzyme-linked immunosorbent assay
ER	endoplasmic reticulum
FACIT	fibril-associated collagens with interrupted triple helices
FAP-a	fibroblast activation protein alpha
FCS	foetal calf serum
FGF	fibroblast growth factor
FGFR	fibroblast growth factor receptor
GOI	genes of interest
GWAS	genome wide associated study
HA	hyaluronic acid; hyaluronan
H&E	haematoxylin & eosin
HGDC	human genomic DNA control
HGF	hepatocyte growth factor
hpx	hemopexin
HRP	horseradish peroxidase
HSP46	heat-shock protein 47
ICC	immunocytochemistry
IF	immunofluorescence
IFN	interferon
IGF	insulin-like growth factor

IGFR	insulin-like growth factor receptor
IHC	immunohistochemistry
IL	interleukin
IMS	industrial methylated spirit
IR	insulin receptor
Jag-1	jagged-1
JNK	c-Jun N-terminal kinase
KCM	keratinocyte conditioned medium
KGF	keratinocyte growth factor
KSFM	keratinocyte serum-free medium
MAPK	mitogen activated protein kinase
MI	myocardial infarction
MMP	matrix metalloproteinase
MT-MMP	membrane-tethered matrix metalloproteinase
NFkB	nuclear factor kappa b
P/S	penicillin / streptomycin
PAGE	polyacrylamide gel electrophoresis
PAI-1	plasminogen activator inhibitor -1
PBS	phosphate buffered saline
PCR	polymerase chain reaction
PDGF	platelet derived growth factor
PDGFR	platelet derived growth factor receptor
PDL	pulsed-dye laser
PI3K	phosphatidylinositol-3 kinase
PIAS2	protein inhibitor of activated signal transducer and activator of transcription 2
PO	pressure overload
POSTN	osteoblast specific factor
PPAR	peroxisome proliferator-activated receptor
PPC	positive PCR control
RIPA	Radioimmunoprecipitation assay buffer
RNA	ribonucleic acid
RT	reverse transcription
RTC	reverse transcription control
RUNX3	Runt-related transcription factor 3
SDS	sodium dodecyl sulphate
SFRP1	secreted frizzled related protein1
SMAD	mothers against decapentaplegic homolog
STP	signal transduction pathwayfindar (array)
TAA	thioacetimide
TGF	transforming growth factor
TNC	tenascin-C

TNF	tumour necrosis factor
TNFAIP6	tumour necrosis factor, alpha induced protein 6
UV	ultraviolet
VEGF	vascular endothelial growth factor
YAP-TAZ	Yes-associated protein – Transcriptional coactivator with PDZ binding motif

Acknowledgements

While it is impossible to thank individually everyone who helped make this challenging project possible, thanks must first go to the late Professor Harshad (Harry) Navsaria who offered me the opportunity to join his team. Unfortunately, his extended absences due to ill health quite early on, and eventual untimely death made for a number of difficulties.

I therefore express my very special appreciation and heartfelt thanks to Professor Mike Philpott who stepped in to become my main supervisor and who has been a wonderfully supportive mentor throughout. His guidance and confidence in me throughout this study have been vital. Special thanks go to my second supervisor, Professor Simon Myers for his constant support. A deep debt of gratitude must also go to Dr Kristin Braun whose well-timed comments and criticisms were of inestimable value.

I make special mention of Head Research Nurse – Sister Lyn (Floderlyn Selim) for her staunch support in accessing patients and collecting samples for my lab research, as well as Chris Evagora and his team for their never-ending help with my histology needs!

My heartfelt thanks and gratitude go to Sreekanth Vootukuri-Reddy (Skee), who I could always count on to help out, and Dr Eleni Pantazi who has been like a big sister. Special thanks to Dr Mat Caley, Dr Su Marsh, Viv Robles, Dr Jamie Upton, Dr Ros Hannen, Dr Diana Velutto, Dr Danielle Lavery, Dr Wes Harrison, Dr Allon Hazan, Dr Matt Brooke, Dr Louise Russell, Sam Matthew - not forgetting my wonderful students Kous and Monty, who were an absolute joy to mentor.

I am truly grateful to Ruth Angus (Sparkles), Louise Adams (Lou-Lou), Robert Abrehart (Mr Hug), Dr Hemanth Tummala, Fiona Kenny and George Theocharidis for their friendship and support – not forgetting the always reliable Sam and Gordon!

My big brother Mike has always been there for me and given helpful guidance. A huge thank you goes to my parents, Diane and Ioannis Drymoussis, who, throughout my life have given me their love, encouragement and support. Finally, I cannot thank my Geordie (John Spoors) enough for his love and total support from the very beginning and throughout.

1 Introduction

1.1 Human Skin

The skin is a large, complex organ consisting of 17% of the body's weight, which provides an essential barrier for the body against the environment, giving protection against mechanical stress and invasion of pathogens (Farage et al., 2010, Simpson et al., 2011). Skin protects the body from water loss and temperature change, as well as providing sensory roles, vitamin D synthesis, immune surveillance and excretion of wastes through sweat glands (Farage et al., 2010). The two major compartments in skin are the epidermis, and the dermis (**Figure 1-1**).

1.1.1 Epidermis

The epidermis is a multi-layered epithelium consisting of a terminally differentiated stratified squamous epithelium, which has to maintain equilibrium between cell proliferation and death. Keratinocytes are the main cell type in the epidermis, making up 95% of the skin's cell population. Other cell types within the epidermis include melanocytes which provide pigmentation to skin and hair, Langerhans cells which function immunologically, and Merkel cells which are sensory receptor cells (Farage et al., 2010).

The epidermis consists of five specialized layers: the stratum basale (basal layer), and the suprabasal layers incorporating the stratum spinosum (spinous layer); stratum granulosum (granular layer); stratum lucidum (clear cell layer); and the outermost layer stratum corneum (cornified layer) (**Figure 1-1**). Keratinocytes proliferate and form a stratified squamous epithelium made of flattened (squamous) epithelial cells which migrate from the undifferentiated basal epithelia to the terminally differentiated stratified squamous of the external layer of the skin. During this process called keratinisation, the keratinocytes increase in size and then flatten, as they differentiate out (Farage et al., 2010, McGrath et al., 2004). The basal layer keratinocytes synthesise keratins K5 and K14, whereas the intermediate suprabasal layers express K1 and K10, allowing for clear differentiation between the two populations (Markey et al., 1992, Leigh et al.,

1993, Blanpain and Fuchs, 2006, Fuchs, 1990). In the granular layer, keratinocytes begin to lose their nuclei, and dense cytoplasmic granules form, containing profilaggrin – the precursor to the interfilamentous protein filaggrin. Loricrin and involucrin are additional proteins expressed in this epidermal layer (Fuchs, 1990, McGrath et al., 2004). The stratum lucidum is a thin layer of clear cells, transluscent under a microscope. This layer functions as a waterproof layer between the two most differentiated epidermal layers (McGrath et al., 2004). Once cells transition to granular cells, they collapse into a flattened shape, and express filaggrin.

Epidermal stem cells reside in the basal layer of the epidermis, as well as the bulge region of hair follicles, where they maintain homeostasis in skin, by regenerating and repairing hair and the epidermis post-injury (Alberts, 2008, McGrath et al., 2004). The stem cells in the hair follicle can give rise to the eight differentiated cell types within the hair follicle: Outer Root Sheath (ORS), Companion layer of the ORS, Henle, Huxley layers of the Inner Root sheath (IRS) plus the IRS Cuticle, Cortex of the hair fibre and hair fibre cuticle and finally hair follicle germinative epithelium (Owens and Watt, 2003, Youssef et al., 2010).

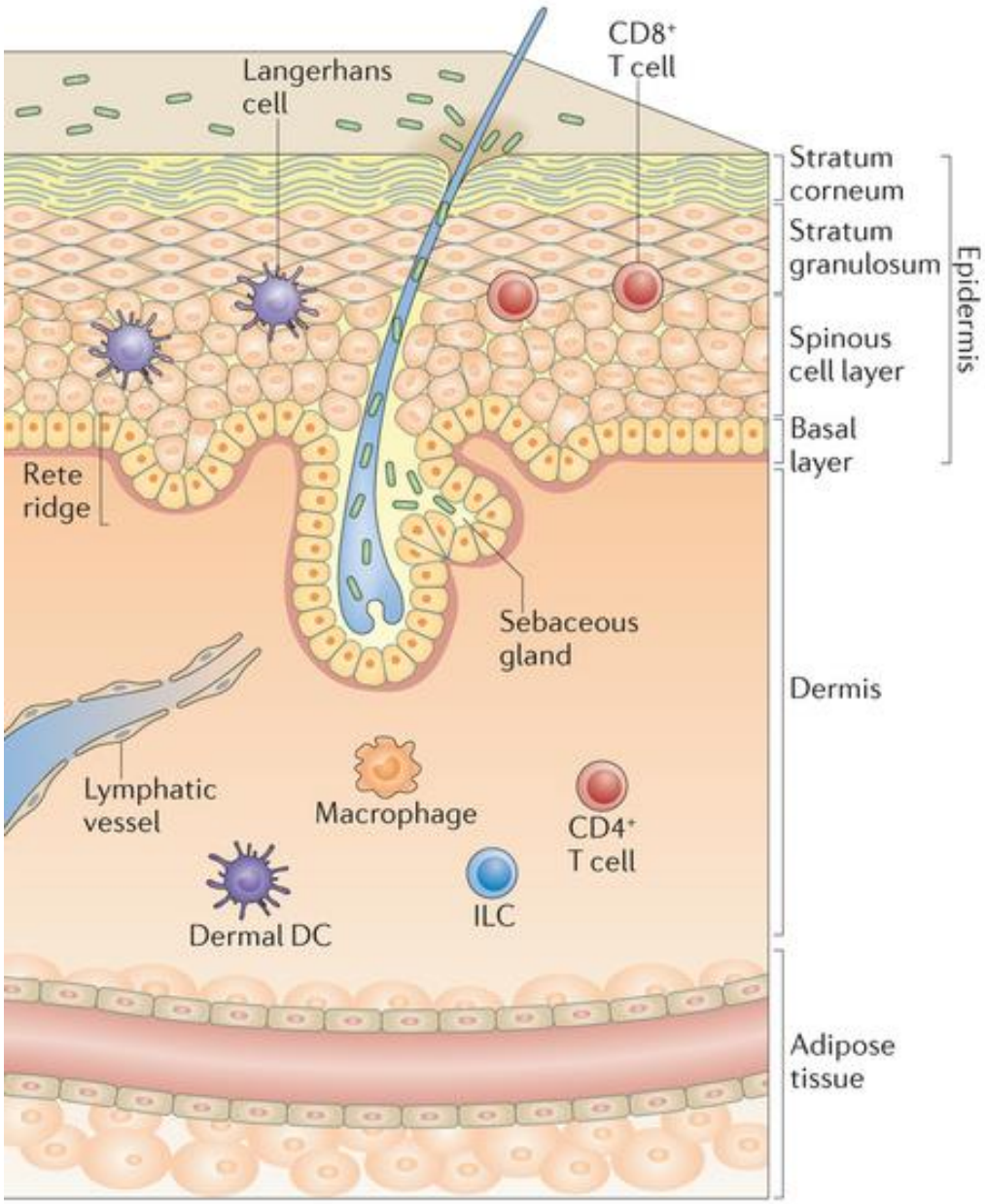

Figure 1-1 Structure of human skin

Human skin is composed of the epidermis, the dermis, and adipose tissue. Within the epidermis, there is the basal layer and four suprabasal layers of keratinocytes. The suprabasal layers include the spinous layer, granular layer (stratum granulosum), stratum lucidum (clear cell layer – not visible here), and the stratum corneum (cornified layer). The dermis is made up of extracellular matrix (ECM) molecules, lymphatic and blood vessels, immune cells and fibroblasts. Adapted from (Pasparakis et al., 2014).

1.1.2 Dermis

The dermis, also known as the stromal tissue, is mainly made up of connective tissue containing various extracellular matrix (ECM) components, immune and inflammatory cells, as well as fibroblast cells. The dermis is traversed by blood and lymphatic vessels as well as nerves (Rinn et al., 2006). The dermal-epidermal junction (or basement membrane) is undulating with epidermal ridges, rete ridges, projecting into the dermis. This provides not only mechanical support for the epidermis, but also is a barrier against the exchange of molecules and cells (McGrath et al., 2004). Below the dermis, but not strictly part of the skin, is a fatty layer of adipose, the subcutaneous layer.

There are three major components to the dermis ECM: collagen, elastin and hyaluronic acid (hyaluronan; HA) (Farage et al., 2010). Dermal fibroblasts can synthesise components of the ECM and basement membrane proteins such as collagen, fibronectin, laminin and elastin. Epithelial cells depend on this stroma for their organisation (Farage et al., 2010, Ghaffari et al., 2009a, Bremnes et al., 2011). Within the dermis and adipose tissue there is also a number of appendages, including hair follicles, sebaceous glands, sweat glands and nails. Each of these contribute to a number of critical functions of the skin (Farage et al., 2010).

1.1.2.1 Fibroblasts

Fibroblasts are mesenchymal cells and a member of the connective tissue family of cells. They are non-vascular, non–epithelial and non-inflammatory cells. Fibroblasts were first described in the late 19th century based upon their location and morphology (Kalluri and Zeisberg, 2006). They play a vital role during development of organs such as skin, eyes, lungs, and then later play a supportive and structural role in the body. Fibroblasts are important in maintaining homeostasis of adjacent epithelium through the secretion of growth factors. During processes such as wound healing, fibroblasts are activated and produce matrix degrading enzymes, cytokines and epithelial growth factors. Collagen types I, III, IV and V, fibronectin, and MMPs are some of the constituents of the ECM that fibroblasts are responsible for producing (Kalluri and Zeisberg, 2006, Bierie and

Moses, 2006). Fibroblasts are consistently spindle shaped even when the cells originate in different anatomical sites (Chang et al., 2002, Krtolica and Campisi, 2002). Despite their morphological similarities, fibroblasts originating from these independent sites all have diverse gene expressions (Rinn et al., 2006, Kalluri and Zeisberg, 2006). However, as members of the connective tissue family of cells they are characterised by the expression of the intermediate filament Vimentin.

1.1.2.2 Collagens: Fibril forming

The collagens are a large family of 28 ECM triple helical proteins that are distributed across many tissue types in the body (Ricard-Blum, 2011, Söderhäll et al., 2007). Depending on the development stage, and the tissue type, collagen fibril lengths range between 12nm and over 500nm (Kadler et al., 2007). They have a wide range of functions including providing tissue structure, aiding cell adhesion and migration, angiogenesis, tissue repair, and tissue remodelling (Gordon and Hahn, 2010, Kadler et al., 2007, Ricard-Blum, 2011). Based on their supramolecular assemblies (as observed through electron microscopy), collagens have been categorized into subfamilies: fibril-forming, fibril-associated with interrupted triple helices (FACITs), beaded filaments, anchoring fibrils, transmembrane collagens, and network-forming (Ricard-Blum, 2011, Kadler et al., 2007).

Fibril-forming collagens have a primary role in contributing to the architecture and mechanical properties of tissues, and are synthesized as procollagens with N- and C-propeptides at either end of the triple helical region (Kadler et al., 2007, Ricard-Blum, 2011). Specific pro-collagen proteinases cleave off the N- and C-propeptides, revealing telopeptides (non-triple helical extensions of the protein chains). This enables fibrillogenesis, via binding sites within the telopeptides to form covalent cross-links with residues in the triple helix domain (Ricard-Blum, 2011, Prockop and Fertala, 1998). Most collagen fibrils consist of multiple collagen types, lending the term “heterotypic”. The most abundant collagen is fibril-forming collagen I, making up more than 90% of bone mass, and providing crucial biomechanical properties including tensile strength and torsional stiffness(Gelse et

al., 2003). Collagen I is also the major collagen in a range of other tissues including tendons, skin, cartilage, ligaments, and the cornea (Gelse et al., 2003). Collagen I is usually formed as a heterotrimer (two identical α1(I)-chains and one α2(I)-chain), though it can be found as a homotrimer (three α1(I)-chain) (Gelse et al., 2003, Ricard-Blum, 2011). In normal skin, collagen triple helical fibrils are usually part of composite fibres containing type III collagen, whereas in cartilage the common combinations are types II with XI and IX, or type II with III (Ricard-Blum, 2011, Wu et al., 2010, Bruckner, 2010, Fleischmajer et al., 1990). In bone, tendon or the cornea, collagen I as well as collagen III can be found to incorporate into fibres containing collagen type V (Gelse et al., 2003, Niyibizi and Eyre, 1989). Non-collagenous macromolecules such as fibronectin, proteoglycans, or integrins, as well as other collagens containing large non-collagenous domains such as collagen V, are thought to help regulate fibrillogenesis by influencing collagen assembly and growth (Ricard-Blum, 2011, Wenstrup et al., 2004, Kalamajski and Oldberg, 2010, Gelse et al., 2003, Fessler et al., 1985).

1.1.2.3 Collagens: Fibril-Associated with Interrupted Triple Helices (FACIT)

Fibril-Associated Collagens with Interrupted Triple helices, or FACITs, such as collagens IX, XII and XIV, are shorter collagens and do not form fibrils on their own. The collagenous domains of these structures are interrupted with short non-helical domains, and are associated with the surfaces of other collagen fibrils (Gelse et al., 2003). Collagens XII and XIV covalently crosslink to collagen I-containing fibrils, whereas collagen IX covalently links to collagen II-containing fibrils (Ricard-Blum, 2011, Amenta et al., 2005, Olsen, 1997). One unique FACIT, collagen XVI, can integrate itself into distinct suprastructural aggregates, depending on the tissue context. In the papillary dermis of the skin for example, it crosslinks with and integrates into specialised microfibrils containing fibrillin-1 (Kassner et al., 2003). Whereas in cartilage, collagen XVI does not integrate into fibrillin-1 containing microfibrils, but instead crosslinks with weakly banded collagen fibrils containing collagens II and XI (Kassner et al., 2003, Ricard-Blum, 2011).

1.1.2.4 Collagens: Beaded filaments and anchoring fibrils

Collagen VI forms beaded filaments, making structural links with cells. Collagen VI monomers crosslink into tetramers which then assemble into long microfibrils, leading to the appearance of a beaded repeat every 105nm (Kadler et al., 2007). Together with collagen VII anchoring fibrils, collagen VI connects the epidermis to the dermis, playing an important role in the basement membrane (Ricard-Blum, 2011, Gordon and Hahn, 2010).

1.2 Normal cutaneous wound healing

Cutaneous wound healing is a complex response to injury, which aims to restore skin integrity and function as efficiently as possible. It is a highly organised and dynamic process of interactions between numerous cell-types, extracellular matrix and signalling molecules. Four precisely and highly programmed phases are observed (**Figure 1-2** and **1-3)** (Guo and Dipietro, 2010, Mathieu et al., 2006): haemostasis (immediately post-injury) (Guo and Dipietro, 2010); inflammation (2-5 days) (Guo and Dipietro, 2010, Gosain and DiPietro, 2004, Broughton et al., 2006a, Campos et al., 2008); proliferation and re-epithelialisation (2 days – 3 weeks) (Campos et al., 2008, Guo and Dipietro, 2010, Gosain and DiPietro, 2004); and tissue remodelling (3 weeks to 2 years or more) (Guo and Dipietro, 2010, Wolfram et al., 2009). Increasingly, these phases of wound healing are thought to be overlapping, and not necessarily distinct from each other (**Figures 1-2** and **1-3**).

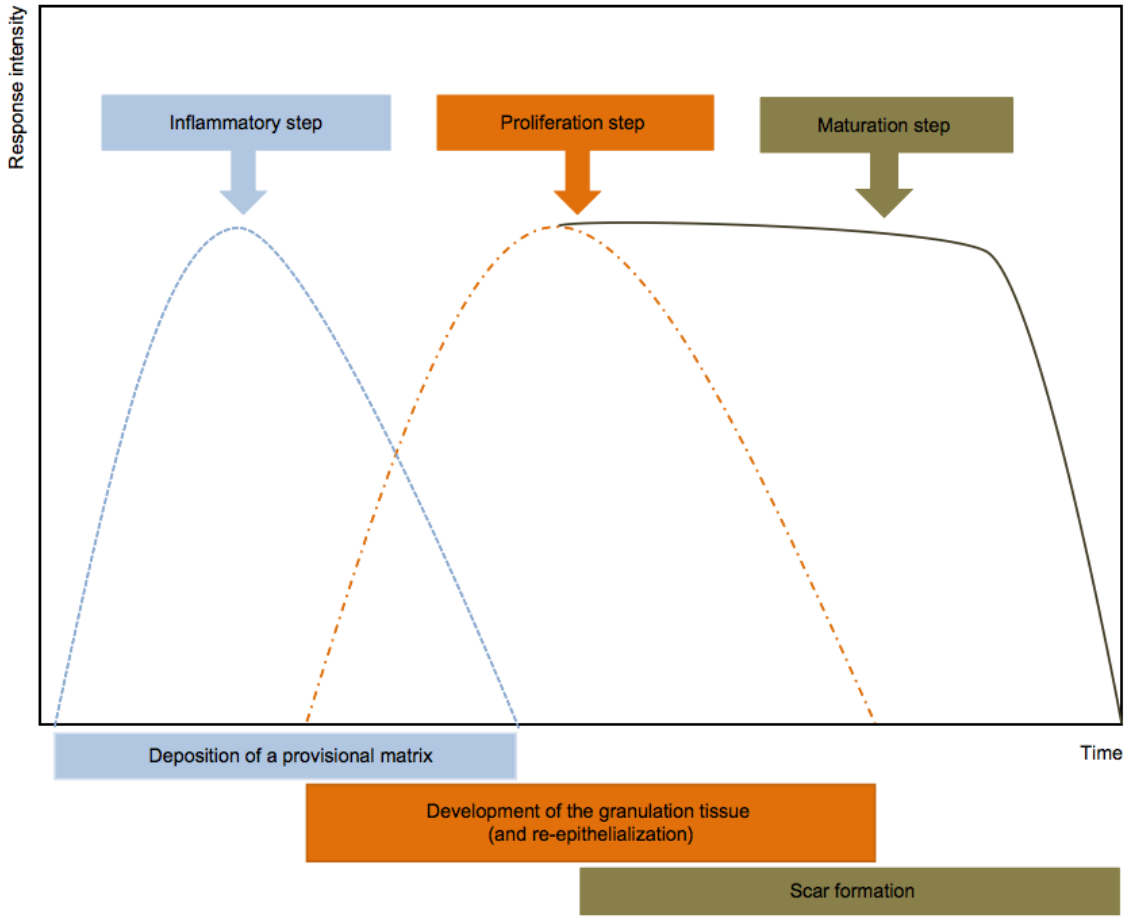

Figure 1-2 The phases of wound healing

Three of the four main phases in wound healing are shown here: after hemostasis, the inflammatory phase, proliferation and re-epithelialisation phase, and the maturation or tissue remodelling phase. These three phases are often overlapping, and not always distinct from each other. Adapted from (Darby et al., 2014)

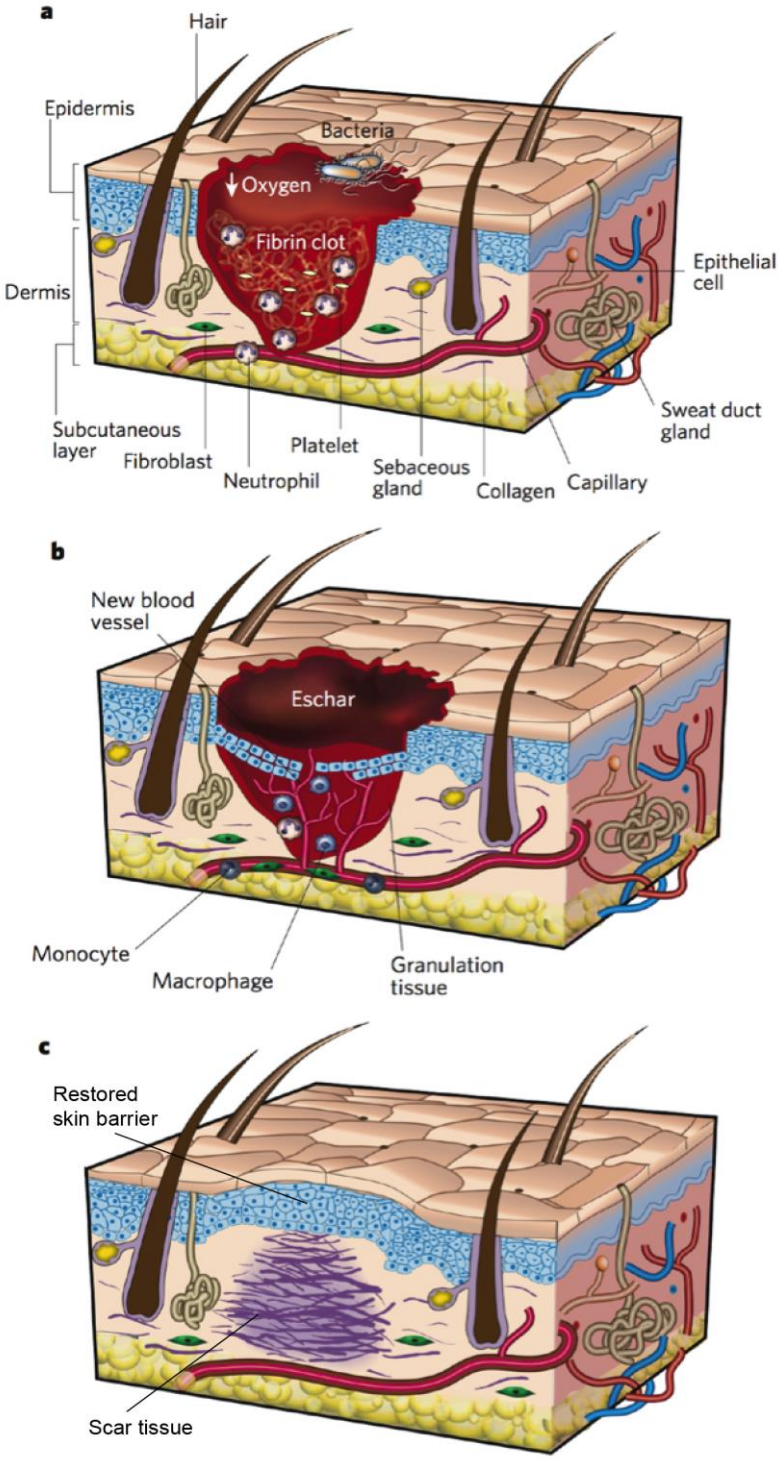

Figure 1-3 Normal wound healing phases

Normal wound healing comprises of three stages after the initial hemostasis. **(a)** Clot formation and inflammatory infiltration occurs from 2 days post-injury. **(b)** Granulation tissue formation and re-epithelialisation during the proliferation phase, occurs 2-10 days post-injury. **(c)** Once integrity of the epithelial layer is restored, the granulation tissue matures into a scar. Tissue remodelling can last for up to 2 years post-injury. Adapted from (Gurtner et al., 2008b)

1.2.1 Haemostasis and inflammation

After the initial bleeding, vascular constriction occurs, followed by blood coagulation and platelet aggregation. These lead to the formation of a temporary clot and restoration of haemostasis (Guo and Dipietro, 2010, Broughton et al., 2006b). Potent vasoconstrictors thromboxane A2 and prostaglandin 2-α are released shortly after injury, after which the clotting cascade is activated. The clot that forms is made up of collagen, platelets, thrombin and fibronectin which all together initiate an inflammatory response (Witte and Barbul, 1997). The clot also protects against invasion of microorganisms and provides a substrate for migration of fibroblasts, monocytes, neutrophils, and endothelial cells to infiltrate this temporary scaffolding (Broughton et al., 2006b, Kurkinen et al., 1980). Pro-inflammatory factors are released at this stage, to initiate the inflammatory response (Broughton et al., 2006b). Platelet migration is promoted by the release of EGF (epidermal growth factor), PDGF (platelet derived growth factor), and TGF-β (transforming growth factor); macrophages infiltration is stimulated by the release of FGF (fibroblast growth factor), ILs (interleukins) 1, 2, 6 and 8, PDGF, TNF (tumour necrosis factor), and TGF-α; and fibroblasts and keratinocytes are attracted by IFNs (interferons) α, β, and γ, KGF (keratinocyte growth factor), as well as TGF- α and β (Broughton et al., 2006b, Henry and Garner, 2003, Lawrence and Diegelmann, 1994).

Infiltrating neutrophils help to clear up any invading microbes and cellular debris (Guo and Dipietro, 2010, Gosain and DiPietro, 2004, Broughton et al., 2006a, Campos et al., 2008). Then macrophages and leukocytes infiltrate the area to prepare the wound bed for the next phase of healing. Macrophage activation is important as these cells mediate angiogenesis, fibroplasia and synthesise nitric oxide (Witte and Barbul, 2002). They also release numerous cytokines which then stimulate fibroblast infiltration and further wound debridement (Broughton et al., 2006b).

1.2.2 Proliferation and re-epithelialisation

Re-epithelialisation, angiogenesis, collagen deposition, and granulation tissue formation are the key events in the later stages of wound healing. If the basement membrane has been destroyed, epithelial cells at the edges of the wound begin proliferating and migrating, thereby causing wound contraction and eventually re-establishing the protective barrier (Lawrence and Diegelmann, 1994, Grotendorst et al., 1989). TNF-α stimulates endothelial cell migration and capillary formation. Angiogenesis is critical to supply oxygen, nutrients and circulating growth factors, required for local cellular metabolism. Without this, the granulation tissue will not form properly, and can result in chronically unhealed wounds. Local fibroblasts synthesise and secrete KGF and IL-6 which further stimulate neighbouring keratinocytes to migrate to the wound area, proliferate and differentiate into a newly formed epidermis (Smola et al., 1993, Xia et al., 1999, Broughton et al., 2006b).

For granulation tissue formation, fibroblasts and keratinocytes are recruited to the wound area where, alongside more mature immune cells, they secrete growth factors such as TGF-beta and EGF, and synthesize temporary ECM components. These include fibronectin, vitronectin, laminin, and collagen (mainly type III) (Campos et al., 2008, Guo and Dipietro, 2010, Gosain and DiPietro, 2004). Fibroblasts already located in the wound site begin to be activated into myofibroblasts, as they acquire smooth muscle cell characteristics, and express α-SMA (Darby et al., 2014). These myofibroblastic cells show contractile properties, with α-SMA being present in microfilament bundles and stress fibers. Other related proteins have also been found to be expressed in myofibroblasts, including desmin, cytoglobin, and transgelin, however α-SMA is thought to be the most reliable marker for this cell type (Tomasek et al., 2002). The main function of myofibroblasts is to synthesise ECM components, in order to eventually replace the temporary matrix of the granulation tissue, and begin the remodelling phase of wound healing (Hinz and Gabbiani, 2003).

1.2.3 Tissue remodelling

In the final scar maturation stages, which can last between a few days and up to 2 years post-injury, there is an attempt to recover normal tissue structure. The ECM is re-organised through the replacement of less resilient ECM proteins with stronger components. Collagen type III is replaced by collagen type I, proteoglycans, and glycosaminoglycans are deposited, and vascular density regresses to normal levels. Physical contraction is ongoing throughout the wound healing process, in which myofibroblasts appear to have a central role. Crucially, amongst all the new ECM synthesis, there is also great complexity in regulated ECM degradation through proteases such as matrix metalloproteases (MMPs), their inhibitors – tissue inhibitors of metalloproteases (TIMPs), and the plasminogen activator system (PA). Once tissue remodelling is coming to an end and tissue integrity has been restored, vascular cells and myofibroblasts are lost through apoptosis (Desmoulière et al., 1995). The balance between ECM synthesis and degradation is essential to the resulting architecture of the tissue. The ultimate normal scar will contain collagen bundles running in parallel to the surface (Guo and Dipietro, 2010, Wolfram et al., 2009).

1.3 Aberrant scarring

Deregulation of any of the stages described above can lead to insufficient or excessive healing activities, resulting in a whole range of conditions, including ulcers, hypotrophic scars, hypertrophic scars, or keloids. It is thought that an extended proliferation phase is key to keloid scar development, where many proliferation factors, which are up-regulated during normal granulation tissue formation, remain enhanced and do not undergo degradation once tissue integrity is restored (Jumper et al., 2015). The keloid epidermis shows a flattened but thickened epidermis, with a highly collagenous dermis (Lee et al., 2004). As there are no definitive biomarkers established for keloid scarring, a combination of clinical appearance and histopathology is used in order to differentiate between keloid scarring and other forms of cutaneous fibrosis (Jumper et al., 2015). **Table 1-1** summarises some of the key histological features that keloids have with other

dermal fibroses. **Figure 1-4** demonstrates differences between hypertrophic and keloid scar formation, as well as clinical images from keloid patients.

1.3.1 Hypertrophic scarring

Hypertrophic scars are very similar to keloids, which often makes it difficult to distinguish between the two clinically. Both tend to be raised, pruritic, erythematous, and painful, however hypertrophic scars remain within the boundaries of the original wound, and can spontaneously regress over time. Keloids, on the other hand, infiltrate the surrounding healthy tissue, and continue to develop over time, without a quiescent or regressive phase (Guo and Dipietro, 2010, Wolfram et al., 2009, Le et al., 2008) **(Figure 1-4)**. After surgical excision, hypertrophic scars do not usually recur, though are more associated with contractures than keloids (Mustoe et al., 2002, Jumper et al., 2015).

Figure 1-4 Hypertrophic and keloid scarring

Top panel depicts spectrum of normal to abnormal wound healing, resulting in keloid scar formation, adapted from (Shih et al., 2010a). Bottom panel presents clinical images of three keloid patients. The smaller scars were initiated by ear piercing, the enlarged bulbous scars in the far right image were instigated by childhood smallpox.

1.3.2 Other dermal fibroses

Dermatofibrosarcoma protuberans (DFSP) could easily be confused with keloids, especially in the early stages of development. It is a slow-growing sarcoma of the skin, not usually found on the hands and feet, found to be at a higher rate of incidence in darker skinned individuals, may recur post-surgical excision, and usually occurs between the ages of 20-50 years (Criscione and Weinstock, 2007, Sabater-Marco et al., 2006). One key histological feature of DFSP is that it shows a honeycomb pattern when the fibrous stroma extends into the underlying adipose tissue (Sabater-Marco et al., 2006). Non-polarised collagen (Barr et al., 1986) and positive $CD34^+$ staining (Aiba et al., 1992) have been used to discriminate DSFP against other cutaneous scarring, though parts of the keloid margin have also shown to express $CD34^+$, where it may inversely correlate with collagen I production (Aiba et al., 1992, Jumper et al., 2015).

Another condition, distinct from keloid and DSFP, though with features in common, is *dermatofibroma*. Like keloid scarring, dermatofibromas have a hyperplastic epidermis, are hyperkeratotic, and show hyalinised collagen in the dermis (Alves et al., 2014, Jumper et al., 2015). It differs from keloid scarring, as it tends to be a more uniform, scaly lesion, and does not recur post-excision. The epidermis shows increased rete ridges, and the hair follicle structures are also increased (Luzar and Calonje, 2010). Dermatofibroma is easily distinguished from DSFP, as histological examination shows a $CD34^-$ and factor XVIIIα positive stain for dermatofibroma, though a $CD34^+$ and factor XVIIIα negative stain for DSFP (Altman et al., 1993).

Cutaneous scleroderma (or morphea) can also resemble dermatofibroma or keloid. It is characterized by a thickened dermis, which occasionally presents dense nodules, and a lack of appendages. Histologically, morphea lesions have a lower level of cellularity compared to keloids (Rencic et al., 2003), though they express similar proteins to keloid scars, including diffuse TNC (tenascin) (Lacour et al., 1992), and COMP (cartilage oligomeric matrix protein) (Moinzadeh et al., 2013). They have flattened rete ridges, as in keloids, increased collagen in the dermis, and

increased immune cell infiltration (Buechner et al., 1993). The key difference in this cutaneous fibrosis is that scleroderma is a systemic disease, therefore clinical assessment must first rule out any signs of systemic sclerosis (Jumper et al., 2015).

Table 1-1 Cutaneous fibroses with similarities to keloid scarring

Adapted from (Jumper et al., 2015). **DSFP =** Dermatofibrosarcoma protuberans

Type of fibrosis	In common with Keloids	Different from keloids	Markers used
Hypertrophic scarring	Raised scar; thickened collagen nodules; increased cellularity	Non-flattened epidermis; organised collagen fibres; no recurrence	H&E, α-SMA
DSFP	Raised, pigmented skin; recurrence post-excision	Honeycomb pattern in dermis; non-polarising collagen fibres	Vimentin, α-SMA, $CD34^{+}$, factor $XVIII\alpha^{-}$
Dermatofibroma	Thickened epidermis; hyperkeratosis; hyalinised collagen	Scaly lesions; no recurrence; reduced cellularity	$CD34^{-}$, factor $XVIII\alpha^{+}$
Cutaneous scleroderma	Pigmented; flattened rete ridges	Reduced cellularity; organised collagen fibres; systemic features	$CD34^{-}$, CD1a, CD3, CD8, CD25, $CD20^{+}$, $CD57^{+}$

1.4 Keloid Scarring

1.4.1 Clinical aspects

One of the most defining features of fibrosis, and indeed keloid scarring, is the high accumulation of ECM, particularly collagen type I. The structure and distinct organisation of keloidal collagen is one of the clearest histopathological differences between keloids and other forms of cutaneous fibroses. In normal skin, collagen is contained within distinct bundles which are mostly organised in parallel to the epidermis, yet randomly connected to each other. Hypertrophic scars show flat collagen fibers organised in a wavy pattern, usually in parallel to the epithelial surface. In contrast, the collagen fibers in keloids tend to be haphazardly organised, with some lying in parallel to the epidermis and some not. Keloids also show dense, acellular bundles of collagen fibres, particularly in the central region (Atiyeh et al., 2005, Jumper et al., 2015). The ratio of collagen type I to type III is higher in keloid scars than in normal skin, and the highest expression of these collagens has been observed in the marginal region of the keloid (Syed et al., 2011).

Aside from the aesthetic issues most patients face, these fibroproliferative scars can lead to disfigurement, possible obstruction to movement, and debilitating psychological strain (Stucker and Shaw, 1992, Le et al., 2008). Keloid pathogenesis has been studied for several decades, but is still poorly understood. They have only been observed in humans, and so the lack of reliable animal models has hindered progress in this area of research (Le et al., 2008, Chang et al., 2009). Some *in vitro* models are becoming increasingly reliable, especially with the advancement in 3D culture technologies, though there is still little consistency between research groups. The fibrotic lesion is known to be induced by skin trauma, but forms in predisposed individuals. Skin trauma can be as major as a surgical wound, or as minor as a body piercing or acne. Most keloids develop within 3 months of injury, though it can take up to 1 year to appear (Le et al., 2008, Rohde et al., 2009). One theory involves the constant forces of tension as a contributing factor to keloid development, as they are more likely to form across joints and skin that creases at

a right angle – with the exception of earlobe keloids (Rudolph, 1987, Rohde et al., 2009).

Keloid scarring occurs in all ethnicities, with the highest prevalence observed in darker skin types, such as in African and Asian populations, estimated up to 16% of the population (Jagadeesan and Bayat, 2007, Shih and Bayat, 2010b, Brown et al., 2008a). Prevalence in Caucasian populations are reported to be no more than 1%. A slight predominance in females has also been noted, though this could be linked to a higher rate of earlobe piercing in females (Le et al., 2008, Zips et al., 2008). Keloids can occur at any age, though they more often develop between the ages of 11 and 30 years (Le et al., 2008, Aarabi et al., 2008). This has been explained by the fact that younger individuals more frequently injure themselves, and their skin is more elastic than in older persons (Wolfram et al., 2009, Gurtner et al., 2008a). Furthermore, keloid formation has also been associated with endocrine factors. Menopause prompts the recession of keloids, whereas women report keloid onset or enlargement during pregnancy (Wolfram et al., 2009, Curry and Osteen, 2003).

1.4.2 Clinical management of keloids

As keloid pathogenesis is so complex and still unclear to date, clinical management is varied, and there is no "golden standard". There are numerous reports on retrospective, uncontrolled studies with small sample sizes, meaning that statistical significance is usually hard to evaluate. Other than study design, other factors such as patient selection, patient treatment history, and long-term follow-up is inconsistent between clinical studies. This makes interpretation confusing, and the variety of therapies being investigated shows just how little is understood about the disorder (Broughton et al., 2006b). Prevention of injuries is the obvious solution, though highly impractical. If it is known a certain individual is prone to keloid scarring, any surgical wounds should be closed with minimal tension, avoiding incisions across joint spaces, and following skin creases where possible (Wolfram et al., 2009, Rudolph, 1987, Lim et al., 2002a, Boyce et al., 2002). Total keloid excision with no adjuvant therapy stimulates further fibrogenesis, and can

lead to the quick recurrence of larger scars. Recurrence rates range from 45% to 100% (Wolfram et al., 2009, Smiley et al., 2005, Broughton et al., 2006b). Surgical intervention is usually performed intralesionally so as to "de-bulk" larger scars, and always in combination with another therapy such as pressure therapy, chemotherapy, radiotherapy, or steroid injections (Wolfram et al., 2009, Broughton et al., 2006b). Less common is extralesional surgical excision, principally performed in more recent clinical trials, in combination with chemotherapy or radiotherapy. If the lesion is particularly large, a partial thickness skin graft may be used to close the wound with as little tension as possible.

1.4.2.1 Pharmacologic therapies

The first-line treatments for keloids are corticosteroids, the most common of which is triamcinolone acetonide (TA). These are commonly administered intralesionally (within the margins of the keloid) into the upper layers of the dermis, and function as a global anti-inflammatory agent, which inhibits cell growth and proliferation (Petratos et al., 2002). Vasoconstriction is increased, and the inflammatory infiltrate is reduced, meaning effective phagocytosis and collagenase production by macrophages and polymorphonuclear neutrophils in the wound bed is also reduced (Broughton et al., 2006b, Rudolph, 1987, Wolfram et al., 2009, Rohde et al., 2009, Menon et al., 2012). Inhibition of both fibroblast and keratinocyte proliferation has been observed in culture, with fibroblasts from different regions of the keloid even showing differential response to the glucocorticoids (Smith et al., 2008). It appears that the subset of fibroblasts residing in the reticular dermis of the central scar nodules, where TGF-β signalling is increased, are more resistant to glucocorticoids than fibroblasts from the superficial dermis or adjacent normal tissue (Smith et al., 2008). In the clinical setting, if effects such as tissue atrophy, hypopigmentation, or telangiectasia develop during treatment, it is halted (Wolfram et al., 2009, Veleirinho et al.).

Immunomodulators such as imiquimob and interferon-α2b, induce cytokine and interferon release at the site of application, which in turn act to deactivate fibroblasts from producing excessive collagen fibrils. There has been limited

success with these therapies, showing up to a 54% recurrence rate, compared with 15% when using TA (Wolfram et al., 2009, Rudolph, 1987).

The chemotherapy 5-Fluorouracil (5-FU) is well known in the oncology field, where it has been in use for over 50 years (Philandrianos et al.). It works by targeting rapidly proliferating cells, which in the case of the keloids, would be the fibroblasts. It has also been shown to interfere with TGF-β signalling, and to reduce gene expression of Type I Collagen in keloid fibroblasts (Wolfram et al., 2009, Zigrino et al.). Intralesional injection of 5-FU has been used with some success, particularly when in combination with corticosteroids, and even more so when administered after extralesional excision (inclusive of a small margin of the adjacent healthy skin) (Huang et al., 2013b). A combination of low-dose 5-FU, with triamcinolone on cultured keloid fibroblasts led to reduced cell proliferation (due to the corticosteroid), followed by cell-cycle arrest and apoptosis (due to the 5-FU). Collagen I production and TGF-β signalling was reduced, while MMP2 expression was induced, all to a statistically significant level (Huang et al., 2013b). This is a promising route for keloid treatment, nevertheless 5-FU can demonstrate side effects such as ulceration, pain, and hyperpigmentation (Wolfram et al., 2009, Rudolph, 1987).

1.4.2.2 Other therapies

Occlusive dressings, including silicone and non-silicone gel sheeting, have been increasingly used over the last 20-30 years in the treatment of abnormal scars, with reasonable success. Reports have shown occlusive dressings to soften scars and reduce their size, erythema, pruritis and pain (Le et al., 2008, Bagabir et al., 2012). Keloid prevention was noted in up to 80% of cases post-excision (Le et al., 2008, Jin et al.). The mechanism of action is unclear, however the theory is that occlusion provides hydration and increased temperature to the scar, thereby affecting local keratinocytes to alter growth factor secretion, and as a result influence fibroblast regulation (Wolfram et al., 2009, Bagabir et al., 2012, Li et al., 2012a, Li et al., 2012b).

Radiotherapy is most successfully used as an adjunct to surgical excision, with reports of around 30% recurrence rate. Although radiotherapy technologies are ever evolving, using lower effective doses and increasing the specificity of their action, there are still major risks for the patient. Postoperative complications include impaired wound healing, fibrosis, and the potential for malignancy in the surrounding healthy tissues (Le et al., 2008).

Cryotherapy has shown good outcomes in patients with smaller lesions, and in fair-skinned individuals. It involves the use of a freezing medium to ablate the targeted lesions. Intralesional cryosurgery has shown higher success rates compared with contact cryotherapy, as well as causing less pain – the major factor for lack of compliance to the full course of treatment by patients (Le et al., 2008, Chung et al., 2007).

1.4.3 Genetics of keloid scarring

Keloid formation has been described in individuals with other connective-tissue genetic disorders, including Rubinstein-Taybi syndrome (Siraganian et al., 1989), Ehlers-Danlos syndrome (Pope et al., 1977, Char, 1971), pachydermoperiostosis (Hambrick and Carter, 1966), and Dupuyten's disease (González-Martínez et al., 1995, Shih and Bayat, 2010b). Rubinstein-Taybi syndrome is characterised by abnormalities such as developmental delay, mental retardation, broad thumbs, and distinctive facial features (Mishra et al., 2015). One study reported a 5% occurrence rate of keloids in individuals with Rubinstein-Taybi syndrome, though there was no conclusive evidence that the two are necessarily associated, as the keloid occurrence rate was not calculated in the control patient group (Siraganian et al., 1989). The observation of keloid formation in Ehlers-Danlos syndrome patients was interesting as this genetic disorder displays a collagen type III deficiency (Pope et al., 1975).

Most keloids occur sporadically, but some cases are hereditary. Over the relatively small number of studies on the genetics of familial keloids, the most commonly reported mode of inheritance is autosomal dominant with incomplete penetrance

and variable expression (Shih et al., 2010a, Marneros et al., 2001). While there have been several studies on keloid inheritance and on isolating responsible genes for keloid scarring, select genes have not yet been verified. So far, genome-wide studies have been performed on Japanese and Chinese families (Nakashima et al., 2010a, Marneros et al., 2004b), but only small-scale studies have been performed on the highest prevalent ethnicities, such as African-Caribbean (Shih and Bayat, 2010a, Bella et al., 2011). An African-American family showed linkage to the 7p11 locus, where EGFR might be affected, and in a Japanese family, a keloid susceptibility locus was mapped to 2q23, where TNFAIP6 (tumour necrosis factor, alpha induced protein 6) may be of interest (Marneros et al., 2004b, Shih and Bayat, 2010b). In a large Chinese family spanning five generations, the linkage locus 18q21.1 was thought to be important – a region where SMADs 2, 4, and 7 (mothers against decapentaplegic homologs) and PIAS2 (protein inhibitor of activated signal transducer and activator of transcription 2) are coded for (Shih and Bayat, 2010b, Yan et al., 2007). The SMAD genes are involved in the TGF-β pathway, which has been associated with fibrosis, and will be discussed below (**section 1.4.5**).

A number of genes within the TGF-β pathway, as well as other factors such as EGFR, p53, and RUNX3 (Runt-related transcription factor 3), have been investigated for polymorphisms and mutations. As with much of keloid research, the results are often conflicting and inconsistent in use of methodologies. To date, no polymorphisms or mutations have been identified in TGF-β ligands TGF-β1, 2, and 3, or in their receptors TGF-βRI, II and III, or in SMADS 3, 6 and 7 (Bayat et al., 2004, Bayat et al., 2005, Brown et al., 2008b, Saed et al., 1998). Similarly, although p53 mutations were found in cultured keloid-derived fibroblasts, these were non-existent in the original tissues, meaning the mutations were likely to be acquired during the cell culture process (Saed et al., 1998). Zhang et al. found a higher rate of gene mutations in TNF receptor II in keloid tissue, compared to the same patients' venous blood control (Zhang et al., 2008).

1.4.4 ECM remodelling in keloids

The balance of ECM protein production and degradation is clearly deregulated in keloid scarring, and numerous studies have shown how this deregulation can be seen in all phases of wound healing (Shih et al., 2010a). In the inflammatory phase, fibronectin and fibrinogen form a temporary matrix to allow cells to migrate through the wounded area. At this stage, fibronectin and collagen type I levels are increased, along with a decrease in fibrin degradation (Babu et al., 1989, Kischer and Hendrix, 1983, Shih et al., 2010a, Friedman et al., 1993, Tuan et al., 1996). Elevated levels of hyaluronic acid has been debated over a number of studies, not agreeing to whether it's due to increased production in early wound healing, or a lack of degradation in the later phases of healing (Meyer et al., 2000, Alaish et al., 1995). The proliferative phase is where ECM production increases momentum in normal wound healing, and in keloid scarring even more so. Arguably, keloids never fully end their proliferative phase, as they continue expanding over time. As growth factors are recruited to the wound bed, neovascularisation, collagen deposition, granulation tissue formation and wound contraction take place (Shih et al., 2010a).

As the wound enters the later stages of repair, enzymes such as collagenases, gelatinases, and elastases ensure initial ECM structures are digested and replenished with more stable versions, until the injury has been reconstituted to its original state (O'Kane and Ferguson, 1997, Shih et al., 2010a). The major enzymes in this complex, yet delicately balanced, process include the matrix metalloproteinases (MMPs), plasminogen activator (PA)-plasmin, and a disintegrin and metalloproteases (ADAMs). PA converts plasminogen into plasmin, which consecutively breaks down fibrin (Toriseva and Kahari, 2009), and activates procollagenase to breakdown collagen (Tuan and Nichter, 1998). Several factors have been suggested as inhibitors of ECM breakdown, including interferon-γ (IFN-γ). In normal wound healing, IFN-γ inhibits fibroblast proliferation, decreases synthesis of collagen types I, II and III, and increases collagenase synthesis (Adelmann-Grill et al., 1987, Jimenez et al., 1984, Shih et al., 2010a). IFN-γ has been reported as reduced in keloids, where collagen synthesis is increased and

collagenase activity appears ineffective in degrading the fibrotic scar tissue (Shih et al., 2010a, McCauley et al., 1992).

It is accepted that α-SMA-expressing fibroblasts in granulation tissue signifies the presence of ECM-producing myofibroblasts (Darby et al., 2014, Darby et al., 1990, Jumper et al., 2015). When local populations of fibroblasts are not available or sufficient for granulation tissue remodelling, alternative sources of myofibroblasts have been reported to be mesenchymal stem cells (Jahoda et al., 2003), circulating bone marrow derived cells (Pittenger et al., 1999, Opalenik and Davidson, 2005), as well as differentiated cells undergoing epithelial- or endothelial-to-mesenchymal transition (Darby et al., 2014, Nakamura and Tokura, 2011). During prolonged wound healing processes, myofibroblasts are implicated with excessive scarring, where they fail to undergo cell death once the granulation tissue has matured and tissue remodelling is underway (Desmoulière et al., 1995, Darby et al., 1990). In fact, it was suggested that α-SMA expression is present in hypertrophic scars but not in keloid scars, making it a potential marker for differentiating between these two histologically similar formations (Ehrlich et al., 1994). Since then however, α-SMA expression has been observed in both keloids and hypertrophic scarring (Lee et al., 2004, Lee et al., 2012), with increased intensity surrounding the thickened collagenous nodules characteristic of keloid scars (Santucci et al., 2001, Jumper et al., 2015). Understandably, the potential regulation of myofibroblast disappearance through apoptosis is of increasing interest in terms therapeutics (Hinz and Gabbiani, 2003).

Along with the myofibroblasts normally present in many fibrotic diseases, mesenchymal stem cell (MSC) populations have been identified in keloid dermis, at an elevated level compared to healthy control skin. Iqbal et al support that there is in fact a hybrid haematopoietic/ mesenchymal cell population, called fibrocytes, present as a distinct population alongside the MSCs (Iqbal et al., 2012).

1.4.4.1 Structural ECM proteins in keloids

The abundant structural protein collagen type I accounts for the majority of the fibrotic scar tissue seen in the keloid dermis. It is generally accepted that thickened

collagen I fibres are organized in a haphazard manner, termed as "keloidal collagen" (Lee et al., 2004). They have a glassy appearance, are hyalinised, oesinophilic, and can form acellular nodules in parts of the reticular dermis (Ehrlich et al., 1994). The ratio of collagen I/ collagen III is also increased in keloids (Abergel et al., 1985, Kischer and Brody, 1981, Lee et al., 2004). In normal skin the ratio is approximately 6, whereas in keloid scars the collagen type I/III ratio is close to 17 (Friedman et al., 1993, Shih et al., 2010a). It has not been concluded whether this effect is due to the lack of collagenase activity (particularly for type III), or an increased production of both collagen types (Niessen et al., 1999, Abergel et al., 1985, Shih et al., 2010a). It is likely that both actions contribute to the problem. Collagens V and VI have also been found to be overexpressed in keloids (Shih and Bayat, 2010b), which may indicate changes to the basement membrane integrity, where these collagens reside (Gordon and Hahn, 2010, Ricard-Blum, 2011).

Fibronectin is a key glycoprotein of the ECM, which binds to integrins and other ECM-related molecules, forming an early granulation tissue (Martino et al., 2011). It has shown increased expression in keloids compared to normal skin (Kischer and Hendrix, 1983), especially at the dermal-epidermal junction, and co-localised with fibroblasts located between the thickened collagen nodules (Sible et al., 1994). Fibronectin can also be stimulated by the growth factor TGF-β1 (Lee et al., 2013, Jumper et al., 2015).

Hyaluronan, an essential glycosaminoglycan of the ECM, has shown a unique expression pattern in keloid tissue. It has shown minimal expression in the papillary dermis, with intense expression in the subrabasal layers of the epidermis. In contrast, hypertrophic scars have shown a stronger expression in the papillary dermis, and very low expression in the epidermis (Hellström et al., 2014), making this protein a potential useful marker for differentiating between hypertrophic scars and keloids (Sidgwick and Bayat, 2012). HA is thought to be important in effective epithelialization, and well as for regulating fibroblast cell morphology (Tan et al., 2011).

Elastin and fibrillin were found to be disorganised in keloid lesions, as compared to normal skin. Fibrillin-1 was decreased across the whole tissue, whereas elastin showed no expression in the papillary dermis, and a significantly increased level in the reticular dermis (Amadeu et al., 2004).

More recently, molecules such as dermatopontin, periostin, and tenascin have been linked to keloid histopathology (Jumper et al., 2015, Sidgwick and Bayat, 2012). Dermatopontin has shown a decreased level of both gene and protein expression in keloids compared to normal skin (Russell et al., 2010, Catherino et al., 2004). In keloids, periostin has shown increased expression in the dermis and epidermis, compared to normal skin, as well as strong co-localisation with CD31, suggesting periostin may affect blood vessel density (Zhang et al., 2015). In hypertrophic scars, dermal fibroblast proliferation and differentiation were enhanced (Crawford et al., 2015).

1.4.5 Fibrogenic Signalling Pathways

There is growing evidence that epithelial-mesenchymal cross talk has a significant impact in wound healing and fibrotic disorders (Tuan et al., 1996, Ashcroft et al., 1997a). During wound healing, keratinocytes stimulate fibroblasts to produce growth factors as well as ECM proteins, which then stimulate keratinocyte proliferation in a double paracrine manner (Werner et al., 2007). In keloids, a similar pattern has been reported in numerous studies, though the extended effect on the keratinocytes has not been thoroughly examined (Ashcroft et al., 1997a, Wachsstock et al., 1987, Rasp et al., 1987, Adelmann-Grill et al., 1987, Shih et al., 2010a). Co-culturing keloid keratinocytes with normal fibroblasts resulted in an enhanced TGF-β-induced collagen production by the fibroblasts (Ashcroft et al., 1997a, Ashcroft et al., 1997b, Freneaux et al., 2000). Also, increased differentiation of fibroblasts was noted when treated with conditioned media from co-cultured cells, compared to when treated with conditioned media from single layer cultures (Freneaux et al., 2000).

When grown under co-culture conditions, keratinocytes and fibroblasts have shown to produce increased levels of TGF-β – also shown to induce α-SMA expression in the fibroblasts. The increased fibroblast differentiation is noted by increased cell contractility (Werner et al., 2007). Other than TGF-β, overexpression of other cytokines and growth factors, such as IGF, PDGF, and TNF-α in keloids show there is a lack of control of the wound healing signals (Wolfram et al., 2009, Diegelmann et al., 1979, Niessen et al., 1999, Blackburn and Cosman, 1966, Ehrlich et al., 1994, Rohde et al., 2009, Zips et al., 2008, Aarabi et al., 2008). PDGFR-α is at least four times enhanced in keloid fibroblasts (Shih et al., 2010a, Haisa et al., 1994), which could be due to TGF-β1 action (Shih et al., 2010a, Messadi et al., 1998), compared to healthy control skin fibroblasts.

Moreover, there is an apparent imbalance between proliferative and apoptotic pathways, thought to be due to a combination of increased myofibroblast proliferation, and a downregulation of apoptotic related genes (Chipev et al., 2000, Luo et al., 2001, Ladin et al., 1998, Akasaka et al., 2001, Shih and Bayat, Syed et al., 2011). Though more recently, evidence is growing that levels of apoptosis and proliferation vary between regions within the keloid lesion, with the central part of the scar showing increased levels of apoptosis, and the marginal region showing the highest level of proliferation.

1.4.5.1 TGF-β/SMAD signalling in keloids

The TGF-β system is a superfamily of proteins that regulate several different processes, including morphogenesis, embryonic development, adult stem cell differentiation, immune regulation, wound healing and inflammation. TGF-β uses protein kinase receptors and SMAD mediators to transduce signals (Derynck and Zhang, 2003), and any deregulation of the pathways can contribute to pathologies such as cancer, cardiovascular issues, fibrosis, and congenital disorders. In fibrotic conditions, abnormal TGF-β regulation has been linked to pulmonary fibrosis, liver cirrhosis, congestive heart failure, rheumatoid arthritis, Marfan syndrome, hypertrophic scars, systemic sclerosis, as well as keloids (Santibañez et al., 2011, He et al., 2010, Varga and Pasche, 2008, Fujiwara et al., 2005a). More specifically,

TGF-β1 has been established as an important fibrogenic factor that promotes ECM production and fibrosis in tissues, including in keloids (He et al., 2010, Leask and Abraham, 2004, Fujiwara et al., 2005a). Keloid fibroblasts are believed to express increased levels of TGF-β1, which induces collagen overproduction in the dermis. Additionally, CTGF expression is induced by TGF-β, which encourages fibroblast differentiation into myofibroblasts, and eventually collagen synthesis (Santibañez et al., 2011). The TGF-β receptors (TGF-βR) I and II and some of their intracellular signalling mediators, SMAD2, SMAD3 and the SMAD2/3/4 complex, have been shown to be elevated in keloids compared to normal skin (Phan et al., 2005, He et al., 2010). The SMADs also interact with the mitogen-activated protein kinase (MAPK) pathway, which in combination with JNK promotes cell invasion and ECM synthesis through mesenchymal cell activation (He et al., 2010, Furukawa et al., 2003, Matsuzaki and Okazaki, 2006). TGF-β1–induced SMAD2/3 phosphorylation at the linker region serves as a cross-talk platform for phosphorylation by the MAPK pathway, making TGF-β1 a key factor in keloid pathogenesis (He et al., 2010).

TGF-β1/SMAD signalling (**Fig 1-5**) is achieved when the appropriate SMAD complexes translocate to the nucleus to propagate transcription. Phosphorylated SMAD2/3 link with SMAD4 to form a complex, and together with the ERK and JNK pathways translocate to the nucleus (Shi and Massague, 2003, He et al., 2010, Derynck and Zhang, 2003). From there, gene expression for proteins crucial to ECM regulation are targeted. One example is plasminogen activator inhibitor-1 (PAI-1), an important factor in cell invasion and ECM deposition, and has increased activity in keloids (Yang et al., 2008, Tuan et al., 2003, He et al., 2010). He et al demonstrated that ERK, JNK and p38 inhibitors significantly suppressed TGF-β1-induced PAI-1 expression, meaning that these pathways also play a role in PAI-1 transcription (He et al., 2010). SMAD7 acts as an inhibitor of the SMAD2/3 complex, through its interaction with activated TGF-βRI, thus preventing SMAD2/3 phosphorylation, and as a result decreasing fibrogenic proteins. In keloid fibroblasts, SMAD7 appeared significantly reduced, and even more so when the cells are treated with TGF-β1 (Nakao et al., 1997, Kopp et al., 2005, Yu et al., 2006). This could explain the lack of a negative feedback loop in keloids, which would

ordinarily keep ECM production in balance. He et al showed that inhibiting p38 in keloid fibroblasts reversed the SMAD7 reduction, which supports their hypothesis that the p38 pathway is involved in regulating fibrogenesis in keloids (He et al., 2010).

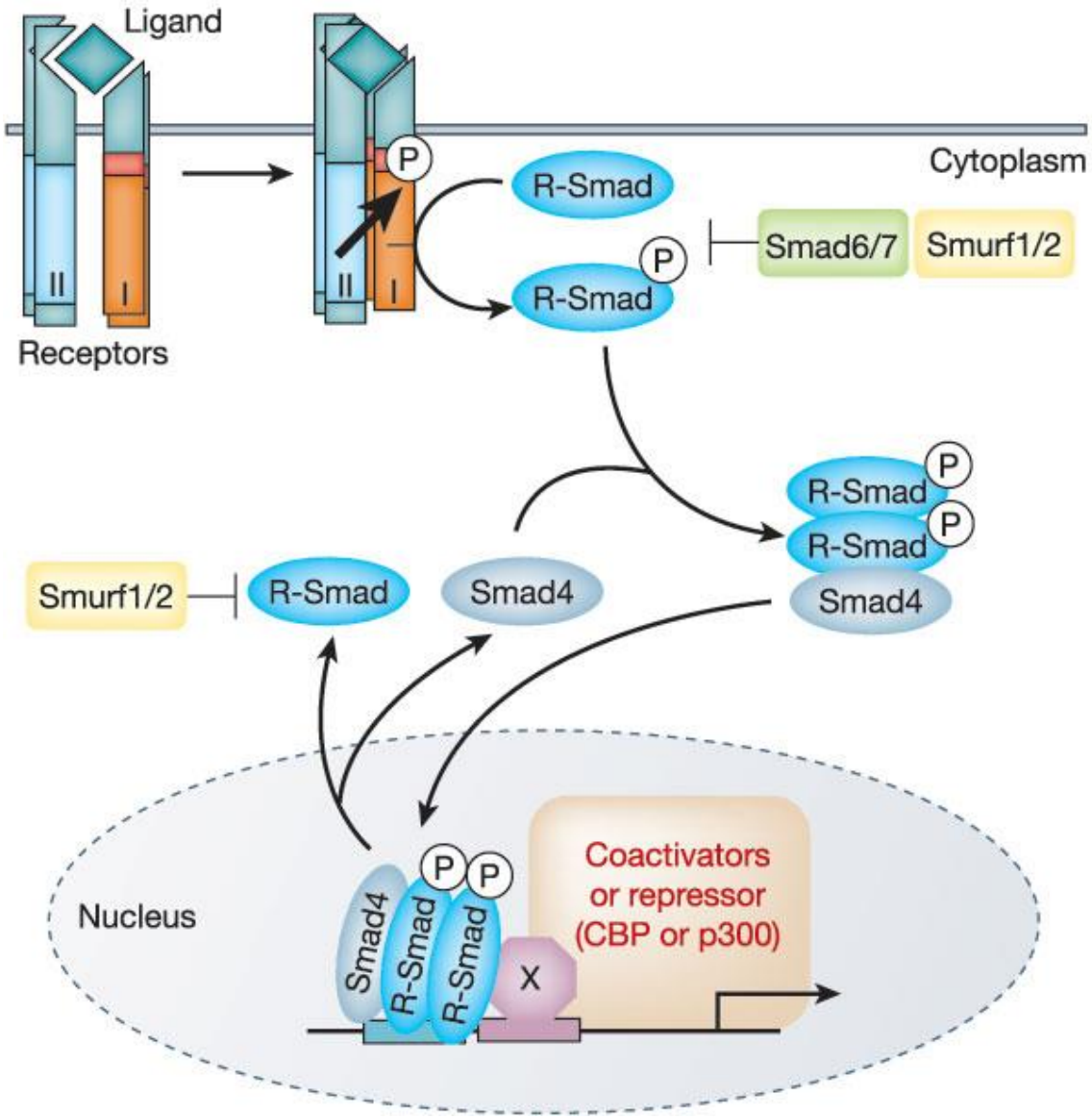

Figure 1-5 The TGF-β/ SMAD signalling pathway

Once bound to its ligand, the TGF-β receptor kinases induce phosphorylation of the R-SMADs (receptor-activated SMADs 2 and 3), which then form a complex with co-SMAD (SMAD4). The SMAD 2/3/4 complex is then translocated to the nucleus to regulate transcription of target genes. SMAD6 or 7 along with Smurf1/2 inhibit this process, by blocking R-SMADs from forming a complex, and therefore contribute to a negative feedback to TGF-β action. Image adapted from (Derynck and Zhang, 2003).

1.4.5.2 Other signalling pathways, growth factors and cytokines in keloids

The Wnt pathway has long been implicated in fibrosis, though only a small number of studies have shown its role in keloid scarring (Igota et al., 2013). There are two main pathways to Wnt signalling: β-catenin-dependent, which leads to downstream transcription of genes related to cell proliferation and growth; and β-catenin-independent, linked to cell polarity and migration (Niehrs, 2012). There is also a third pathway involving Ca^{2+}, where calceneurin induces NFAT (nuclear factor of activated T-cells), leading to effects on cell migration and cell fate (see **Figure 1-6**) (Niehrs, 2012). Igota et al. demonstrated Wnt5a was overexpressed in keloid fibroblasts compared to normal fibroblasts, due to the β-catenin-dependent Wnt activation (Igota et al., 2013). In hypertrophic and keloid scar tissue, histological examination demonstrated TGF-β-induced activation of the β-catenin-dependent Wnt signalling pathway (Sato, 2006). In isolated keloid fibroblasts, a range of IGF-(insulin growth factor) binding proteins were found to be overexpressed, compared to normal fibroblasts, whereas expression of Wnt pathway inhibitors DKKs (dickkopf homolog) 1 and 3, and SFRP1 (secreted frizzled related protein 1) were decreased. JAG-1 (jagged-1), an effector of the Notch pathway and a target of Wnt signalling, was also over-expressed in keloid fibroblasts (Smith et al., 2008). When comparing the central and marginal regions of the keloid scar separately, apoptosis-inducing genes were found to be over-expressed in the central region, whereas apoptosis inhibitor AVEN was increased in the keloid edge, supporting the notion that the keloid margin is expanding whereas the centre is regressive (Seifert et al., 2008)

Another signalling pathway known to impact on fibrosis is the Notch pathway, which requires cell-cell contact for activation, and is important in regulating several processes including proliferation, differentiation and apoptosis (He and Dai, 2015). In systemic sclerosis and scleroderma, Notch activation appeared to impact on myofibroblast activation (Dees et al., 2011). Very little has been reported on Notch signalling in keloids, though Syed et al. observed a significant up-regulation of Notch receptors and ligand Jagged-1 (JAG-1) in keloid scars

compared to both adjacent normal skin to the keloids and external control skin (Syed and Bayat, 2012).

During the proliferative phase, neovascularisation helps to form an initial granulation tissue, where nutrient and oxygen transfer is enabled. Keloids demonstrate increased neovascularisation, with VEGF signalling playing a major role (Shih et al., 2010a, Beer, 2005, Gira et al., 2004). PDGF, CTGF (connective tissue growth factor), EGF, and IGF are among the cytokines shown to impact on fibrogenesis, and have been reported as increasing the proliferative response in keloids (Shih et al., 2010a).

EGF action in keloids is inconclusive at present, with reports of increased, decreased and no significant difference in expression levels in keloids (Shih et al., 2010a, Harper, 1989, Satish et al., 2004). Aside from re-epithelialisation, CTGF plays an important role in ECM production and tissue remodelling in the later stages of wound healing (Shih et al., 2010a, Abreu et al., 2002). In keloid epidermis, CTGF shows increased expression at the basal layer. Co-culturing keloid keratinocytes and fibroblasts leads to increased secretory CTGF and decreased endogenous CTGF, together suggesting that keratinocytes secrete CTGF into the dermis and from there promotes fibrogenesis (Shih et al., 2010a, Khoo et al., 2006). CTGF also impacts on TGF-β signalling (Abreu et al., 2002, Shih et al., 2010a), discussed earlier on. IGF-I also encourages keloid fibrogenesis through TGF-β1 signalling. Keloid tissues and fibroblasts demonstrate increased levels of IGF-I receptor (IGF-IR), which could partly explain the proliferative, anti-apoptotic, invasive nature of keloids (Shih et al., 2010a, Ishihara et al., 2000).

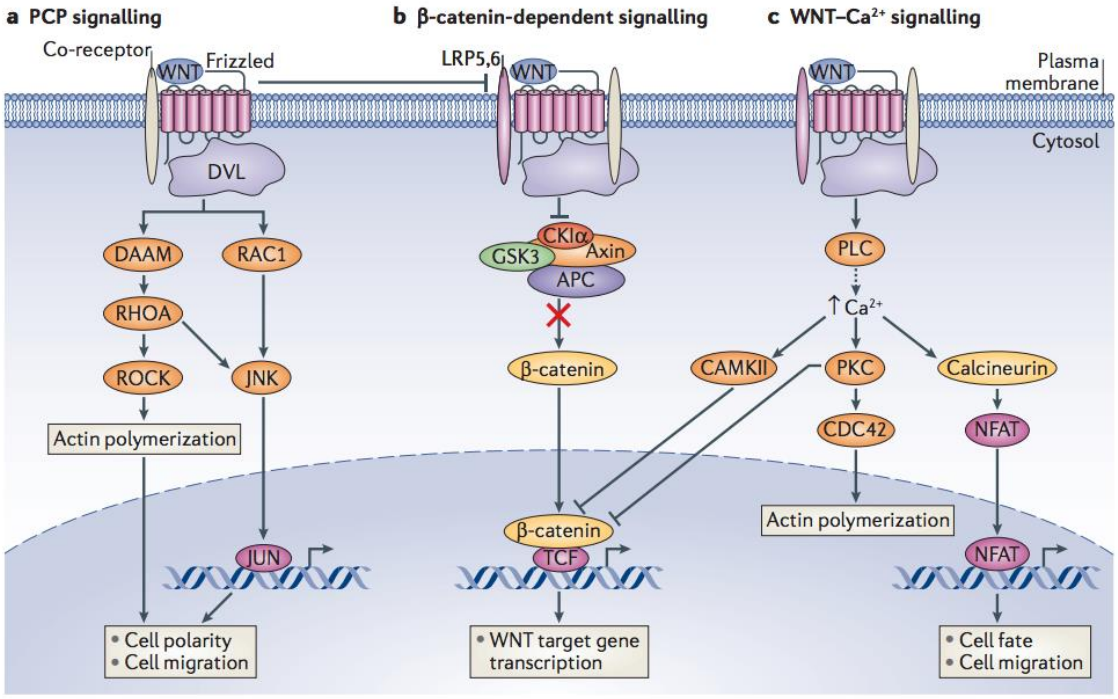

Figure 1-6 Wnt signalling pathways

Schematic of the main pathways involved in Wnt signalling. **(a)** The β-catenin-independent pathway: PCP (planar cell polarity) signalling is primarily involved in regulating cell polarity and motility. **(b)** In the β-catenin-dependent pathway, when Wnt ligand is present, the destruction complex (comprising of GSK3, APC, Axin and CKIα) is inactivated. This allows β-catenin to be translocated to the nucleus and activate gene transcription. **(c)** The Wnt-Ca^{2+} pathway leads to activation of NFAT (nuclear factor of activated T cells) which once translocated to the nucleus, triggers transcription of genes regulating cell fate and migration.

Adapted from (Niehrs, 2012)

1.5 Research aims and objectives

1.5.1 Research aim

In the current literature, it becomes clear that there is a high degree of variability reported in a large proportion of keloid scars. Whether in relation to the disorder's histopathology, genetic analysis, or signalling processes taking place, it is difficult to reach firm conclusions on the cause of keloid scarring. The prevailing inconsistencies in methodologies applied, experimental design, source materials used, as well as control material used, make it even more challenging to establish a causative link to keloids.

The overall aim of my research was, as far as possible, to identify a marker of keloid scarring, in a uniform as possible group of clinical samples, so that this could be used to further elucidate keloid pathogenesis. I examined the keloid scars as a whole entity, inclusive of the epidermis and dermis, containing the central, marginal, and adjacent normal sites of the scars.

1.5.2 Objectives

- To characterise the keloid scar and control skin biopsies, by assessing their tissue morphology, cell proliferation, and fibroblast activation. Also, to investigate protein expression patterns of MMPs 1, 2, 13, and 14 in the same tissues.

- To explore gene expression alteration in whole keloid tissues, using a focused approach. Real Time qPCR arrays were used to examine 84 genes linked to the ECM, and a further 84 genes linked to 10 of the most well known signalling pathways.

- To validate the gene expression results in whole tissue, as well as in primary cultured keratinocytes and fibroblasts from the same cohort of specimens.

- To conclude with an identified biomarker for future investigations in keloid biology.

2 Materials and Methods

2.1 Patient samples

Keloid specimens were received from The Royal London Hospital in Whitechapel, London. Ethical approval for these has been made under the ethical registration number 2011-000626-29. The nature of keloid scarring is such, that it is deemed unethical to harvest matched control healthy skin biopsies from keloid patients, as this would lead to a new keloid forming. Therefore, healthy control skin samples were retrieved from unaffected patients undergoing routine procedures within the plastic surgery department of The Royal London Hospital, where there was excess unwanted skin. Most of the available normal skin came from Caucasian individuals, however African-Caribbean skin was collected wherever possible, so as to at least match the keloid scars by ethnicity. Full patient consent was collected in all cases. Refer to **Tables 2-1** and **2-2** for detailed information relating to all patient samples used in this thesis.

All keloids were extralesionally excised, including a margin of the adjacent normal tissue. Almost all the keloids showed vertical growth, with only K36 and K42 showing a "butterfly" appearance, where the central part of the keloid is flattened and only the edges protrude vertically.

Table 2-1 Patient information for keloid, normal and hypertrophic scars used throughout thesis.

NB: **ECM PCR** (Extracellular matrix and adhesion molecules qPCR array – see section 2.3.2); **STP PCR** (signal transduction pathway finder qPCR array – see section 2.3.2); **IHC** (Immunohistochemistry – see sections 2.2.1-2.2.3)

Keloid Sample ID	Gender	Ethnicity	Body location	IHC	ECM PCR array	STP PCR array	Primary Fibroblasts	Primary Keratinocytes
Chapter ref.				3	4	4	5	5
NSc	F	African-Caribbean	Neck	X				
HSc	Unknown	Caucasian	Unknown	X				
K20	Unknown	African-Caribbean	Unknown				X	X
K26	Unknown	African-Caribbean	Earlobe - Recurrence	X				
K28	F	African-Caribbean	Abdomen		X	X		
K32	M	Asian	Ear	X				
K34	F	African-Caribbean	Post-auricular	X	X	X	X	
K35	M	African-Caribbean	Scapula	X	X	X		
K36	F	African-Caribbean	Breast (butterfly)	X	X	X	X	X
K40	M	African-Caribbean	Cheek	X	X	X		
K42	F	Caucasian	Abdomen (butterfly)	X				
K51	M	African-Caribbean	Sternum	X			X	X
K55	M	African-Caribbean	Nape of neck	X			X	X
K70	M	Caucasian	Post-auricular	X			X	

Table 2-2 Patient information of healthy control tissues used throughout thesis.

NB: **ECM PCR** (Extracellular matrix and adhesion molecules qPCR array – see section 2.3.2); **STP PCR** (signal transduction pathway finder qPCR array – see section 2.3.2); **IHC** (Immunohistochemistry – see sections 2.2.1-2.2.3)

Normal Skin Sample ID	Gender	Ethnicity	Body location	IHC	ECM array	STP array	Primary Fibroblasts	Primary Keratinocytes
Chapter ref.				3	4	4	5	5
NS4	F	Caucasian	Unknown	X			X	
NS6	F	African-Caribbean	Breast	X	X	X	X	X
NS7	F	Caucasian	Facelift		X			
NS8	F	Caucasian	Breast				X	X
NS9	F	African-Caribbean	Breast	X	X			
NS14	F	Caucasian	Breast		X	X		
NS16	F	Caucasian	Breast	X	X	X		
NS17	F	African-Caribbean	Abdomen	X		X		
NS18	M	Caucasian	Thigh	X				
NS21	F	African-Caribbean	Breast	X		X		
NS22	F	African-Caribbean	Abdomen	X				
NS24	F	African-Caribbean	Breast				X	
NS25	F	African-Caribbean	Breast	X				
NS29	F	Caucasian	Abdomen					X

2.1.1 Tissue fixation and wax embedding

Clinical samples were cut with a disposable surgical scalpel (cat. SCA-310-030K, Fisher) into approximately 5-20mm^3 pieces and incubated in 4% (v/v) formaldehyde (diluted from 37 wt% solution in water, stabilized with 5-15% methanol; cat. 119690010, Acros Organics, Fisher Scientific UK) or 10% Neutral Buffered Formalin (cat. HT501128-4L, Sigma Life Science, Poole, UK) for 16-48hrs at room temperature, then transferred to 70% (v/v) ethanol (made up with ≥99.8% Ethanol, absolute; cat. E/0650DF/17, Fisher Scientific) until embedding in paraffin (cat. 36114 4V, VWR Chemicals) within 2-7 days. The system used for embedding the tissues in paraffin is the Tissue-Tek VIP 5 Vaccuum Infiltration Processor (Sakura). The system processes the tissue samples in graded alcohols (70% (v/v), 80% (v/v), 95% (v/v), and 100% (v/v) Ethanol), Xylene, and Paraffin. The tissue samples are held in the processing chamber in solution under pressure. The graded alcohols dehydrate the tissue, the xylene removes the alcohol from the tissue, and the paraffin interpenetrates the tissue. See **Table 2-3** for the processing program used.

Formalin-fixed paraffin-embedded tissues were sectioned using a HM 325 Rotary Microtome (cat. 902100, Thermo-Fisher Scientific) and Low-profile Tissue-Tek Accu-Edge disposable microtome blades (cat. 25608-964, Sakura Finetek, supplied by VWR Chemicals), to cut sections at 3-4μm thick, and placed on Superfrost Plus Micro glass slides (cat. 48311-703, VWR Chemicals). Before carrying on with any chosen staining procedure described below, tissue sections were placed in an oven at 57°C for 30min, to allow sections to fully adhere to the glass slides.

Table 2-3 Processing schedule for paraffin embedding of fixed human tissue. All steps were carried out under vaccuum conditions, while mixing.

Step	Solution	Time (min)	Temperature (°C)
1	70% Ethanol	60	Room Temperature
2	90% Ethanol	60	Room Temperature
3	95% Ethanol	60	Room Temperature
4	100% Ethanol	60	Room Temperature
5	100% Ethanol	60	Room Temperature
6	100% Ethanol	60	Room Temperature
7	Xylene	90	Room Temperature
8	Xylene	90	Room Temperature
9	Paraffin wax	90	60° C
10	Paraffin wax	90	60° C
11	Paraffin wax	60	60° C

2.1.2 Snap-freezing fresh tissue

After thoroughly washing with PBS containing 1% (v/v) antibiotic/ antimycotic (containing 10,000 units penicillin, 10mg streptomycin, and 25µg amphotericin B per mL in 0.9% (w/v) NaCl; cat. P11-002, PAA Laboratories GmbH, Austria), clinical samples were cut into approximately 2-5mm^3 pieces, placed into 2mL cryovials (cat. 430488, Corning Incorporated) and fully immersed for at least 5 seconds in liquid nitrogen. These were then stored at -80°C, and were later homogenized for either protein or RNA extraction (see below).

2.2 Protein assays

2.1.1 Haematoxylin and Eosin (H&E)

The Varistain Gemini ES Slide Stainer (Shandon) was used to carry out the Haematoxylin and Eosin (H&E) stain on paraffin-embedded tissue sections. The slides were submerged in xylene for 2min, then again in xylene twice for 1min. Next the slides are submerged in IMS alcohol (Industrial Methylated Spirit; cat. 302434C, VWR Chemicals) for 2min, and again in alcohol twice for 1min, before washing in tap water for 30sec. The sections are incubated in Mayer's Haematoxylin solution (cat. 72804, Thermo Scientific) for 12min, washed with tap water for 3min, differentiated in 0.3% Acid alcohol (concentrated HCl in 70% Ethanol) for 10sec, and washed again for 3min. Next, the sections are placed in Eosin solution (cat. 10061830, Fisher Scientific) for 2min, and washed in tap water for 90sec. Finally, the slides are dehydrated in alcohol once for 2min and twice for 3min, then cleared in xylene twice for 2min and once for 1min, before mounting coverslips onto the slides with DPX mountant (cat. 360294H, VWR Chemicals).

2.1.2 Herovici's special stain

2.1.2.1 Solutions for Herovici's special stain

Celestine Blue: 50g Iron Alum (Ammonium iron (III) sulphate 12-hydrate; cat. 10021, VWR Chemicals) was stirred into 1000mL cold distilled water until fully

dissolved. 5g Celestine Blue (cat. HD1240, TCS Biosciences Ltd) was added and the mixture boiled for a few minutes. After cooling, the solution was filtered and 140mL Glycerol (cat. 10118, VWR Chemicals) added.

Mayer's Haemalum: 1g Haematein (cat. 34036, VWR Chemicals) was dissolved in 50mL 90% (v/v) Ethanol, with a gentle heat. 1000mL distilled water was added and the solution brought to boil. When the colour deepened, 50g Potassium Alum (Aluminium potassium sulphate 12-hydrate; cat. 10009, VWR Chemicals) was added. The mixture was cooled and filtered before using.

Van Gieson: 100mL Saturated Aqueous Picric Acid (Trinitrophenol; cat. 10192, VWR Chemicals) were mixed with 10mL 1% (w/v) Aqueous Acid Fuchsin (Acid magenta; cat. 34031, VWR Chemicals).
Herovici's stain: 50mL Van Gieson was added to 50mL 0.05% (w/v) Aqueous Methyl Blue (cat. M6900, Sigma-Aldrich, Poole, UK). Once well mixed, 10mL glycerol was added, before adding 0.5mL Saturated Aqueous Lithium Carbonate (cat. 10329, VWR Chemicals).

2.1.2.2 Herovici protocol

Tissue sections were de-waxed by soaking in xylene twice for 3min each, then soaking in IMS alcohol twice for 3min. The sections were rehydrated by soaking in distilled water for at least 5min. Sections were covered with Celestine Blue solution for 2min, the solution was tipped off, then Mayer's Haemalum was added for 2min. Slides were washed in distilled water for 5min, before differentiating in 1% (v/v) Acid Alcohol for a few seconds. After washing in distilled water for a further 5min, sections were covered with Herovici's stain for 2min, briefly rinsed in distilled water, then differentiated in 1% (v/v) Acetic Acid (ethanoic acid; cat. 10498, VWR Chemicals) for 2min. Finally, slides were rinsed in distilled water, dehydrated by rinsing in IMS alcohol, cleared by rinsing in xylene, and mounted with DPX. With this special stain, young collagen (type III) will show up in blue, mature collagen (type I) in red, muscle in yellow, and nuclei blue/ black.

2.2.1 3,3'-Diaminobenzidine (DAB) Immunohistochemistry (IHC)

Tissue sections were de-waxed by soaking in xylene twice for 3min each, then soaking in IMS alcohol twice for 3min. The sections were rehydrated, by soaking in distilled water for at least 5min. For antigen retrieval, the tissue sections were placed in a plastic slide rack and then submerged in the appropriate antigen retrieval buffer (see **Table 2-4**) within a plastic container. The container with the slides was placed in the microwave at 850W for 35min, then removed from the microwave and allowed to cool for 5min. The slide rack was then removed and submerged in tap water for at least 5min. The antigen retrieval conditions and concentrations used for each primary antibody examined here are shown in **Table 2-4.** After antigen retrieval, sections were dabbed dry and the Dako DAB Peroxidase Substrate kit (Vector Laboratories) was used for subsequent steps. Sections were incubated with 3% (v/v) hydrogen peroxide solution for 15min, and washed twice with Dako wash buffer for 3min, before incubating with normal horse serum for 20min. The primary antibody was appropriately diluted in Dako wash buffer (see **Table 2-4**) then added to the tissue sections for 40min, before washing with Dako wash buffer twice for 3min. Anti-mouse and anti-rabbit secondary antibody solution was added for 30min, sections were washed with Dako wash buffer twice for 3min once more, then were incubated in ABC reagent for 30min. Finally, sections were washed with Dako wash buffer twice for 3min, and DAB solution [1 drop DAB solution per 1mL substrate buffer] was added and left for exactly 5min. The sections were washed in tap water for at least 5min before counterstaining using the Varistain Gemini ES Slide Stainer (as in **section 2.2.1**). Slides were submerged in haematoxylin for 2min, washed in tap water for 3min, then differentiated in acid alcohol for 10sec before washing in tap water for 3min. Finally, the stained tissue sections were dehydrated in alcohol once for 2min and twice for 3min, then cleared in xylene twice for 2min and once for 1min, before mounting coverslips onto the slides with DPX.

Table 2-4 List of antibodies used for immunohistochemistry

Protein	1^{ary} antibody supplier (product code)	1^{ary} antibody description	1^{ary} antibody concentration for IHC	Antigen retrieval method for IHC
Ki67	Novocastra (NCL-L-Ki67-MM1)	Mouse monoclonal IgG1	61.2mg/mL used at	pH6, microwave, 35min
α-SMA	Dako (M0851)	Mouse monoclonal IgG2a kappa	Used at 1:100	pH6, microwave, 35min
MMP1	Protein Tech (17873-1-AP)	Rabbit polyclonal IgG	0.5mg/mL used at 1:100	pH6, microwave, 35min
MMP2	Abcam (ab37150)	Rabbit polyclonal IgG	1mg/mL used at 1:100	pH8.1, microwave, 35min
MMP13	Protein Tech (18165-1AP)	Rabbit polyclonal IgG	0.7mg/mL used at 1:100	pH6, microwave, 35min
MMP14	Abcam (ab88618)	Rabbit polyclonal IgG	1mg/mL used at 1:100	pH8.1, microwave, 35min
SPP1	Proteintech (22952-1-AP)	Rabbit polyclonal IgG	0.36mg/mL used at 1:50	pH6, microwave, 10min

2.2.2 Immunofluorescence

For immunofluorescent detection, the same antigen retrieval methods were used for each antibody described in the previous section (see **Table 2-4**), though blocking was carried out for 1hr using 5% (v/v) normal goat serum (cat. 50-197Z, Invitrogen) diluted in PBS. Tissue sections were incubated for 1hr at room temperature with primary antibody diluted as in **Table 2-4** in PBST [PBS containing 0.1% (v/v) Tween (Polyoxyethylene-sorbitan monolaurate; cat. P-1379, Sigma Life Sciences, Poole UK)]. Sections were washed thoroughly, then incubated with Alexa Fluor 568 Goat-anti-Rabbit secondary antibody (cat. A11011, Life Technologies) diluted in the same buffer as for the primary, at a dilution ratio of 1:500, for 1hr at room temperature, in the dark. After washing thoroughly once more, sections were mounted with ProLong Gold antifade reagent containing DAPI (4', 6-diamidino-2-phenylindole; cat. P-36931, Life Technologies).

2.2.3 Protein sample preparation

2.2.3.1 Tissue homogenisation

Two similar methods were used for tissue homogenization, according to the equipment available throughout the duration of this project. In the first one, snap frozen tissue samples of 20-50mg were ground in a stainless steel pestle and mortar, previously cooled on dry ice to ensure the tissue remained frozen and broke up into a powder. The frozen powdered sample was then scraped out into a nuclease-free 1.5mL microfuge tube (cat. AM12400, Ambion), 100µL of lysis RIPA buffer containing protease inhibitors (see **Table 2-5** - contains inhibitors of serine, cysteine and acid proteases, and aminopeptidases in DMSO; cat. P8340-1ML, Sigma-Aldrich, Poole UK) and phosphatase inhibitors (see **Table 2-5** - contains inhibitors of serine, threonine and tyrosine phosphatases; cat. 5870S, Cell Signalling) was added, and kept on ice until the next step.

The alternative method involved using the Tissue Lyser LT (cat. 85600, QIAGEN, Germany). Here, one or two 7mm stainless steel beads (cat. 69990, QIAGEN) were pre-cooled in a 2mL microfuge tube on dry ice, to which 20-50mg of snap frozen

tissue were added. 100µL of RIPA protein lysis buffer containing protease and phosphatase inhibitors as above were added to the tube, before placing in the Tissue Lyser LT and oscillating at a frequency of 50Hz, 3 times for 3min. After each 3min the tubes were inspected for sufficient tissue lysis, and if the mixture began to warm to room temperature, the sample was cooled for 2min on dry ice before oscillating for a further 3min. Once the tissue was sufficiently homogenized, the mixture was carefully removed and placed into a fresh 1.5mL microfuge tube. The tube containing the bead was then washed with a further 50µL of lysis buffer, which was then carefully removed and added to the rest of the mixture. After the first part of mechanical homogenization, an electric pestle (cat. K749510-1500, Fisher Scientific) was used to help lyse the sample further, before continuing with protein extraction.

Table 2-5 Constituents of protease and phosphatase inhibitor mixes, used in protein extraction methods.

Reagent	Groups of enzymes targeted by inhibitors	Inhibitor names (stock concentration)
Protease Inhibitor Cocktail (100x) P8340-1ML, Sigma	Serine proteases (e.g. trypsin, chymotrypsin, and plasmin)	AEBSF (104mM), Aprotinin (80µM), Leupeptin (2mM)
	Aminopeptidases	Bestatin (4mM)
	Cystein proteases	E-64 (1.4mM), Leupeptin (2mM)
	Acid proteases	Pepstatin A (1.5mM)
Phosphatase Inhibitor Cocktail (100x) 5870S, Cell Signalling	Serin/ threonine and acidic phosphatases	Sodium fluoride
	Serin/ threonine phosphatases	Sodium pyrophosphate
		β-glycerophosphate
	Tyrosine and alkaline phosphatases	Sodium orthovanadate

2.2.3.2 Protein extraction from tissues and cells

Homogenised tissue samples were put through 2-3 freeze/ thaw cycles to further break up the fibrous tissue, before overnight incubation at 4°C on rotation (SB3 Rotator, Stuart Equipment, UK). Samples were then centrifuged at 13,000rpm (Heraeus Fresco 17 Microcentrifuge, cat. 75002420, Thermo Scientific, Germany), at 4°C for 10 min, and the supernatant collected. The insoluble pellet was re-suspended in 50µL of RIPA protein lysis buffer containing protease and phosphatase inhibitors as before, then centrifuged again at 13000rpm, 4°C for 10min, before collecting the supernatant. This process was followed a total of three times, and all three supernatants were collated into one sample. During optimization steps, it was found that around 90-95% of the total protein from the fibrous tissue samples is collected within the first three fractions.

For cultured cells, protein extraction was completed when the cells reached close to 70% confluency. The conditioned media was reserved for other assays described below, before thoroughly washing the cells with cold tissue culture-grade PBS (Dulbecco's Phosphate Buffered Saline; cat. D8537, Sigma Life Sciences, Poole, UK). The PBS was aspirated, and then cold RIPA protein lysis buffer, containing protease and phosphatase inhibitors as described above, was added to the cells. For 0.5 x 10^6 cells 100µL of the RIPA protein lysis buffer was used, to ensure as high a final protein concentration as possible. Once the RIPA protein lysis buffer was added, the cells were scraped and collected into a 1.5mL microfuge tube, and stored at -80°C until the next step. Cell lysates were then incubated on ice for 0.5-2hrs, with agitation by vortexing for 10sec every 15-20min, before being spun down at 13,000rpm, at 4°C for 10min. The supernatants were collected, and any remaining pellets discarded.

2.2.3.3 Protein quantification assay

Protein quantification was carried out using the DC Protein Assay Kit II (cat. 500-0112, Bio-Rad, UK). First of all, a 1:5 dilution of each sample was made for the assay. If samples appeared highly concentrated, a 1:10 or 1:20 dilution was used, to ensure the sample concentration values were within the linear range of the

standard curve. Seven dilutions of the protein standard Bovine Serum Albumin (BSA) containing from 0mg/mL to 1.2mg/mL protein, were prepared in the same RIPA protein lysis buffer used for tissue or cell lysis. For the assay, at least duplicates of 5µL of each diluted sample or standard were placed in a clear flat-bottomed 96-well microplate (cat. 353075, Falcon, Fisher Scientific), followed by 25µL of **solution A'**. Solution A' consists of 20µL of **reagent S** (surfactant solution) to every 1mL of **reagent A** (alkaline copper tartrate solution). Finally, 200µL of **reagent B** (dilute Folin reagent) was added per well. The plate was gently shaken, while avoiding the formation of bubbles, and incubated at room temperature for a minimum of 15min, though the reaction is stable for upto 2hrs. Absorbance levels were measured at 750nm using the Synergy HT microplate reader (cat. 12926527, Bio-Tek Instruments, Thermo Fisher Scientific, UK), before estimating the individual protein concentrations.

2.2.4 Western Blotting

Western blotting was used to detect the expression of specific proteins in cell lysates. The isolated protein samples are first denatured, then separated according to size, by sodium-dodecyl sulphate (SDS) gel electrophoresis. The SDS applies a negative charge to positive ions on the proteins, allowing the proteins to be transferred to a nitrocellulose membrane by electrophoresis. Specific proteins can then be detected using a primary antibody, to which a secondary antibody binds. The secondary antibody is coupled to horseradish peroxidase (HRP), which upon the addition of ECL (enhanced chemiluminescent) reagent, a chemical reaction occurs and becomes luminescent. The resulting light emission is finally detected using autoradiography film.

2.2.4.1 Sodium dodecyl sulphate (SDS) – polyacrylamide gel electrophoresis (PAGE)

Protein lysates were diluted with 4x NuPAGE LDS Sample Buffer (cat. NP0008, Invitrogen Life Technologies) containing 10% (v/v) β-mercaptoethanol as a reducing agent, then heated at 95-100°C for 3-5 min. 12-well or 15-well Bis-Tris precast gels (cat. NP0336BOX, Invitrogen Life Technologies) were secured in the

gel electrophoresis tank (XCell SureLock Electrophoresis Mini-Cell; cat. EI0001, Invitrogen Life Technologies), before loading samples into the gels: 8µL of protein ladder (cat. 161-0374, PrecisionPlus Dual Color Protein Standards, BIORAD) and 20µL of each sample (10-20µg per well). NuPAGE 20x MOPS SDS running buffer (cat. NP0001, Invitrogen Life Technologies) was diluted 1:20 with distilled water, and added to the gel electrophoresis tank. Electrophoresis was achieved at a current of 60v, 200mA, 100-200W for 15-20mins, then increased to 200v for a further 45-60min.

2.2.4.2 Protein transfer and immunoblotting

The proteins separated on the gels were then transferred onto nitrocellulose membranes (Hybond-C Extra Nitrocellulose 0.45µm; cat. RPN303E, GE Healthcare Life Sciences), using the Hoefer TE22 Mighty Small transfer tank (cat. TE22, Hoefer, supplied by GE Healthcare Life Sciences), and 1x Transfer Buffer [200mL Methanol + 700mL water + 100mL 10x Transfer Buffer; see **Table 2-6**]. The current was set at 39mA, 400v for 2hrs.

Any background signal on the membranes was then blocked with 5% (w/v) Blocking Buffer [5% (w/v) non-fat dry milk in TBST [Tris-buffered saline (see **Table 2-6**)] containing 0.1% (v/v) Tween], at room temperature for 1hr, under agitation. Primary antibody incubation followed, diluting the antibody at the appropriate concentration in 3% (w/v) Blocking buffer [3% (w/v) non-fat dry milk in TBST; see **Table 2-6**] and incubating at room temperature for 1hr, under agitation. See **Table 2-7** for antibody details. MMPs 2 and 14 show 2 expected product sizes, as the smaller one represents the active form of the proteins, and the larger one represents the inactive form.

The membranes were thoroughly washed with TBST 3 times for 5min, before incubating with the appropriate HRP immunoglobulins diluted in 3% (w/v) Blocking buffer for 1hr, at room temperature, under agitation. For primary antibodies raised in mouse, the Goat-anti-Mouse HRP immunoglobulins (cat. P0447, Dako, Agilent Technologies) was used an appropriate dilution optimized for each assay (see **Table 2-7**); whereas for primary antibodies raised in rabbit,

the Goat-anti-Rabbit HRP immunoglobulins (cat. P0448, Dako, Agilent Technologies) was used (see **Table 2-7**). Finally, the membranes were thoroughly washed 3 times with TBST, and once with TBS before development.

Table 2-6 Constituents of buffers used in Western Blotting

Buffer	Constituents	Amount	Product details	Notes
10x TBS (pH7.6)	Tris-Base	24g	cat. T1503-1KG; Sigma-Aldrich	For 1L TBST: 100mL 10x TBS + 899mL distilled water + 1mL Tween
	NaCl	88g	cat. S7653-1KG; Sigma-Aldrich	
	Distilled water	1000mL	Millipore filtered water	
10x Transfer Buffer	Tris-Base	30.35g	cat. T1503-1KG; Sigma-Aldrich	For 1L 1x Transfer buffer: 100mL 10x Transfer Buffer + 200mL Methanol + 700mL distilled water
	Glycine	144g	cat. G8898-1KG; Sigma-Aldrich	
	Distilled water	1000mL	Millipore filtered water	
Blocking Buffer	Non-fat milk powder	5g (Block) or 3g (Antibody)	Marvel dried skimmed milk; Marvel	5% used for blocking membranes, whereas 3% used for diluting primary and secondary antibodies
	TBST	100mL	1:10 dilution of 10x TBS in distilled water plus 0.1% Tween	
Stripping Buffer (pH6.7)	Tris-Base	5.75g	cat. T1503-1KG; Sigma-Aldrich	Used for stripping membranes of antibody probing, in order to blot for a different protein on the same samples
	SDS	10g	cat. 23500.260; VWR International	
	β-Mercaptoethanol	3.47mL	cat. M-3148; Sigma Life Sciences	
	Distilled water	500mL	Millipore filtered water	

Table 2-7 Primary and secondary antibodies used for Western Blotting.

Protein	1ary antibody supplier (product code)	1ary antibody (dilution used)	2ary antibody (dilution used)	Expected product size
MMP2	Abcam (ab37150)	Rabbit polyclonal IgG (1:1000 dilution)	HRP Rabbit Immunoglobulins; cat. P0448, Dako; (1:30.000)	66/72 kDa
MMP14	Abcam (ab88618)	Rabbit polyclonal IgG (1:1000 dilution)	HRP Rabbit Immunoglobulins; cat. P0448, Dako; (1:10.000)	58/65 kDa
β-Actin (loading control)	Sigma (A2228)	Mouse monoclonal IgG (1:50.000 dilution)	HRP Mouse Immunoglobulins; cat. P0447, Dako; (1:50.000)	42 kDa

2.2.4.3 Image capture and quantification

The western blots were developed using the Amersham ECL Prime Western Blotting reagent (cat. RPN2232, GE Healthcare), containing a luminol solution and a peroxide solution. These two solutions were first brought to room temperature, before mixing an aliquot of the solutions at a 1:1 ratio (taking care not to cross-contaminate the bottles of solution). Each membrane was blotted to remove excess liquid, then placed on a plastic sheet, and roughly 1mL of the mixture was placed per $10cm^2$ membrane, and incubated at room temperature for 5min. The membrane was then enclosed in the plastic sheeting, any excess liquid blotted, and stabilized with some tape inside a 18 x 24cm autoradiography Hypercassette (cat. RPN13642, Amersham, GE Healthcare). Development then continued in a dark room, where a sheet of Amersham Hyperfilm ECL was carefully placed on the membrane and incubated for 5sec to 30min in the dark, depending on the strength of the signal. The films were then developed using the Xograph Film Autoprocessor (Xograph).

The developed films from the western blots were captured on the CanoScan LiDE220 flatbed scanner (Canon). Quantification was achieved using ImageJ 1.49v. The scanned images were first converted to 8-bit gray-scale images, before rectangles of equal size were drawn around each lane of bands to be quantified. Next, the profile plot of all the lanes was created via ImageJ, and a straight line was drawn across the bottom of each peak, so as to remove any background noise from the calculations. The area and size of each peak (representing each band) was then measured automatically, and the relative values of band density plotted in Excel. To take into account any human error at the time of running the SDS-PAGE gel, the values obtained from the protein of interest were corrected with the values obtained from the loading control (β-Actin). Finally, the relative difference in band density was measured between the normal and keloid samples, representing the relative difference in levels of expression for the proteins analysed.

2.3 Nucleic acid assays

2.3.1 RNA extraction from tissue

Before starting any nucleic acid work, all surfaces and pipettes were first cleaned with 70% (v/v) ethanol, then with RNase AWAY solution (cat. 7002, Thermo Scientific), and finally with nuclease-free water, to ensure all nucleases and contaminants had been removed. Tissue homogenization prior to total RNA extraction was carried out in exactly the same way as described in **section 2.2.5.1**. The key difference was the type and volume of lysis buffer used: here, 300-600µL in total of Buffer RLT Plus (from the RNeasy Fibrous Tissue Mini Kit; cat. 74704, QIAGEN) containing 0.01% (v/v) β-Mercaptoethanol (cat. M-3148, Sigma Life Sciences, Poole, UK) was used. As above, an electric pestle was used to help lyse the sample further, before continuing with the method for the RNeasy fibrous tissue kit.

All samples were treated with proteinase K (from the RNeasy Fibrous Tissue Mini Kit) for 10min at 55°C, before centrifuging the samples at ≥10,000rpm for 3min. The supernatant was removed and placed in a fresh microtube, to which an equal volume of 70% (v/v) ethanol was added and thoroughly mixed. The mixture was transferred to the RNeasy spin columns in 700µL aliquots, and centrifuged at ≥10,000rpm for 30sec, while discarding the flow-through each time. At this stage, the RNA in the sample had bound to the column membrane, and so it was washed once by adding 350µL of Buffer RW1 to the column, centrifuging at ≥10,000rpm for 30sec, and discarding the flow-through. Next, 10µL of DNase stock solution mixed with 70µL of Buffer RDD were added to each RNeasy membrane for removal of any DNA contamination, and incubated for 15min at room temperature. The columns were washed with a further 350µL of Buffer RW1, centrifuged at ≥10,000rpm for 30sec, and the flow-through discarded. This was followed by 2 washes with 500µL of Buffer RPE, centrifuging at ≥10,000rpm for 30sec-2min, and discarding the flow-through. The RNeasy columns were then placed in fresh collection tubes, and centrifuged at ≥10,000rpm for a further 1min to ensure all remnants of ethanol and wash buffer constituents had been completely removed from the RNeasy membranes. Finally, the bound RNA was eluted from the

membranes with 20-40µL of nuclease-free water (cat. BP2484-100, Fisher BioReagents, Fisher Scientific). The concentrations were subsequently calculated by measuring absorbance levels at 260nm, using the NanoDrop 1000 spectrophotometer (Thermo Scientific).

In order to ensure the RNA samples were of acceptable purity for use in downstream applications described below, the ratio of absorbance levels at 260nm and 280nm was used to assess the purity of RNA. A 260/280 ratio of approximately 2.0 was considered to be a pure RNA sample, with values near 1.8 considered to be contaminated with DNA, and values lower than ≈1.8 to be potentially contaminated with protein, phenol or other chemical contaminants (NanoDrop, 2012, NanoDrop, 2007).

2.3.2 Real Time quantitative Polymerase Chain Reaction (qPCR) RT² Profiler arrays

Two different RT² Profiler Real Time qPCR arrays were used to examine 5 keloid and 5 normal skin samples (**Tables 2-1 and 2-2**): the Human Extracellular Matrix and Adhesion Molecules (ECM) array (cat. 330231 PAHS-013ZA, QIAGEN); and the Human Signal Transduction Pathway Finder (STP) array (cat. 330231 PAHS-014ZA, QIAGEN). A full description of the genes tested in each array is presented in **Appendices A and B.**

2.3.2.1 Reverse transcription and qPCR run for arrays

The RT² Profiler Real Time qPCR arrays are provided in 96-well plates containing the primer assays for 84 pathway-focused genes, 5 reference genes, 1 gDNA (genomic DNA) control, 3 reverse transcripting (RT) controls, and 3 positive PCR controls. cDNA synthesis by RT was performed using the RT² First Strand kit (cat. 330401, Qiagen). First of all, 1µg RNA was mixed with 2µL of Buffer GE and made up to a total of 10µL with non-DEPC treated nuclease-free water, to eliminate any remaining gDNA. This gDNA mix was incubated at 42°C for 5min, then placed on ice for at least 1min. The reverse transcription mix was made up of 4µL 5x Buffer BC3, 1µL Control P2, 2µL RE3 Reverse Transcriptase Mix, and 3µL of nuclease-free

water per sample. This 10µL reverse transcription mix was combined with the 10µL of gDNA elimination mix, before incubating at 42°C for 15min, and 95°C for 5min to stop the reaction. A further 91µL of nuclease-free water were added to the RT reaction mixture, and thoroughly mixed by pipetting. The cDNA synthesis reactions were kept on ice until proceeding.

For the RT^2 Real Time qPCR arrays, 102µL of cDNA synthesis reaction was mixed with 1350µL of 2x RT^2 SYBR Green Mastermix. This was thoroughly mixed by pipetting, and then 20µL was aliquoted in each well of the array plates. The PCR reaction was performed on the ABI 7500 standard system (Applied Biosystems), with the following thermal profile: 10min at 95°C, and 40 cycles of 30sec at 95°C and 60sec at 60°C. Data was then analysed using the $\Delta\Delta C_T$ method, using the predesigned excel template provided by Qiagen (www.SABiosciences.com/pcrarraydataanalysis.php.)

2.3.2.2 Statistical analysis for qPCR arrays

Calculations were carried out as follows. In each sample, Ct values for each gene were firstly normalized against the average of the 5 reference genes (this gives the ΔCt values). Next, the ΔCt values were converted to the log scale, making the assumption that all assays were close to 100% efficient. This was achieved using the formula $2^{-\Delta Ct}$. For each gene, the average log scale value of the three control samples (AVG_{ctrl}) was calculated, and $\Delta\Delta C_T$ was estimated by dividing the log scale value of each of the 10 samples by the AVG_{ctrl}. The resulting data shows the fold-change in gene expression in each sample, relative to the average of the 5 controls. Fold-change of 1 or over was considered as gene up-regulation, whereas a fold-change of less than 1 was considered as gene down-regulation. For statistical analysis to test whether keloid expression was significantly different to control, a student's t-test was applied ($p<0.05$), with no consecutive correction for multiple comparisons.

2.3.3 Real Time qPCR by relative standard curve method

2.3.3.1 Reverse transcription and qPCR run

Complementary DNA (cDNA) synthesis was achieved using the SuperScript VILO cDNA synthesis kit (cat. 11754-050, Invitrogen Life Technologies). Per reaction, 4µL of 5x VILO Reaction Mix and 2µL 10x SuperScript Enzyme Mix were added to 1-1.5µg of RNA, according to yield of RNA extraction from each batch of samples. The final reaction volume was made up to 20µL with nuclease-free water, and gently mixed by pipetting. The RT reaction was carried out in a thermal cycler (peqSTAR 2X double block thermocycler; cat. PEQL95-07002, VWR), incubating at 25°C for 10min, then 42°C for 60min, and terminated at 85°C for 5min. Synthesised cDNA was diluted 1:30 for use in Real Time qPCR reactions described below.

Forward and reverse primer pairs were designed and tested for specificity in silico using the NCBI Primer-BLAST function (http://www.ncbi.nlm.nih.gov/tools/primer-blast/). Alternatively, the PrimerBank (http://pga.mgh.harvard.edu/primerbank/) was used to select previously tested primer sets. All selected primer oligos were then synthesized by Sigma. In certain cases where primer optimization proved unsuccessful, off-the-shelf QuantiTect primer assays were used (QIAGEN). See **Table 2-8** for oligo sequences and associated melting temperatures optimised for the qPCR reactions.

Table 2-8 Real Time qPCR primer sequences and assay melting temperatures used.

Gene	Sense Primer sequence	Anti-sense Primer sequence	T_m (°C)
BCL2	AGGCTGGGATGCCTTTGTGG	TTTGTTTGGGGCAGGCATGT	64
BMP2	ACTACCAGAAACGAGTGGGAA	GCATCTGTTCTCGGAAAACCT	64
COL1A1	ACTTGCTTGAAGACCCATGC	GGTGTTTGAGCATTGCCTTT	64
EGFR	TGCACCTACGGATGCACTG	CGATGGACGGGATCTTAGGC	64
GATA3	Hs_GATA3_1_SG (QuantiTect Primer Assay)		62
HEY1	CGGCTCTAGGTTCCATGTCC	GCTTAGCAGATCCCTGCTTCT	62
MMP1	GAGCAAACACATCTGAGGTACAGGA	TTGTCCCGATGATCTCCCCTGACA	64
MMP2	Hs_MMP2_1_SG (QuantiTect Primer Assay)		62
MMP3	Hs_MMP3_1_SG (QuantiTect Primer Assay)		62
MMP13	TCCTGATGTGGGTGAATACAATG	GCCATCGTGAAGTCTGGTAAAAT	62
MMP14	CGAGGTGCCCTATGCCTAC	CTCGGCAGAGTCAAAGTGG	62
SFN	GGATCCCACTCTTCTTGCAG	CTGCCACTGTCCAGTTCTCA	64
SORBS1	TGGGCAAGACAAAGACATGGA	AGCACTGGAAGAAAGCCTCC	60
SPARC	ACGGCAAGGTGTGCGAGCTG	TTGGTGCCCTCCAGGGTGCA	64
SPP1	ATCACCTGTGCCATACCAGT	CTTACTTGGAAGGGTCTGTGG	64
TNC	ACAGCCACGACAGAGGC	AGCAGCTTCCCAGAATCCAC	58
VEGFA	Hs_VEGFA_6_SG (QuantiTect Primer Assay)		62
WISP1	CCAGCCTAACTGCAAGTACAA	GGCGTCGTCCTCACATACC	62
HPRT	GAAGAGCTATTGTAATGACC	GCGACCTTGACCATCTTTG	62
B2M	GAGGCTATCCAGCGTACTCCA	CGGCAGGCATACTCATCTTTT	62

The KAPA SYBR FAST qPCR kit (cat. K4602, Kapa Biosystems, supplied by Anachem Ltd) was used for making up the qPCR reaction mixtures. For a total reaction volume of 10µL per well, 9µL were the qPCR master mix, and 1µL the diluted cDNA at approximately 5ng/µL. The qPCR master mix was made up as follows: 5µL of 2x KAPA SYBR FAST qPCR Master Mix Universal, 0.2µL of 50x ROX Low (reference dye), 0.2µL of 10µM Sense Primer, 0.2µL of 10µM Anti-sense Primer, and 3.4µL nuclease-free water. Reactions were performed in triplicate, in 96-well plates (cat. N8010560, Life Technologies), and sealed with MicroAmp Optical Adhesive Films (cat. 4311971, Applied Biosystems). The ABI 7500 standard system (Applied Biosystems) was used for Real Time qPCR analysis. The thermal profile was as follows: 5min at 95°C, 40 cycles of 30sec at 95°C and 60sec at 58-64°C (see **Table 2-8** for individual assay melting temperatures), followed by 1 min at 95°C to end the reaction. A consecutive melting curve was acquired at the end of the PCR, to ensure reaction efficiency and primer specificity. During assay optimization steps, the PCR reactions were carried out on the thermal cycler, and the resulting PCR products run on an agarose gel (see below), to establish assay specificity.

Data was analysed using the Relative Standard Curve method. For this, a reference cDNA synthesized from the Stratagene qPCR Human Reference Total RNA (cat. 750500, Agilent Technologies) was used to create 1:10 serial dilutions for a 4-point standard curve. The standard curves were tested for each of the 18 genes of interest (GOI) and 2 reference genes tested. The GOI Ct values for each sample were normalized against the 2 reference genes (HPRT and B2M), and further normalized against each gene's standard curve. This aimed to take into account varying assay efficiencies more accurately. Finally, values obtained for each keloid sample was compared against the mean value for the combined normal samples. This resulted in gene expression fold-changes being reported, and then adjusted to show a positive or negative value, representing an up- or down-regulation respectively.

All Real Time qPCR samples destined for comparison against one another were processed at the same time. More precisely, their RNA extractions, RT reactions, as

well as the final qPCR reactions were performed simultaneously for each group of samples being examined. Fold-change values of normalized gene expression levels in Keloid *vs* Normal Skin (control) samples from different groups of samples could then be assessed all together.

2.3.3.2 Agarose gel electrophoresis

A 2% (w/v) agarose/ Tris-acetate ethylediamine-tetra-acetic acid (TAE) gel was cast, containing 10µL GelRed (Nucleic Acid Gel Stain 10.000X; cat. 41003, Biotium) per 100mL of agarose gel mixture. GelRed is an environmentally safe nucleic acid dye, used as an alternative to the highly toxic ethidium bromide. It intercalates with DNA, which causes the GELRed to strongly fluoresce when exposed to U.V. (ultra violet) light, allowing the location of DNA molecules to be visualized on the gel. PCR products resulting from assay optimization steps above were loaded on to the gel, mixing 8µL PCR product with 2µL sample loading buffer (5x DNA Loading Buffer Blue; cat. BIO-37045, Bioline, London, UK). The samples were run alongside 10µL DNA ladder (HyperLadder 25bp; cat. BIO-33057, Bioline, London, UK) to estimate product size, and separated by electrophoresis at a current of 120V for 30min. Finally, the PCR products were visualised by U.V. light and the gel photographed using a Multi Image Light Cabinet (Alpha Innotech Corporation, San Leandro, CA, USA).

2.3.3.3 Statistical analysis of Relative Standard Curve method Real Time qPCR data

Calculations were carried out similar to the qPCR arrays, described in **section 2.3.2.2**. The differences were as such: normalization was carried out using the average of 2 reference genes, giving the ΔCt values; and assay efficiencies were calculated based on the standard curves for each assay. Relative differences in ΔCt values for each gene were calculated between the keloid and control group of samples, by dividing the average keloid value by the average control value. For statistical analysis to test whether keloid expression was significantly different to control, a student's t-test was applied ($p<0.05$), with no consecutive correction for multiple comparisons.

2.4 Cell culture methods

All cell culture was performed in a laminar flow hood under aseptic conditions. All sterile disposable culture flasks, plates and dishes, as well as disposable strippettes, were from Nunc (Roskilde, Denmark). All centrifuge steps were carried out using a Centrifuge 5702 (Eppendorf). All fibroblasts were cultured at 37°C in a humidified chamber at 5% CO_2/ 95% atmospheric air, whereas all keratinocytes were cultured at 10% CO_2/ 90% atmospheric air. The difference in CO_2 levels were adjusted dependent on the sodium bicarbonate concentration present in the culture media used, to ensure they buffered to pH7.4. Culture media was changed every 2-3 days in all cases.

2.4.1 3T3 mouse fibroblast feeder layer

NIH/3T3 mouse fibroblast cells (CRL-1658, ATCC, LGC Standards, UK), were cultured and expanded in T175 cm^2, 3-layer or 5-layer polystyrene culture flasks, in Dulbecco's Modified Eagle's Medium (DMEM; cat. 21331-046, Gibco, Life Technologies), supplemented with 10% (v/v) foetal calf serum (FCS; cat. FCS-SA/500-50115, Labtech International), 1% (v/v) penicillin/ streptomycin (with 10000 units penicillin and 10mg streptomycin per mL in 0.9% (w/v) NaCl; cat. P0781-100mL, Sigma Life Science, Poole, UK) and 1% (v/v) L-Glutamine (200mM stock concentration; cat. G2713, Sigma-Aldrich, St Louis, USA). Culture medium was changed every 2-3 days, and the cells were passaged when they became 60-70% confluent, to avoid transformation.

For cell growth arrest, 3T3 cells at no more than 70% confluency were washed with cell-culture grade sterile PBS before incubating in 0.05% (v/v) trypsin/ 0.02% (v/v) versene (1:10 dilution of 10X solution; cat. 59418C-100ML, Sigma-Aldrich, UK) for 2-5 min, at 37°C. Once cells had detached fully, at least an equal volume of DMEM medium was added to the flask (the serum in the medium thereby quenching the enzyme action of trypsin/ versene), the cells were resuspended and transferred to a falcon tube. The cells were then centrifuged at 1000rpm for 5min, the supernatant aspirated off, and the pellet resuspended in fresh pre-warmed DMEM medium. This ensured any remaining trypsin/ versene

solution was fully removed from the cell mixture. 3T3 fibroblasts resuspended at a density of 3-4 x10^6 cells/ mL of DMEM medium were irradiated with 60 Gy. The irradiated 3T3 fibroblasts were counted with a haemocytometer and cryopreserved in aliquots of 2-4x10^6 cells per vial, as described below until required.

2.4.2 Primary keratinocyte isolation and culture

Primary keratinocytes were isolated based on the Rheinwald and Green method (Rheinwald and Green, 1977, Rheinwald and Green, 1975). Tissues were washed at least 3 times with sterile PBS containing 1% (v/v) antibiotic/ antimycotic solution (100X solution of penicillin/ streptomycin/ amphotericin B; cat. 15240-062, Life Technologies). Excess fatty tissue was trimmed off the bottom using a disposable scalpel to avoid interference in the cell extraction procedure, and the tissue was cut into approximately 3-5mm^2 pieces. In fibrotic keloid tissues, the majority of the dermis was initially removed and kept wet in PBS for later fibroblast extraction, and to avoid interference to keratinocyte extraction. The tissue pieces still containing the epidermis were then incubated in a 2.5mg/mL Dispase II (cat. 17105-041, Gibco, Life Technologies) solution diluted with PBS containing 1% (v/v) penicillin/ streptomycin, either overnight at 4°C or for 45–90min at 37°C. The epidermis was consecutively peeled off the dermis, placed in a falcon tube containing 0.25% (v/v) trypsin solution (cat. L11-002, GE Healthcare), and kept at 37°C in a waterbath for 30-60min. Within this 30-60min timeframe, the falcon tube was shaken vigorously every 2-10min, the cloudy solution carefully removed and placed in RM+ Medium (see **Table 2-9**), to quench the trypsin activity. Fresh, pre-warmed 0.25% (v/v) trypsin was added to the remaining epidermis, and the process repeated until no further cells were being released. The cell mixture in serum-containing medium was then spun at 800-1000rpm for 10min, the supernatant carefully removed and discarded, and the cell pellet re-suspended in fresh pre-warmed RM+ culture medium.

Table 2-9 Cell culture media compositions used for keratinocyte culture

SFM (serum-free medium); **DMEM** (Dulbecco's Modified Eagle's Medium); **FCS** (foetal calf serum); **EGF** (epidermal growth factor); **BPE** (bovine pituitary extract); **P/S** (penicillin / streptomycin).

RM+ Medium		**SFM Medium 1**	**SFM Medium 2**	**SFM Medium 3**
1:1 DMEM and F12 (cat. 21331-020, Gibco, Life Technologies)		**KSFM** (cat. 17005-075, Gibco, Life Technologies)	**1:1 mixture of DMEM** (cat. 21068-028) and **Ham's F12** (cat. 21765-029; both Gibco, Life Technologies)	1:1 mixture of SFM Medium 1 and SFM Medium 2
Supplements (final concentrations)	**Product order info**	**Supplements (final concentrations)**	**Supplements (final concentrations)**	**Product order info**
1% (v/v) P/S	cat. 15140122, Life Technologies	1% (v/v) P/S	1% (v/v) P/S	cat. 15140122, Life Technologies
5% (v/v) FCS	cat. FCS-SA/500-50115, Labtech International	EGF 0.2ng/mL	EGF 0.2ng/mL	cat. 10450-013, Life Technologies
1% (w/v) Adenine (100x stock = 0.018M in 0.05M HCl)	cat. A2786-5G, Sigma-Aldrich	BPE 25ng/mL	BPE 25ng/mL	cat. 13028-014, Life Technologies
1% (v/v) RM+ : 1. transferrin 5µg/mL 2. hydrocortisone 0.4µg/mL 3. cholera toxin 10nM 4. insulin 5µg/mL 5. liothyronine 200nM 6. EGF 10ng/mL	1. cat. T2252, Sigma-Aldrich 2. cat. H4881, Sigma-Aldrich 3. cat. C8052, Sigma-Aldrich 4. cat. I5500, Sigma-Aldrich 5. cat. T6397, Sigma-Aldrich 6. cat. EGF-1, Serotec	$CaCl_2$ 0.4mM	$CaCl_2$ 0.4mM	cat. 21115, Sigma-Aldrich
			L-Glutamine 2mM	cat. G7513, Sigma-Aldrich

For cell expansion, 3-4x10^6 (per T75 flask) irradiated 3T3s were first seeded in RM+ DMEM medium (**Table 2-9**) 2-24 hrs before seeding 3x10^6 keratinocytes in the same flask.

For the experiments presented in **Chapter 5**, primary keratinocytes were expanded in RM+ medium on a 3T3 feeder layer, from the initial extraction through to the first 2 or 3 passages, before switching to culturing to serum-free keratinocyte media. This consisted of two different serum-free media with slight differences in composition, to allow for the different growth factor requirements of low and highly confluent cells (**Table 2-9**). For cells of up to 40-50% confluency, "**Medium 1**" was used. Next, "**Medium 2**" was assembled, which was then used to assemble "**Medium 3**" for cells above 50% confluency. **Medium 3** consisted of a 1:1 mixture of Medium 1 and Medium 2.

2.4.2.1 Primary keratinocyte passaging

Once cells reached 60-70% confluency, they were first washed with PBS to remove any remnant serum-containing medium, and any cell debris. For keratinocytes grown on a feeder layer, the fibroblasts were first detached by adding 0.02% (v/v) versene to the culture flask and incubating at 37°C for no longer than 2-3min. The flask was given a sharp tap on the side to loosen the feeder cells, which were carefully aspirated. The remaining keratinocytes were detached by incubating in 0.05% (v/v) trypsin/ 0.02% (v/v) versene for 5min. At least an equal volume of serum-containing cell culture medium was added to the culture flask, the cell mixture well resuspended, then placed in a suitable falcon tube to centrifuge at 800-1000rpm, for 5min at room temperature. The supernatant was aspirated, the cell pellet resuspended in 10mL culture medium, and the cells counted using a haemocytometer. Finally, keratinocytes were expanded as described below, switched to serum-free media for subsequent experiments, or cryopreserved.

To switch keratinocytes to serum-free media, the pellet of detached keratinocytes obtained during the regular procedure for cell passaging was gently resuspended in PBS twice, to remove as much of the serum-containing RM+ medium as possible.

The washed pellet of keratinocytes was then resuspended in Medium 1, centrifuged at 800-1000 rpm to form a pellet again, and finally resuspended in Medium 1 to seed in a culture flask (3-4x10^6 cells per T75 flask). After 1 passage in Medium 1, keratinocytes were detached by adding 0.05% (v/v) trypsin/ 0.02% (v/v) versene, and incubating for 5min as above. The enzyme action was neutralised with Trypsin Neutraliset Solution 1x (cat. R-002-100, Gibco, Life Technologies), and the cell mixture centrifuged at 800-1000rpm to form a pellet. The keratinocytes were either seeded for experiments, or cryopreserved.

2.4.3 Primary fibroblast isolation and culture

The remaining dermis from the primary keratinocyte isolation procedure was scraped and roughly sliced into 3-5mm^2 pieces, before incubating in 0.5-0.75mg/mL Collagenase D solution (activity at 0.180 U/mg lyophilized enzyme; cat. 11088866001, Roche Diagnostics, Germany) diluted in serum-free DMEM cell culture medium (1% (v/v) penicillin/ streptomycin, 1% (v/v) L-Glutamine), overnight at 37°C. The falcon tubes containing the dissociated fibroblasts were then shaken vigorously for 3-5min before filtering through a 100µm pored cell strainer, into serum-containing DMEM cell culture medium (10% (v/v) FCS, 1% (v/v) penicillin/ streptomycin, 1% (v/v) L-Glutamine), thereby quenching any enzyme activity. Cells were spun at 1000rpm for 10 min before seeding at a density of 25.000-30.000 cells/cm^2

2.4.3.1 Primary fibroblast cell passaging

Once cells had reached 70% confluency, they were first washed with PBS to remove any remnant serum-containing media, plus any cell debris. The fibroblasts were then incubated for 2-5 min in 0.05% (v/v) trypsin/ 0.02% (v/v) versene, until they had all detached. At least an equal volume of serum-containing cell culture media was added to the culture flask, the cell mixture well resuspended then placed in a suitable falcon tube to centrifuge at 1000rpm, for 5min at room temperature. The supernatant was aspirated, the cell pellet resuspended in 10mL culture medium, and the cells counted using a haemocytometer. Finally, fibroblasts

were seeded into appropriate culture flasks for experiments, expanded at roughly 20% of their original density, or cryopreserved.

2.4.4 Cryopreservation of cultured cells

When cells reached 70% confluency, and were destined for cryopreservation, they were washed and detached from the culture flasks as described in the cell passaging sections above. Once the cells had been counted and their total yield estimated, the cell pellet was resuspended in freezing medium [10% (v/v) diethyl sulphoxide (DMSO; Fisher, Leicestershire, UK), 90% (v/v) FCS], to a concentration of 2 or $4x10^6$ cells/mL. DMSO was included in the freezing medium to prevent the formation of crystals during the freezing process that would otherwise lyse the cells. The cell suspension was transferred in 1mL aliquots to cryovials and frozen slowly at -80°C. After at least 2 days, the cell vials were transferred and stored long term in liquid nitrogen (-170°C).

2.4.5 Cell growth rate estimation

2.4.5.1 Alamar Blue assay

Both isolated fibroblast and keratinocyte populations from passages 3 or 4 were seeded in triplicates in 6-well plates in their respective media, for growth rate evaluation by the Alamar Blue assay. After 16-24h, allowing cells to attach, Alamar Blue (AbD Serotec) was added to the cultured cells at a 1:10 ratio, and incubated at 37°C, in the dark for 2-3 hours. Aliquots were then taken from all samples and fluorimetric analysis at an excitation emission spectra of 560/590 nm was carried out. Metabolism of Alamar Blue was measured as arbitrary units (A.U.). Measurements were taken at days 1, 3, 5 and 7, with the day 0 values subtracted from the data, as normalization. Keloid cells were compared against their normal counterparts.

2.4.5.2 Population doubling

An additional, more exact method of measuring cell growth rate was to estimate population doubling rates. For both fibroblast and keratinocyte cultures, cumulative cell population doubling levels were plotted against time. Calculations began at passage 2 or 3, and at each passage for four passages, a total number of viable cells were counted using a haemocytometer. The exact same number of cells were reseeded at every passage, and performed at exactly the same time interval, when cells reached 60-70% confluence. Keratinocytes were passaged every 5 days, whereas fibroblasts were passaged every 4 days. Population doubling level (PDL) of the cell population was calculated using the following formula:

$$PDL = \frac{\log_{10}(\text{total cell count obtained}) - \log_{10}(\text{total cell count re-seeded})}{\log_{10}(2)}$$

3 Characterisation of normal skin and keloid scars

3.1 Introduction

3.1.1 Keloid scar tissue characterisation

There are well-established morphological differences between keloids, hypertrophic scars, normal scars and normal skin. Their structures and how they link to function have been investigated for decades, yet there is still confusion in the field about the defining characteristics of keloid scarring. A recent comprehensive review by Jumper et al on the histopathology of keloid scarring brings to light the main common features and unresolved hypotheses that have been reported to date (Jumper et al., 2015).

One useful technique used for investigating the scar tissue morphology is the Herovici polychrome stain. This technique was first developed in 1963 (Herovici, 1963, Syed et al., 2011), which selectively stains the nuclei dark blue/ black, and the connective tissues both red/pink and blue. It was later confirmed that the blue fibres were made up of newly synthesised collagen fibres, and the red/pink fibres were made up of mature dense collagen fibres (Lillie et al., 1980, Levame and Meyer, 1987). In fact Levame et al suggested that the blue fibres correlated with collagen type III immunostaining, and the red/pink fibres correlated with collagen type I immunostaining (Levame and Meyer, 1987). This polychrome stain has previously been used to examine the ratio of collagen type I and III secretion in wound healing (Sebastian et al., 2011), mature burn scars (Rawlins et al., 2006), and keloids (Syed et al., 2011). In relation to the Herovici analyses presented in the current chapter, the red/pink and blue stains will be interpreted more broadly, referring to the collagen fibre thickness and maturity, rather than typesetting into collagens I or III.

As described in Chapter 1, during the proliferative phase of wound healing (the development of granulation tissue) there is increased angiogenesis, allowing increased proliferation of fibroblasts (Darby and Hewitson, 2007). At this stage, fibroblasts are activated and begin to express large stress fibres, which are not normally seen in quiescent fibroblasts, as well as microfilament bundles (Darby

and Hewitson, 2007). The activated fibroblasts become much more contractile, then synthesise and deposit matrix molecules in the ECM, thereby playing a major role in granulation tissue maturation (Hinz, 2007, Hinz and Gabbiani, 2003). Once the activated fibroblasts are fully differentiated, they begin to express the cytoskeletal protein α-SMA (alpha-Smooth Muscle Actin), which is now a recognized marker for the myofibroblast phenotype (Darby et al., 1990, Sandbo and Dulin, 2011, Darby and Hewitson, 2007, Skalli et al., 1986, Darby et al., 2014). It has been well described that myofibroblasts appear for a short time in granulation tissue during wound healing (Darby et al., 1990, Darby and Hewitson, 2007, Eddy et al., 1988). In fibrotic conditions however, myofibroblast expression is known to persist, leading to excessive matrix deposition and increased tissue contraction. For this reason, an increased myofibroblast expression has been linked to pathological fibrosis, including hypertrophic and keloid scarring (Skalli et al., 1989, Baur et al., 1975, Darby and Hewitson, 2007, Shih et al., 2010a).

α-SMA, as the name suggests, is expressed in vascular smooth muscle cells, which are found within the walls of larger blood vessels such as the aorta, as well as small arteries, arterioles and veins (Gabbiani et al., 1981). Small blood vessels are often found in the deep dermal layers of skin, where they aid in transporting nutrients to the skin appendages (Darby and Hewitson, 2007). In an event of infection or injury, capillaries also enable the transportation of white blood cells to the site of inflammation. For extensive tissue vascularisation analyses, more robust endothelial markers such as CD31 (Kurokawa et al., 2010, Connolly et al., 2014) have previously been used in keloid and scar characterisation studies. However, as angiogenesis was not the main focus of the research in this chapter, it was deemed acceptable to comment on general differences between normal skin and keloid regions, using α-SMA alone. Added to this, α-SMA had the advantage of a dual functionality, being able to detect both blood vessel walls and myofibroblasts simultaneously.

3.1.2 Extracellular matrix regulation

As fully described in Chapter 1, the deregulated balance in ECM production and degradation is key to keloid scarring. When a normal wound enters the later stages of repair, enzymes such as collagenases, gelatinases, and elastases ensure initial ECM structures are digested and replenished with more stable versions, until the injury has been reconstituted to its original state (O'Kane and Ferguson, 1997, Shih et al., 2010a). The major enzymes in this delicately balanced process include the matrix metalloproteinases (MMPs), plasminogen activator (PA)-plasmin, and a disintegrin and metalloproteases (ADAMs) (Shih et al., 2010a). PA converts plasminogen into plasmin, which consecutively breaks down fibrin (Toriseva and Kahari, 2009), and activates procollagenases to breakdown collagen (Tuan and Nichter, 1998). It is at this stage where young collagen type III is replaced by more mature, collagen type I to a ratio (type I/III) of approximately 6 in normal scars (Shih et al., 2010a). This is in contrast to keloid scars where the collagen type I/III ratio is close to 17 (Friedman et al., 1993, Shih et al., 2010a). It has not been concluded whether this effect is due to the lack of collagenase activity (particularly for type III), or an increased production of both collagen types (Niessen et al., 1999, Abergel et al., 1985, Shih et al., 2010a). It is likely that both the lack of collagenase activity and increased collagen synthesis contribute to the problem.

A number of proteases in the MMP family, including MMPs 1, 2, 3, 9, and 13, have been reported as overregulated in keloids at the protein level, but with conflicting results at the gene level. These MMPs are thought to contribute to scar tissue expansion beyond the injury site, as is characteristic of keloids (Leake et al., 2003, Oriente et al., 2000, Neely et al., 1999). One report in keloids showed MMP2 levels to be increased, though MMP9 levels to be decreased (Neely et al., 1999). Contradictory reports on MMP and TIMP expressions perhaps reflect the variable conditions and types of controls used across different studies. When testing serum from keloid patients and healthy individuals, there was no significant difference in expression of MMPs 1, 2 and 9, and TIMP1 and 2 (Ulrich et al., 2010). However, cultured fibroblasts from keloid patients and control healthy individuals showed an increased expression of all these proteins in the keloid cells (Ulrich et al., 2010, Fujiwara et al., 2005a). MMP13 was shown to be increased in keloid-derived

fibroblasts, which along with MMP1, was down-regulated upon treatment with decorin (Li et al., 2013). Other reports demonstrated MMP2 to be down-regulated in keloid-derived fibroblasts (Uchida et al., 2003). MMP14, also known as membrane tethered 1-MMP (MT1-MMP), has had little attention in the fibrotic scarring field, though it is considered as one of the important regulators of matrix re-modelling in the normal healing process (Imaizumi et al., 2009, Gillard et al., 2004, Parks, 1999). Imaizumi et al (2009) indicated that in keloid fibroblasts, MMP2 activity is promoted in collagen bundles, with the cooperation of MMP14 and TIMP2 (Seifert et al., 2008, Imaizumi et al., 2009). Despite all this, the imbalanced ECM production and degradation machinery is still poorly understood, and the mechanisms of action of seemingly crucial factors are unclear to date.

3.1.3 Aims

The primary aim of the work presented in this chapter was to characterise a range of normal skin and keloid specimens to be used in the following chapters. Overall tissue morphology of each normal skin and keloid will be explored, using routine H&E staining and herovici polychrome staining. Immunostaining for Ki67 and α-SMA were used to investigate cell proliferation and fibrogenesis in keloid scars, compared to normal skin. Following this, protein expression patterns for MMPs 1, 13, 2, and 14 were examined in the normal and keloid specimens by immunohistochemistry, to evaluate the potential imbalance in ECM production and degradation, characteristic of keloids.

3.2 Results

3.2.1 Human keloid scar tissue collection

Throughout the course of the research presented in this thesis, a total of 70 keloid scars were collected from both male and female patients, with a range of ages, ethnic origins, body locations, and types of surgical excision. Biopsies from each keloid were snap-frozen and stored at -80°C for nucleic acid or protein analysis, as well as fixed and processed into paraffin embedded blocks for immunohistochemical methods. Wherever possible, keratinocytes and fibroblasts were also extracted from the keloids and the resulting primary cultures stored in liquid nitrogen. A similar approach was taken with a total of 29 normal skin samples, which were collected for use as healthy controls. Only a small number of the collected keloid scars are presented in this thesis, as I aimed to focus on two common characteristics within the group of keloids: they are all inclusive of extralesional (adjacent normal) tissue; and the majority are from African-Caribbean patients. Where possible, the same keloid and healthy control tissues were used for all the analyses presented in this and the following chapters, to minimize the effects of inter-patient variability as much as possible.

3.2.2 Normal healthy skin characterisation

A total of 9 healthy donor skin specimens were used for characterisation. Of these, 8 were female and 1 male; 4 of the female samples were of Caucasian origin and the rest were of African-Caribbean origin patients (see **Tables 2-1** and **2-2** in Chapter 2) for full patient details). It is deemed unethical to resect unaffected normal skin from keloid patients, as this will knowingly cause a new keloid to form. Therefore control tissue cannot be completely matched to each keloid patient, and must be retrieved from unrelated healthy individuals. As this disorder is highly correlated to the ethnicity of individuals (see **section 1.4** in Chapter 1), it was of interest to use African-Caribbean control tissues, as the majority of keloids being analysed were from African-Caribbean patients. As the majority of published keloid research to date has used Caucasian control skin, regardless of the keloid patient ethnicity, it was also of interest to include a number of Caucasian control

samples in this thesis, so as to be able to compare the data with previously published research. Where possible, body location matches were made between keloid and control tissues, as it has been shown that fibroblasts can behave differently depending on which part of the body they originate from (Chipev and Simon, 2002).

3.2.2.1 Normal skin tissue structure

The overall structure and collagen make-up of the dermal compartment for each healthy skin specimen was evaluated through H&E and Herovici staining. In all patients, the epidermal thickness was uniform throughout the length of each sample, with no apparent differences between Caucasian and African-Caribbean individuals. Three representative patients are presented below, which show the variability seen within the group of control tissues used (n=9). The epidermis of facelift skin (**Figures 3-1**) had the least undulating appearance, with breast skin (**Figures 3-3**) showing more ridges, and abdominal skin (**Figure 3-5**) showing the most undulation. Almost all normal skin samples contained skin appendages such as hair follicles, sweat glands and sebaceous glands.

Herovici staining allowed for visualization of young and mature types of collagen, coloured blue and pink, respectively. In all normal skin samples, the collagen fibres appear finer and more tightly packed in the papillary dermis, whereas they are slightly thicker in the reticular dermis. The thicker mature fibres in the deep dermal layers are characteristically loosely organised in no particular orientation. This holds true for all healthy normal skin specimens analysed (**Figures 3-1, 3-3, and 3-5)**.

3.2.2.2 Ki67 cell proliferation marker in normal skin

All normal skin samples showed a similar level of Ki67 nuclear expression in the basal epidermal keratinocytes, with no expression in the suprabasal layers of the epidermis (**Figures 3-2, 3-4, and 3-6**). Patient 22 was the exception, showing almost no proliferative cells in the epidermis (**Figure 3-6**). Note that Ki67 expression is restricted to the cell nuclei, and any diffuse brown chromogen

observed in the basal epidermal cell layer of certain patients is due to melanin pigmentation contained within melanocytes. Cell proliferation was observed at a higher rate in skin appendages such as hair follicles. Additionally, patients 4 and 21 (**Figures 3-2** and **3-4** respectively) showed a very small number of proliferative cells within the dermis.

3.2.2.3 α-SMA expression in normal skin

In the normal skin specimens analysed here, α-SMA expression was observed mainly in small blood vessels in all dermal layers (**Figures 3-2, 3-4,** and **3-6**). This included larger vessels found in the lower reticular dermis near the subcutaneous fat layer, as well as very small capillaries surrounding hair follicle bulbs and sweat glands, and even in between the epidermal ridges in the papillary dermis. There was no evidence of myofibroblasts present in the dermis.

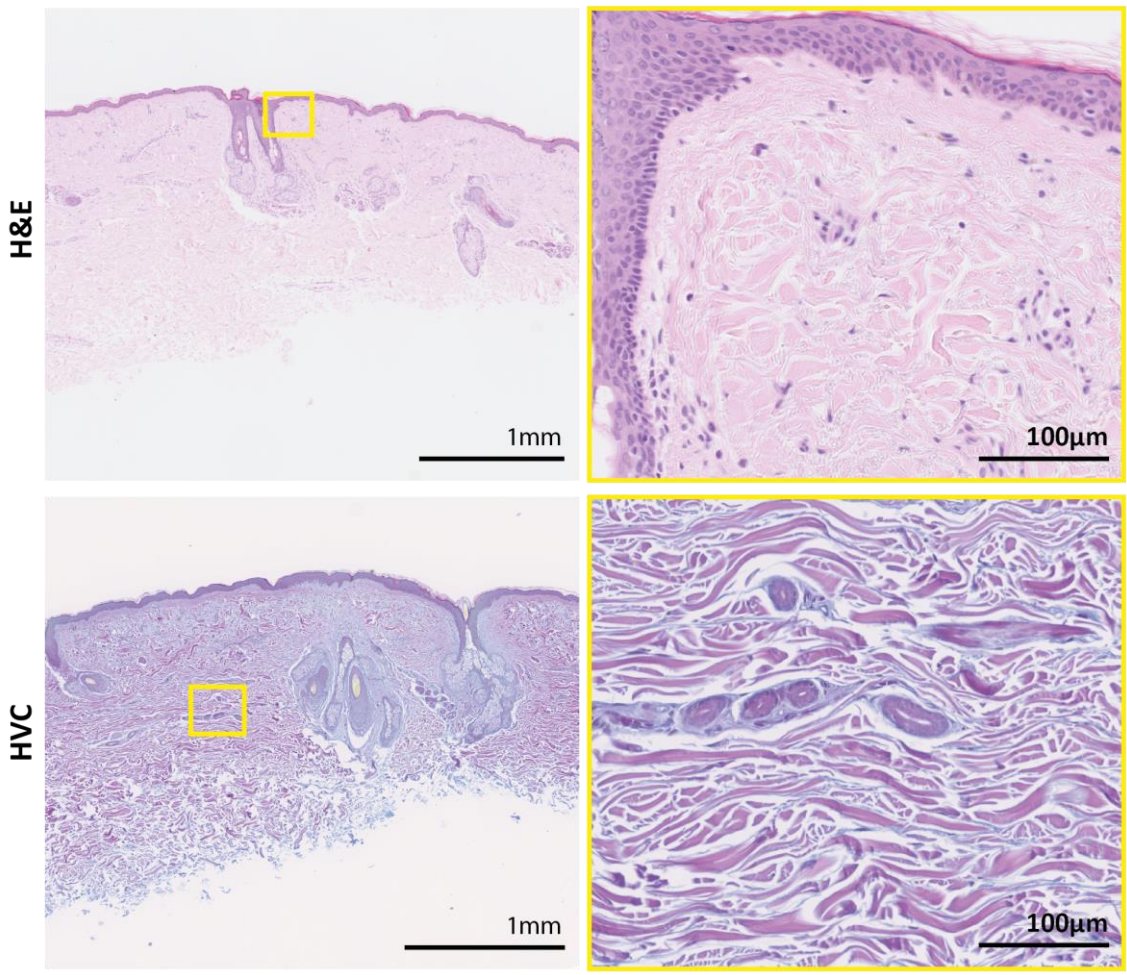

Figure 3-1 H&E and Herovici staining of normal skin from patient 4.

Skin from a facelift of an over 40-year old Caucasian female patient. The top two panels show a H&E stain, whereas the lower two panels show a herovici (HVC) stain. There is a mixture of loosely organised young and mature collagen fibres in the whole dermis. [**In pink** = Mature Collagen fibres; **In blue** = Young Collagen fibres]. Images are representative of **n=9** normal skin biopsies investigated.

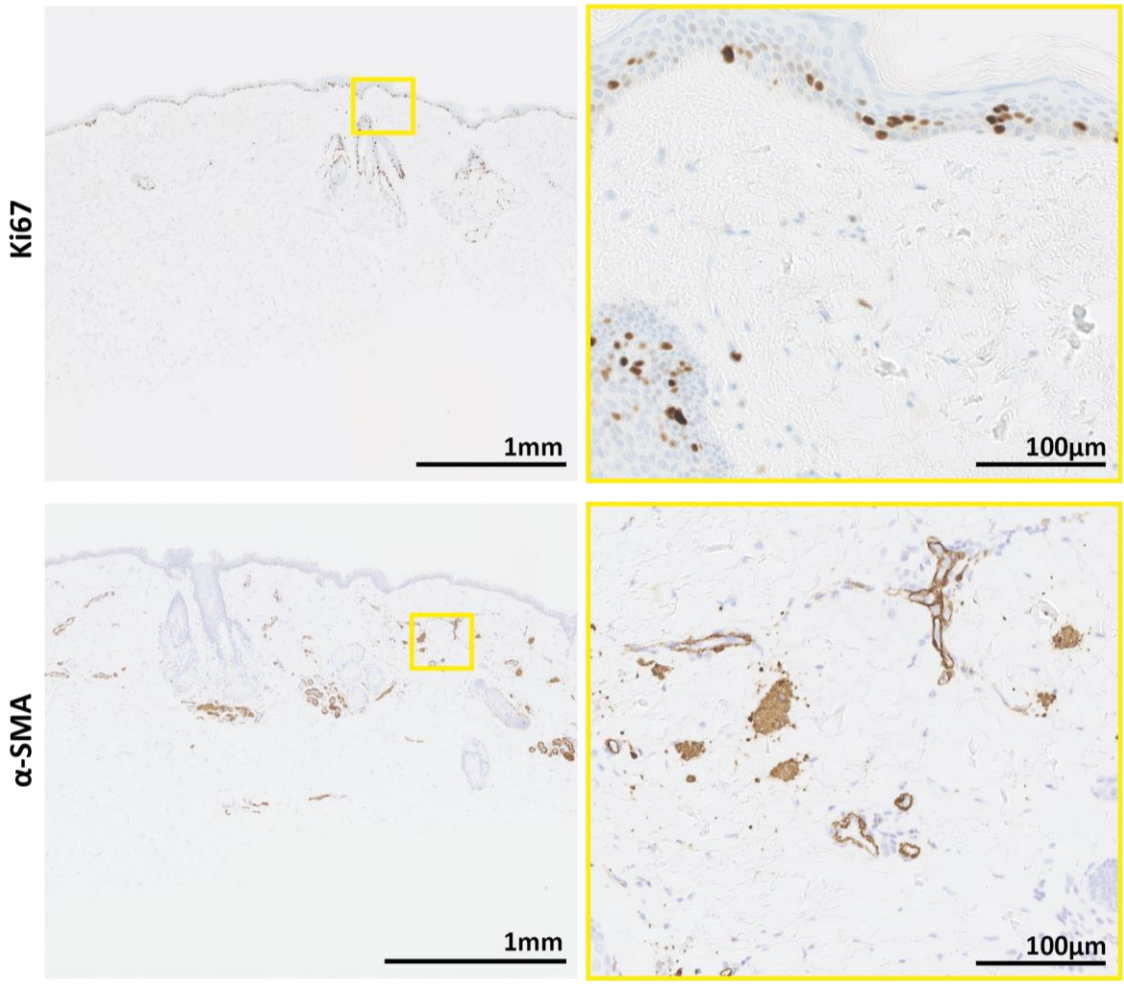

Figure 3-2 Ki67 and α-SMA protein expression in normal skin patient 4

DAB-Immunohistochemistry of patient 4 normal skin. Cell proliferation marker **Ki67** (top two panels) showed strong nuclear expression in cells within skin appendages such as hair follicles, and in the basal layer of the epidermis. **α-SMA** (α-Smooth Muscle Actin) expression was observed solely in the dermis, though was restricted to blood vessel walls. Images are representative of **n=9** normal skin biopsies investigated.

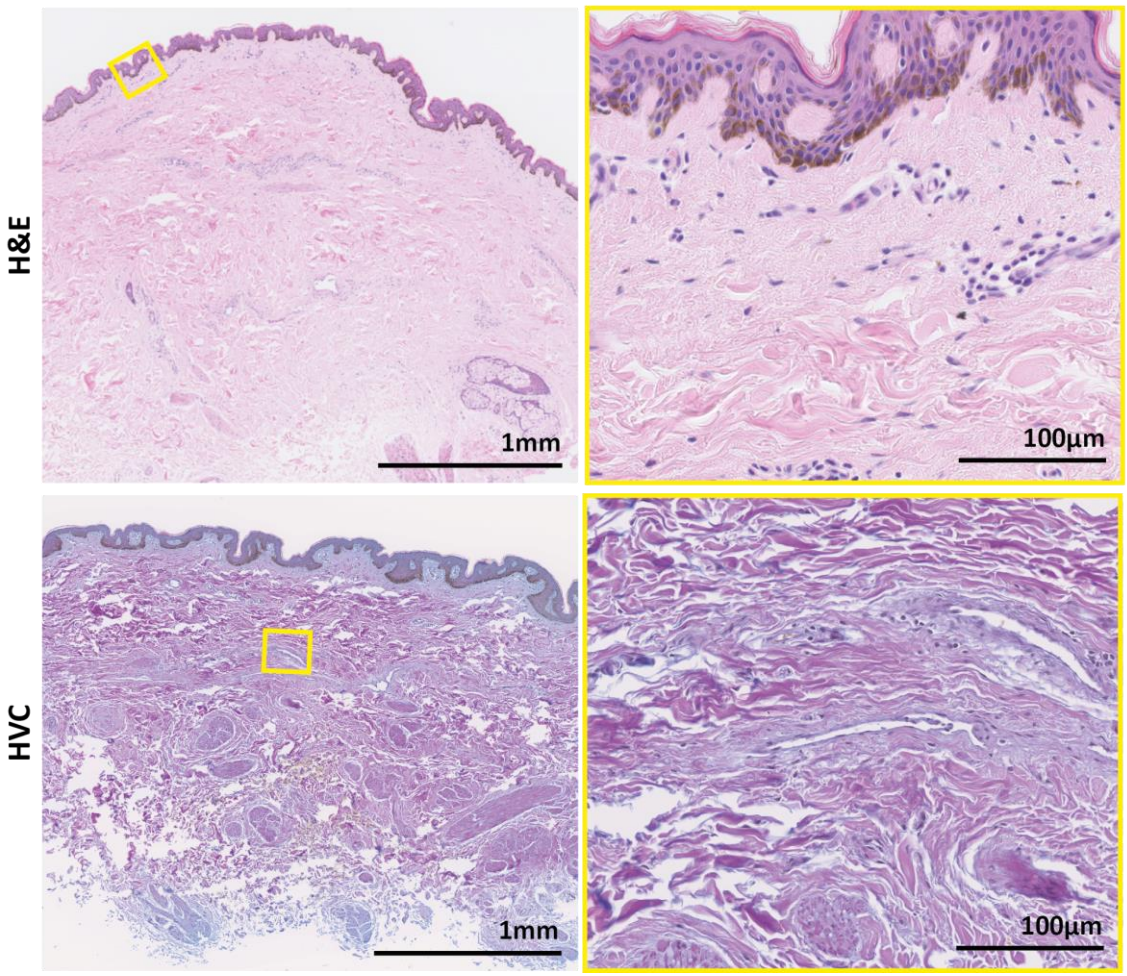

Figure 3-3 H&E and Herovici stain for normal skin patient 21

From the breast of an African-Caribbean female patient. The increased levels of melanin pigment in this patient can be seen as a diffuse brown colour in the basal epidermis. The top two panels show a H&E stain, whereas the two bottom panels show a herovici (HVC) stain. All collagen fibres in the dermis are loosely organised and randomly oriented. Mature collagen fibres are predominant here. [**In pink** = Mature Collagen fibres; **In blue** = Young Collagen fibres]. Images are representative of **n=9** normal skin biopsies investigated.

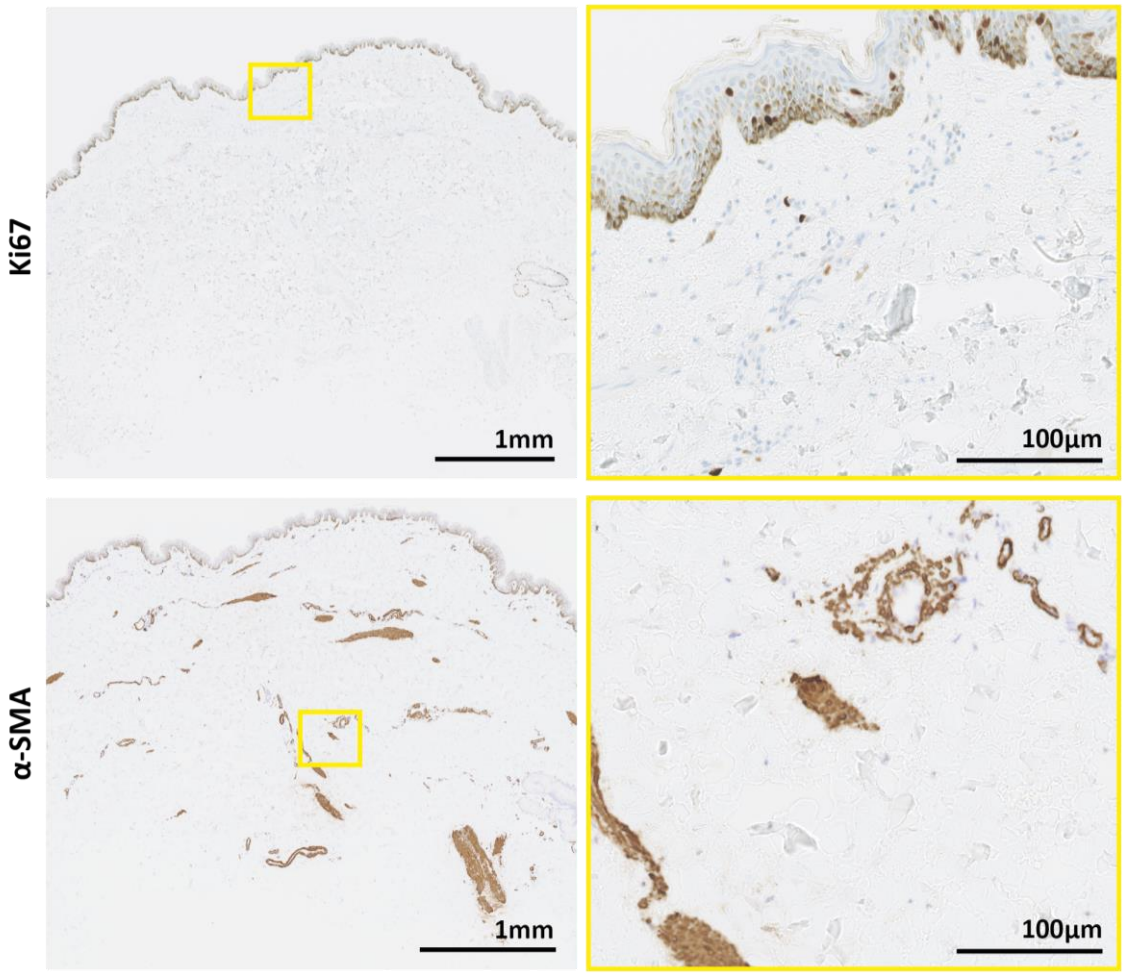

Figure 3-4 Ki67 and α-SMA protein expression in normal skin patient 21.

DAB-Immunohistochemistry of patient 21 normal skin. Cell proliferation marker **Ki67** showed clear nuclear expression in a small number of basal keratinocytes, as well as a small number of dermal cells. **α-SMA** (α-Smooth Muscle Actin) expression showed mainly the presence of small blood vessels, although there was a small number of cells in the dermis indicating myofibroblasts. In both cases, the diffuse brown shading in the basal layer of the epidermis is the melanin pigment. Images are representative of **n=9** normal skin biopsies investigated.

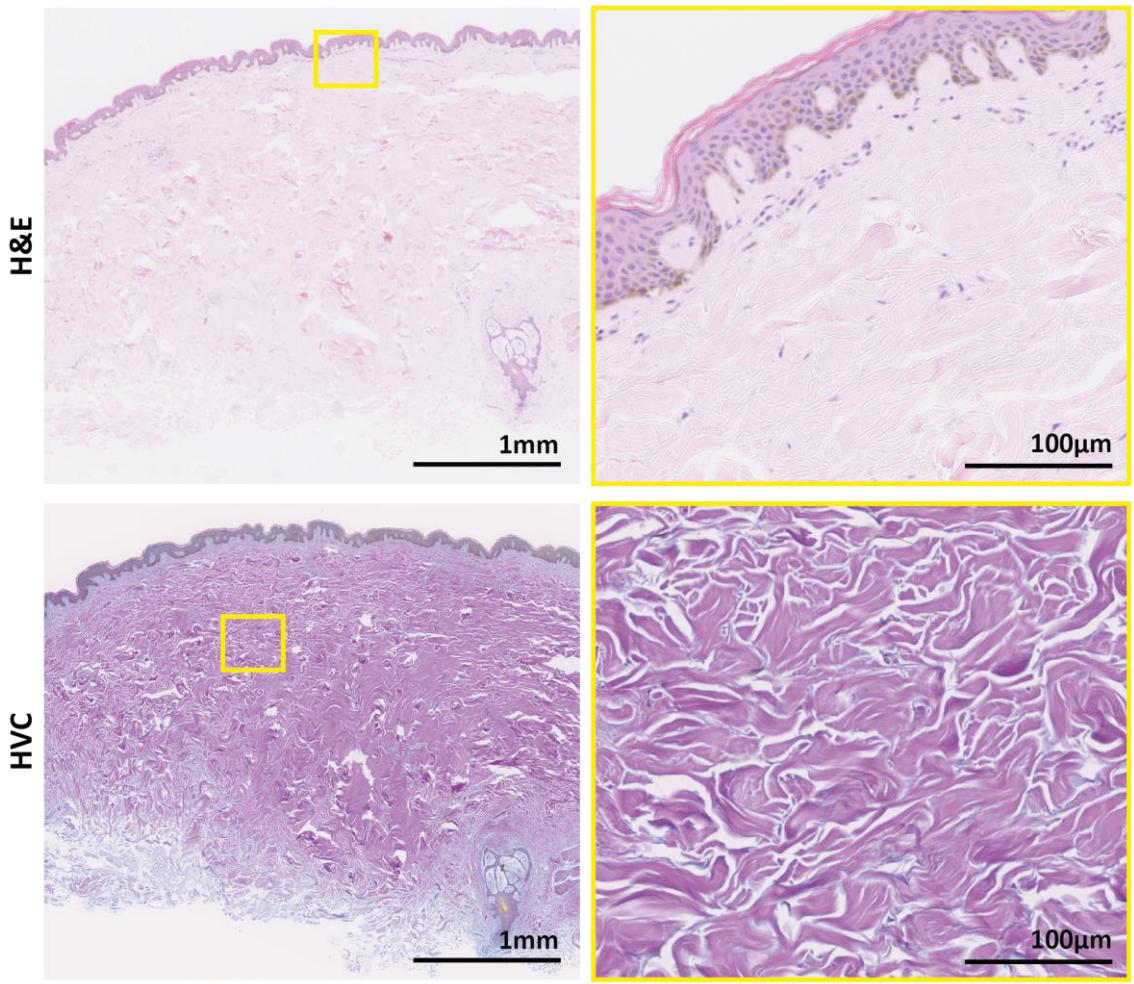

Figure 3-5 H&E and Herovici staining for normal skin patient 22

From the abdomen of an African-Caribbean female patient. Slightly increased levels of melanin pigment can be seen here as a diffuse brown colour in the basal epidermis. The top two panels show a H&E stain, whereas the two bottom panels show a herovici (HVC) stain. All collagen fibres in the dermis are loosely organised and randomly oriented. Mature collagen fibres are predominant here. [**In pink** = Mature Collagen fibres; **In blue** = Young Collagen fibres]. Images are representative of **n=9** normal skin biopsies investigated.

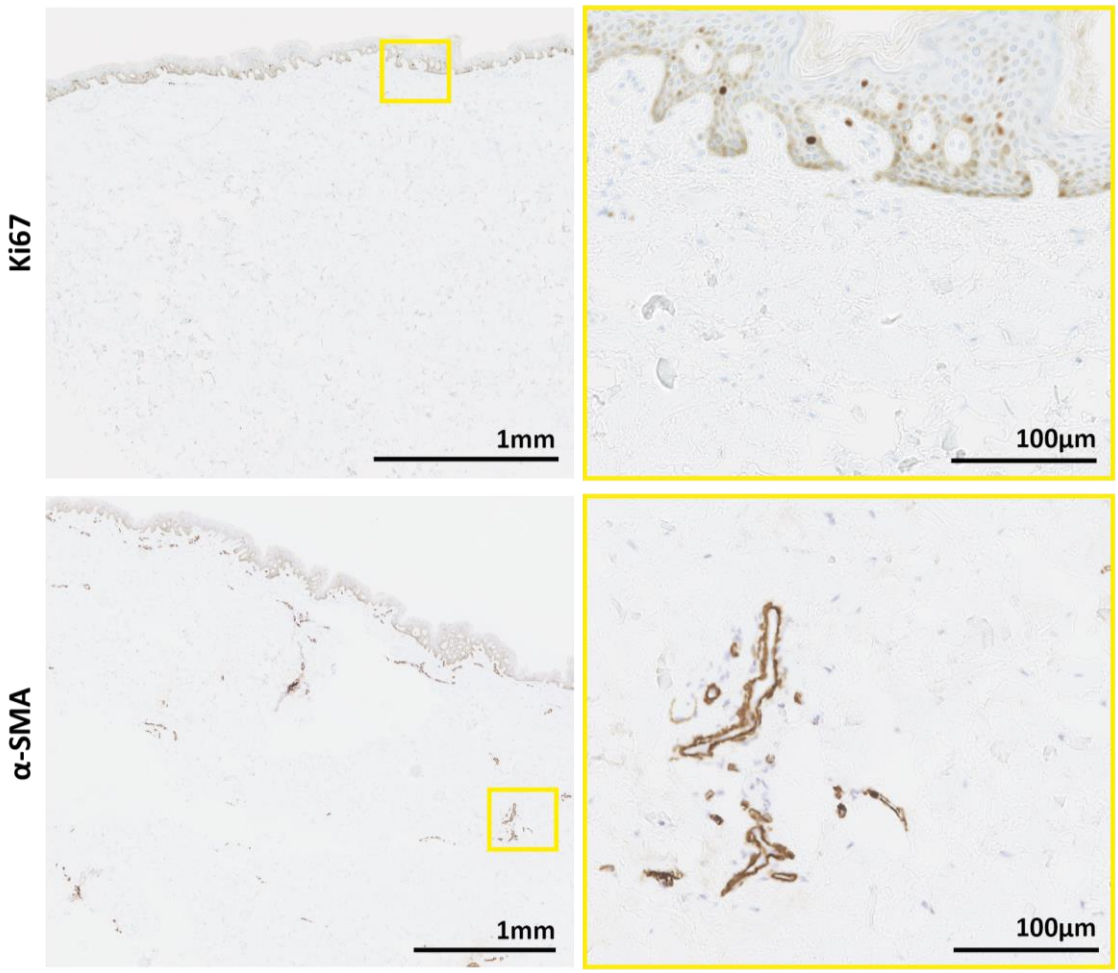

Figure 3-6 Ki67 and α-SMA protein expression in normal skin patient 22.

DAB-Immunohistochemistry of patient 22 normal skin. Cell proliferation marker **Ki67** showed clear nuclear expression in very few basal keratinocytes. The diffuse brown shading in the basal layer of the epidermis is the melanin pigment. **α-SMA** (α-Smooth Muscle Actin) expression revealed no myofibroblasts. Images are representative of **n=9** normal skin biopsies investigated.

3.2.3 Normal, hypertrophic and keloid scars

A total of 10 keloid scar specimens were used for characterisation, alongside one normal scar and one hypertrophic scar added for comparison. Of the keloids, 6 were male, 3 were female and 1 was of unknown gender. There was one male and one female keloid from Caucasian individuals, one male of Asian origin, and the rest of the keloid scars were of African-Caribbean origin. The normal scar was from a female African-Caribbean patient, and the hypertrophic scar is of unknown gender and ethnicity, though it is likely to be Caucasian based on the lack of basal epidermal melanin observed in the H&E stain (**Figure 3-9)**. These keloid scars were selected as they had been excised inclusive of extralesional material, enabling the analysis of the developing keloid into the surrounding normal tissue, as well as the central fibrotic scar. For this reason there is a range of body locations used, including abdomen, breast, neck, ear, and sternum. As mentioned above in **section 3.2.2**, healthy control tissue was matched with the keloid tissue where possible, but only breast and abdomen normal tissue was available as matches.

3.2.3.1 Normal and hypertrophic scar tissue structure

The overall structure of the normal scar (**Figure 3-7**) appeared in part similar to normal skin, in that the epidermis was of similar thickness to normal skin epidermis, and was uniform across the tissue. The dermis however was much deeper than in normal skin, and any hair follicles or sebaceous glands present were restricted to the margins of the scar. Herovici staining of young and mature collagen fibres, showed that the normal scar tissue contained mostly mature collagen fibres. These were slightly thickened in areas, and slightly more densely organised than in normal skin, however they were still randomly oriented, as in normal skin (**Figure 3-7**).

The hypertrophic scar epidermis was thickened and presented distinct ridges and protrusions in to the underlying dermis (**Figure 3-9**), as compared to both normal skin and normal scar tissue. The dermis was hugely thickened compared to both normal skin and normal scar tissue, and showed varying levels of cellular density within the ECM. Herovici staining revealed regions of thickened mature collagen

fibres and nodules in the papillary dermis, with a high density of young collagen fibres in the majority of the reticular dermis. These collagen fibres in the deep dermis were wavy, and highly organised in parallel to the overlying epidermis. In both normal and hypertrophic scar specimens, there were no skin appendages visible (**Figure 3-9**).

3.2.3.2 Ki67 expression in normal and hypertrophic scar tissue

Cell proliferation was minimal in the normal scar sample, with hardly any Ki67 expression in the basal keratinocytes, no expression in the suprabasal epidermal layers, and no expression visible in the dermis (**Figure 3-8**). The hypertrophic scar specimen on the other hand showed an increased level of cell proliferation in the basal layer of the epidermis (**Figure 3-10**), as compared to either normal scar tissue or healthy control skin. There was also some Ki67 expression in the upper dermal layers of the hypertrophic scar, which appeared to be increased, compared to normal skin. These observations are of course limited, due to the single sample analysed for both normal scar and hypertrophic scar tissues. For this reason,

3.2.3.3 α-SMA expression in normal and hypertrophic scar tissue

In the normal scar tissue, α-SMA expression revealed a very small number of dermal cells expressing α-SMA, showing evidence of a small population of myofibroblasts (**Figure 3-8**). The hypertrophic scar tissue (**Figure 3-10**) showed a highly increased level of α-SMA expression in the reticular dermal cells, suggesting increased myofibroblast activation. This pattern of myofibroblast expression correlated with the expression patterns of young collagen fibres identified in section 3.2.3.1 (**Figure 3-9**).

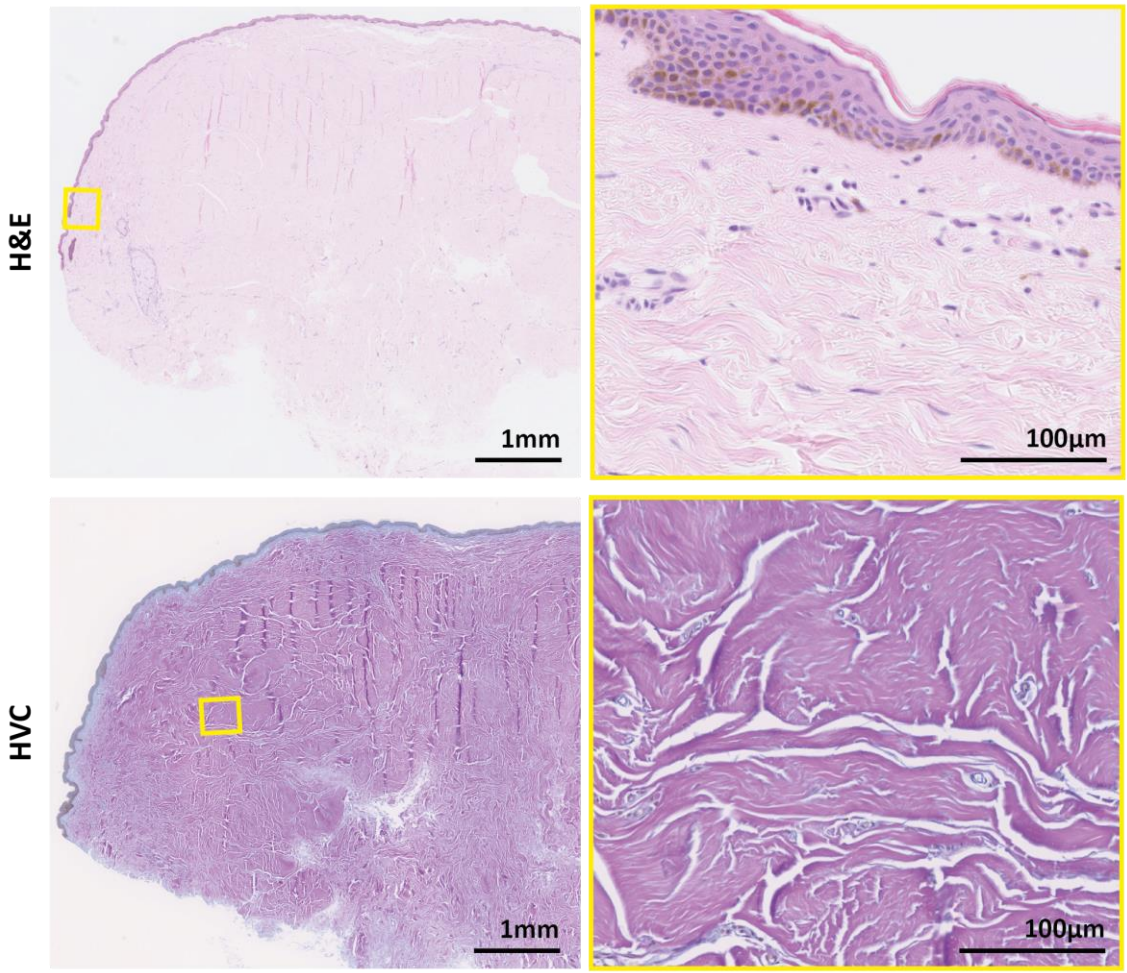

Figure 3-7 H&E and Herovici staining for a normal scar

Normal scar tissue from the neck of a 31-year old African-Caribbean female patient. Skin pigmentation can be seen as a diffuse brown colour in the basal epidermis. Epidermal thickness appears normal, and the dermis is thickened. There is a predominance of mature collagen fibres in the whole dermis, presented as thickened, randomly organised fibres. [**In pink** = Mature Collagen fibres; **In blue** = Young Collagen fibres]

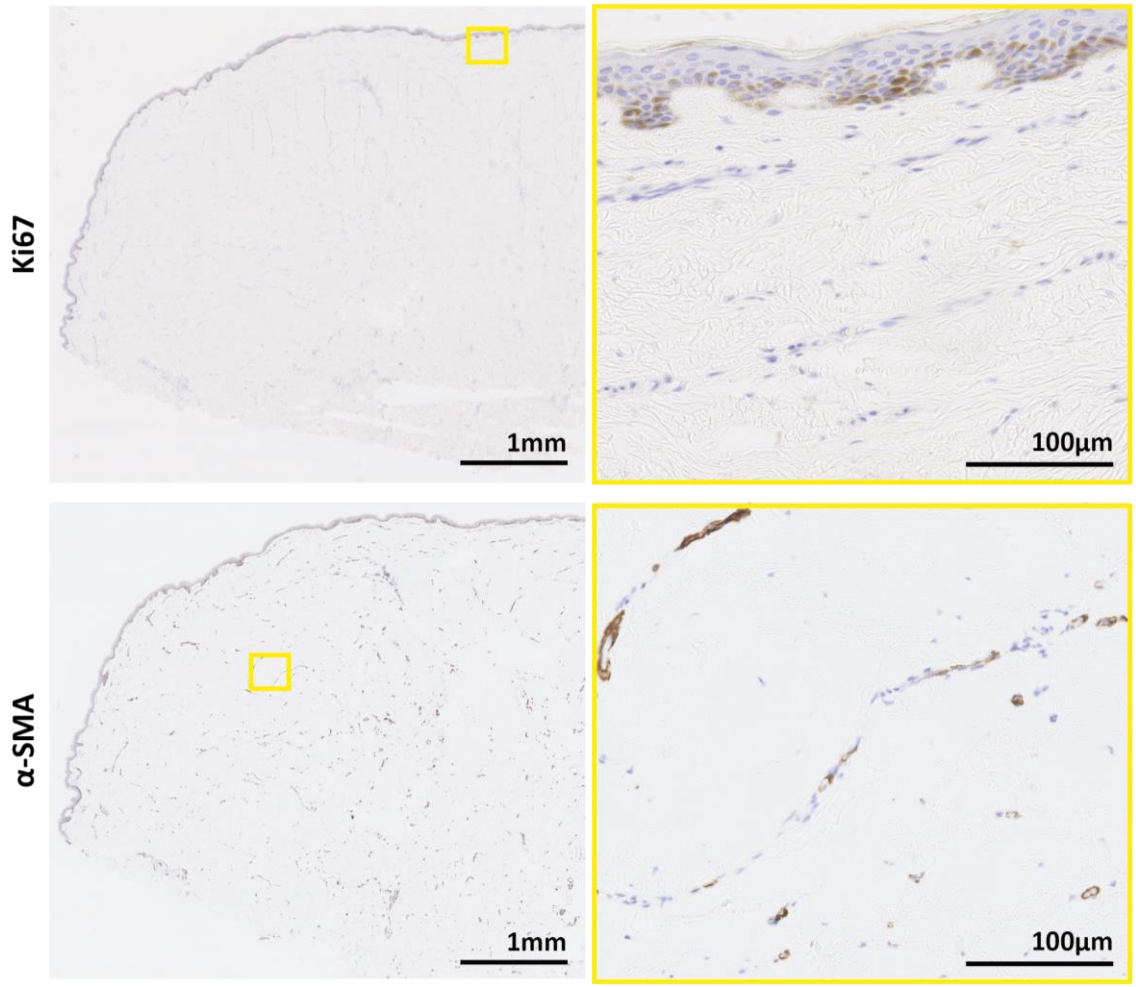

Figure 3-8 Ki67 and α-SMA protein expression in a normal scar.

DAB-Immunohistochemistry of normal scar tissue. Very little **Ki67** expression was found in basal keratinocytes, with almost no expression in the dermis. The diffuse brown shading in the basal layer of the epidermis is the melanin pigment. **α-SMA** (α-Smooth Muscle Actin) expression revealed a number of small blood vessels, as well as a low level of myofibroblasts.

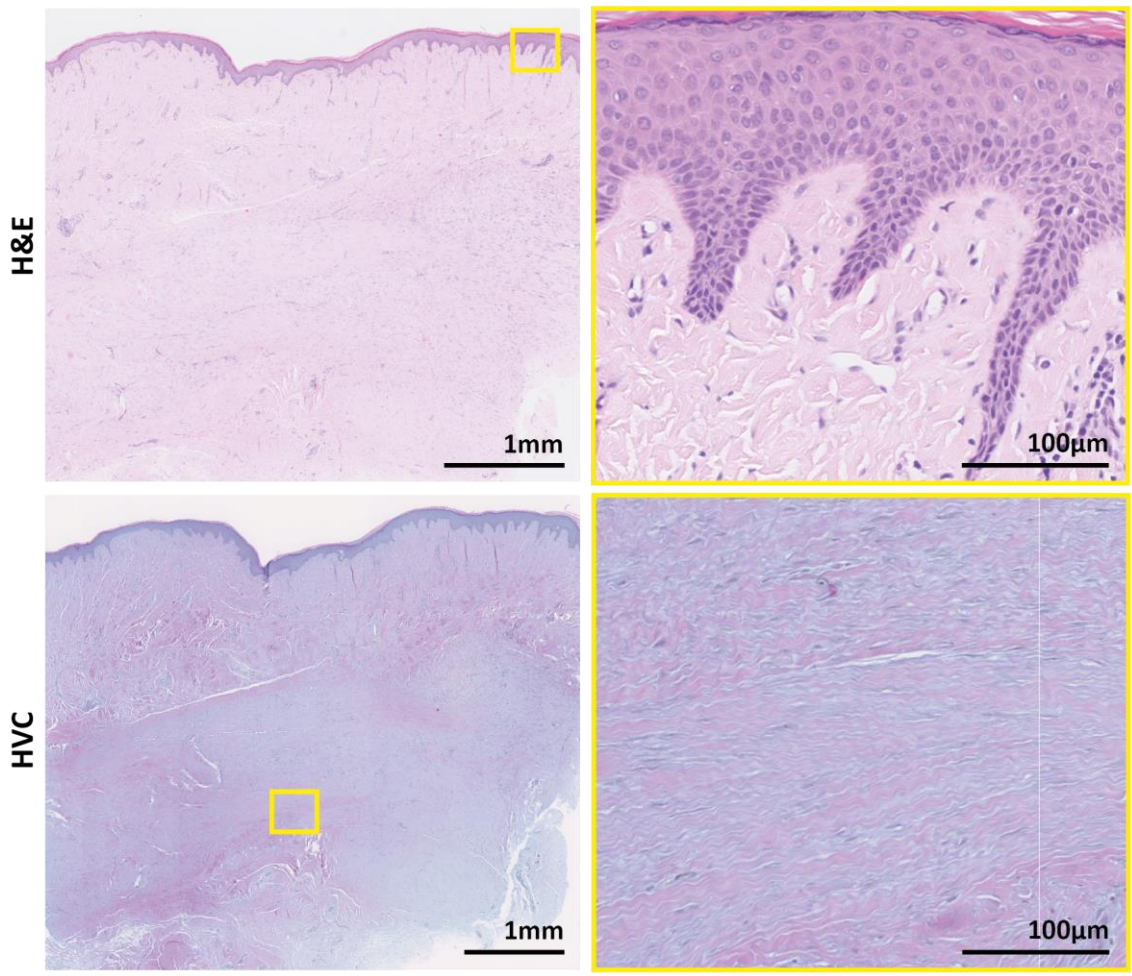

Figure 3-9 H&E and Herovici for a hypertrophic scar

The ethnicity, gender and body region of this specimen is unknown, however the lack of melanin pigmentation in the basal keratinocytes suggests that the patient was Caucasian. The top two panels show a H&E stain, where it is clear the epidermis is thickened, with increased ridges into the collagenous dermis. There is an increased density of young collagen fibres, particularly in the reticular dermis. Both young and mature collagen fibres appear thickened and well-organised in parallel to the epidermis. [**In pink** = Mature Collagen fibres; **In blue** = Young Collagen fibres].

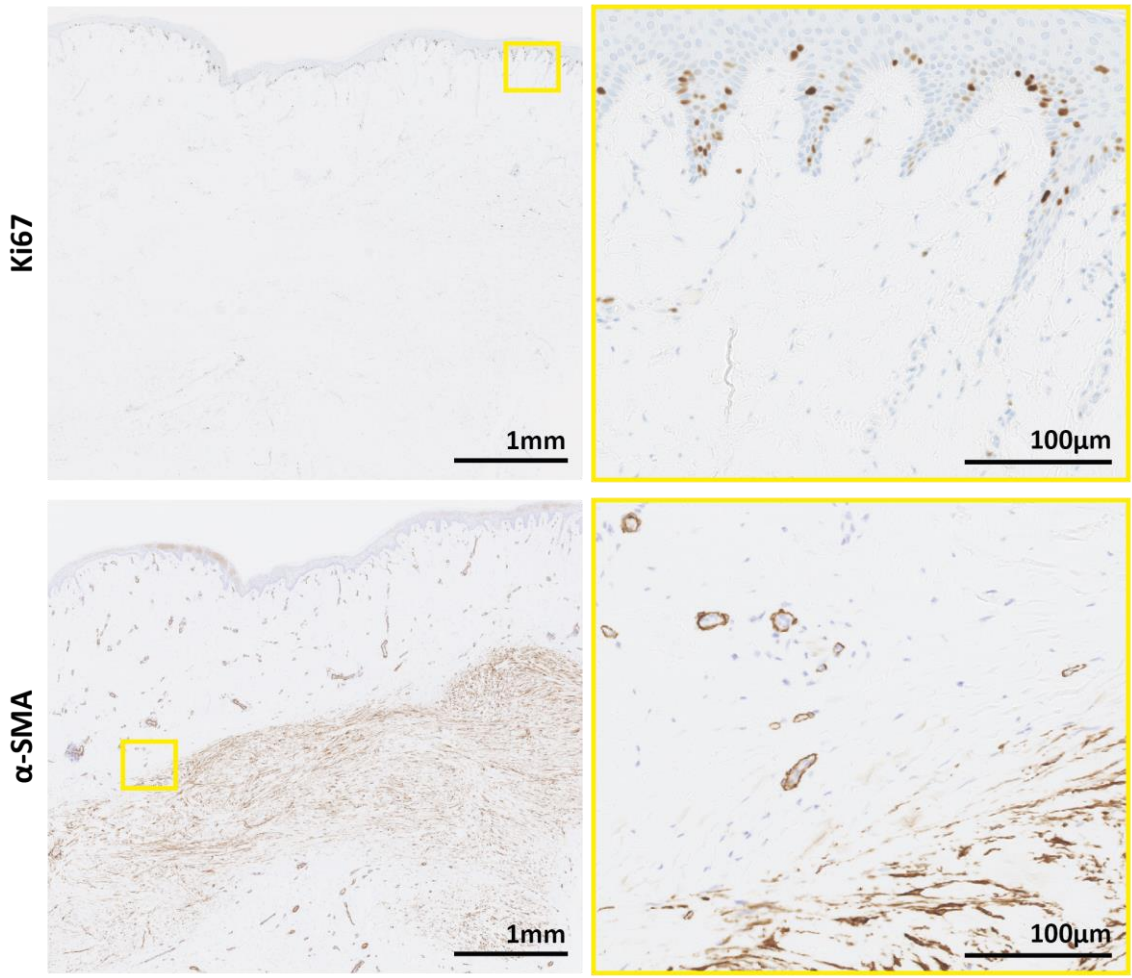

Figure 3-10 Ki67 and α-SMA protein expression in a hypertrophic scar.

DAB-Immunohistochemistry of a hypertrophic scar specimen. Cell proliferation marker **Ki67** showed strong nuclear expression in numerous basal keratinocytes along the whole epidermal layer, with little expression in the dermis. **α-SMA** (α-Smooth Muscle Actin) expression revealed a number of small blood vessels in the papillary dermis, and a high level of myofibroblasts in the reticular dermis. Myofibroblast expression appeared to mirror the pattern and orientation of the predominantly young collagen fibres observed in the previous **Figure 3-9**.

3.2.3.4 Keloid scar tissue structure

When examining histological sections of each keloid sample, it became clear that there was great variability between patients. Just over half of the keloid scar specimens showed distinct differences in epidermal and dermal structures between the central, marginal and adjacent normal skin – demonstrating how the keloid develops as it expands outwards and upwards. Keloid patients 32, 36, 40, 42, 51 and 70 (**Figures 3-13, 3-19, 3-21, 3-23, 3-25,** and **3-29)** demonstrated the recognised keloid morphology. The *central* region of the keloid showed a thickened, fairly uniform epidermis with minimal undulations, and a deep, densely fibrous dermis. Herovici staining revealed randomly organised thick collagen nodules surrounded by finer young collagen fibres, together forming acellular, cigar-shaped structures. These large collagen bundles were found to run in parallel to the surface of the skin. The marginal, or *edge*, region of the keloid then followed, where the epidermis was still thickened but demonstrated particularly deep abnormal protrusions into the dermis. A mixture of young and mature collagen fibres appeared thickened but tightly packed and well organised, sometimes in parallel to the epidermis, sometimes in parallel to the nodular structures described in the keloid centre. Finally, the *adjacent normal* skin region showed a much thinner epidermis than the rest of the keloid, which was however more undulating than normal healthy skin. One defining feature of the adjacent normal skin tissue was that the dermis much resembled that of normal healthy skin, with loosely organised and randomly oriented mature collagen fibres.

The intensity levels of the blue (young) and pink (mature) Herovici staining were measured and quantified, which revealed a statistically significant increase in mature collagen fibres between the keloid centre and edge regions (**Figure 3-31**). Within the keloid edge and adjacent normal regions, there was also a statistically significantly increased level of young collagen fibres, compared to mature fibres (**Figure 3-31**).

Keloid patients 26, 34, and 35 (**Figures 3-11, 3-15** and **3-17**) showed similar distinctions between central and marginal scar regions, however there were no

clearly defined adjacent normal skin areas histologically identifiable. Conversely, the epidermal structure in keloid patient 55 (**Figure 3-27**) was so abnormal and full of irregular protrusions, that there was no distinct central region that appeared similar to other keloid specimens. Additionally, the dermis of keloid patient 55 did not show the characteristic collagen bundles seen in the central regions of other keloids. For this reason, this particular specimen was treated as having only edge and adjacent normal areas. Patient 55 also contained a high number of hair follicles, most of which were concentrated near the subcutaneous fat layer.

3.2.3.5 Ki67 cell proliferation marker in keloid scar tissue

There was a range of Ki67 expression patterns observed in the keloid scars presented in this chapter. The majority of the keloids appeared to demonstrate the highest level of cell proliferation in the *edge* region. Within this category, keloids from patients 26 and 34 (**Figures 3-12** and **3-16**), which had no defined adjacent normal skin, showed an increased basal keratinocyte proliferation in the central region compared to normal healthy control skin. Whereas the central region of keloid patient 35 (**Figure 3-18**), which also lacked adjacent normal tissue, displayed a similar level of Ki67 expression to healthy control skin. Patient 55 (**Figure 3-28**), which lacks a defined central region, showed increased cell proliferation across the basal epidermis and the whole dermis of the main portion of the keloid, leading into a much less proliferative adjacent normal skin region.

Also within the category of keloids displaying the highest cell proliferation rate at their margin, patient 36 (**Figure 3-20**) demonstrated a marked difference between the three regions: the centre basal keratinocytes and dermis had a higher number of Ki67-positive nuclei than healthy control skin, while the adjacent normal skin had almost no evidence of cell proliferation across the epidermis and dermis. Keloid scar 70 (**Figure 3-30**), showed similar Ki67 expression pattern to patient 36, where the edge had the highest number of proliferating cells, followed by the centre, followed by the adjacent normal tissue. An interesting observation for patient 70 was that there was a small section within the central region, where the

epidermis resembled the more invasive morphology of the margin, and showed an increased number Ki67-positive cells (see high power image with dotted line border in **Figure 3-30**).

In keloid patients 32, 40, 42 and 51 (**Figures 3-14, 3-22, 3-24** and **3-26**) there appears to be a fairly constant level of Ki67 expression across all scar regions. The only difference between the regions is that in the central and marginal areas there is a low level Ki67 expression in dermal cells, however in the adjacent normal dermis there is no expression of Ki67.

In terms of quantifying these expression patterns, the number of Ki67-positive nuclei was counted and calculated as a percentage of the total number of nuclei present in the images of each tissue. Despite the impression of keloid scars and in particular the keloid edge regions showing increased cell proliferation levels, there was no significant difference between normal skin, keloid centre, keloid edge, or keloid adjacent normal skin (**Figure 3-32**). There was a high level of variability between patients of the same group, however overall it appears that the qualitative assessment of keloid scar tissue being more proliferative than normal skin is due to the increased number of cells being present in the first place.

It is important to note that Ki67 expression is restricted to the cell nuclei, and any diffuse brown shading observed in the basal epidermal cell layer of most keloid patients (especially notable in patient 40, **Figure 3-22**) is due to melanin pigment contained within melanocytes.

3.2.3.6 α-SMA expression in keloid scar tissue

As for Ki67 expression, there was also a range of α-SMA expression patterns observed in the keloid scars. Keloid patients 26 and 55 (**Figures 3-12** and **3-28**) revealed almost no myofibroblast expression across the whole tissues. In keloid patients 32, 40, 51 and 70 (**Figures 3-14, 3-22, 3-26** and **3-30**) there were numerous myofibroblasts visible in the dermal scar centres and edges. Adjacent normal tissue from these patients displayed no myofibroblasts.

Keloid patients 34, 36 and 42 (**Figures 3-16, 3-20,** and **3-24**) displayed elevated myofibroblast expression in the central and marginal regions, particularly in the deep dermal layers. There were no myofibroblasts present in the adjacent normal tissue. Finally, keloid scar 35 (**Figure 3-18**) demonstrated a distinctly strong myofibroblast expression in the reticular dermis throughout the whole keloid.

When comparing these observations against healthy control skin, it becomes clear that ECM synthesis-inducing myofibroblasts are increased in scarring tissue. See **Table 3-1** for a summary of the keloid scar morphological and histological assessment presented so far. These results suggest that ECM remodeling is taking place in the fibrotic scars. In the next section of this chapter, protein expression patterns of certain MMPs were examined in the same keloids used above.

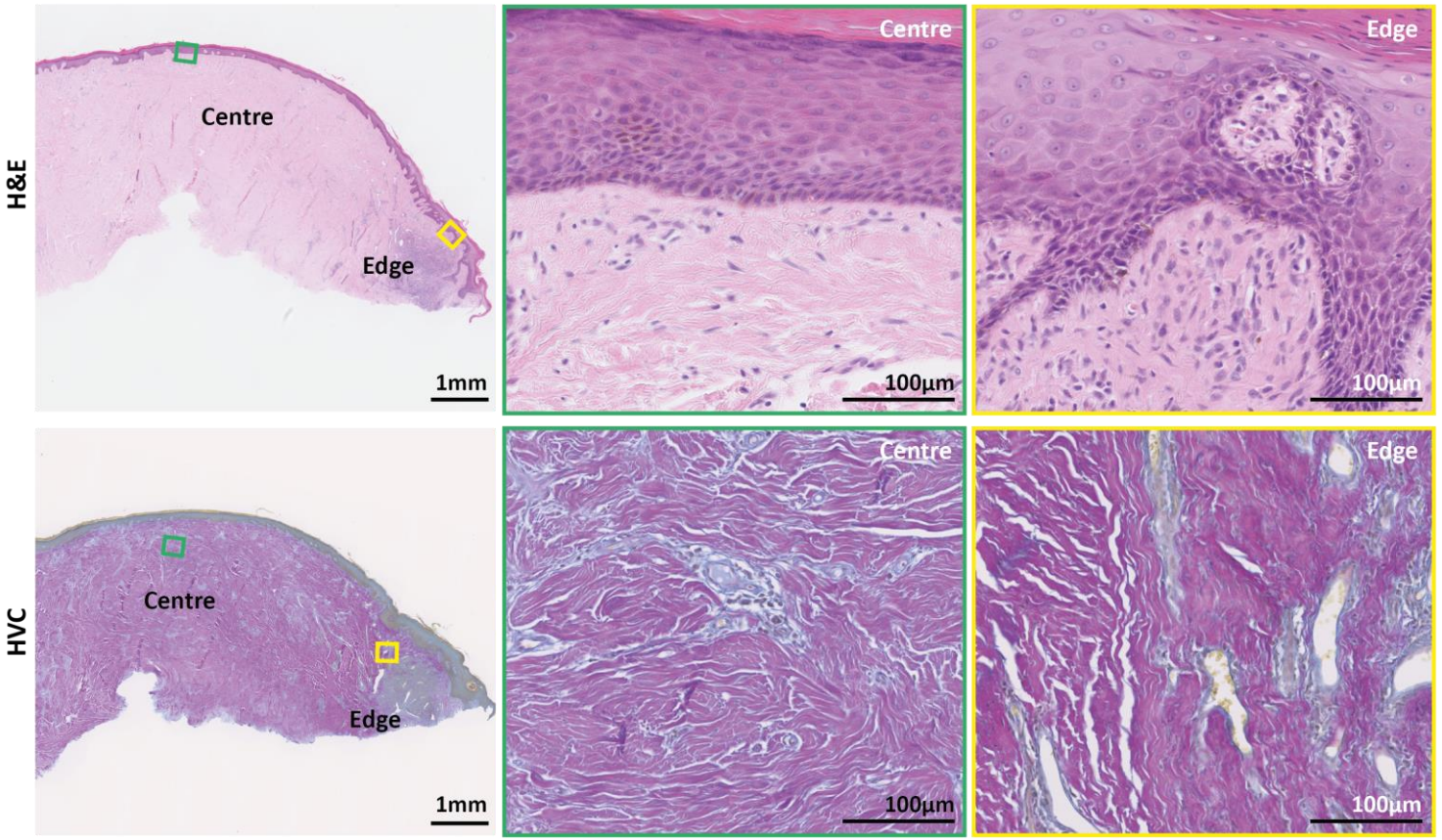

Figure 3-11 H&E and Herovici staining for keloid scar patient 26

A recurrent earlobe keloid from an African-Caribbean female patient. In the H&E stain, it is clear the epidermis is thickened across the keloid, with the *edge* showing increased ridges into the dermis. The herovici (HVC) stain shows thick bundles of mature collagen fibres (in pink) across the whole dermis, with the fibres being more organised at the *edge* of the scar. There was no clear *adjacent normal* tissue distinguishable.

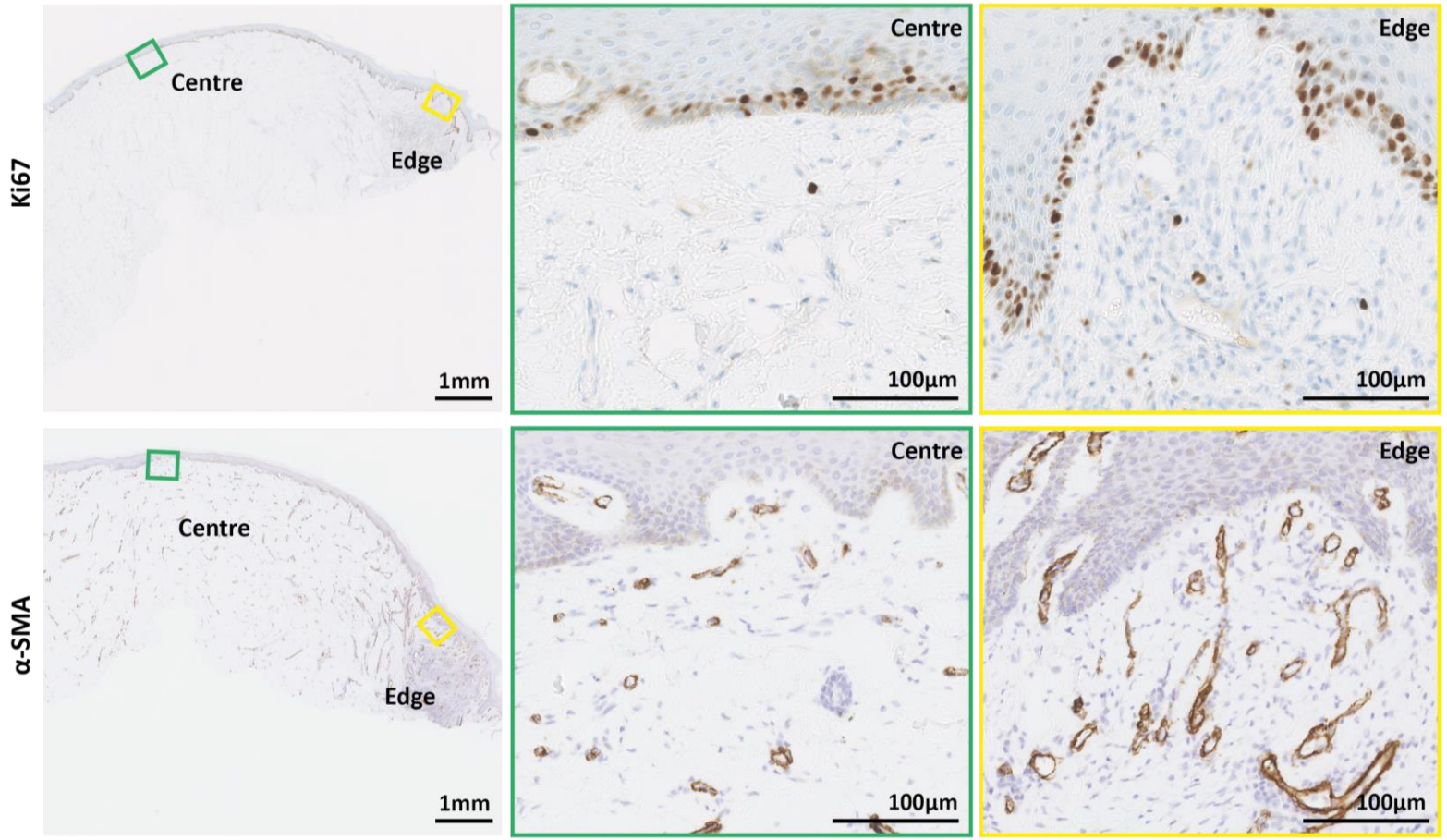

Figure 3-12 Ki67 and α-SMA protein expression in keloid scar patient 26.

DAB-Immunohistochemistry of keloid patient 26. Strong expression of **Ki67** was apparent across the whole keloid basal epidermis, with a slight increase in the *edge*, and very little expression in the dermis. **α-SMA** (α-Smooth Muscle Actin) expression revealed small blood vessels across the whole dermis, and little evidence of myofibroblast expression**.**

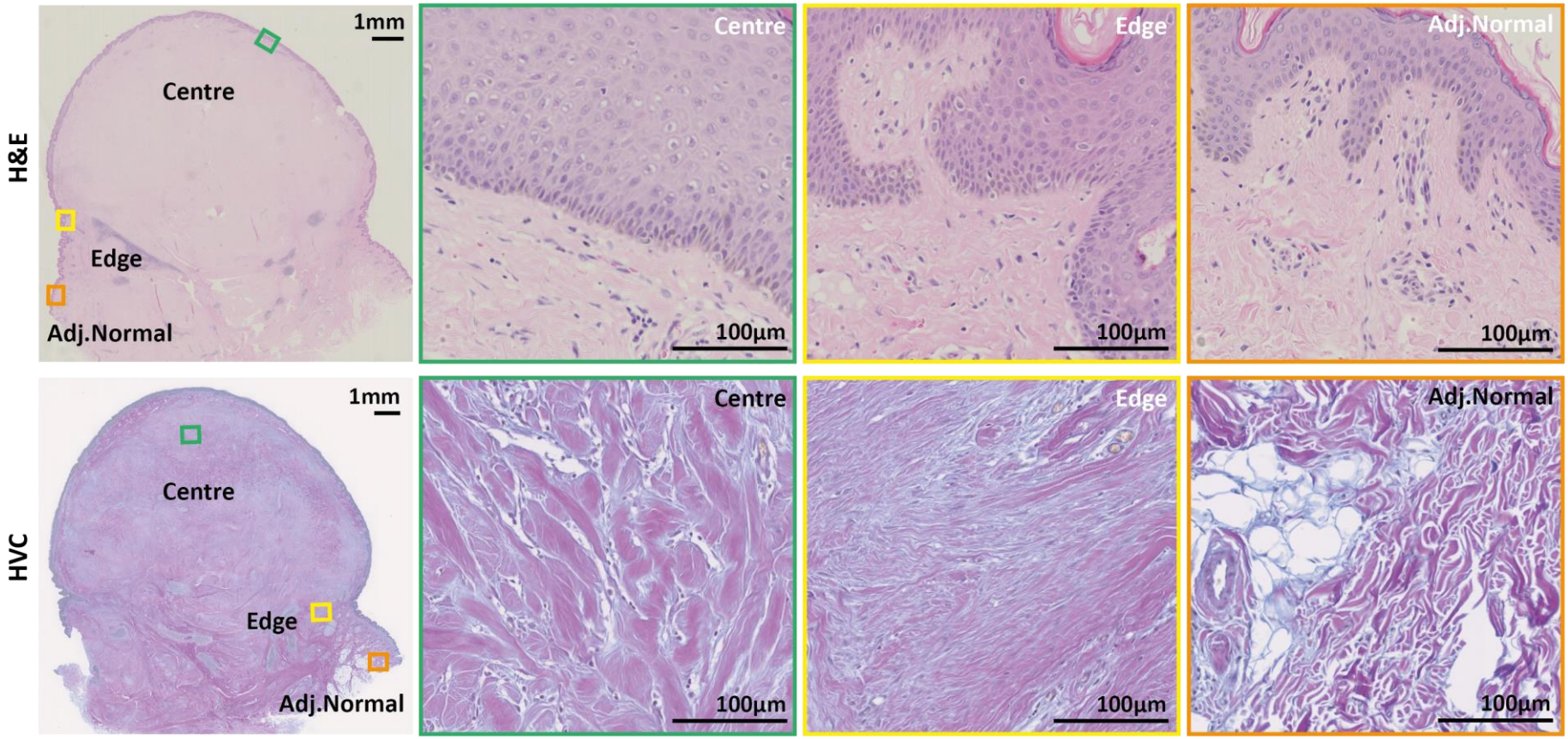

Figure 3-13 H&E and Herovici staining for keloid scar patient 32

From the ear of a 20-year old Asian male patient. The H&E stain showed the epidermis is thickened in the *centre* of the keloid, with the *edge* showing increased ridges into the dermis. The herovici (HVC) stain shows nodules of mature collagen fibres (in pink) surrounded by young collagen fibres (in blue) in the central dermis; a mixture of the two types of collagen fibres organised in parallel in the *edge* dermis; and loosely organised mature collagen fibres in the *adjacent normal* tissue. [**Adj. Normal** = adjacent normal skin]

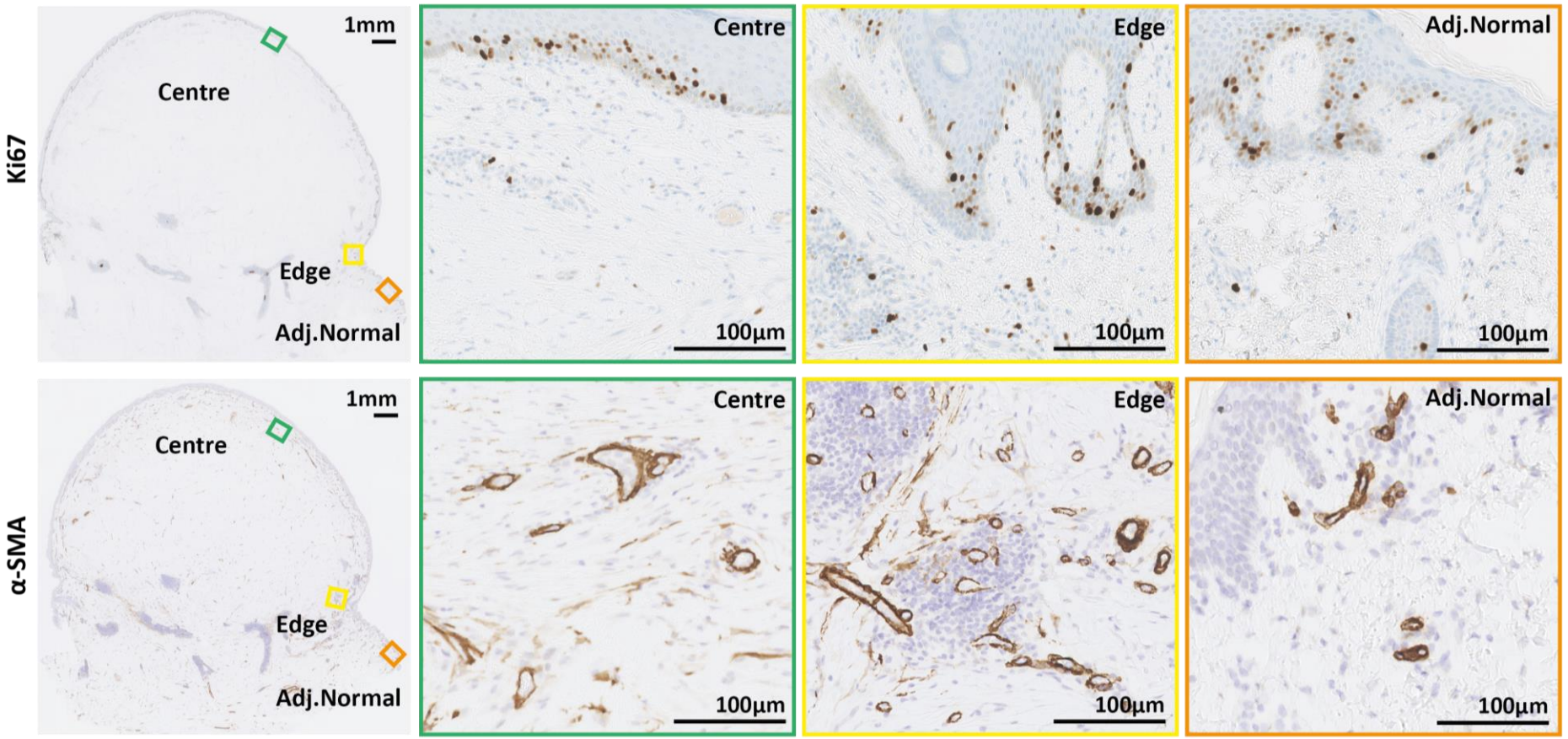

Figure 3-14 Ki67 and α-SMA protein expression in keloid scar patient 32.

DAB-Immunohistochemistry of keloid patient 32. Nuclear expression of **Ki67** was observed across the whole keloid basal epidermis, with slightly increased dermal expression in the *edge*. **α-SMA** (α-Smooth Muscle Actin) expression revealed small blood vessels across the whole dermis, as well as myofibroblasts in the central and edge dermal regions. [**Adj. Normal** = adjacent normal skin]

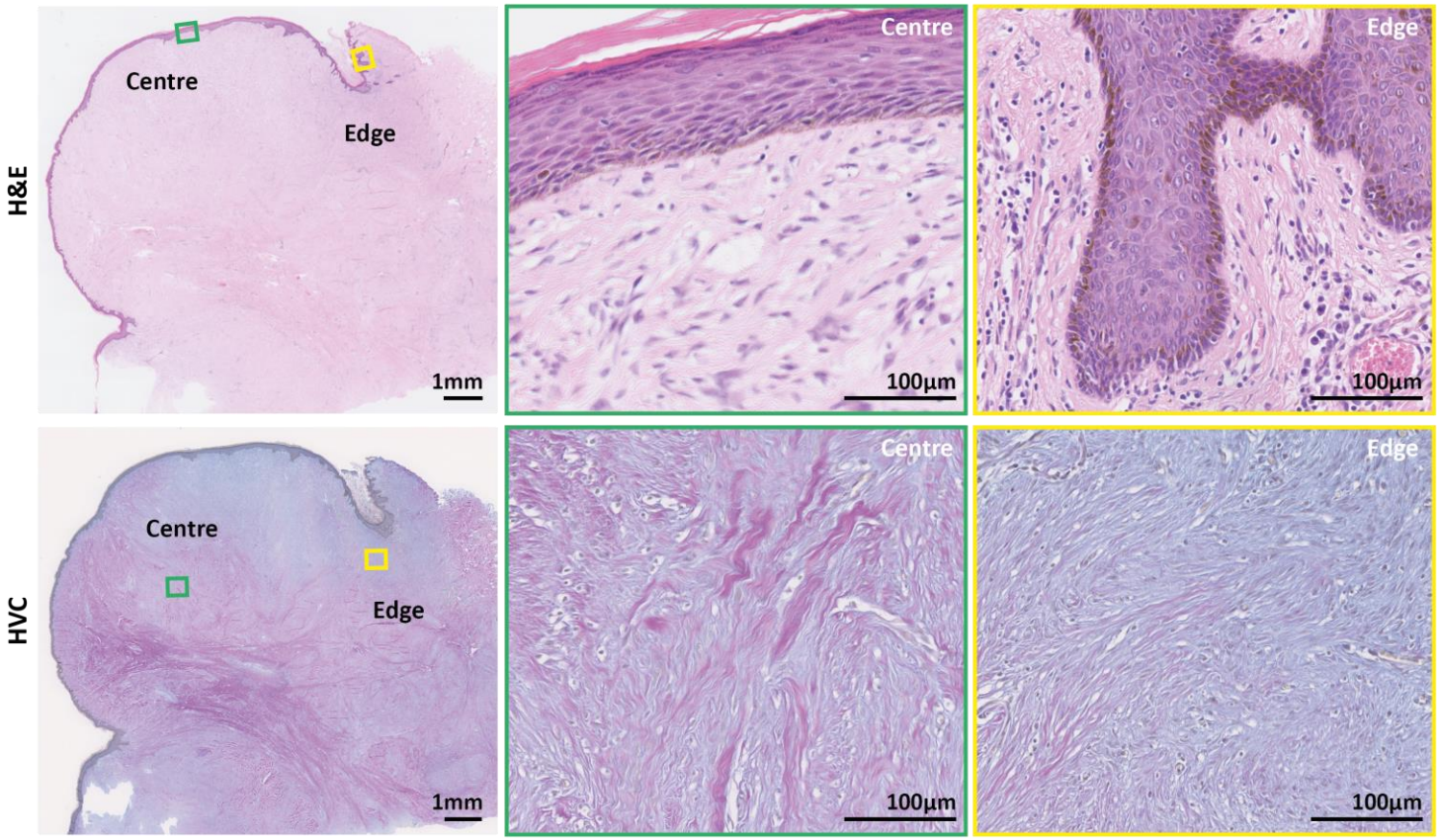

Figure 3-15 H&E and Herovici staining for keloid scar patient 34

From the post-auricular region of an African-Caribbean female patient. The increased melanin pigment is visible as a diffuse brown shading in the basal epidermis. The H&E stain showed the epidermis is thickened in the *centre* of the keloid, with the *edge* showing increased ridges into the dermis. The herovici (HVC) stain shows thickened, mature collagen fibres (in pink) surrounded by finer, young collagen fibres (in blue) in the central dermis; and an increased density of young collagen fibres at the *edge* dermis.

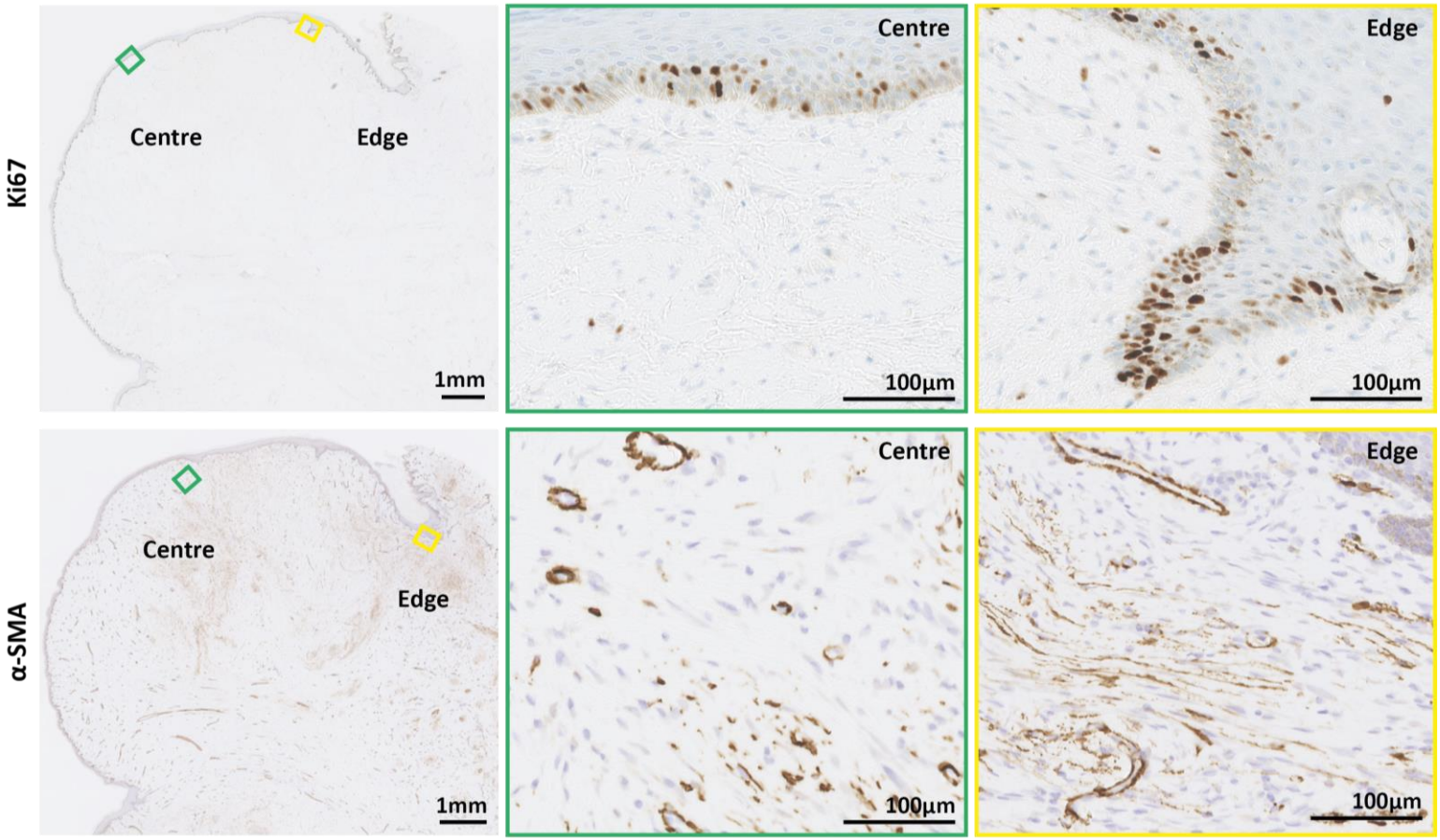

Figure 3-16 Ki67 and α-SMA protein expression in keloid scar patient 34.

DAB-Immunohistochemistry of keloid patient 34. **Ki67** expression was observed across the whole keloid basal epidermis, with a slight increase in the *edge*, and little expression in the dermis. **α-SMA** (α-Smooth Muscle Actin) expression revealed small blood vessels across the whole dermis, and areas of increased levels of myofibroblasts near the *edges* of the keloid.

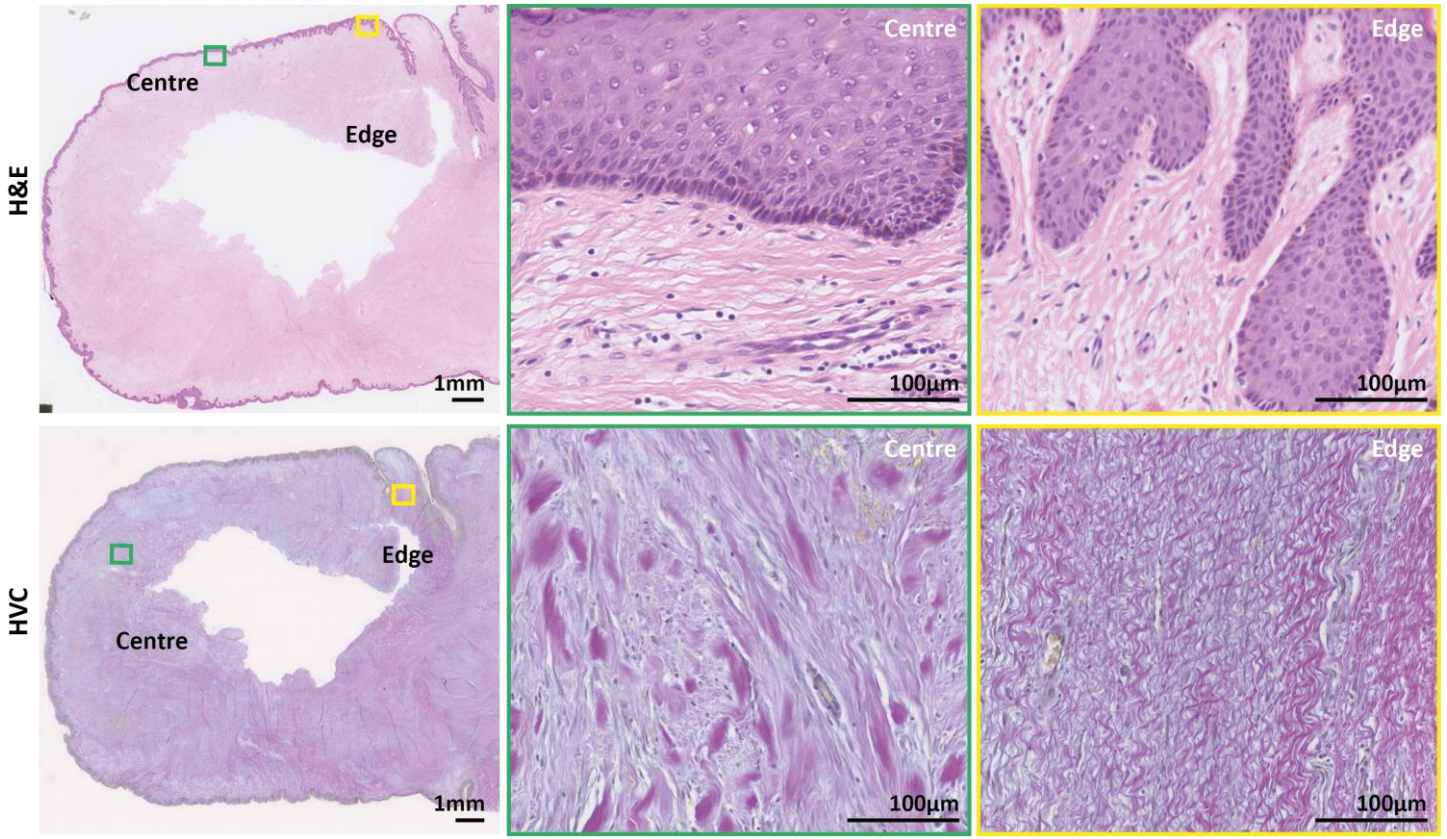

Figure 3-17 H&E and Herovici staining for keloid scar patient 35

From the left scapula of an African-Caribbean male patient. The slightly increased levels of melanin pigment is visible as a faint brown shading in the basal epidermis. The H&E stain showed a thickened epidermis in the keloid *centre*, with the *edge* showing increased ridges. The herovici (HVC) stain showed mature collagen nodules (in pink) surrounded by younger collagen fibres (in blue) in the central dermis; and a mixture of well- organised young and mature collagen fibres at the *edge* dermis.

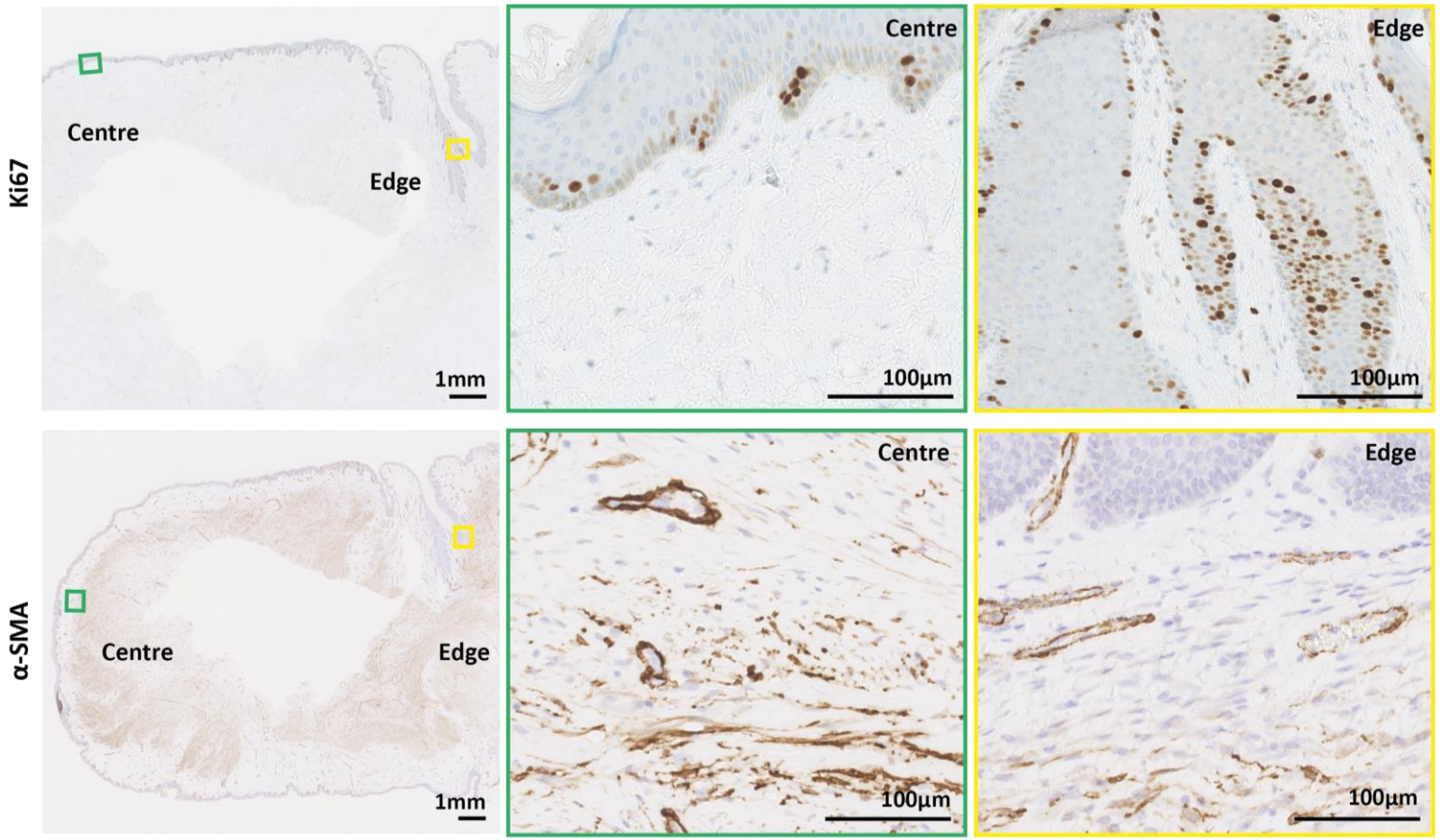

Figure 3-18 Ki67 and α-SMA protein expression in keloid scar patient 35.

DAB-Immunohistochemistry of keloid patient 35. **Ki67** nuclear expression was apparent across the basal layer of the epidermis, with an increased expression at the *edge*, and little expression in the dermis. **α-SMA** (α-Smooth Muscle Actin) expression revealed small blood vessels across the papillary dermis, and an increased level of myofibroblasts in the reticular dermis**.**

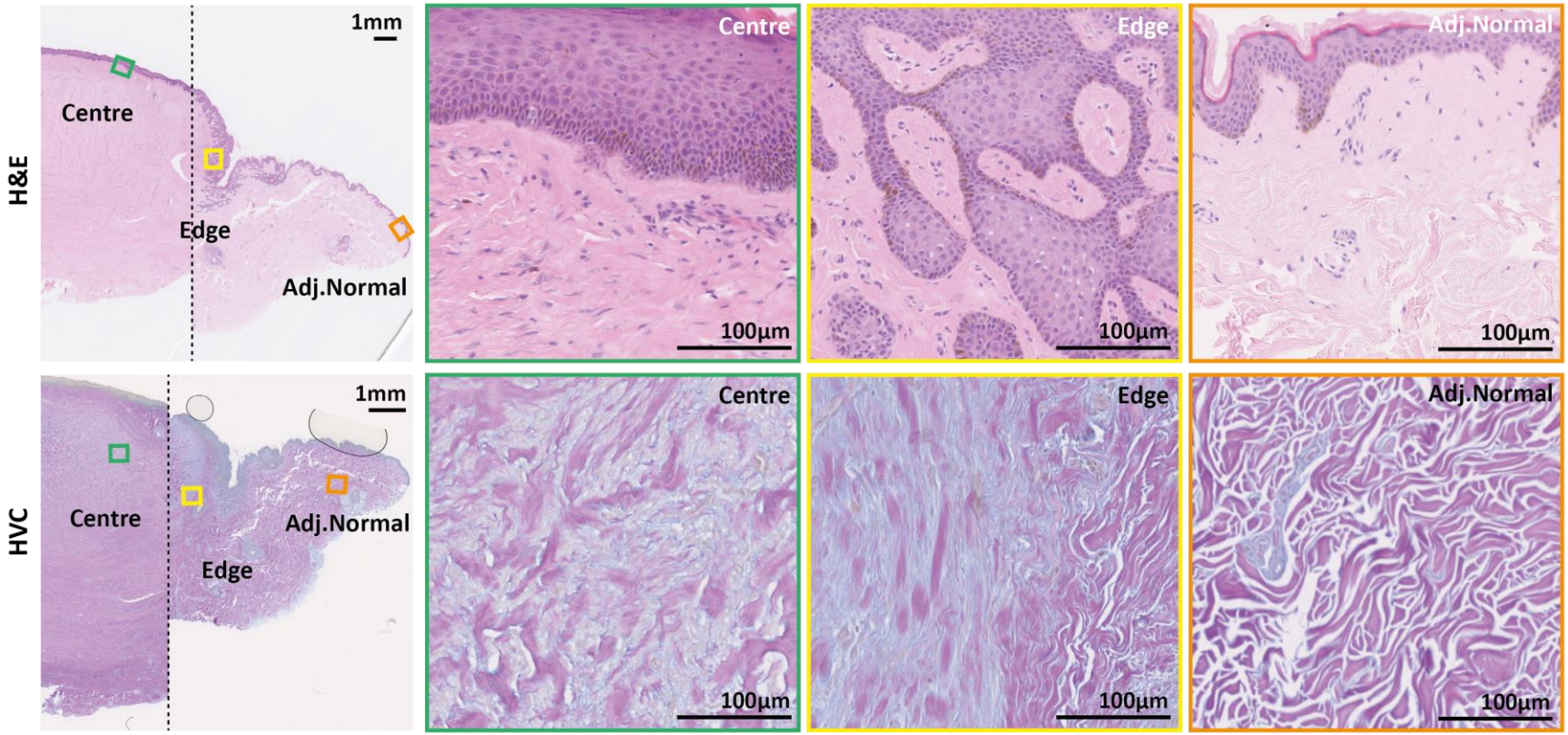

Figure 3-19 H&E and Herovici staining for keloid scar patient 36

A butterfly keloid from the breast of an African-Caribbean female patient. The increased melanin pigment is visible as a diffuse brown shading in the basal epidermis. The H&E stain showed a thickened epidermis in the keloid *centre*, with the *edge* showing invasive-looking ridges into the dermis. The herovici (HVC) stain shows mature collagen nodules (in pink) surrounded by younger collagen fibres (in blue) in the *central* dermis; a mixture of mature collagen nodules and young collagen fibres at the *edge* dermis; and loosely organised mature collagen fibres in the *adjacent normal* tissue.

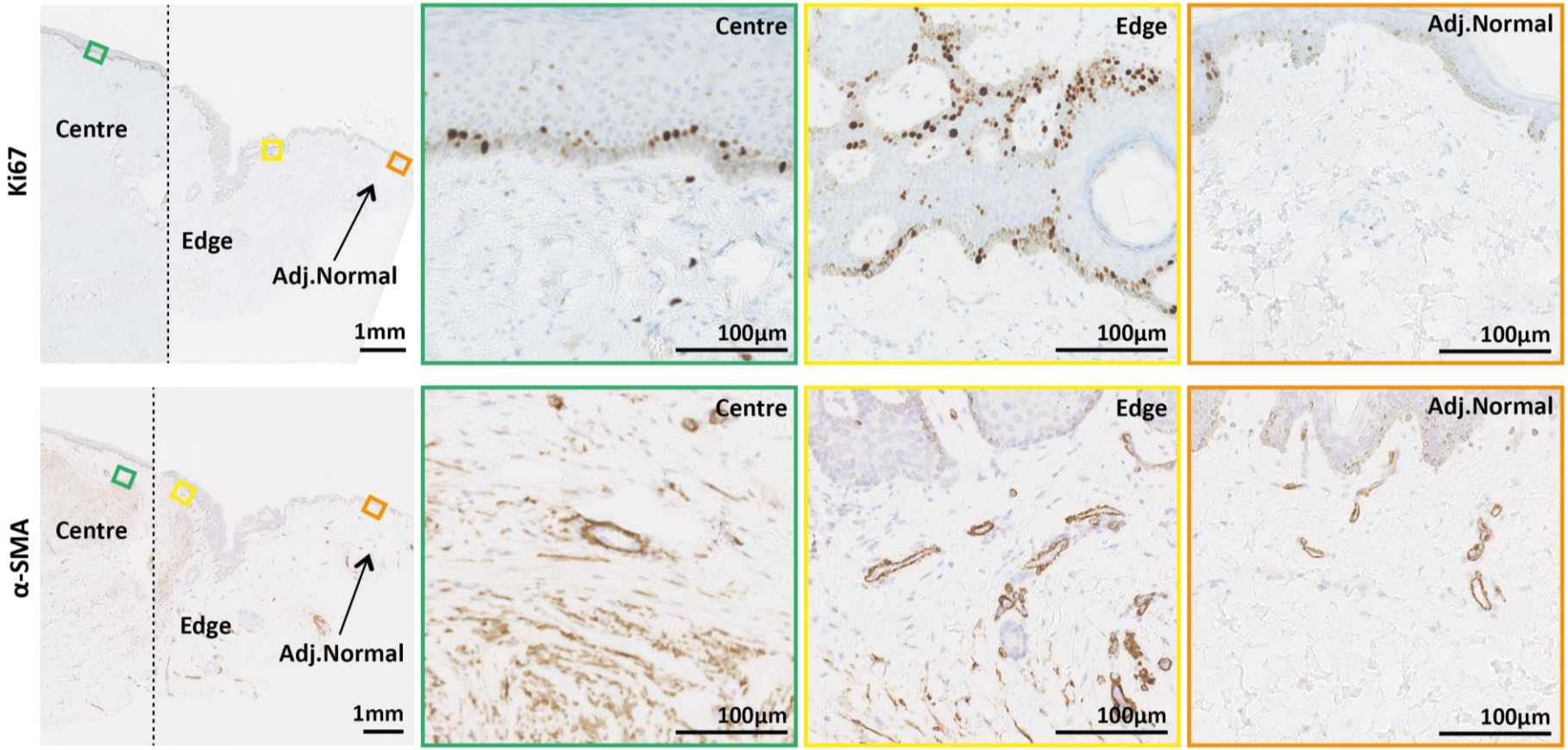

Figure 3-20 Ki67 and α-SMA protein expression in keloid scar patient 36.

DAB-Immunohistochemistry of keloid patient 36. This specimen was particularly large, therefore a small portion of each region is shown in the far left low magnification images. **Ki67** expression was seen in the *centre*, with a high increase in the *edge*, and very little expression in the *adjacent normal* basal keratinocytes. **α-SMA** expression showed capillaries across the papillary dermis, and an increased level of myofibroblasts in the *central* and *edge* reticular dermis**.**

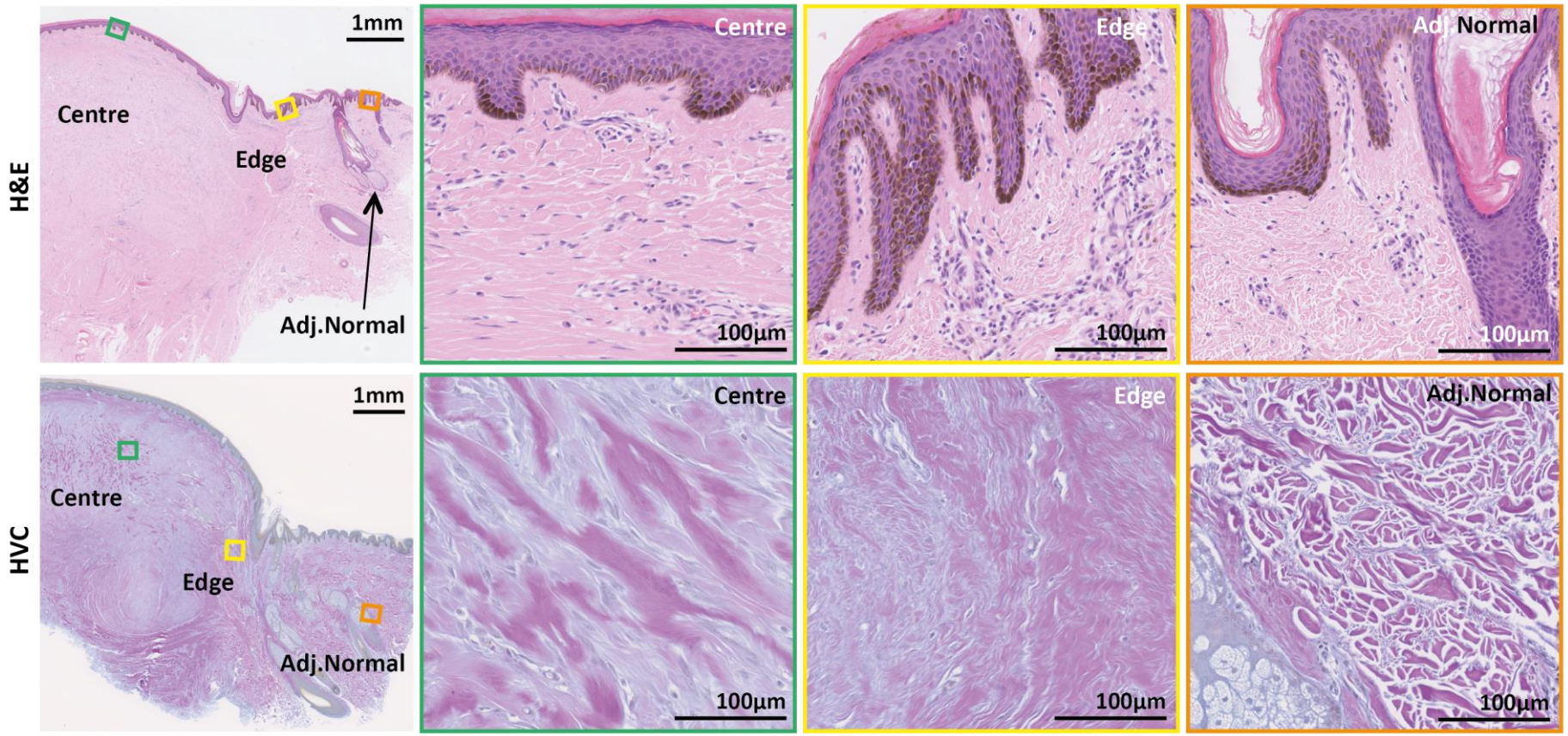

Figure 3-21 H&E and Herovici staining for keloid scar patient 40

From the cheek of a 30-year old African-Caribbean male patient. The increased levels of melanin pigment is visible as a diffuse brown shading in the basal epidermis. The H&E stain showed the *edge* had increased ridges into the dermis. The herovici (HVC) stain showed mature collagen nodules (in pink) surrounded by young collagen fibres (in blue) in the *central* dermis; a mixture of well organised mature and young collagen fibres at the *edge* dermis; and loosely organised mature collagen fibres in the *adjacent normal* tissue.

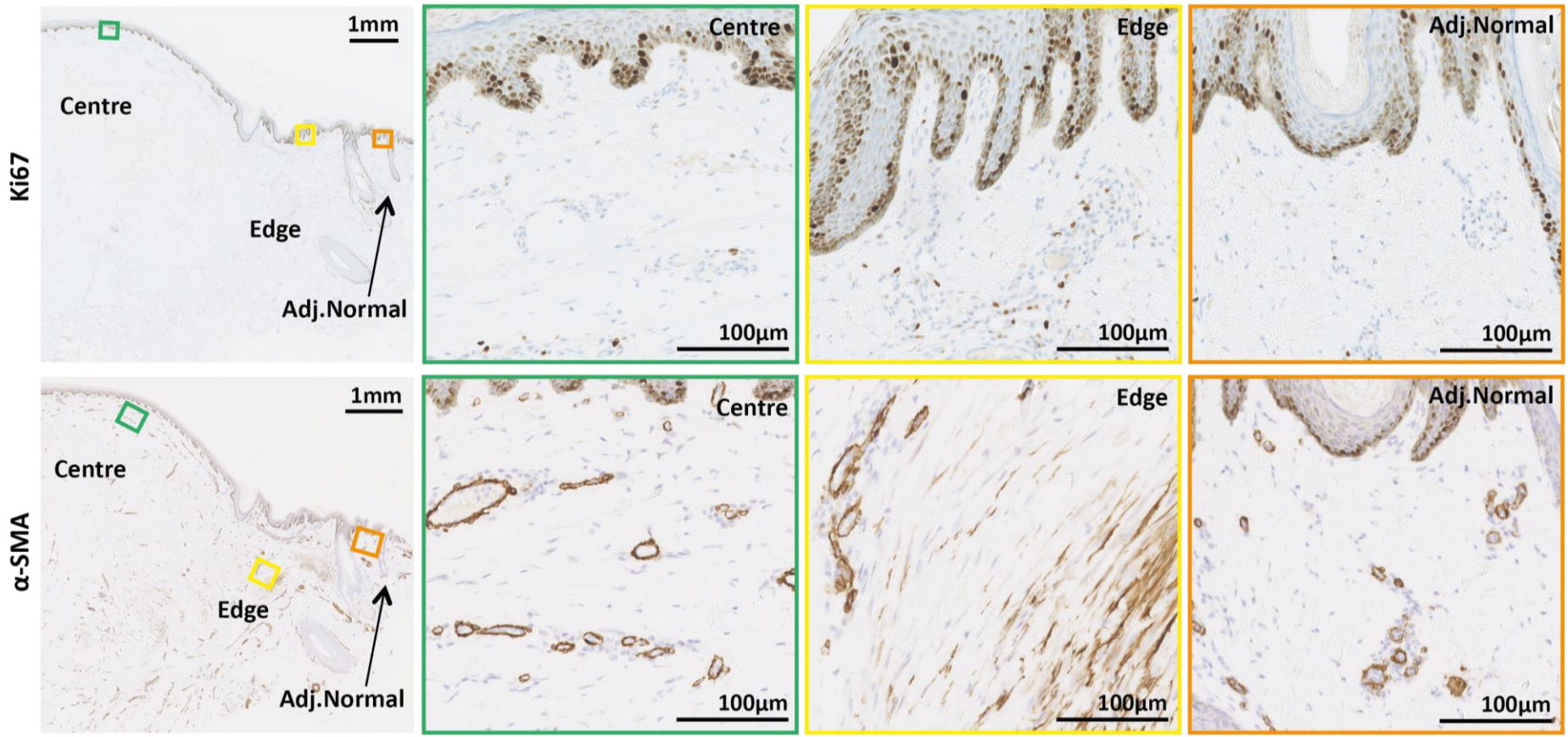

Figure 3-22 Ki67 and α-SMA protein expression in keloid scar patient 40.

DAB-Immunohistochemistry of keloid patient 40. **Ki67** strong nuclear expression was observed in a number of basal keratinocytes, across the whole keloid epidermis. The diffuse brown shading in the basal layer of the epidermis is the melanin pigment. **α-SMA** expression revealed capillaries across the whole dermis, and a number of myofibroblasts in the reticular dermis of the keloid *edge*.

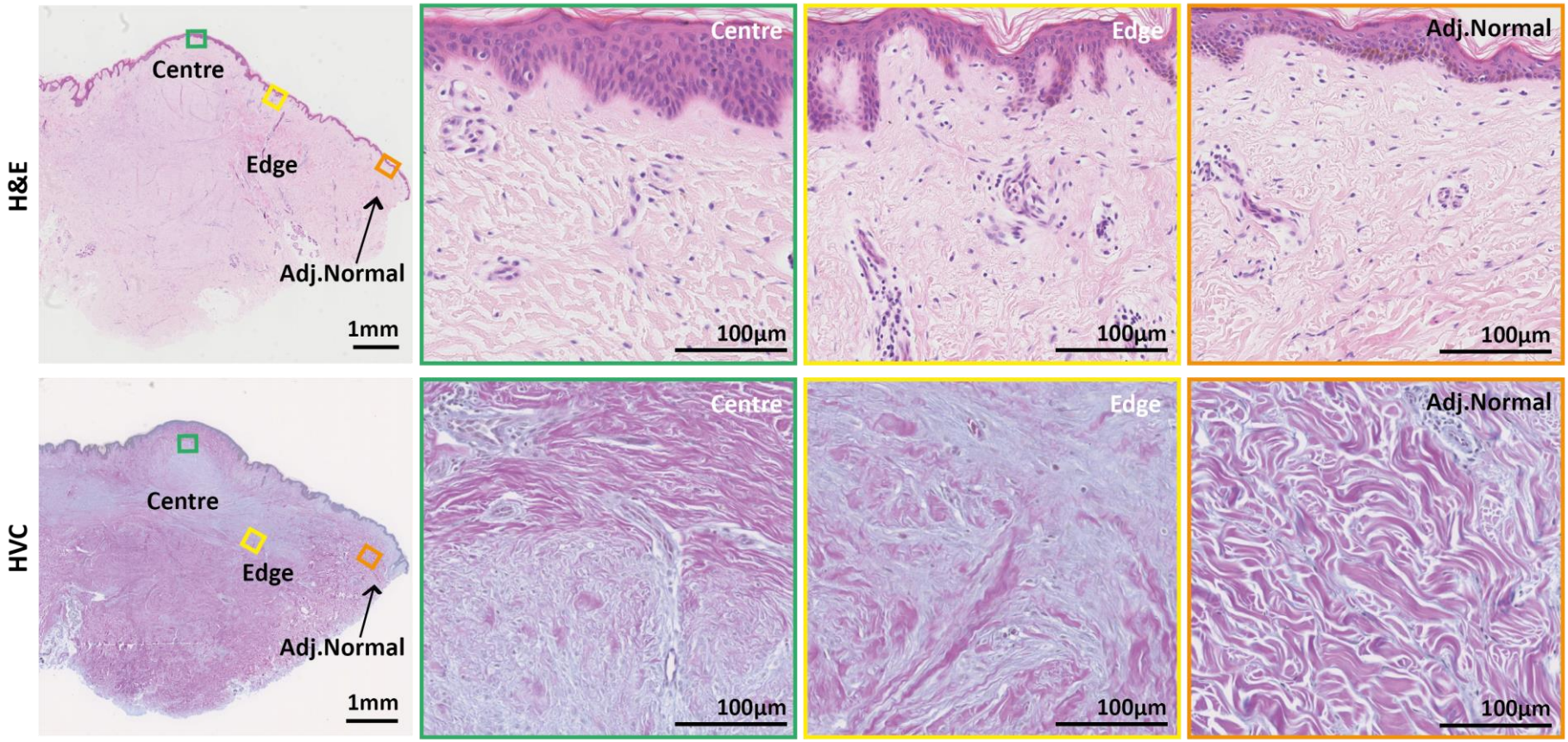

Figure 3-23 H&E and Herovici staining for keloid scar patient 42.

A butterfly keloid from the abdomen of an over 40-year old Caucasian female patient. The H&E stain showed a slightly thickened epidermis in the keloid *centre*, with the *edge* showing increased ridges into the dermis. The Herovici (HVC) stain showed mainly young collagen fibres (in blue) surrounded by mature collagen fibres (in pink) in the *central* dermis; a mixture of mature collagen nodules and young collagen fibres at the *edge* dermis; and loosely organised mature collagen fibres in the *adjacent normal* tissue.

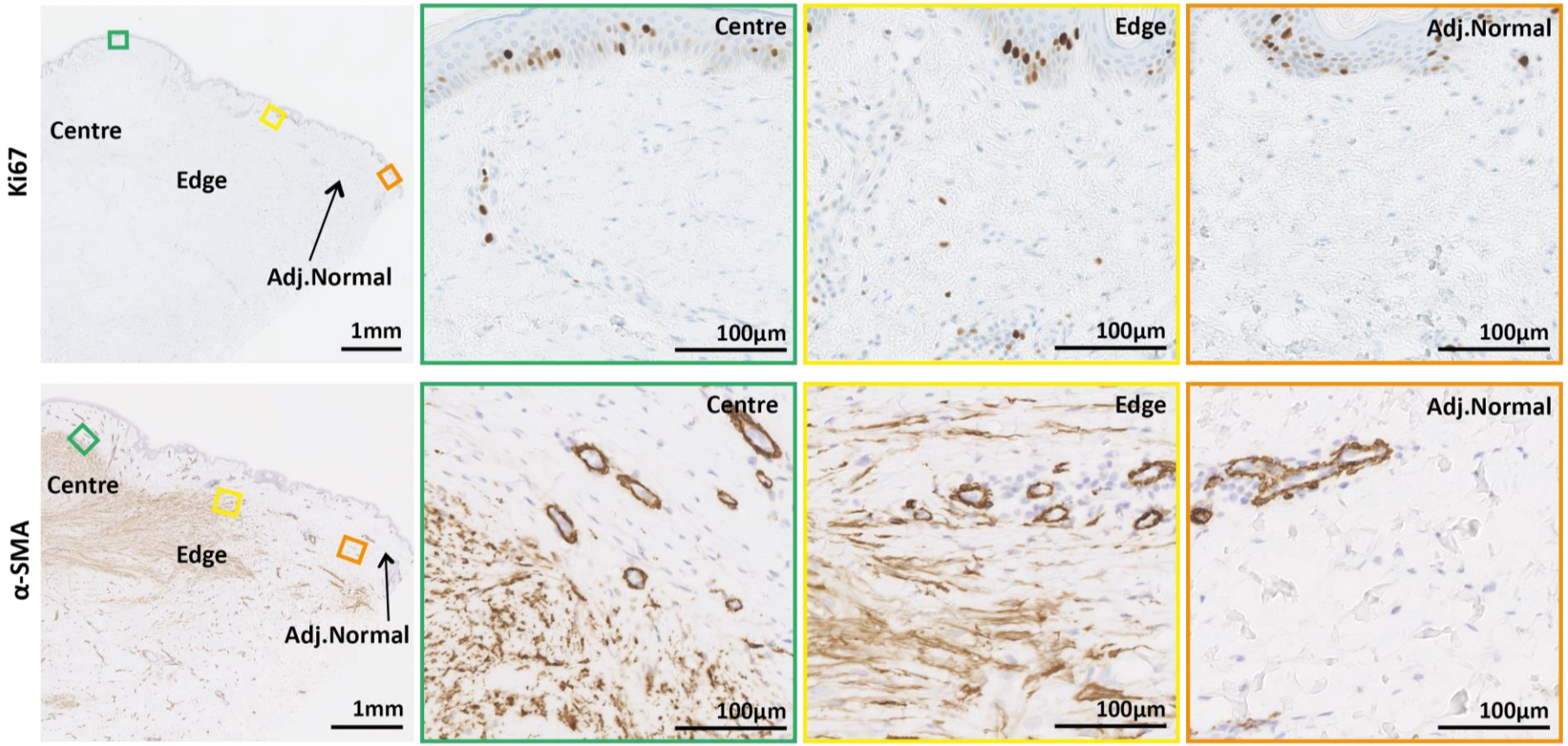

Figure 3-24 Ki67 and α-SMA protein expression in keloid scar patient 42

DAB-Immunohistochemistry of keloid patient 42. **Ki67** strong nuclear expression was observed in a number of basal keratinocytes, across the whole keloid epidermis, with a small number of proliferative cells seen in the *central* and *edge* dermis. **α-SMA** expression revealed capillaries across the whole dermis, and increased levels of myofibroblasts in the reticular dermis of the keloid *centre* and *edge.*

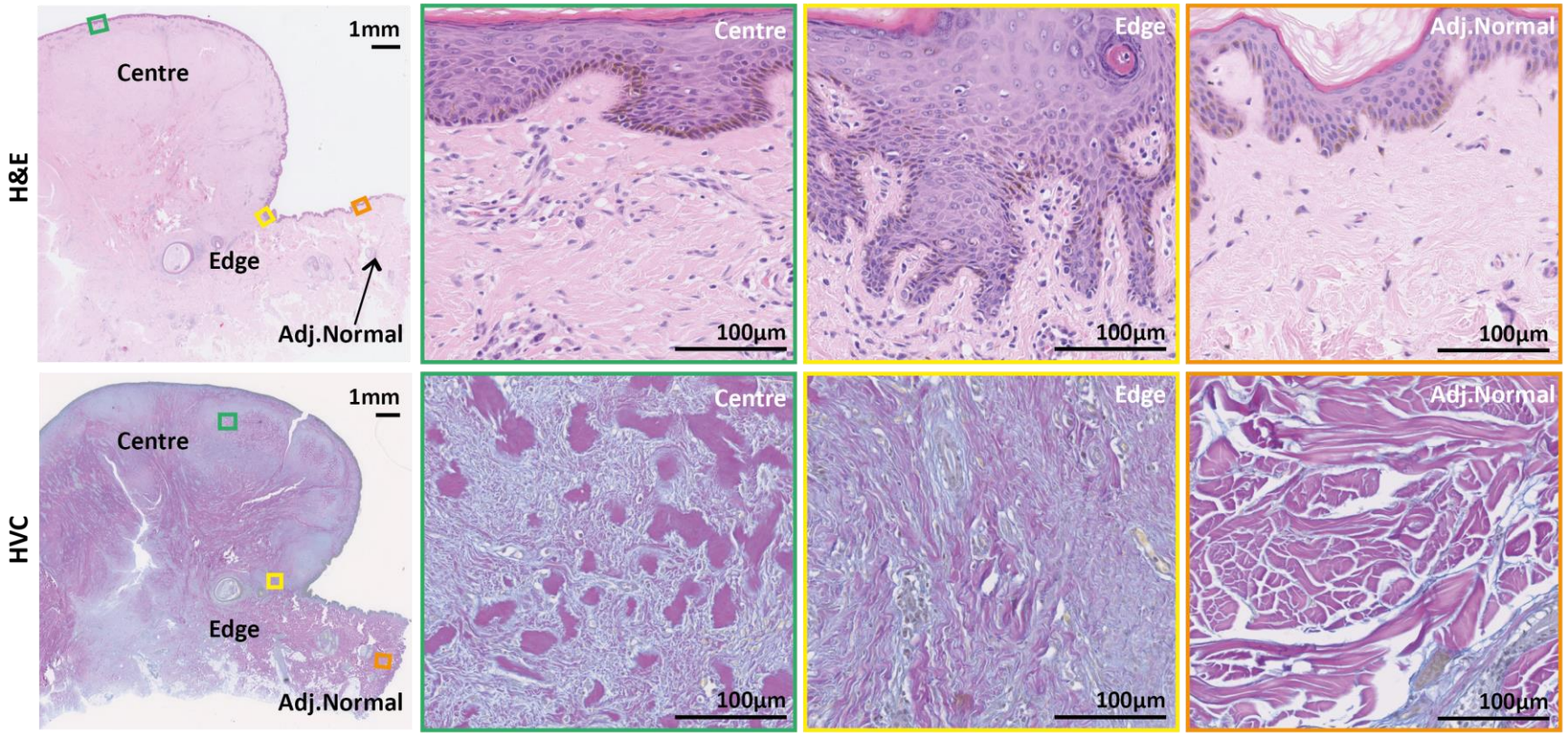

Figure 3-25 H&E and Herovici staining for keloid scar patient 51

1. From the sternum of an African-Caribbean male patient. The increased levels of melanin pigment are visible as diffuse brown shading in the basal epidermis. The H&E stain showed a thickened slightly epidermis in the keloid *centre*, with the *edge* showing invasive-looking ridges into the dermis. The Herovici (HVC) stain shows mature collagen nodules (in pink) surrounded by young collagen fibres (in blue) in the *central* dermis; a mixture of young and mature collagen fibres at the *edge* dermis; and loosely organised mature collagen fibres in the *adjacent normal* tissue.

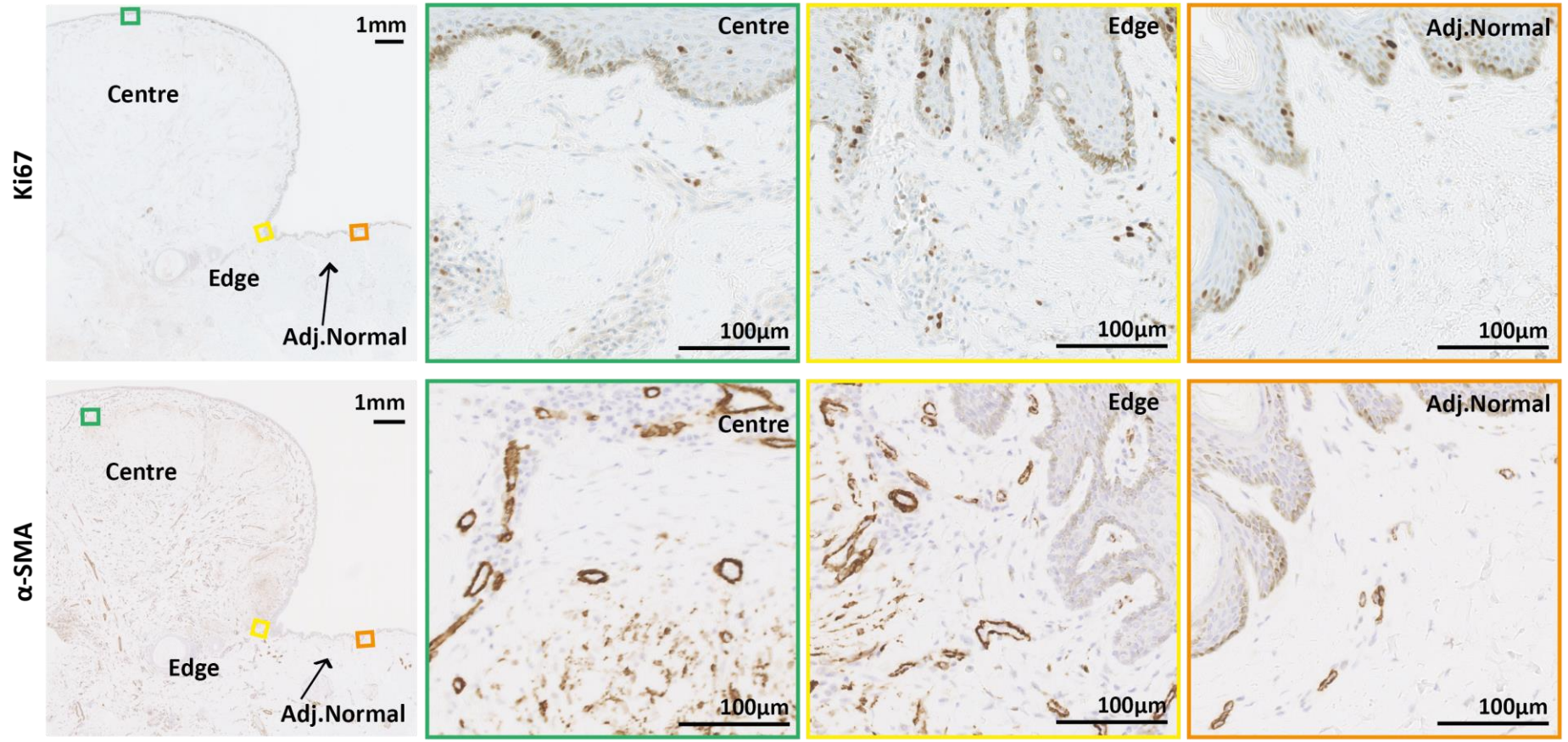

Figure 3-26 Ki67 and α-SMA protein expression in keloid scar patient 51.

DAB-Immunohistochemistry of keloid patient 51. **Ki67-**positive cells were reduced in the *central* and *adjacent normal* basal epidermis. The diffuse brown shading in the basal layer of the epidermis is the melanin pigment. **α-SMA** expression showed increased number of capillaries and myofibroblasts in the *central* and *edge* regions of the dermis.

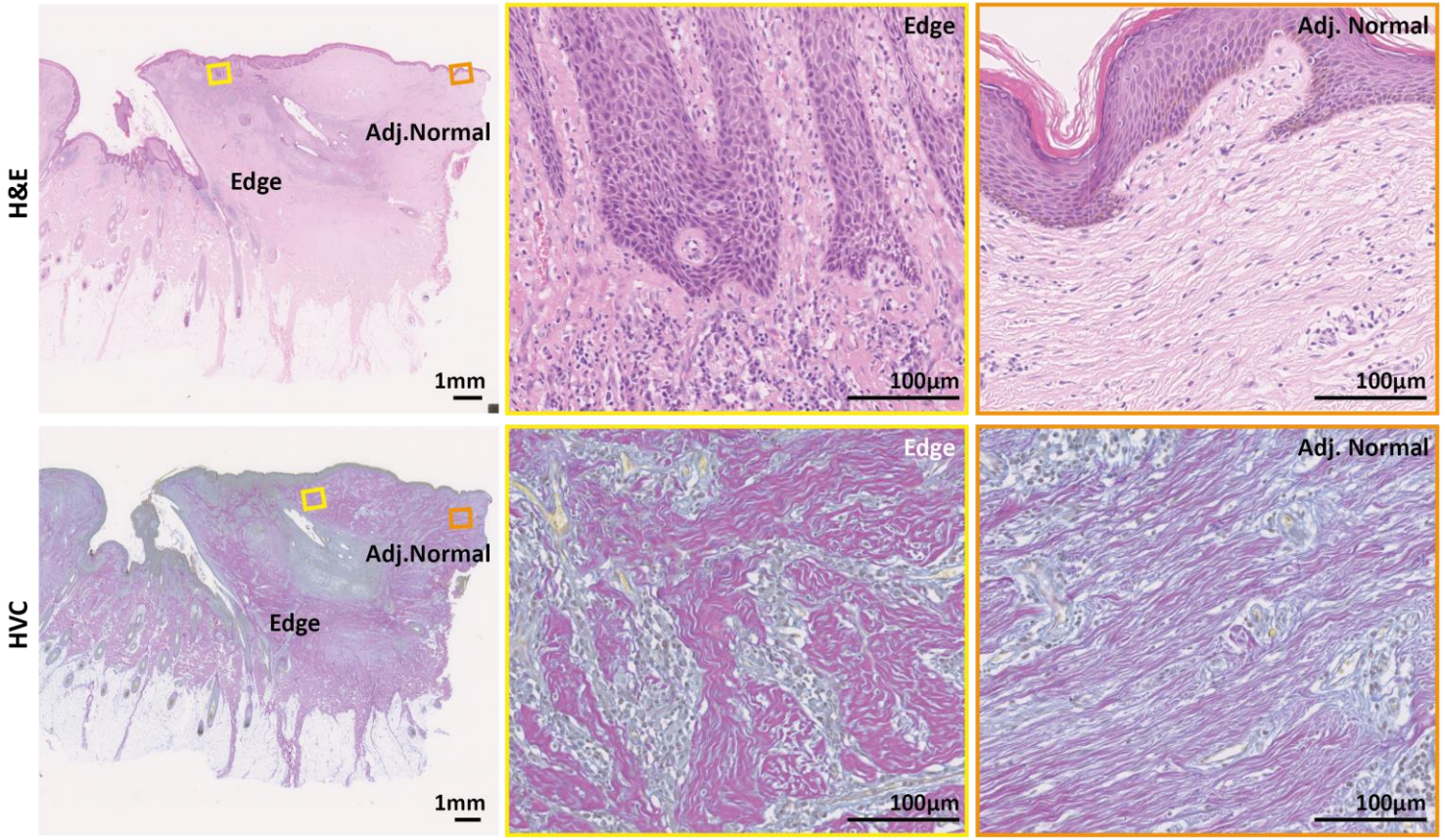

Figure 3-27 H&E and Herovici staining for keloid scar patient 55

From the nape of the neck of an African-Caribbean male patient. The H&E stain showed increased ridges and protrusion into the dermis of the majority of this keloid. The Herovici (HVC) stain showed thickened collagen fibres (in pink) surrounded by finer collagen fibres (in blue) in the main portion of the keloid dermis; and a mixture of young and mature collagen fibres in the *adjacent normal* tissue.

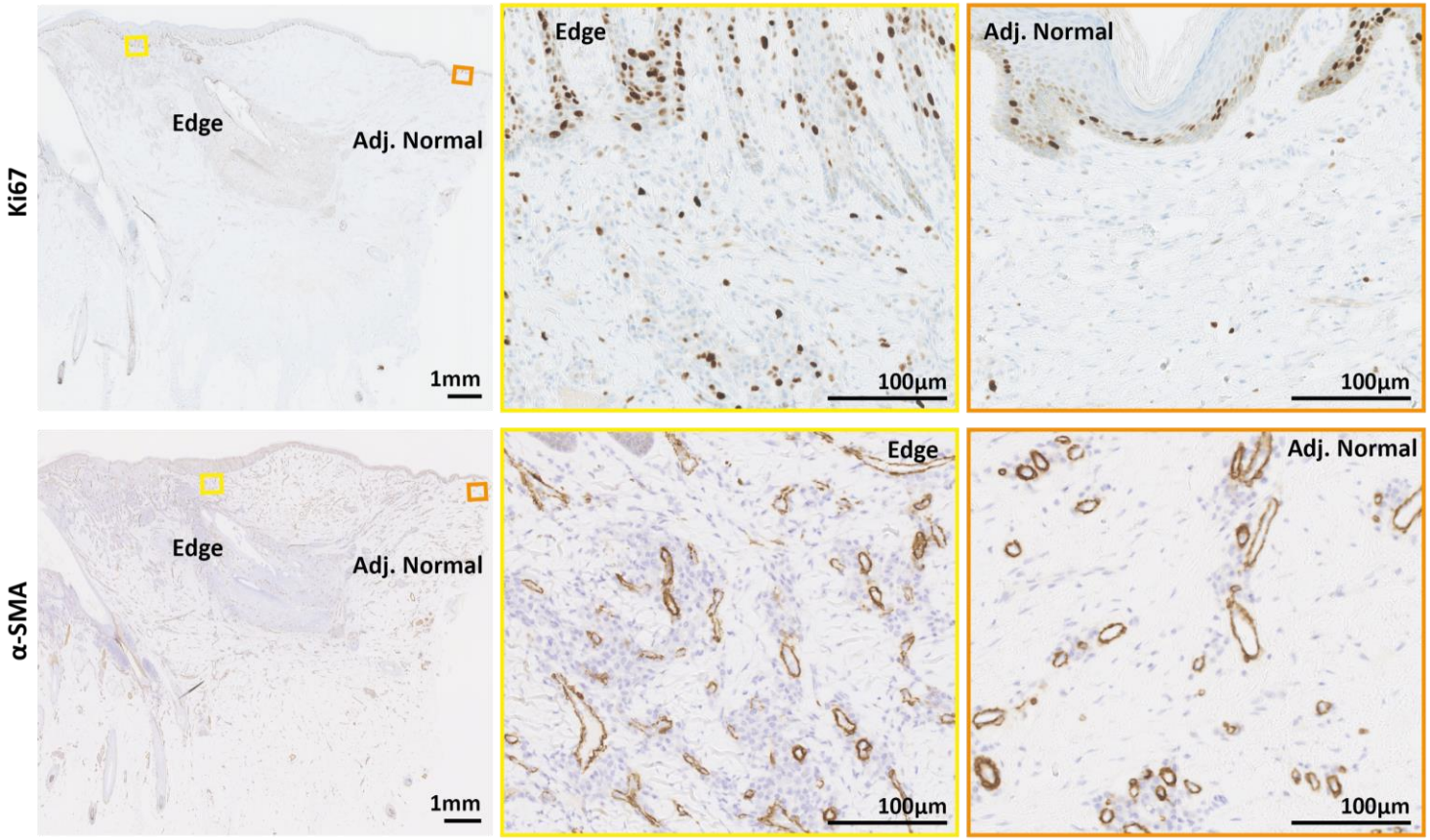

Figure 3-28 Ki67 and α-SMA protein expression in keloid scar patient 55.

DAB-Immunohistochemistry of keloid patient 55. This specimen did not show a typical "*centre*", therefore only "*edge*" and "*adjacent normal*" regions were defined. **Ki67-**positive cells appeared reduced in the *adjacent normal* basal epidermis, and increased in the *edge* dermis. **α-SMA** expression showed revealed a number of capillaries in the dermis, though very few myofibroblasts.

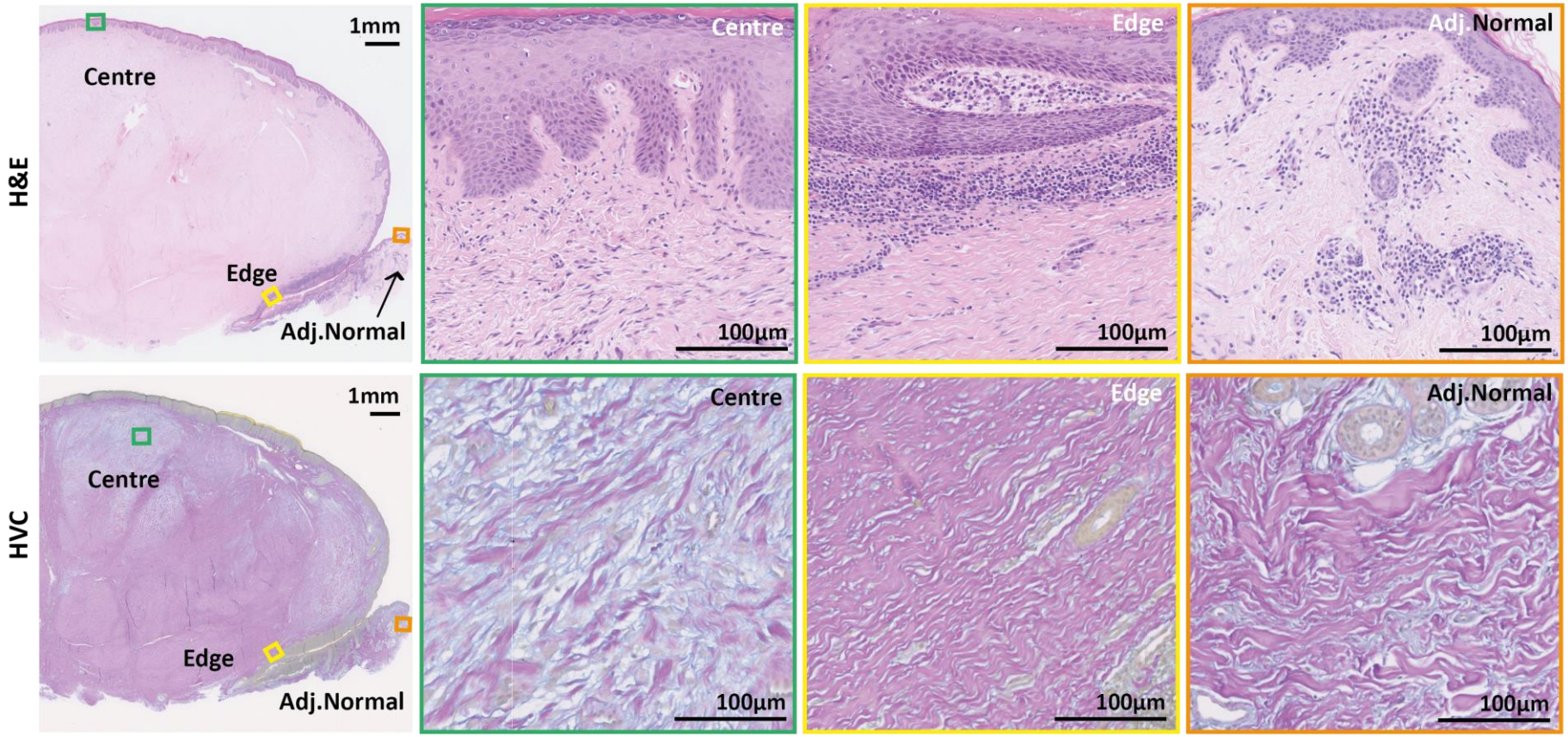

Figure 3-29 H&E and Herovici staining for keloid scar patient 70

From the post-auricular region of a 35-year old Caucasian male patient. The H&E stain showed a thickened epidermis in the *centre*, with the *edge* showing increased ridges into the dermis, and some areas of inflammation in the *edge* and *adjacent normal* tissue. The Herovici (HVC) stain showed mature collagen fibres (in pink) surrounded by young collagen fibres (in blue) in the *centre*; an increased density of well-organised mature collagen fibres at the *edge* dermis; and loosely organised mature collagen fibres in the *adjacent normal* tissue.

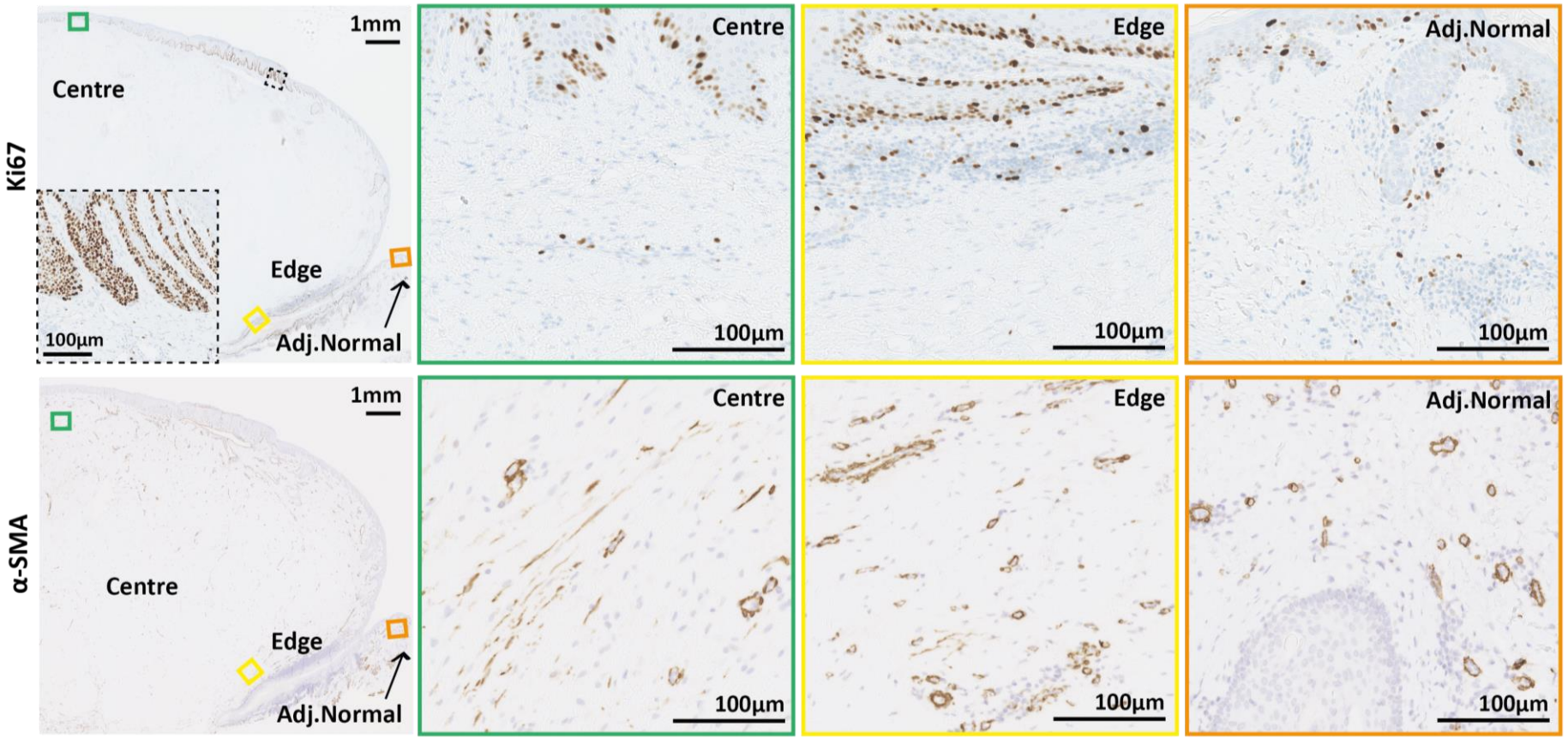

Figure 3-30 Ki67 and α-SMA protein expression in keloid scar patient 70.

DAB-Immunohistochemistry of keloid patient 70. Increased **Ki67** expression was observed in *edge* basal keratinocytes. There was also a highly proliferative epidermal area within the *central* region of the keloid (see high-power image with dotted line border, far left). **α-SMA** expression was low overall, revealing capillaries across the whole dermis, and a small number of myofibroblasts in the keloid *centre* dermis.

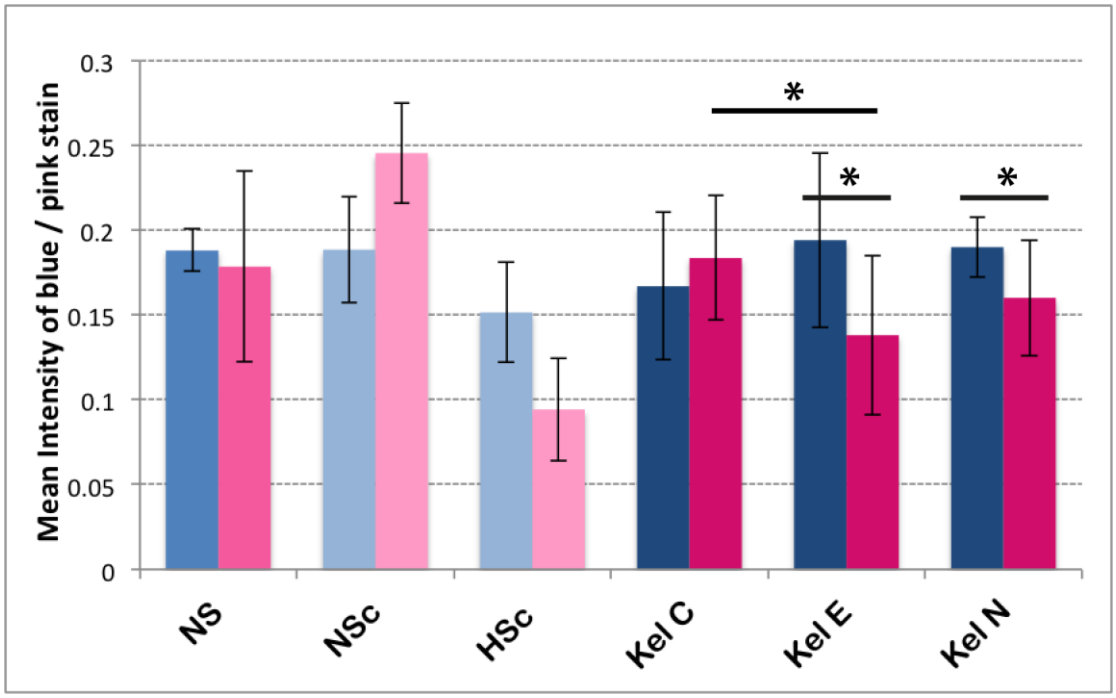

Figure 3-31 Quantification of Herovici staining in Normal skin and Scar tissues

The intensity levels of Blue and Pink/Red staining, representing young and mature collagen fibers respectively, were calculated in at least n=10 images per sample. Note that the NSc (normal scar) and HSc (hypertrophic scar) are from one individual tissue each, so they were not included in the statistical analysis. NS (normal skin) is based on n=9 tissues, and the Kel C, E and N (Keloid Centre, Edge and adjacent Normal regions) are based on n=12 tissues. Statistical analysis revealed no significant differences between normal skin and the keloid as a whole, though there was a statistically significant difference in mature collagen fibres (pink) between Keloid Centre and Edge. There was also an increased level of young collagen fibres compared to mature collagen fibres within the Keloid Edge and Adjacent Normal regions. * = $p<0.05$; Error bars represent the SD.

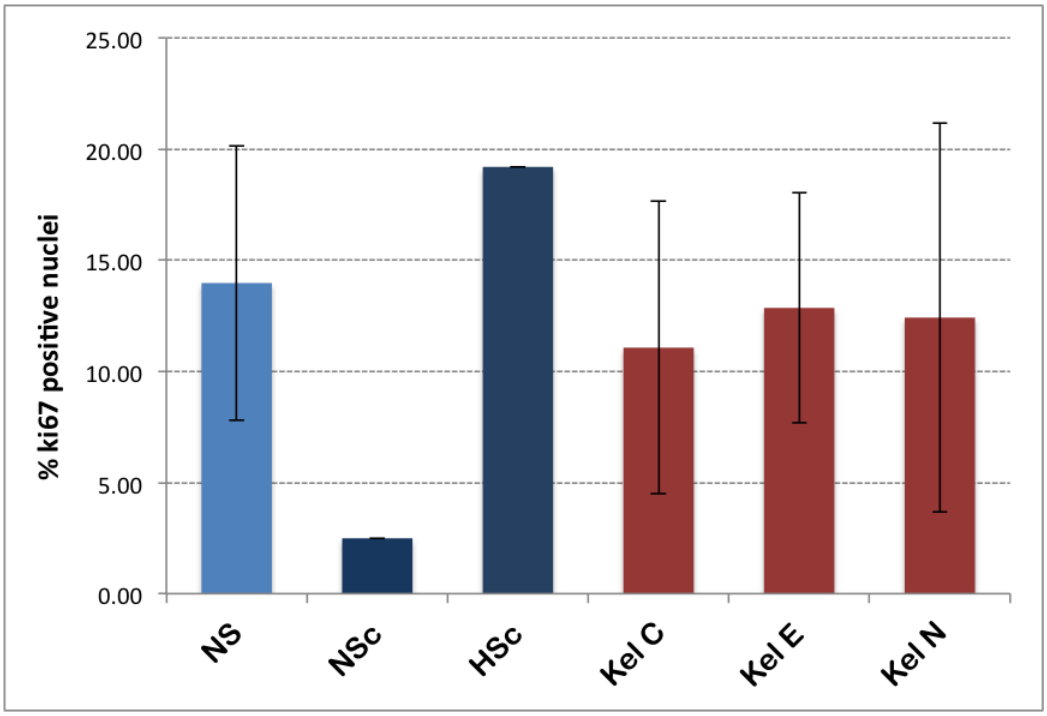

Figure 3-32 Quantification of Ki67 staining in Normal Skin and Scar tissues

The percentage of **Ki67**-positive nuclei per total number of nuclei was calculated in at least n=10 images per sample. Note that the NSc (normal scar) and HSc (hypertrophic scar) are from one individual tissue each, so they were not included in the statistical analysis. NS (normal skin) is based on n=9 tissues, and the Kel C, E and N (Keloid Centre, Edge and adjacent Normal regions) are based on n=12 tissues. There was no statistically significant difference between Normal Skin and any of the Keloid regions, as tested by a Student's T-test. Error bars represent the SD

Table 3-1 A summary of the histological features observed in each keloid region, based on the data from n=10 keloids.

	Centre	Edge	Adjacent normal
Overall morphology of tissue	*Epidermis* thickened and flattened. *Dermis* very thick and highly collagenous. No skin appendages present.	*Epidermis* slightly thickened, with highly irregular ridges. *Dermis* thickened, with some skin appendages visible.	Both e*pidermis* and *dermis closely* resembled healthy control skin morphology. Distance from scar margin to reach normal skin was variable between patients.
Collagen organization	Thickened mature collagen nodules, surrounded by finer collagen fibres, making up large acellular collagen bundles.	A mixture of young and mature collagen fibres, highly organised in parallel bands. Usually in line with the thick collagen bundles of the centre.	Mainly randomly oriented mature collagen fibres, as seen in healthy control skin.
Cell proliferation (Ki67)	No statistically significant differences in Ki67 expression across all keloid regions and normal skin, calculated in relation to the total number of cells present in each tissue.		
α-SMA expression	Variable between patients, though generally strong myofibroblast expression in reticular dermis, as compared to healthy control skin.	Variable between patients, though mostly showing a similar pattern of expression as in the centre keloid region.	Overall little to no expression, comparable to healthy control skin.

3.2.4 Matrix Metalloproteinases in normal and keloid tissue

All 9 healthy control skin samples and 10 keloid specimens characterised above were further analysed for protein expression of MMPs 1, 2, 13 and 14, using DAB-immunohistochemistry. In this section, images from 5 representative healthy control skin donors and 5 keloid scars are shown.

3.2.4.1 MMP1 protein expression

All normal healthy control patient tissues demonstrated a low expression of MMP1 in the epidermis, with faint expression in the upper epidermal layers, and a stronger level of expression in the basal layer (**Figure 3-33**). There was also a small amount of MMP1 expression in the dermis, though most of this was restricted to skin appendages and small blood vessel walls, previously identified in **section 3.2.2.3**.

A similar pattern of epidermal expression was seen in the selection of keloid scars (**Figure 3-34**), though there were some subtle differences between patients, and between keloid regions. Patient 35 showed almost no expression across the whole tissue, whereas patient 42 showed slightly increased MMP1 expression in the marginal epidermis, compared to the central epidermis. Both of these were overall under-regulated compared to normal skin. Keloids 34 and 40 revealed a comparable level of basal epidermal expression as for normal skin, though the central regions of the keloids 34 and 40 showed a reduced basal epidermal expression. For all keloids, there was a very small increase in MMP1 expression in the dermis, compared to healthy control tissue, with no apparent differences between keloid regions. Overall, there were minimal differences between keloid and normal tissues, with either no difference or a slight down-regulation observed in the keloids.

3.2.4.2 MMP13 protein expression

MMP13 expression was similarly distributed across the healthy control tissues, as for MMP1. In healthy skin donors 6, 9, and 18, epidermal expression was uniform across all layers. However, patients 6 and 9 also displayed areas of the epidermis

completely lacking MMP13 expression. Normal skin samples 4 and 21 showed a higher level of expression in the basal epidermis, though it was still overall a relatively weak signal (**Figure 3-35**). It was also noted that MMP13 showed nuclear expression in a number of epidermal cells, other than cytoplasmic expression.

As for the keloid scars, expression of MMP13 in the epidermis ranged from very little expression in keloid patient 26, to inconsistent expression in keloids 34 and 35, to near-uniform expression of the whole epidermis in keloid 42 (**Figure 3-36**). Here too, both nuclear and cytoplasmic expression of MMP13 was observed in the keloid epidermal compartment. Dermal expression of MMP13 in keloids was variable too, though overall slightly increased as compared to normal healthy skin. In keloid patient 42, it was notable that MMP13 expression in the dermis appeared to follow the patterns of the collagen fibre bundles identified with the Herovici stain in **section 3.2.3.4**. Overall, MMP13 protein expression in keloids was very slightly increased compared to normal skin, though no clear differences could be identified between scar regions.

3.2.4.3 MMP2 protein expression

MMP2 expression in both normal healthy skin and keloid scar tissue showed the strongest and most distinctive patterns out of the four MMPs examined here. In healthy normal skin, there was particularly strong MMP2 expression in the epidermis, though it was not uniform across all layers, or across the whole tissue sections. The basal epidermal layer retained the strongest signal, though all normal samples also showed regions of the epidermis where MMP2 expression was completely absent. In the dermis, MMP2 expression was more diffuse, and equally distributed across the whole tissue (**Figure 3-37**).

The keloid scars showed increased MMP2 expression, as compared to normal healthy skin. In the epidermis, MMP2 expression patterns and intensities varied between patients: keloids 26, 34 and 40 showed slightly enhanced expression in the upper epidermal layers; keloid 35 revealed a weak and uniform level of expression across the whole epidermis; whereas keloid 42 demonstrated strong

expression only in the centre and edge regions of the scar (**Figure 3-38**). In the dermis of all the keloid scars, there was a trend of increased MMP2 expression observed in the marginal regions. For keloid patients 34, 35 and 42 in particular, it appeared that MMP2 expression was at its highest in the dermal matrix surrounding the thickened collagen bundles described in **section 3.2.3.4** (**Figures 3-15, 3-17** and **3-23**, respectively for patients 34, 35 and 42). These regions of increased MMP2 expression, and thickened collagen bundles also correlate with the increased myofibroblast expression observed in the same patients (**section 3.2.3.6**, **Figures 3-16, 3-18** and **3-24,** respectively for patients 34, 35 and 42). For both healthy normal skin and keloid scars, MMP2 expression was also concentrated in hair follicle bulbs, their sebaceous glands, and in the lining of some small blood vessels.

3.2.4.4 MMP14 protein expression

MMP14 (MT1-MMP) protein expression demonstrated a very similar pattern to MMP2 expression described above. It was notably weaker than MMP2 overall, though followed the same trend of strong irregular distribution across the epidermis in both normal and keloid tissues. Normal skin patients 4 and 21 showed almost no epidermal expression of MMP14, whereas normal donors 6 and 9 demonstrated regions of strong or completely absent signal, and normal patient 18 had a consistently uniform epidermal expression (**Figure 3-39**). In all healthy skin specimens, the dermal MMP14 expression was low and equally distributed in the ECM. As for the keloid scars, they followed a variety of MMP14 expression patterns. Keloid patients 26, 34 and 40 showed a weak but mostly uniform level of expression across all epidermal layers, though had increased dermal expression in the marginal regions. In keloid 35, MMP14 expression was only seen in the marginal region of the epidermis, though was increased in the reticular dermis of the whole tissue. Finally, keloid patient 42 displayed strong MMP14 expression in the central and marginal epidermis, with no signal in parts of the marginal and adjacent normal epidermis. Dermal expression in this specimen was strongest in the marginal regions, surrounding the thick collagenous bundles in the main portion of the keloid (**Figure 3-40**).

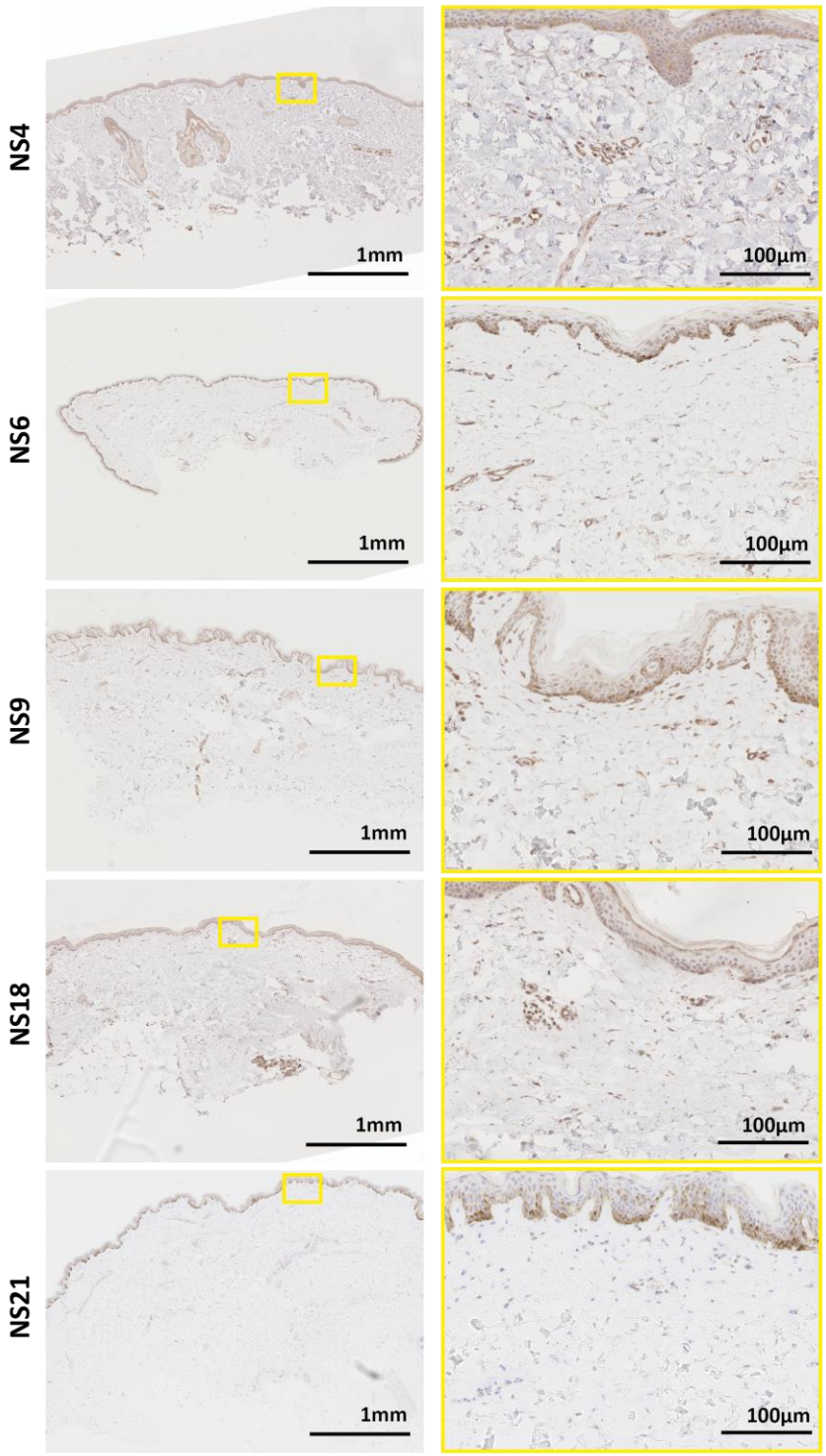

Figure 3-33 MMP1 protein expression in normal skin

Representative DAB-immunohistochemistry images of MMP1 expression examined in n=9 healthy control patients revealed an overall weak level of expression in the epidermis, and almost no expression in the dermis. Appendages and blood vessel walls showed MMP1 expression. In NS6, NS9 and NS21, the intense cytoplasmic brown

colour in the basal epidermis is melanin, due to the patients being of African-Caribbean origin. [**NS** = Normal Skin]

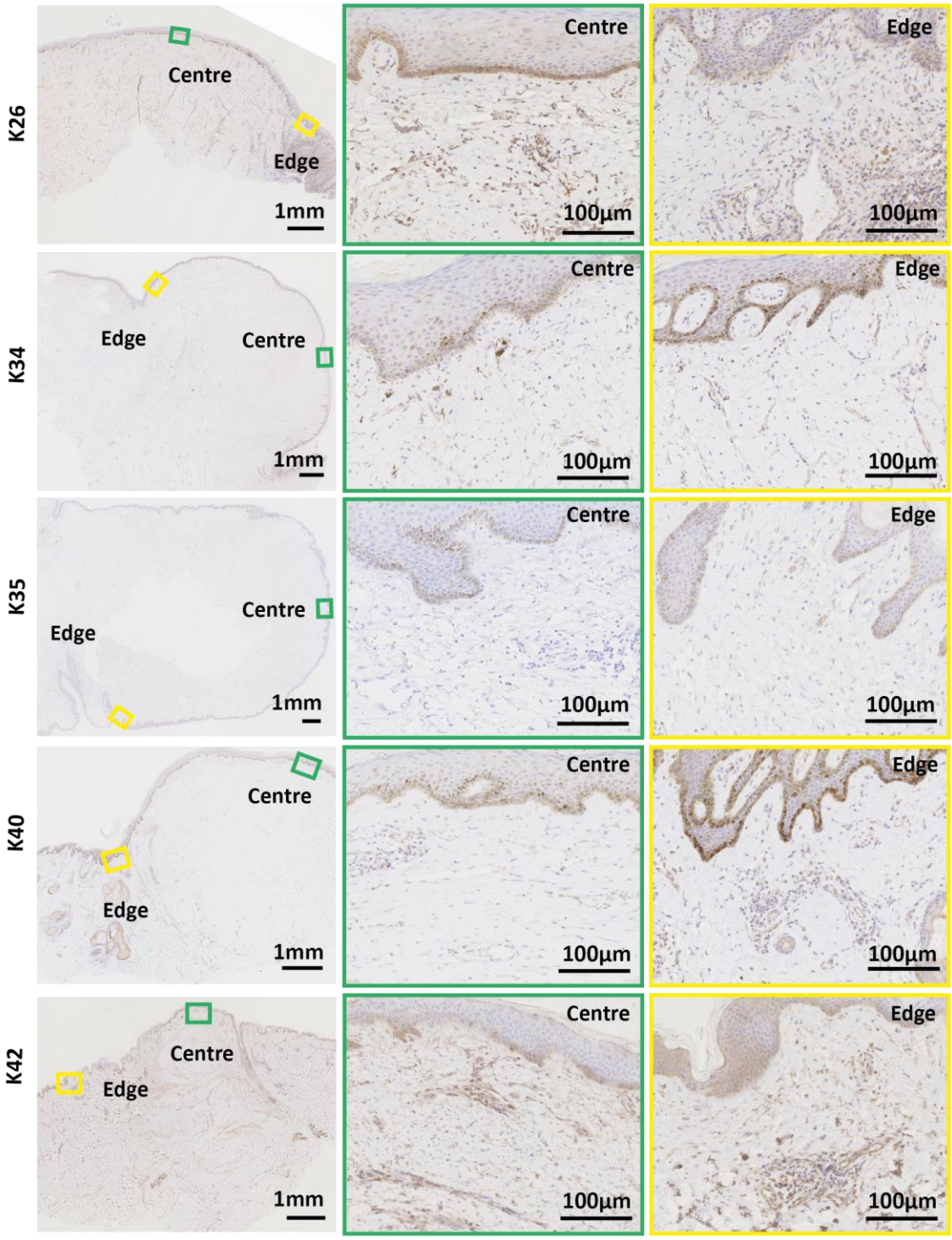

Figure 3-34 MMP1 protein expression in keloid scars

Representative DAB-immunohistochemistry images of MMP1 expression examined in n=12 keloid patients revealed an overall weak level of expression across the scar cross-sections. In patients K26, K40 and K42, the epidermis showed areas of low expression. In most patients, the dermis showed very little expression, mainly concentrated in the edge region of the scar. In all patients apart from K42, the more intense cytoplasmic

brown colour in the basal epidermis is melanin, due to the patients being of African-Caribbean origin. [**K** = Keloid Scar]

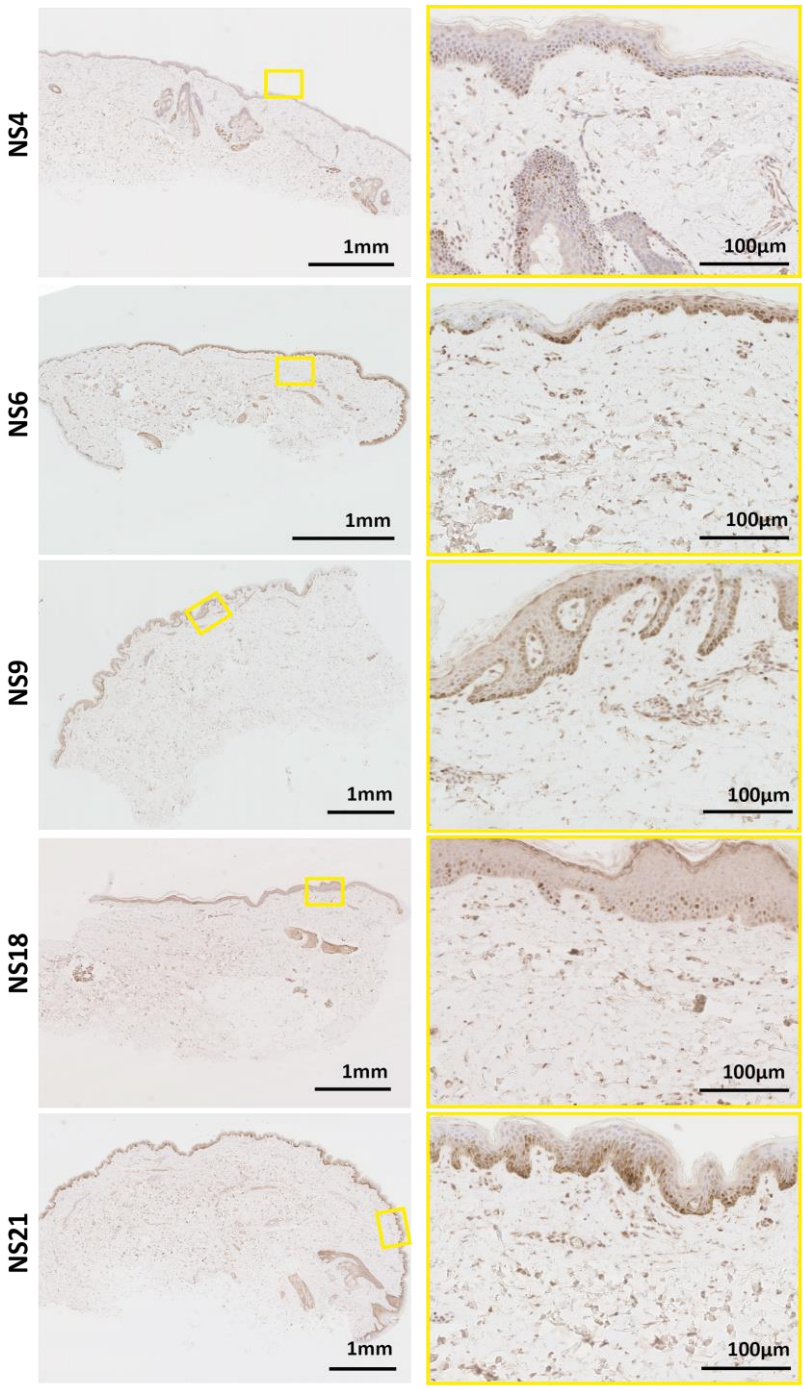

Figure 3-35 MMP13 protein expression in normal skin

Representative DAB-immunohistochemistry images of MMP13 expression examined in n=9 healthy control patients revealed a weak level of expression in both the epidermis, and dermis. Protein localization varied, appearing to be nuclear in some basal keratinocytes and hair follicle cells; cytoplasmic in the rest of the epidermis; and secreted in the ECM of the dermis. Appendages and blood vessel walls showed MMP13 expression. In NS6, NS9 and NS21, the intense cytoplasmic brown colour in

the basal epidermis is melanin, due to the patients being of African-Caribbean origin. [**NS** = Normal Skin]

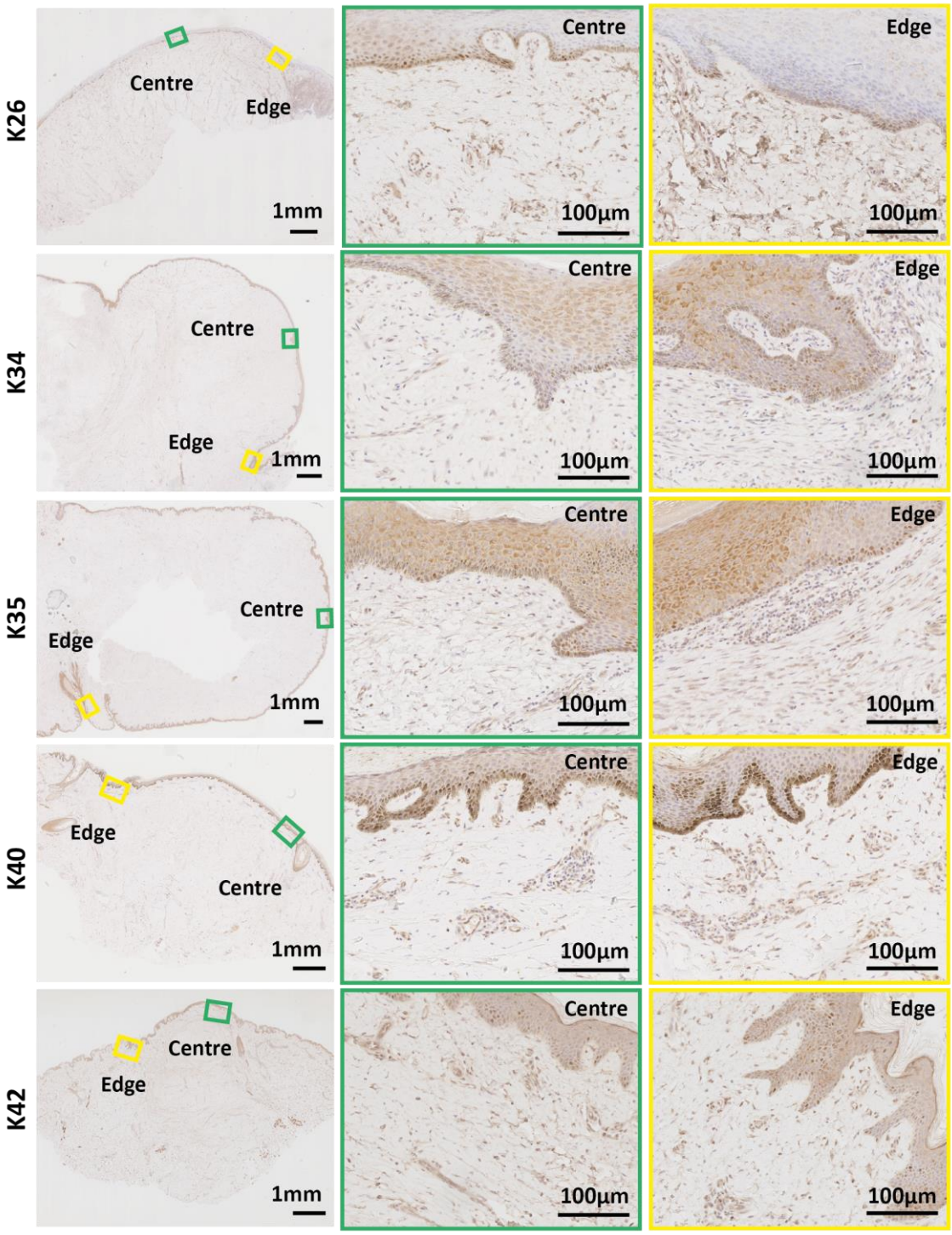

Figure 3-36 MMP13 protein expression in keloid scars

Representative DAB-immunohistochemistry images of MMP13 expression examined in n=12 keloid patients revealed either no expression (K26) or a medium level of mainly cytoplasmic expression (K34, K35, K42) in the epidermis. In most patients, the dermis showed very little expression, mainly concentrated in the edge region of the scar. In all patients apart from K42, the more intense cytoplasmic brown colour in the basal

epidermis is melanin, due to the patients being of African-Caribbean origin. [**K** = Keloid Scar]

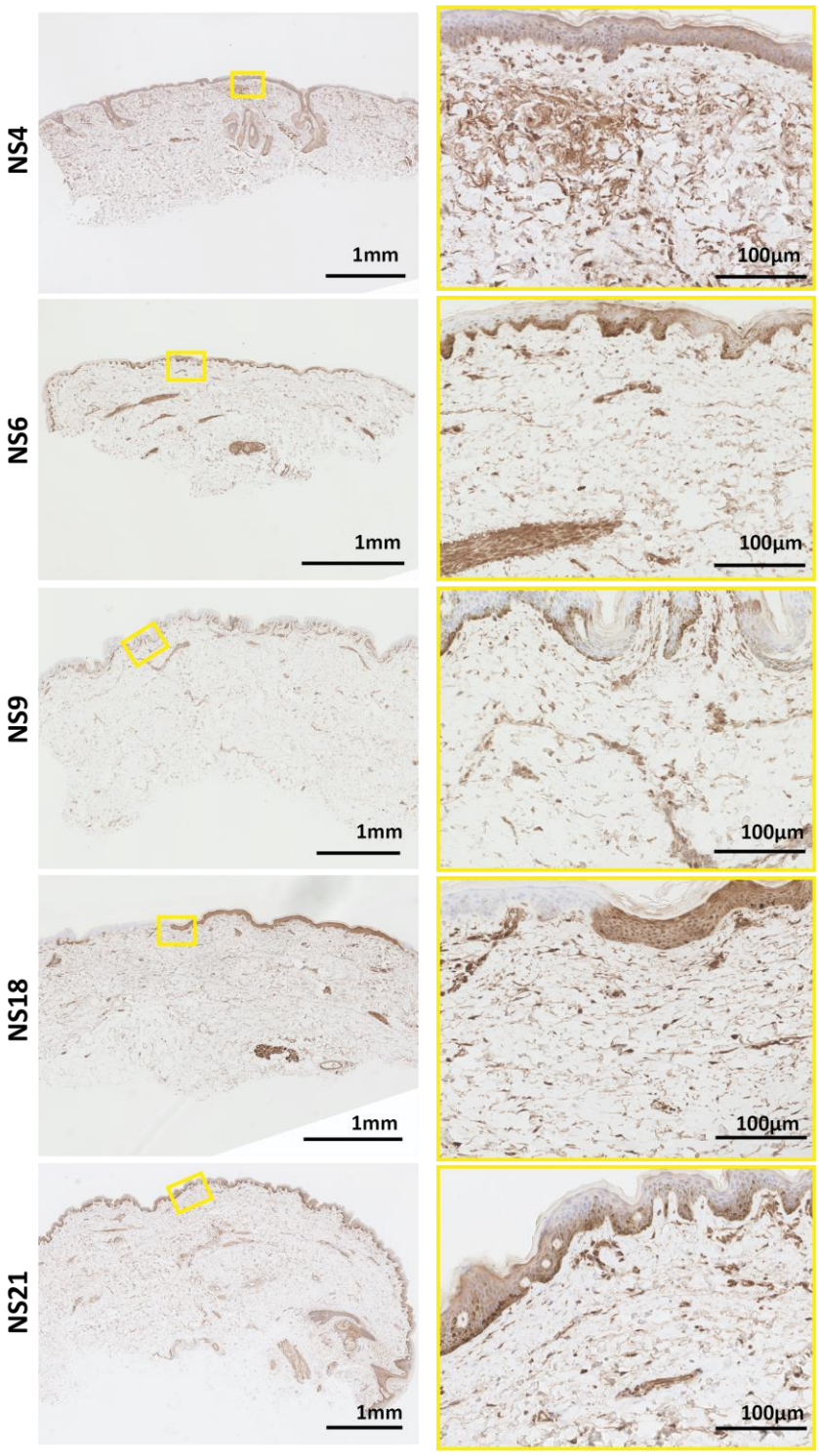

Figure 3-37 MMP2 protein expression in normal skin

Representative DAB-immunohistochemistry images of MMP2 expression examined in n=9 healthy control patients revealed an intermittently strong level of expression in the epidermis, and low levels in the dermis. Appendages, such as hair follicles and sweat glands, as well as blood vessel walls showed MMP2 expression. In NS6, NS9 and

NS21, the intense cytoplasmic brown colour in the basal epidermis is melanin, due to the patients being of African-Caribbean origin. [**NS** = Normal Skin]

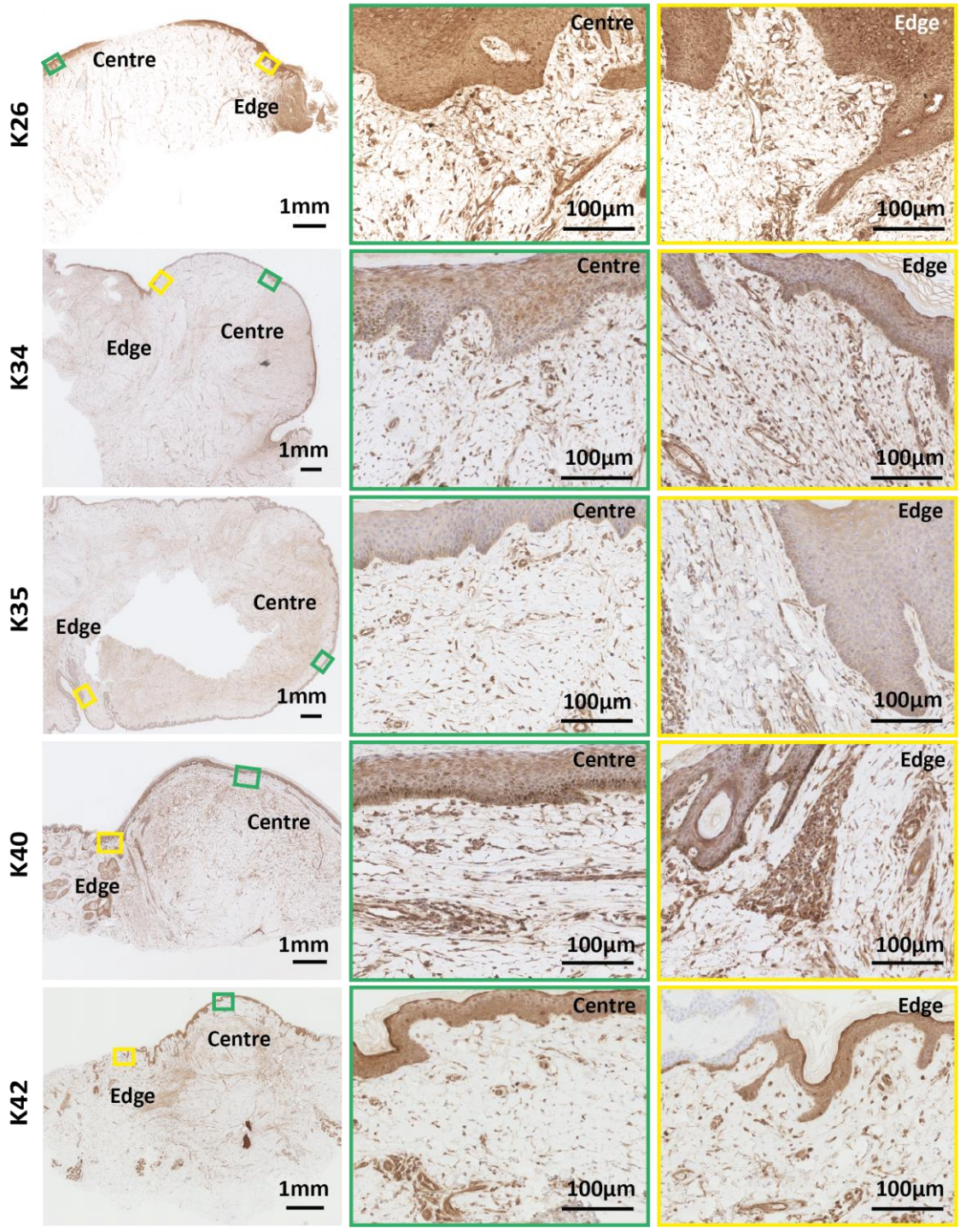

Figure 3-38 MMP2 protein expression in keloid scars

Representative DAB-immunohistochemistry images of MMP2 expression examined in n=12 keloid patients showed strong expression in most of the epidermis, as compared to normal skin. In most patients, the dermis showed increased expression in the edge region of the scar, especially around thickened collagen bundles. In all patients apart from K42, the more intense cytoplasmic brown colour in the basal epidermis is melanin, due to the patients being of African-Caribbean origin. [**K** = Keloid Scar]

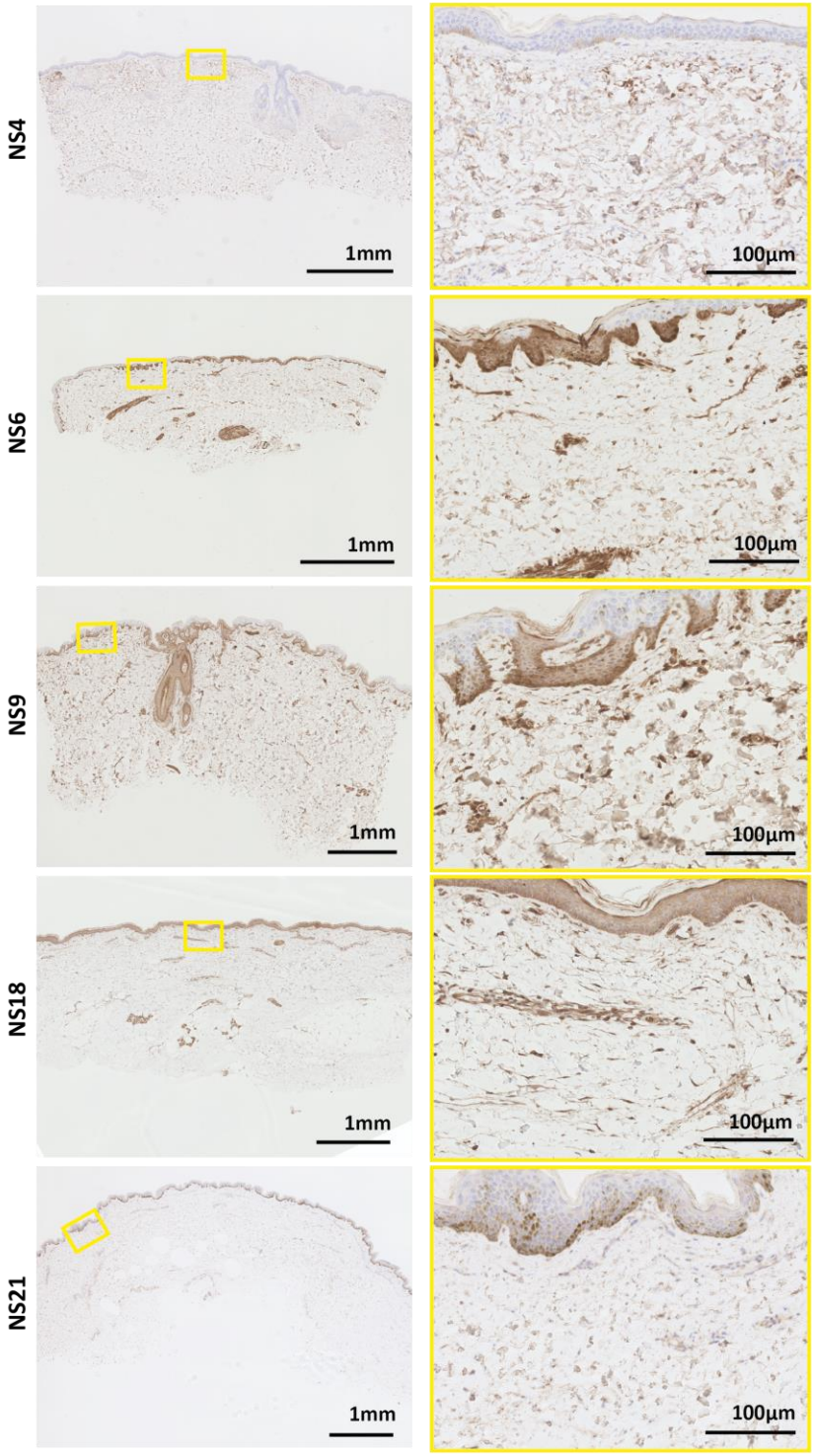

Figure 3-39 MMP14 protein expression in normal skin

Representative DAB-immunohistochemistry images of MMP14 in n=9 healthy control patients revealed a similar pattern of expression to MMP2, though was overall weaker in the epidermis, and almost absent in the dermis. Appendages, such as hair follicles and sweat glands, as well as blood vessel walls showed MMP14 expression. In NS6, NS9 and NS21, the intense cytoplasmic brown colour in the basal epidermis is melanin, due to the patients being of African-Caribbean origin. [**NS** = Normal Skin]

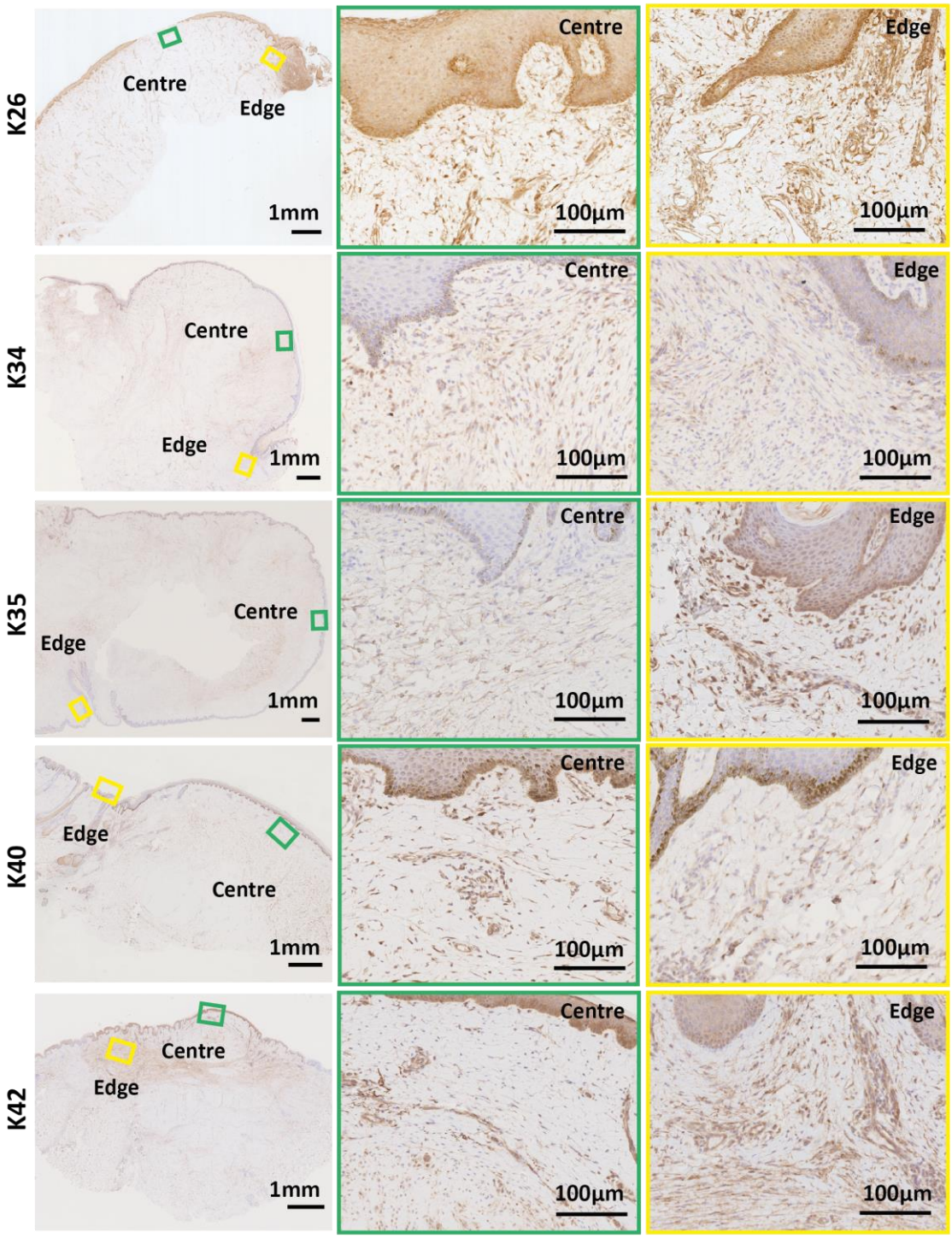

Figure 3-40 MMP14 protein expression in keloid scars

Representative DAB-immunohistochemistry images of MMP14 expression examined in n=12 keloid patients showed a slightly increased expression in the epidermis, as compared to normal skin. In most patients, the dermis showed a modest increase at the edges of the scars, especially around the thickened collagen bundles. In all patients apart from K42, the more intense cytoplasmic brown colour in the basal epidermis is melanin, due to the patients being of African-Caribbean origin. [**K** = Keloid Scar]

3.3 Discussion

3.3.1 Tissue characterisation

In the first half of this chapter, a detailed view of each individual keloid and healthy control skin specimen was characterised in terms of whole tissue morphology, using H&E staining, and collagen fibre formation, using a herovici chromogenic stain, whereby young and mature collagen fibres are visualized in blue or pink, respectively. DAB-Immunohistochemical analysis was used to examine cell proliferation by nuclear expression of Ki67, and fibrogenesis by α-SMA expression in dermal fibroblasts. I also included one normal scar and one hypertrophic scar for comparison against the keloid scars.

The keloids were all extralesionally excised, inclusive of central, marginal and normal tissue adjacent to the scar, however it was not always possible to visualize all three regions under histological examination. In patients 26, 34, 35, the adjacent normal tissue was not distinguishable from the edge keloid tissue. Patient 55 had a high level of inflammation, and the majority of the keloid was very irregular, meaning it was not possible to distinguish a central region, as seen in the rest of the keloid sample set. In the majority of the keloids it was possible to see the progression from the established scar tissue in the centre of the keloid, into the marginal expanding scar tissue at the edge of the keloid, and finally into the adjacent normal tissue.

3.3.1.1 Tissue morphology and collagen fibre structures

Several studies have aimed to define the morphological characteristics that differentiate keloid scars from hypertrophic scars, normal scars and normal skin. This characterisation is based on examining collagen and other ECM protein makeup of the tissues, (Ehrlich et al., 1994, Lee et al., 2004, Hellström et al., 2014, Chong et al., 2015), angiogenesis and hypoxia (Chong et al., 2015), proliferation and cellularity (Ehrlich et al., 1994, Chong et al., 2015), and immune cell infiltration (Chong et al., 2015). The histological hallmark of keloid scarring is an abundance of "keloidal collagen"; where interstitial collagen fibres are thickened, hyalinised, and have a distinct glassy appearance (Lee et al., 2004, Jumper et al., 2015). While

some studies have found keloidal collagen bundles are organised in line with the skin surface (Ehrlich et al., 1994), others have shown these collagen bundles to be haphazardly arranged in the dermis (Knapp et al., 1977, Da Costa et al., 2008). The ratio of collagen type I to type III has also been reported to be increased in keloids (Uitto et al., 1985, Abergel et al., 1985, Peltonen et al., 1991), mostly due to collagen type I being increased in keloid tissue, while collagen type III levels remain similar to normal skin.

In the data presented in this chapter, the central region of the keloid scar showed a flattened and thickened epidermis, as compared to normal skin. The dermis contained thickened and randomly organized mature collagen nodules, surrounded by finer, young collagen fibres. Together they formed large, acellular, cigar-shaped collagen bundles, running in parallel to the skin epithelium. The morphology of the keloid edge was highly variable between keloids, in both epidermal and dermal compartments. On the whole, the epidermis of the keloid edge was more invasive-looking, within which the epidermal cell layers were less defined due to the increased undulating appearance. The dermis generally revealed a higher proportion of young collagen fibres, often interlaced with mature collagen fibres. The collagen fibres were highly organised into parallel wavy bands, which were usually seen in line with the central keloid collagen bundles, and not necessarily in line with the skin surface. This was in contrast to the hypertrophic scar tissue analysed, where the wavy collagen fibres observed in the reticular dermis were organised in parallel to the epidermis.

Many of these findings are in line with findings in a number of earlier studies (Blackburn and Cosman, 1966, Kischer and Brody, 1981, Ehrlich et al., 1994). Ehrlich et al (Ehrlich et al., 1994) showed that bundles of collagen fibrils in mature keloid scars were indeed randomly oriented, however the closely packed parallel collagen fibres were only seen in hypertrophic scars. This was in contrast to my findings, where the collagen parallel band pattern was mostly observed at the keloid edge. It is likely that the keloid specimens used in Ehrlich's study were not inclusive of the marginal scar regions, and so they only observed the collagen fibre patterns in the mature central keloid scars.

The concept that there are structural and functional differences between the central, edge and adjacent normal sites of the keloid has not been thoroughly studied. One clinical study examined the level of disease recurrence and prognosis, after surgical excision of the whole keloid inclusive or not of the extralesional margin (Tan et al., 2010). The study authors found that keloid scar recurrence was increased in patients where the leading edge of the keloid scars had not been fully removed (Tan et al., 2010). In other studies, the different lesional sites of the keloid have revealed differences in gene expression regulation (Seifert et al., 2008, Shih et al., 2010b), more of which will be discussed in **Chapter 4**. In terms of collagen structure and morphology, Syed *et al* found that the thickened collagen bundles were found to be larger and appear more frequent at the edge of the keloid, compared to the central and adjacent normal tissue (Syed et al., 2011). The same study also reported that the ratio of mature-to-young collagen was at its highest at the keloid margin compared to the rest of the keloid, shown in both tissue and cultured fibroblasts (Syed et al., 2011). This was supported by my analysis of the Herovici staining, where the Keloid Edge region showed the largest difference between young and mature collagen fibres, compared to all other regions (**Figure 3-31**).

A distinction of the normal tissue directly adjacent to the keloid has previously been described in terms of differences in gene expression patterns (Seifert et al., 2008, Shih et al., 2010b, Syed et al., 2011), though most studies on keloid scarring only describe the central and marginal regions of the scars. My research shows that the tissue morphology and collagen structure in the adjacent normal tissue of the keloid was very similar to that of healthy control skin, especially in the dermis. The epidermis was sometimes slightly thicker, more proliferative, and with more protrusions than observed in healthy control skin samples. Nonetheless, there was some variability in the size of the keloid margin; i.e. the adjacent normal tissue truly resembling healthy control skin was at a distance of 2-10mm from the leading edge of the keloid. This could be a contributing factor in explaining why certain extralesionally-excised keloids appeared to lack healthy-looking tissue beyond the keloid edges, under histological examination. As it is not universal

practice to excise a larger than 2-4mm margin of normal skin around the keloid margin, it is possible that the majority of extralesionally-excised keloids discussed in the literature, do not in fact contain truly adjacent normal tissue.

A number of keloid specimens demonstrated areas of inflammation, identified by a high concentration of polymorphonuclear cells (characteristic of white blood cells) seen in the dermis. Patients 26, 32, 51 and 70 (**Figures 3-11, 3-13, 3-25,** and **3-29**) showed small patches of inflammatory invasion around the edges of the keloid, whereas patient 55 (**Figure 3-27**) had a high level of inflammation in the main portion of the keloid away from the adjacent normal skin.

3.3.1.2 Cell proliferation

I examined the pattern of cell proliferation in keloid tissues, using Ki67 as a marker of cells in the proliferative state (Scholzen and Gerdes, 2000). Across the whole keloid, it appeared as if the proportion of cells in the proliferative state was increased in comparison to healthy control skin, with the basal layer of the epidermis showing the highest level of Ki67 expression. However, quantifying the number of proliferative cells as a percentage of the total cells present in the tissue, demonstrated that there was no statistically significant difference between any of the sample groups. This held true whether comparing normal skin to keloid scar as a whole, or comparing the individual keloid regions.

During normal wound healing, the proliferation phase is marked by the formation of granulation tissue, re-epithelialisation, angiogenesis, and leads on to tissue remodeling by increasing ECM deposition (Baum and Arpey, 2005, Jumper et al., 2015). It is thought that an extended proliferation phase during wound healing strongly influences keloid scar formation (Jumper et al., 2015, Young et al., 2013). The keloid epidermis is often thickened with flattened rete ridges (Lee et al., 2004, Köse and Waseem, 2008), and the basal keratinocytes express increased levels of keratin 16 – a hyperproliferation marker (Bloor et al., 2003, Ong et al., 2010, Jumper et al., 2015). It has long been known that local autocrine and paracrine signaling occurs between the epidermal and dermal cells, influencing inflammatory responses (Pasparakis et al., 2014) and other wound healing

processes during scar formation (Garner, 1998, Machesney et al., 1998, Jumper et al., 2015). Keratinocytes have been shown to help regulate fibroblast proliferation, apoptosis, and collagen production, during normal wound healing (Jumper et al., 2015, Wang et al., 2015, Köse and Waseem, 2008).

Few studies have been reported on the keratinocyte-fibroblast interaction in keloids, though it has been shown that keloid keratinocytes increase proliferation and reduce apoptosis of the associated fibroblasts (Funayama et al., 2003, Phan et al., 2003). Also, co-culturing keloid keratinocytes with normal fibroblasts leads to increased production of collagen type I by the fibroblasts (Lim et al., 2002b, Mukhopadhyay et al., 2005). Based on this, it is assumed that a prolonged period of increased keratinocyte proliferation would stimulate the associated fibroblasts to continue producing more ECM proteins, eventually leading to the fibrotic state of a keloid scar.

3.3.1.3 α-SMA expression

3.3.1.3.1 Myofibroblasts

I used immunohistochemical detection of α-SMA protein expression, primarily as a marker for fibroblast activation (Darby et al., 1990) in the keloid scars under examination. Myofibroblasts are differentiated fibroblasts which contain cytoplasmic bundles of microfilaments, nuclear indentations, and cell-cell and cell-stroma connections (Ehrlich et al., 1994). Myofibroblasts are thought to develop gradually during wound contraction, from granulation tissue fibroblasts, and temporarily express α-SMA while they help to remodel the wound bed (Eddy et al., 1988, Darby et al., 1990, Welch et al., 1990, Tsukada et al., 1987). In fibrotic conditions, including hypertrophic scars (Baur et al., 1975) and keloids (Ehrlich et al., 1994), myofibroblasts have been shown to persist, continually synthesizing ECM, which leads to the characteristic collagenous tissue of fibrosis (Gabbiani and Majno, 1972, Skalli et al., 1989).

In this chapter, normal skin and the normal scar showed no myofibroblast expression, whereas the hypertrophic scar and the majority (8 out of 10) of the keloid scars displayed increased levels of myofibroblasts in the reticular dermal

layers. Previous work on the role of myofibroblasts and how best to detect them in hypertrophic scarring and keloids has been conflicting (Jumper et al., 2015, Matsuoka et al., 1988, Sarrazy et al., 2011). It has been suggested that α-SMA staining could help differentiate between hypertrophic scars and keloids, as only hypertrophic scars demonstrated myofibroblast expression (Ehrlich et al., 1994). It has since been confirmed that keloids do in fact express α-SMA, though it cannot reliably be used as a predictive marker of distinction between scar types, as there is substantial expression level variability between hypertrophic and keloid patients (Jumper et al., 2015, Lee et al., 2012, Lee et al., 2004). The conflicting results between studies may be linked to the variability in how keloid scars have been excised (as discussed above in **section 3.1.1.1**), i.e. whether the samples analysed are inclusive of the marginal and extralesional keloid sites, as is the case in my sample set. Another observation from my findings was that particularly concentrated areas of myofibroblast expression appeared to correlate well with the acellular collagen bundles identified earlier on (**section 3.1.1.1**). This is in agreement with studies where α-SMA staining was found positive within collagen nodules of keloid tissue (Santucci et al., 2001, Hunasgi et al., 2013, Jumper et al., 2015). In fact, it was postulated that α-SMA expression may decrease overtime in hypertrophic scars, allowing for distinction between young and old lesions; whereas α-SMA expression in keloids remains constant regardless of lesion age. During normal wound healing, myofibroblasts eventually apoptose once wound contraction and re-epithelialisation has been completed. The failure of myofibroblasts to apoptose in keloid scars could explain the ongoing growth and proliferation seen in these fibrotic lesions (Darby et al., 2014, Santucci et al., 2001, Sarrazy et al., 2011, Hinz, 2007, Jumper et al., 2015).

3.3.1.3.2 Tissue vascularisation

As α-SMA is a major component of vascular smooth muscle cells (Gabbiani et al., 1981), blood vessels were also easily visible in the tissues examined in this chapter. There was an apparent increased number of blood vessels in the whole keloid and hypertrophic scar dermis compared to normal skin, with particularly high density of capillaries observed at the keloid scar edge, and in between the epidermal protrusions across all keloid regions. This observation is supported by

an early study, where through scanning electron microscopy, they observed a higher number of blood vessels in the hypertrophic and keloid scars, compared to normal scar tissue (Lametschwandtner and Staindl, 1990, Ehrlich et al., 1994). Later, it was found that keloid scars actually demonstrate a decreased level of angiogenesis, compared to hypertrophic and normotrophic scars, as tested by measuring factor VIII-related antigen by IHC staining (Beer et al., 1998). Since then there have been several studies showing increased vascularization in keloid scars, compared to normal skin (Gira et al., 2004, Trompezinski et al., 2000, Mogili et al., 2012, Fujiwara et al., 2005b). Vascular endothelial growth factor (VEGF) gene expression was found to be increased in keloid epidermis (Gira et al., 2004); TGF-β1 action appeared to promote VEGF secretion in keloid fibroblasts *in vitro* (Trompezinski et al., 2000, Fujiwara et al., 2005b) and *in vivo* (Fujiwara et al., 2005b); and in keloid patient sera and tissues, VEGF was found to be increased, while endostatin (anti-angiogenic factor) was decreased compared to healthy controls (Mogili et al., 2012).

Using α-SMA as a sole marker of angiogenesis or tissue vascularization is clearly very limited, with several growth factors being responsible for this process (Syed and Bayat, 2012, Zhang et al., 2015). Imaging techniques for vessel detection would also provide a much more comprehensive examination of vascularization within tissues (Cole and Herron, 2010). Given the inherent variability between keloid patients, a much more thorough, multi-faceted examination of angiogenesis and vascularization would be interesting to complete in a wide array of keloid lesions, as this may help to further elucidate some of the variable histopathology of this disorder.

It is clear that the definition of the separate keloid regions is subject to bias, as there are no definitive boundaries between each region. In most cases, the scar tissue morphology changes gradually from region to region, with each individual keloid demonstrating unique differences in morphology and fibrogenic characteristics. It would be interesting to further classify keloid specimens according to gender, patient age, scar age, body location of scar, and treatment history, in order to be able to correlate the observed characteristics to specific

changes in tissue morphology, and thereby establish a more clear cut method of defining the different keloid sites. This, however, would require a much larger number of samples, to enable the application of more sophisticated and rigorous statistical analysis for sound conclusions to be made, which was beyond the boundaries of the research presented in this thesis.

It would have been interesting to also look at keratin expression and apoptosis markers for a more comprehensive characterisation, however as keloid tissue morphology and states of proliferation and apoptosis have been widely published, I focused on confirming that these keloids were indeed fibrogenic and displayed the basic characteristics previously observed. The data presented in this chapter provide additional tissue morphology information derived from the marginal and extralesional sites of the keloids, which is rather limited in current literature. Accordingly, I aim to present a more complete impression of the keloid development.

3.3.2 MMP expression in keloids

Matrix metalloproteinases are a subfamily of extracellular zinc- and calcium-dependent endopeptidases, which are part of the metzincin superfamily of proteins (Bode et al., 1993, Huxley-Jones et al., 2007). Moreover, MMPs are historically recognized for their role in catabolizing specific ECM molecules. More recently however, it has become clear that the primary role of the MMPs is to process bioactive molecules such as growth factors, cytokines and chemokines, thereby regulating the activity of these proteins and the downstream effects on cell behaviour (Gill and Parks, 2008, Egeblad and Werb, 2002, Mott and Werb, 2004). Such cell processes include leucocyte activation, chemokine processing, and antimicrobial defense (Parks et al., 2004, Manicone and McGuire, 2008, Gill and Parks, 2008). During wound healing (described in detail earlier in **Chapter 1**), MMPs participate in the regulating mechanisms of all the tissue repair phases: inflammatory cells express MMPs, which then regulate trans-epithelial migration of leukocytes and chemokine activity (Parks et al., 2004); MMPs cleave components of cell-cell junctions and cell-ECM contacts at the wound edges in order to achieve re-epithelialization (Singer and Clark, 1999); and finally tissue

remodeling is aided by MMP activity, both via direct proteolytic degradation of ECM proteins and through their effects on cell migration (Gill and Parks, 2008).

In fibrosis of the liver, lung and kidney, MMPs have shown to be both inhibitory and stimulatory, depending on the tissue type, cell types involved, and other MMPs present (Giannandrea and Parks, 2014). Some research groups have supported using circulating levels of certain MMPs, including MMPs 1, 2, 7, 8, 9, and 13, or their degradation products (collagen fragments) as potential biomarkers of active fibrosis taking place (Veidal et al., 2011, Leeming et al., 2011, Rosas et al., 2008). Nonetheless, identified roles for specific MMPs are usually not the same across different organ systems (Giannandrea and Parks, 2014). MMP research within keloid scarring has been varied, but conflicting, as discussed earlier on (**section 3.1.2**).

In this chapter, protein expression patterns of MMPs 1, 2, 13 and 14 were examined in all of the characterised normal (n=9) and keloid (n=10) specimens. Images from 5 representative normal skin samples and 5 representative keloid scars were presented in the data, showing the varied patterns of MMP expression observed across the full sample set.

3.3.2.1 Collagenases -1 and -3 (MMP1 and MMP13)

MMP1 (collagenase-1) and MMP13 (collagenase-3) are capable of cleaving fibrillar collagen types I, II, III, V and IX (Reynolds, 1996, Ulrich et al., 2010, Ala-aho and Kähäri, 2005), though they have been shown to act on a wide range of ECM substrates including fibronectin, aggrecan, laminin, vitronectin, and perlecan (Ala-aho and Kähäri, 2005). As with most MMP family members, MMPs 1 and 13 also have a major role in regulating chemokine activity, affecting cell migration and proliferation in inflammatory and wound repair responses (Parks et al., 2004, McCawley and Matrisian, 2001).

In the keloid samples analysed in this chapter, both MMPs 1 and 13 showed a very low level of protein expression overall, in both the epidermis and dermis, with very few differences between normal skin and keloid scars. MMP1 protein

expression in keloid scars was either the same as in normal skin, or slightly lower than in normal skin. MMP13 protein expression appeared to be very slightly increased in keloids compared to normal skin. These findings are in line with previous studies, though there are also areas of conflict. Looking at primary cultured fibroblasts, MMP1 gene and protein expression was significantly decreased, while MMP13 was significantly increased in keloid-derived fibroblasts compared to normal fibroblasts (Uchida et al., 2003). By contrast, MMP1 protein expression levels were shown to be increased by 6-fold in keloid-derived fibroblasts compared to normal fibroblasts, in another study (Fujiwara et al., 2005a). This discrepancy could be due to *in vitro* studies on MMPs being notoriously poor at predicting their physiologic functions (Giannandrea and Parks, 2014, Parks et al., 2004, Gill and Parks, 2008). In keloid patients who underwent pulsed-dye laser (PDL) treatment, some scar tissue regression was observed, and MMP13 protein expression was significantly increased, while there was no change in MMP1 protein expression, as tested by IHC and Western Blot (Kuo et al., 2005). This suggests that MMP13 could be acting as an anti-fibrotic enzyme through PDL treatment, though it was not clear from the study whether MMPs 1 and 13 were altered in keloid tissues compared the normal tissues, regardless of the effect of the PDL treatment.

In other forms of fibrosis, Iimuro *et al* used a thioacetamide (TAA)-induced rat model of acute hepatocellular injury to show that overexpressing MMP1 in fibrosis increased scar tissue degradation (Iimuro et al., 2003). This proposed potential therapeutic strategy was further tested in myocardial (Foronjy et al., 2008) and muscle (Kaar et al., 2008) fibrosis mouse models, where a degradation of the scar tissue was also observed. In a chronic liver fibrosis mouse model, where mice are treated with carbon tetrachloride (CCl_4) over a period of at least 10 weeks, MMP13 also demonstrated anti-fibrotic effects. Fibrosis was seen to persist in MMP13-deficient CCl_4-treated mice (Fallowfield et al., 2007); and overexpression of MMP13 in CCl_4-treated rats appeared to promote hepatocyte proliferation and tissue remodeling, via the activation of HGF (hepatocyte growth factor), MMP2 and MMP9 (Endo et al., 2011). However, it is unlikely that the anti-fibrotic effect of MMP13 is due to MMP2 and MMP9 acting directly on interstitial collagen, as their

catalytic domain structures do not interact easily with the large fibrillar triple chains of interstitial collagens (Giannandrea and Parks, 2014, Parks et al., 2004). Conversely, MMP13 also demonstrated pro-fibrotic effects, in a bile-duct ligation (BDL) model of liver injury, where a loss of MMP13 led to a reduction in cytokine production, myofibroblast activation, collagen expression, and of the fibrotic tissue in general (Uchinami et al., 2006).

My findings support elements of the literature discussed above, which show MMP1 to be unaltered or decreased in keloids and other fibroses, and MMP13 to be increased, compared to healthy control tissue. Kuo et al suggested that increased MMP13 production may be involved in the remodeling of keloid scar tissue, by cleaving collagen type III and allowing new collagen type I to be synthesized (Kuo et al., 2004, Kuo et al., 2005). The high concentration of collagen type I present in the keloid dermis, alongside the increased level of MMP13 and minimal difference in MMP1 expression in the keloid dermis noted in this chapter, would support this hypothesis.

3.3.2.2 Gelatinase A (MMP2)

MMP2 is capable of cleaving collagen types IV, V, VII, X, XI and XIV, gelatin, elastin, proteoglycan and fibronectin, and is expressed by a range of cell types including keratinocytes, fibroblasts, and endothelial cells (Hernández-Pérez and Mahalingam, 2012, Kerkelä and Saarialho-Kere, 2003, Sawicki et al., 2005). MMP2 is also widely studied in the context of inflammation and modulating chemokine activity (Parks et al., 2004, McQuibban et al., 2000).

In my findings, MMP2 showed a marked increase in protein expression in the keloid scars, particularly in the dermis. This supports several studies where MMP2 has been shown to be overexpressed in keloids (Ulrich et al., 2010, Bran et al., 2010, Fujiwara et al., 2005a, Tanriverdi-Akhisaroglu et al., 2009, Imaizumi et al., 2009). MMPs 1, 2 and 9 circulating protein expression in hypertrophic scar and keloid patient sera showed no significant differences to healthy control patients. However, when the same patients' scar tissues were analysed for gene expression levels, only MMP2 was significantly increased in keloid and hypertrophic scars

compared to normal scar tissue (Ulrich et al., 2010). Interestingly, TIMP1 and TIMP2 also showed significantly increased gene expression in the aberrant scars, compared to normal scar tissue (Ulrich et al., 2010). In cultured cells, MMP2 gene expression (Fujiwara et al., 2005a), and protein secretion (Bran et al., 2010) was shown to be increased in keloid-derived fibroblasts, compared to normal fibroblasts. In patient material, normal skin showed the highest level of pro-MMP2 compared to hypertrophic and keloid scars as tested by ELISA, though fibroblasts derived from the same keloids revealed the highest levels of active MMP2 compared to normal fibroblasts, as tested by gelatin zymography (Tanriverdi-Akhisaroglu et al., 2009).

In terms of keloid regional differences, there appeared to be increased levels of MMP2 expression at the keloid edge, particularly surrounding the enlarged collagen bundles identified in the characterisation steps. Imaizumi et al reported a similar finding, when comparing keloid and mature scar tissue. They found that MMP2, TIMP2 and TIMP3 were all significantly increased in keloids compared to mature scar tissue (Imaizumi et al., 2009). However in my findings, I also observed a high MMP2 expression in the keloid epidermis, which appeared not to be seen (and not addressed) by Imaizumi et al. Another interesting finding in the same study, was the co-expression of MMP2, MMP14 and TIMP2 in keloid fibroblasts, supporting the hypothesis that these three enzymes regulate each other's activity (Imaizumi et al., 2009). More specifically, it is thought that MMP14 binds to the N-terminal of TIMP2, which then allows for the catalytic domain of TIMP2 to bind to the HPX (hemopexin) domain of pro-MMP2. Another MMP14 molecule then binds to pro-MMP2 leading to a two-step activation step of MMP2 (Hadler-Olsen et al., 2011, Visse and Nagase, 2003). Taken together, the MMP2 overexpression and increased activity may aid the keloid expansion, by breaking down surrounding ECM, and allowing the resident myofibroblasts to migrate and deposit new collagen fibres (Neely et al., 1999).

3.3.2.3 MT1-MMP (Membrane tethered 1-MMP; MMP14)

MMP14 is a membrane-tethered family member, which is best known as an activator of pro-MMP2, though can also facilitate the proteolysis of fibrillar

collagens, syndecan-1 and laminin, as well as cleave monocyte chemotactic proteins (Parks et al., 2004, Goldsmith et al., 2013). In terms of fibrosis, it is thought to enhance pro-fibrotic signaling pathways (Goldsmith et al., 2013).

In the data above, MMP14 showed a very similar pattern of expression as MMP2, though was overall weaker than MMP2 in both normal skin and keloid scars. Certain keloids did show a marked increase in dermal expression compared to normal skin, especially in the marginal dermal regions, surrounding the dense collagen bundles, as for MMP2. This is most likely due to MMP14 being recognized as an activator of pro-MMP2 (Visse and Nagase, 2003, Itoh and Seiki, 2006, Imaizumi et al., 2009, Hadler-Olsen et al., 2011). MMP14 has not been widely studied in keloids or hypertrophic scarring, though its role in keloid development could be interesting, as it has been suggested that it has a key role in epithelial cell proliferation, post-injury (Atkinson et al., 2007). In this study, MMP14 knockouts of an airway epithelial-specific injury mouse model showed impaired wound healing compared to wildtype. This was thought to be linked to keratinocyte growth factor (KGF) receptor, which was seen to be overexpressed in the wildtype mice, but not the MMP14 knockouts (Atkinson et al., 2007).

In myocardial fibrosis, it has been reported that MMP14 is likely to play an important role in the activation of the pro-fibrotic molecule TGFβ (Goldsmith et al., 2013, Tatti et al., 2008). In animal models of pressure overload (PO) – a precursor to cardiac hypertrophy – early and sustained induction of MMP14 has been observed (Zile et al., 2012). In a myocardial infarction (MI) mouse model, MMP14 activity was found to have different effects within the MI region, and in the surrounding tissue. MMP14 appeared over-expressed in the MI region, in conjunction with MMP2 increased activity, whereas the increased MMP14 levels in the surrounding tissue was correlated with an increase in TGF-β signaling and collagen synthesis (Spinale et al., 2010). This pattern ties in with some of my observations, where MMP14 and MMP2 over-expression in the keloid tissues were identified in the similar regions to each other, and showed an increased concentration at the scar edges, where the thickened collagen bundles were located.

In most studies where MMP levels have been linked to keloid scarring, primary cell cultures have been used, of which mostly the fibroblasts have been monitored. Where histological analyses of MMPs have been made, the main focus has been on the dermis. This is undoubtedly important, however, with growing evidence that epithelial-mesenchymal interactions lead to alterations in cell behaviour of either compartments (Ghaffari et al., 2009b, Mukhopadhyay et al., 2005, Funayama et al., 2003, Lim et al., 2002b, Hahn et al., 2013), it is likely that the aberrant mechanisms taking place here are present in both epidermis and dermis.

Evaluating the protein expression of MMPs 1, 2, 13 and 14 in keloid and normal tissues show a first impression of the kind of MMP activity that might be taking place in the keloid scars. The high concentration of collagen I present in the keloid dermis, shows there is an imbalance of tissue remodeling processes. The small, almost non-existent differences in protein expressions of MMPs 1 and 13 support the fibrotic condition of the keloids. Whereas the clear overexpression of MMP2 and its activator, MMP14, in keloids suggests that fibrotic expansion is taking place. Seeing as MMPs are known to be regulated by their microenvironment, depending on which cell types, chemokines, cytokines and ECM molecules are present, it becomes clear that studying their expression and function in isolated cell cultures will most likely not be representative of their actual action *in vivo* (Giannandrea and Parks, 2014, Parks et al., 2004, Gill and Parks, 2008). As their action depends on which effectors and inhibitors are in their microenvironment, it becomes important to examine the composition of this microenvironment. In the following chapter, a more focused approach has been applied to explore which genes are expressed differently in keloid scars compared to normal skin, in the context of the ECM and related adhesion molecules.

4 Gene expression analysis of keloid ECM in whole tissue

4.1 Introduction

4.1.1 Gene expression analyses in keloids

To date, there have been a number of studies investigating the genetic aspects of keloid scarring (Shih and Bayat, 2010b), including inheritance patterns (Clark et al., 2009, Marneros et al., 2001, Omo-Dare, 1975), genome-wide association studies (GWAS) (Nakashima et al., 2010b, Marneros et al., 2004a, Velez Edwards et al., 2014), and whole genome microarrays (Tosa et al., 2005, Smith et al., 2008, Na et al., 2004, Chen et al., 2003, Hahn et al., 2013).

Across a number of studies, a variety of sample types have been tested, different technology platforms used, and the stringency of the analyses performed has been inconsistent, in terms of the threshold set for statistical significance (Shih and Bayat, 2010b, Huang et al., 2013a). Using keloid scar tissue, Chen et al. compared against internal control samples (Chen et al., 2003), whereas Naitoh et al. used a combination of internal and external control skin (Naitoh et al., 2005). Some examined keloid-derived fibroblasts (Smith et al., 2008, Seifert et al., 2008), whilst Hahn et al. are the only ones to date to report on microarray analysis of keloid-derived keratinocytes (Hahn et al., 2013). The ethnicity of the patients is not always mentioned, though Chen et al. examined Chinese patients (Chen et al., 2003), Nakashima et al. focused on the Japanese population (Nakashima et al., 2010b), Velez Edwards et al. recruited mainly African-American keloid patients (Velez Edwards et al., 2014), and Hahn et al. examined a Caucasian and African-American patients (Hahn et al., 2013).

Two groups have aimed to collate the current published gene expression profile datasets, and identify which genes showed to be significantly altered in keloids compared to normal skin, across at least two separate microarray studies (Shih and Bayat, 2010b, Huang et al., 2013a). Shih et al. found a total of 25 genes reported to be up- or down-regulated in more than one microarray study, loosely categorized into three functional groups: ECM (extracellular matrix), inflammation, and apoptosis (Shih and Bayat, 2010b). Three years later, Huang et al. identified a

total of 64 genes to be altered in keloids, 48 of which appeared to also be altered in hypertrophic scarring (Huang et al., 2013a). This relatively small proportion of overlap between microarray studies where over 1100 genes have been identified as altered collectively over the last decade, was most likely affected by the lack of consistency between microarray studies, as mentioned above. Overall, genes related to ECM and tissue structure were over-expressed in keloid tissue and fibroblasts, such as collagens, fibronectin, aggrecan, and versican. MMP (matrix metalloproteinase) gene expression was inconsistent, with MMPs 2 and 14 found to be over-expressed, while MMPs 1 and 3 were under-expressed in keloids. Genes linked to the TGF-β pathway were overexpressed in keloids, as were cell survival and cell proliferation related genes. Across both keloid and hypertrophic samples, genes related to skeletal development were significantly altered in keloids compared to normal skin (Huang et al., 2013a). See **Table 4-1** for a summary of some of these altered genes.

Very few gene expression studies have been reported comparing the different keloid sites. One group examined the differences in gene expression profiles between the deep dermis of the centre, superficial dermis of the centre, and the edge (Seifert et al., 2008). Overall there were some small differences in levels of gene expression between the regions, however they all followed similar trends, i.e. all three regions were either overexpressed or underexpressed compared to external control skin, with no genes showing an overexpression in one region and an underexpression in another region. Interestingly, the superficial central scar showed a slight increase in apoptosis-related gene expression, compared to the rest of the keloid. This supports the notion that the keloid is not a static fibrotic tissue, and is continually undergoing gradual remodelling, with an expanding edge and apoptotic centre (Seifert et al., 2008).

Table 4-1A Summary of genes found to be altered in at least two microarray studies (continued on next page)

All genes were up-regulated in keloid compared to normal skin, except where indicated with an asterisk (*), signifying a down-regulation in keloids. Based on two reports (Shih and Bayat, 2010b, Huang et al., 2013a).

Gene code	Gene full name	Involved in…	References
A2M	Alpha-2-macroglobulin	Inflammation, protease inhibitor	(Chen et al., 2003, Hu et al., 2006)
ACAN	Aggrecan	ECM, inflammation	(Naitoh et al., 2005, Seifert et al., 2008)
ADIPOQ	Adiponectin, C1Q and collagen domain binding	Fat metabolism, ECM remodelling	(Huang et al., 2013a)
ANXA1	Annexin-A1	Inflammation, apoptosis	(Hu et al., 2006, Seifert et al., 2008)
BMP6	Bone morphogenetic protein 6	Apoptosis	(Huang et al., 2013a)
NREP (C5ORF13)	Neuronal regeneration related protein	ECM remodelling	(Smith et al., 2008, Hu et al., 2006, Naitoh et al., 2005)
COL1A1	Collagen I alpha1	ECM	(Naitoh et al., 2005, Seifert et al., 2008)
COL1A2	Collagen I alpha2	ECM	(Chen et al., 2003, Hu et al., 2006)
COL4A2	Collagen IV alpha2	ECM	(Hu et al., 2006, Seifert et al., 2008)
COL5A2	Collagen V alpha2	ECM	(Chen et al., 2003, Hu et al., 2006)
COL6A1	Collagen VI alpha1	ECM	(Hu et al., 2006)
COL15A1	Collagen XV alpha1	ECM	(Naitoh et al., 2005, Seifert et al., 2008)
DCN	Decorin	ECM	(Hu et al., 2006, Chen et al., 2003)
EGFR *	Epidermal growth factor receptor	Inflammation, apoptosis	(Seifert et al., 2008)
FAP	Fibroblast activation protein alpha	Proliferation, inflammation	(Naitoh et al., 2005, Seifert et al., 2008)
FN1	Fibronectin 1	ECM, inflammation, apoptosis	(Chen et al., 2003, Naitoh et al., 2005, Seifert et al., 2008)
HIF-1A	Hypoxia-inducible factor alpha subunit 1	Apoptosis	(Seifert et al., 2008)

Table 4-1B (Continued from Table 4-1A)

Gene code	Gene full name	Involved in…	References
IGFBP7	Insulin-like growth factor binding protein 7	Inflammation	(Seifert et al., 2008, Smith et al., 2008)
JAG-1	Jagged-1	Angiogenesis, ECM remodelling	(Smith et al., 2008, Hu et al., 2006)
JUP *	Junction plakoglobin	Cell junction organisation	(Hu et al., 2006, Smith et al., 2008, Hahn et al., 2013)
MMP1 *	Matrix Metalloproteinase 1 (collagenase 1)	ECM remodelling	(Smith et al., 2008)
MMP2	Matrix Metalloproteinase 2 (gelatinase A)	ECM remodelling	(Huang et al., 2013a)
MMP3 *	Matrix Metalloproteinase 3 (stromelysin 1)	ECM remodelling	(Smith et al., 2008, Seifert et al., 2008, Hahn et al., 2013)
MMP14	Matrix Metalloproteinase 14 (MT1-MMP)	ECM remodelling	(Huang et al., 2013a)
NRP1 *	Neuropilin 1	Cell migration, apoptosis	(Smith et al., 2008, Chen et al., 2003)
OGN	Osteoglycin	ECM, ossification	(Naitoh et al., 2005, Smith et al., 2008)
POSTN	Periostin, osteoblast specific factor	ECM remodelling	(Naitoh et al., 2005, Hu et al., 2006, Hahn et al., 2013)
SERPINF1 *	Serpin peptidase inhibitor, clade F	Apoptosis	(Seifert et al., 2008, Smith et al., 2008)
TGF-β1	Transforming growth factor beta 1	ECM, proliferation	(Seifert et al., 2008, Chen et al., 2003)
TGF-βRIII *	Transforming growth factor beta receptor III	ECM, inflammation	(Hu et al., 2006, Seifert et al., 2008)
THBS2 *	Thrombospondin 2	Angiogenesis, ECM interactions	(Seifert et al., 2008)
THBS4	Thrombospondin 4	ECM interactions & remodelling	(Naitoh et al., 2005)
TNC *	Tenascin C	ECM remodelling	(Huang et al., 2013a, Hahn et al., 2013)
VCAN	Versican	ECM, inflammation	(Naitoh et al., 2005, Chen et al., 2003, Seifert et al., 2008)

It is possible that the gene expression studies described above, are based on keloid scars which have been excised with varying margins of adjacent normal skin. As discussed in Chapter 3, defining the different keloid regions is subject to bias, and highly variable between patients. For this reason, most attempts at analyzing the different keloid regions separately are not easily reproducible across research groups. In the case of the expression data on isolated fibroblasts, the expression patterns observed may not be representative of the processes taking place *in vivo*. The impact of the resident keratinocytes, possible immune cell infiltration, underlying adipocytes, as well as circulating growth factors and cytokines from the increased blood supply to the scar tissue are not accounted for in a fibroblast-only analysis. This complication is partly explored in Hahn et al.'s study, where they performed microarray analysis on isolated keloid fibroblasts and keratinocytes, then followed up with RT-PCR analysis on whole keloid tissue (Hahn et al., 2013). A total of 25 genes were significantly altered in keloid fibroblasts, 31 genes were significantly different in keloid keratinocytes, though only 9 of these genes continued to be altered in whole tissue. Interestingly, when they compared lesional to non-lesional cells taken from the same patient, there was little difference in gene expression levels despite there being a significant difference between keloid and external control cells (Hahn et al., 2013).

Consequently, the gene expression data described below are based on analyzing a cross-section of whole keloid scars – containing central, edge and adjacent normal tissue, with both dermal and epidermal compartments. This way, a snapshot of the complete fibrotic lesion is taken into consideration, inclusive of all cell types, and all tissue compartments.

4.1.2 Aim

The primary aim of the work presented in this chapter was to identify which genes are differentially expressed in keloid scar tissue, compared to normal skin, in the context of the ECM. In particular, Real-Time qPCR arrays were selected as a relatively focused approach to examine 84 genes thought to be key in ECM structure and regulation. Additionally, a further 84 genes were examined under

the same technology platform, which are associated with 10 of the most well studied signalling pathways. Finally, a selection of the most significantly altered genes were validated by individually designed Real Time qPCR assays, using the relative standard curve method. Put together, this will give an insight into the processes potentially taking place in this subset of keloid scars.

4.2 Results

4.2.1 Gene expression levels of extracellular matrix & adhesion molecules, in keloid scars

The Human ECM and Adhesion Molecules RT^2 Profiler qPCR array (see **section 2.3.2, Chapter 2**) was used to evaluate the expression profiles of 84 genes related to cell-cell and cell-matrix interactions, as well as key structural ECM proteins. Complete cross-sections of five extralesionally-excised keloids (encompassing central, marginal and adjacent normal skin regions) and five healthy control skin specimens were used in the analyses (see **Tables 2-1 and 2-2** for patient details, **Chapter 2**). The specimens were inclusive of the epidermal and dermal compartments of the tissues, so as to obtain an overall impression of the whole tissues.

4.2.1.1 Differences within normal skin specimens

Seeing as this disorder shows a very high level of inter-patient variability, and a high correlation of severity level to patient ethnicity, I aimed to include healthy controls of African-Caribbean origin to be in keeping with the keloid scars used here. At the time of completing the ECM qPCR array analyses, I had only two African-Caribbean normal skin samples available, which were combined with three Caucasian normal skin samples to increase the healthy control sample group number.

Analysis started with examining the differences in gene expression within the control group, between Caucasian and African-Caribbean normal skin to ensure there were no significant differences within the control group. The majority of the genes on the Human ECM and Adhesion Molecules RT^2 Profiler qPCR arrays showed no significant differences between Caucasian and African-Caribbean normal skin. There was a total of 7 genes with decreased expression in normal African-Caribbean skin compared to normal Caucasian skin: COL11A1 (collagen XI; 42.73-fold down-regulated), CTNND1 (delta 1 catenin; 10.35-fold down-regulated), HAS1 (hyaluronan synthase 1; 3.74-fold down-regulated), ITGA4

(integrin alpha 4; 3.18-fold down-regulated), MMP1 (2.38-fold down-regulated), MMP7 (11.28-fold down-regulated), MMP10 (4.11-fold down-regulated), MMP11 (3.03-fold down-regulated), and MMP12 (8.07-fold down-regulated) (**Figure 4-1**) One gene showed an increased expression in normal African-Caribbean skin compared to normal Caucasian skin: MMP3 (3.15-fold up-regulation). Notably, the fact that I had only two African-Carribean samples of normal skin meant it was not possible to test the statistical significance against the three Caucasian samples. Nonetheless, the most obvious changes were taken into consideration when examining the fold-differences in gene expression in the keloids *vs* normal skin samples, which is described in the following section.

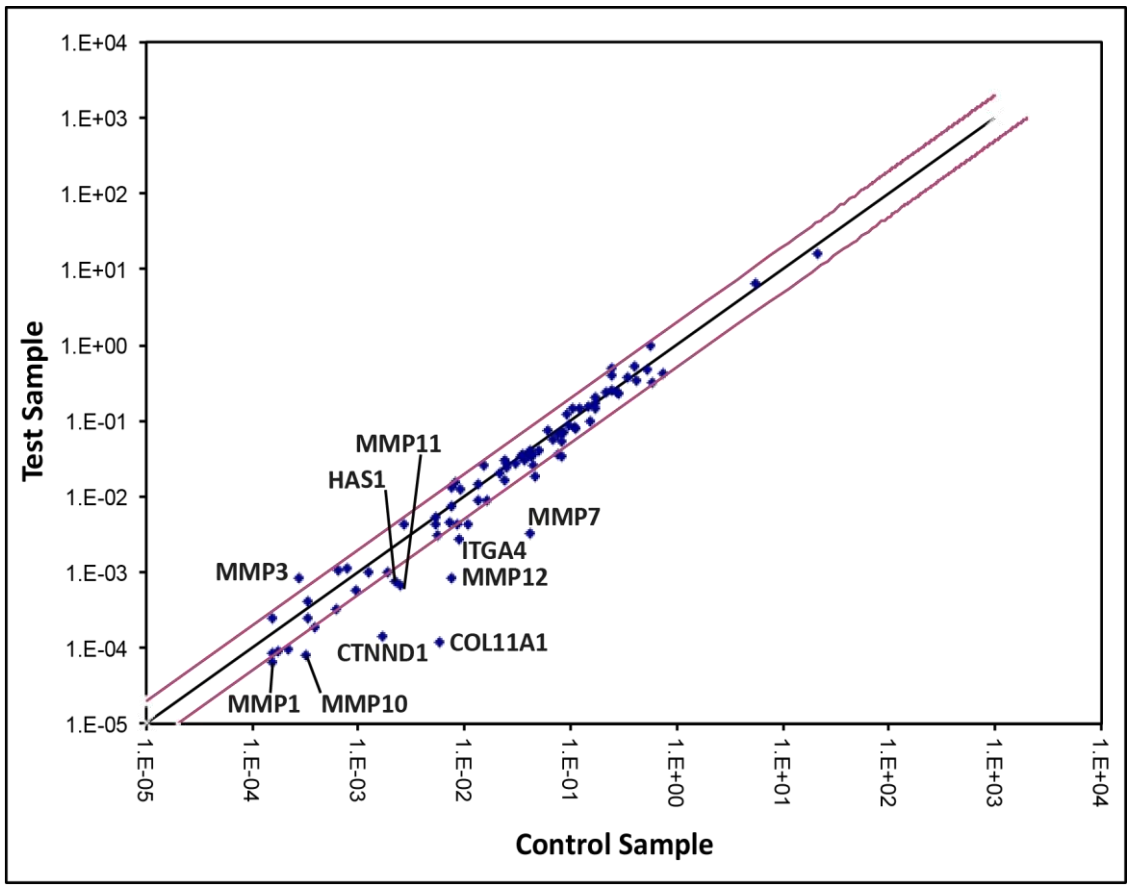

Figure 4-1 Scatterplot showing fold-changes in expression of ECM genes between African-Caribbean and Caucasian normal skin samples, using an ECM qPCR array.

All values outside of the two pink lines show a more than 2-fold difference in gene expression in African-Caribbean normal skin (n=2), compared to Caucasian normal skin (n=3). In total there were 7 genes that showed a down-regulation in African-Caribbean skin compared to Caucasian normal skin: COL11A1 (-42.73), CTNND1 (-10.35), HAS1 (-3.74), ITGA4 (-3.18), MMP1 (-2.38), MMP7 (-11.28), MMP10 (-4.11), MMP11 (-3.03), and MMP12 (-8.07). By contrast, MMP3 showed an up-regulation of 3.15-fold. Statistical analysis of data was not carried out due to the very small number of African-Caribbean samples. **X axis (Control)**= Caucasian normal skin; **Y axis (Test)**= Afro-Caribbean normal skin.

4.2.1.2 Differences between keloid and normal skin

Out of the original 84 ECM-related genes examined, a total of 34 genes demonstrated a minimum of 2-fold up-regulation in keloid tissue compared to normal skin, with 18 showing statistical significance (at least $p<0.05$), as tested by an unpaired Student's T-test. A further 8 genes showed a minimum of 2-fold down-regulation in keloids, 3 of which did so in a statistically significant way (at least $p<0.05$) (**Figure 4-2**) A summary of all the statistically significantly altered genes, with a 2-fold change or more, is presented in **Table 4-2.** See **Appendix C** for the full list of results for all 84 genes tested.

It is worth noting that almost all the genes that were altered between the African-Caribbean and Caucasian control samples (**Figure 4-2**) did not demonstrate any significant change in expression when comparing the keloid and normal tissues. The exceptions were MMP1 and MMP3. MMP1 had a 2.38-fold lower expression in normal African-Caribbean skin compared to normal Caucasian skin, however when comparing keloid to normal skin samples, MMP1 showed a great up-regulation of 51.78-fold. On the other hand, MMP3 had a 3.15-fold higher expression in normal African-Caribbean skin compared to normal Caucasian skin, and an even higher up-regulation of 9.22-fold in keloid samples compared to all normal skin samples.

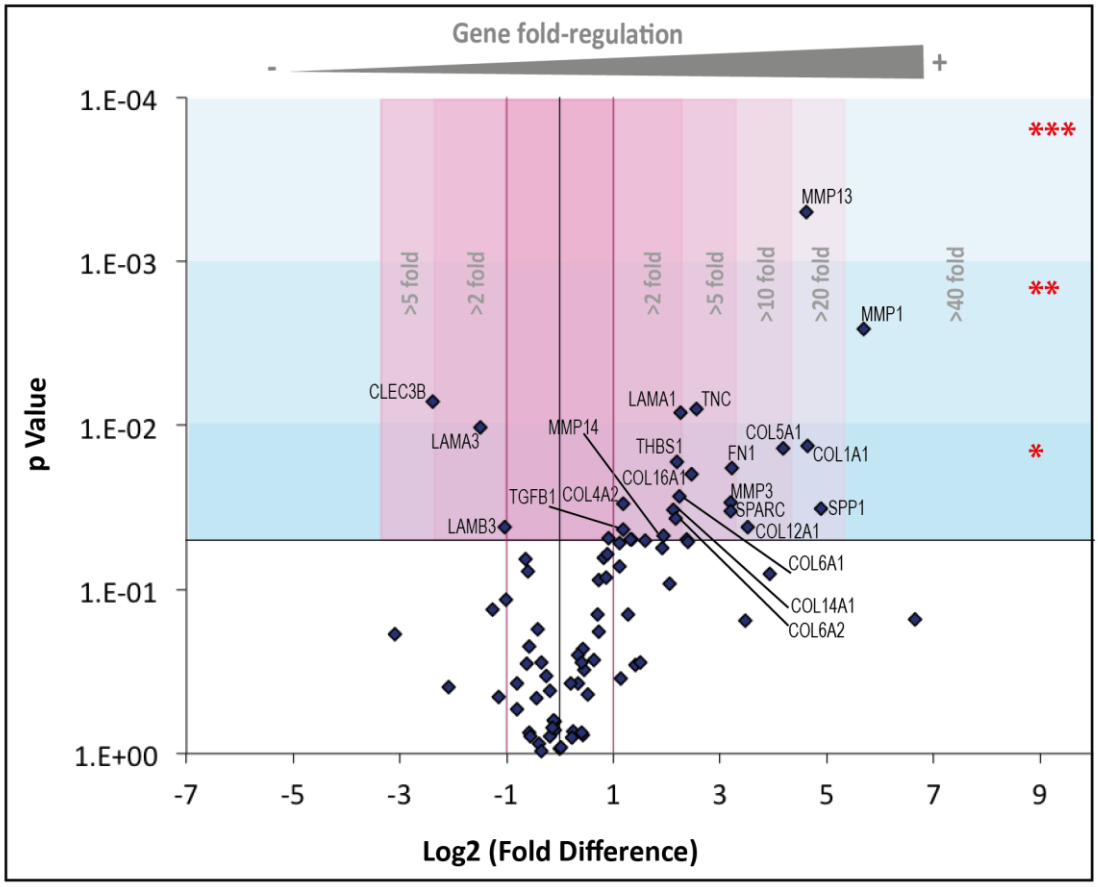

Figure 4-2 Volcano plot of Extracellular Matrix & Adhesion Molecule RT^2 Profiler qPCR array.

A total of 21 genes were shown to be more than 2-fold significantly altered in keloid scars compared to normal skin (n=5). The pink shaded areas show the levels of fold-changes: up-regulation to the right (positive values on X axis), and down-regulation to the left (negative values on X axis). The blue shaded areas show increasing levels of statistical significance. Statistical analysis was carried out using the Student's T-test, with * = $p<0.05$; ** = $p<0.01$; and *** = $p<0.001$. See **Table 4.2** for specific values of gene expression fold-changes and their associated p values.

Table 4-2 Genes from the ECM qPCR array that were significantly different between keloid and control skin. (n=5)

Gene symbol	Fold change in expression	P value (Student's T-test)
MMP1	51.78	0.0026
SPP1	29.59	0.0320
COL1A1	24.84	0.0134
MMP13	24.34	0.0005
COL5A1	18.26	0.0137
COL12A1	11.44	0.0416
FN1	9.28	0.0183
SPARC	9.24	0.0334
MMP3	9.22	0.0293
TNC	5.85	0.0080
COL16A1	5.50	0.0199
MMP16	5.18	0.0496
LAMA1	4.81	0.0084
COL6A1	4.73	0.0269
THBS2	4.58	0.0168
COL6A2	4.52	0.0368
COL14A1	4.33	0.0329
MMP14	3.85	0.0469
LAMB3	-2.04	0.0419
LAMA3	-2.80	0.0103
CLEC3B	-5.20	0.0071

Examining more closely the significantly altered genes in this sample group, it becomes evident that several functions within the ECM environment are affected. Other than the well-established fibrogenic marker Collagen I (COL1A1), there is over-expression of several structural protein genes including Collagens V, VI, XII, XIV, and XVI; and Fibronectin (FN). In parallel, a number of members from the matrix metalloproteinase (MMP) family were highly up-regulated in keloid skin compared to normal skin, including MMPs 1 and 13.

4.2.2 Gene expression levels from 10 signal transduction pathways, in keloid scars

The Human Signal Transduction PathwayFinder (STP) RT^2 Profiler qPCR array (see **section 2.2.2, Chapter 2**) was used to evaluate the expression profiles of 84 target genes responsive to activation or inhibition of 10 of the most commonly studied signalling pathways. Gene expression results from the same pathway can vary widely, depending on the tissue and experimental conditions. This array aimed to avoid this confusion by focusing on pathway target genes, thereby giving a more complete impression of alterations in developmental, immunological, metabolic and stress-activated processes.

As for the previous ECM qPCR array, complete cross-sections of five extralesionally-excised keloids (encompassing central, marginal and adjacent normal skin regions) and five healthy control skin specimens were used in the analyses (see **Tables 2-1 and 2-2** for patient details, **Chapter 2**). The specimens were inclusive of the epidermal and dermal compartments of the tissues, in order to get an overview of changes in gene expression across the whole tissues.

4.2.2.1 Differences within normal skin specimens

As for the previous ECM qPCR array, the five normal skin control samples were of varying ethnic origin, therefore the differences in gene expression between African-Caribbean and Caucasian skin within the control group were examined. In contrast to the ECM qPCR array (**section 4.2.1.1**), the STP qPCR array investigations included three African-Caribbean and two Caucasian normal skin

samples (rather than two African-Caribbean and three Caucasian samples). The difference in sample make-up was due to the timing of the investigations – at the time of the ECM qPCR arrays, I had no expectation that there would be more than two African-Caribbean samples available. However, at the time of the STP qPCR array investigations, an additional African-Caribbean control skin was made available.

The majority of the genes examined showed no significant differences between the two ethnicities, within the normal control group. However, three genes did show increased fold changes in normal African-Caribbean skin: ADM (adrenomedullin; 2.77-fold up-regulated), EMP1 (epithelial membrane protein 1; 4.44-fold up-regulated), and WNT6 (wingless-type MMTV integration site family member 6; 2.6-fold up-regulated). Additionally, seven genes presented decreased expression in normal African-Caribbean skin compared to normal Caucasian skin: EPO (erythropoietin; 4.39-fold down-regulation), FABP1 (fatty acid binding protein 1; 7.59-fold down-regulation), FOSL1 (FOS-like antigen 1; 2.43-fold down-regulation), LRG1 (leucine-rich alpha-2-glycoprotein-1; 3.95-fold down-regulation), MMP7 (matrix metalloproteinase 7; 4.74-fold down-regulation), TNF (tumour necrosis factor; 3.94-fold down-regulation), and WNT3A (wingless-type MMTV integration site family member 3A; 2.77-fold down-regulation) **(Figure 4-3)**. It is worth noting that MMP7 also appeared down-regulated in normal African-Caribbean skin in the ECM qPCR array (**Figure 4-1**) providing an extra level of confidence in the data. The small number of Caucasian samples used meant statistical significance was not tested. Nonetheless, these gene alterations were taken into consideration when investigating the fold-differences in gene expression in the keloids, as compared to the whole normal control group of samples.

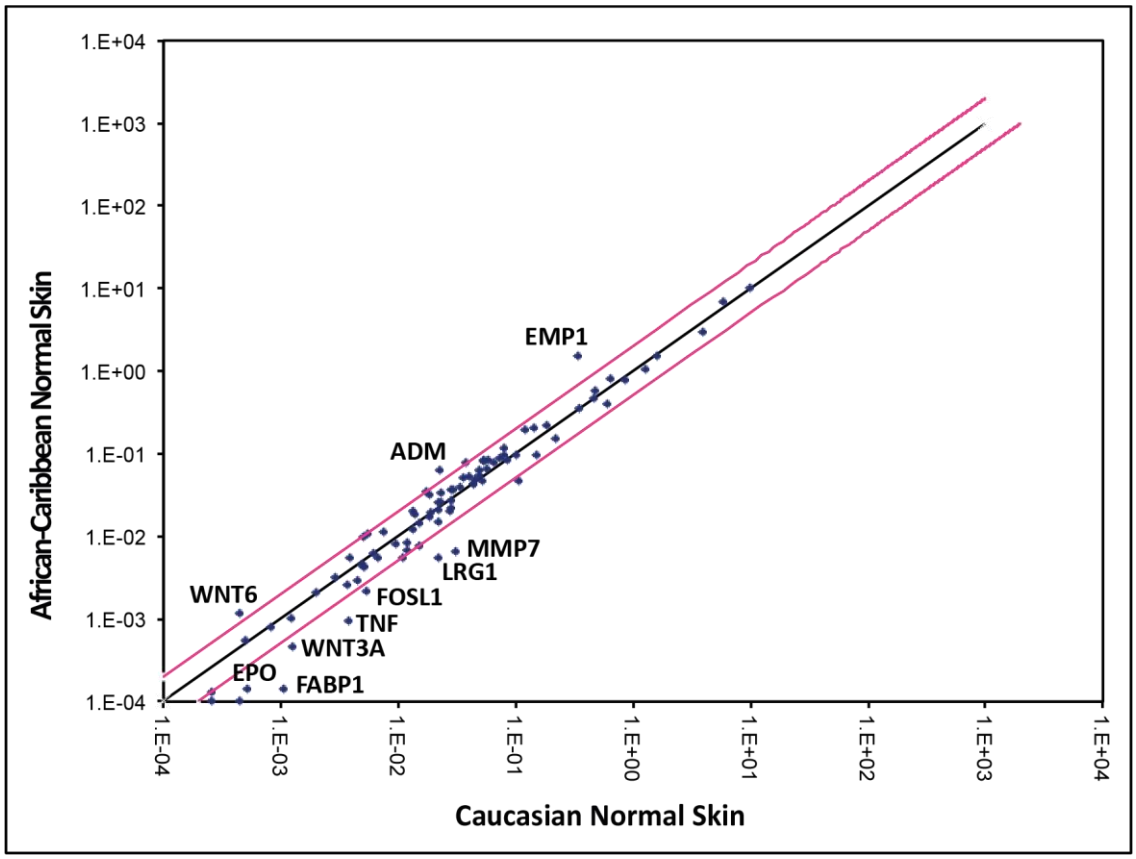

Figure 4-3 Scatterplot showing fold-changes in expression of Signal Transduction Pathway genes between African-Caribbean and Caucasian normal skin, using the STP qPCR array.

All values outside of the two pink lines show a more than 2-fold difference in gene expression in African-Caribbean normal skin (n=3), compared to Caucasian normal skin (n=2). In total, 3 genes demonstrated an up-regulation in normal African-Caribbean skin compared to normal Caucasian skin: ADM (+2.77), EMP1 (+4.44), and WNT6 (+2.6). By contrast, a total of 7 genes revealed a down-regulation in African-Caribbean skin: EPO (-4.39), FABP1 (-7.59), FOSL1 (-2.43), LRG1 (-3.95), MMP7 (-4.74), TNF (-3.94), and WNT3A (-2.77). Statistical analysis was not performed due to the small group numbers.

4.2.2.2 Differences between keloid and normal specimens

Out of the original 84 STP-related genes examined, a total of 10 genes demonstrated a minimum of 2-fold up-regulation in keloid tissue compared to normal skin, with 4 showing statistical significance (at least $p<0.05$), as tested by a Student's T-test. A further 16 genes showed a minimum of 2-fold down-regulation in keloids, with 6 being significant (at least $p<0.05$) (**Figure 4-4**). A summary of all the significantly altered genes, with a 2-fold change or more, can be seen in **Table 4-3**. See **Appendix D** for the full list of results for all 84 genes.

In this qPCR array, none of the genes previously shown to be altered between African-Caribbean and Caucasian normal skin samples (**Figure 4-3**) revealed any difference between keloid and normal skin sample groups.

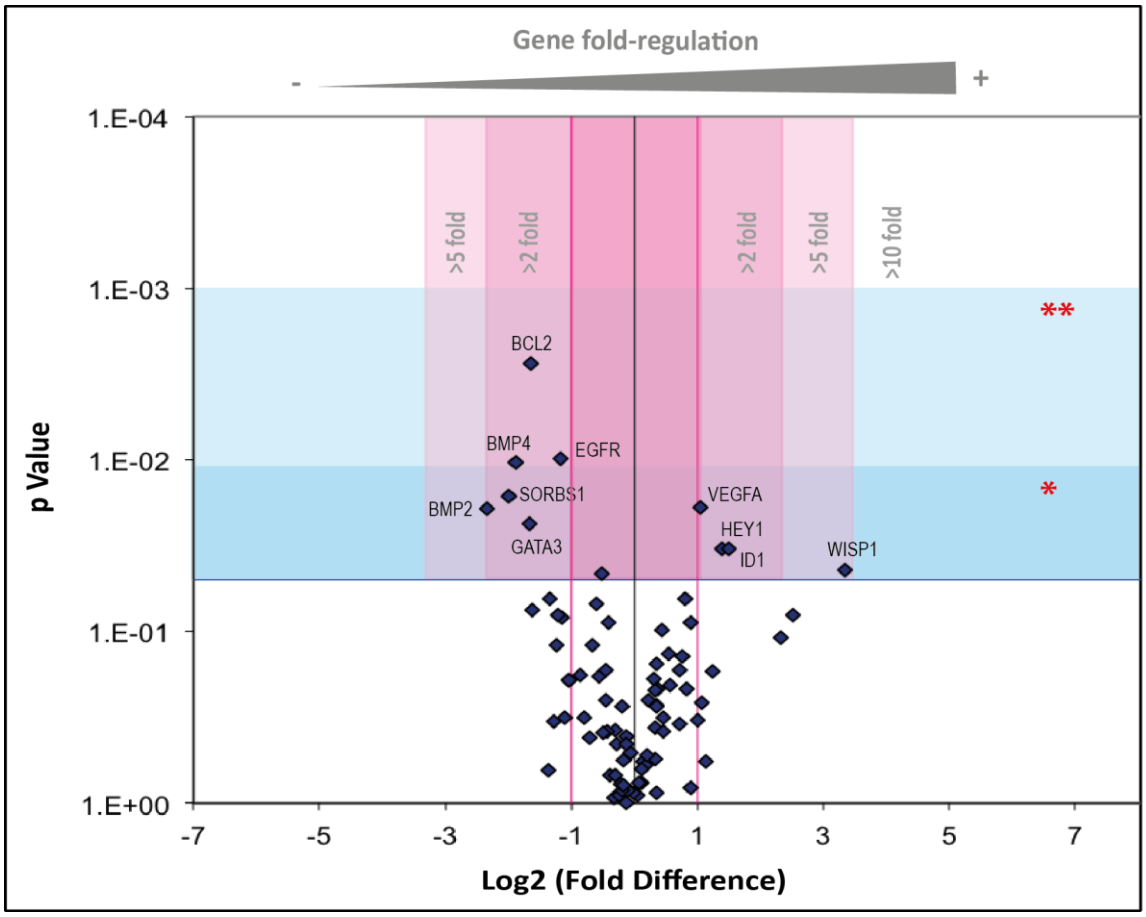

Figure 4-4 Volcano plot of Signal Transduction Pathway Finder Real-Time qPCR array.

A total of 10 genes were shown to be more than 2-fold significantly deregulated in keloid scars *vs*. normal skin (n=5). The pink shaded areas show the levels of fold-deregulation: up-regulation to the right (positive values on X axis), and down-regulation to the left (negative values on X axis). The blue shaded areas show increasing levels of statistical significance. Statistical analysis was carried out using Student's T-test with * = $p<0.05$; ** = $p<0.01$; and *** = $p<0.001$. See **Table 4-3** for specific values of gene expression fold-changes and their associated p values.

Table 4-3 Genes from the STP qPCR array that were significantly different between keloid scars and control skin. (n=5)

Gene symbol	Fold change in expression	P value (Student's T-test)
WISP1	10.10	0.0439
ID1	2.84	0.0328
HEY1	2.62	0.0327
VEGFA	2.06	0.0191
EGFR	-2.23	0.0098
BCL2	-3.12	0.0027
GATA3	-3.15	0.0237
BMP4	-3.67	0.0104
SORBS1	-3.97	0.0162
BMP2	-5.04	0.0191

4.2.2.3 Summary of statistically significantly altered genes analysed

The results of the data presented in **Table 4-2 and 4-3** are summarised in **Figure 4-5.** A relatively high level of inter-patient variability was observed within the selection of keloids. This, along with the relatively low number of samples examined, could explain why the standard deviation values were very high. It becomes clear that keloid tissue has a gene overexpression of structural ECM proteins such as collagens, fibronectin and osteogenic-related proteins SPARC and SPP1, as well as ECM-degrading MMPs. It is also clear that apoptosis-related genes such as BCL2, BMP2 and BMP4 are underexpressed in keloids, while proliferation-linked genes such as WISP1 are overexpressed in keloid tissue.

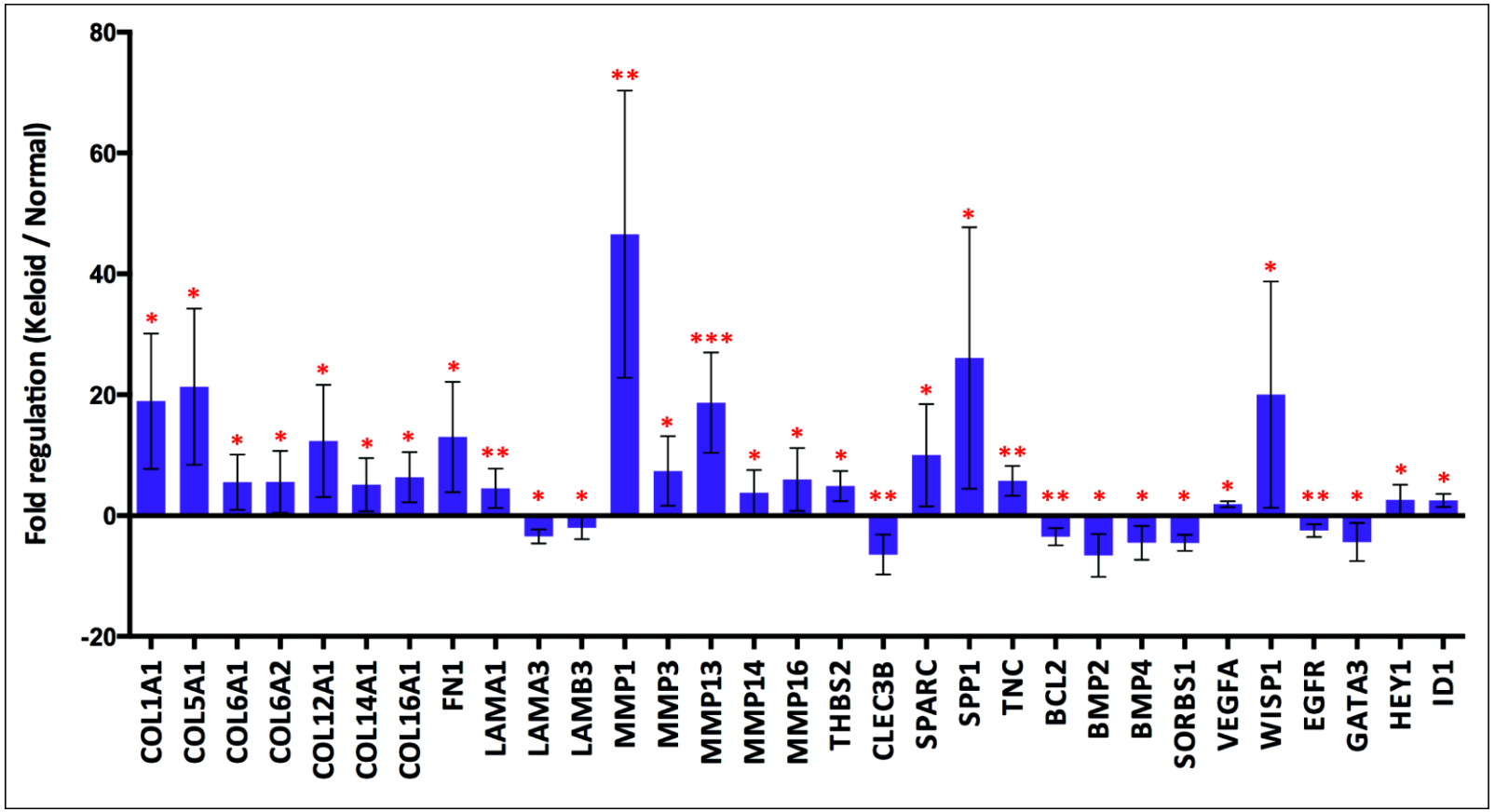

Figure 4-5 Summary of genes identified from both ECM and STP qPCR arrays, that showed significant up- or down-regulation in keloid scars compared to normal skin.

This graph is derived from the data presented in **Tables 4-2** and **4-3**, all of which were statistically significant (at **least p<0.05**). Error bars show the SD of the mean of n=5 keloid patients, each compared to the mean of all n=5 healthy controls.* = p<0.05; ** = p<0.01; and *** = p<0.001.

4.2.3 Validation of qPCR array findings

Taking into account the high inter-patient variability in the qPCR array findings, as well as the fact that the qPCR array investigations were performed once per patient, a selection of the top 31 most altered genes were validated by Real Time qPCR, using the Relative Standard Curve method.

4.2.3.1 Development of Real Time qPCR assays by Relative Standard Curve method

In order to validate the qPCR array findings outlined in **sections 4.2.1** and **4.2.2**, primer sets were manually designed (see **Table 2-8, Chapter 2**) and the qPCR assays were optimized for the Relative Standard Curve method. As opposed to the $\Delta\Delta C_t$ method, where the assumption is that all assays are 100% efficient and the reaction product doubles with each round of polymerisation ($2^{\Delta\Delta C_t}$), a 4- to 6-point standard curve is made from a pooled RNA sample, known to express most genes (see **section 2.2.3.1, Chapter 2**), and used to calculate the specific reaction efficiency rate for each individual Real Time qPCR assay. This way, even though the final data is still relatively quantified, there is a lower chance of false positives occurring (Larionov et al., 2005). The 18 genes of interest (GOI), plus the two reference genes selected for validation are listed in **Table 2-8, Chapter 2**. Due to the large number of samples and genes being tested, two reference genes were included, providing a higher level of confidence during data normalization (ΔC_t). HPRT1 (hypoxanthine phosphoribosyltransferase 1) and B2M (beta-2-microglobulin) were selected based on the results from both qPCR arrays, where these two genes were the most stably expressed out of the original five reference gene used in the qPCR arrays (see **Appendices C** and **D**). The $\Delta\Delta C_t$ values were calculated by normalizing each keloid or normal skin value against the mean from all five normal skin ΔC_t values.

To optimise the qPCR assays, they were first run using the serially diluted control samples at a combined annealing/ extension temperature of 62°C. For the assays which showed non-specificity at 62°C, a range of temperatures from 58 - 64°C was tested, and the PCR products run on a 2% (w/v) agarose gel to establish which conditions resulted in the highest specificity (**Figure 4-6A to C**).

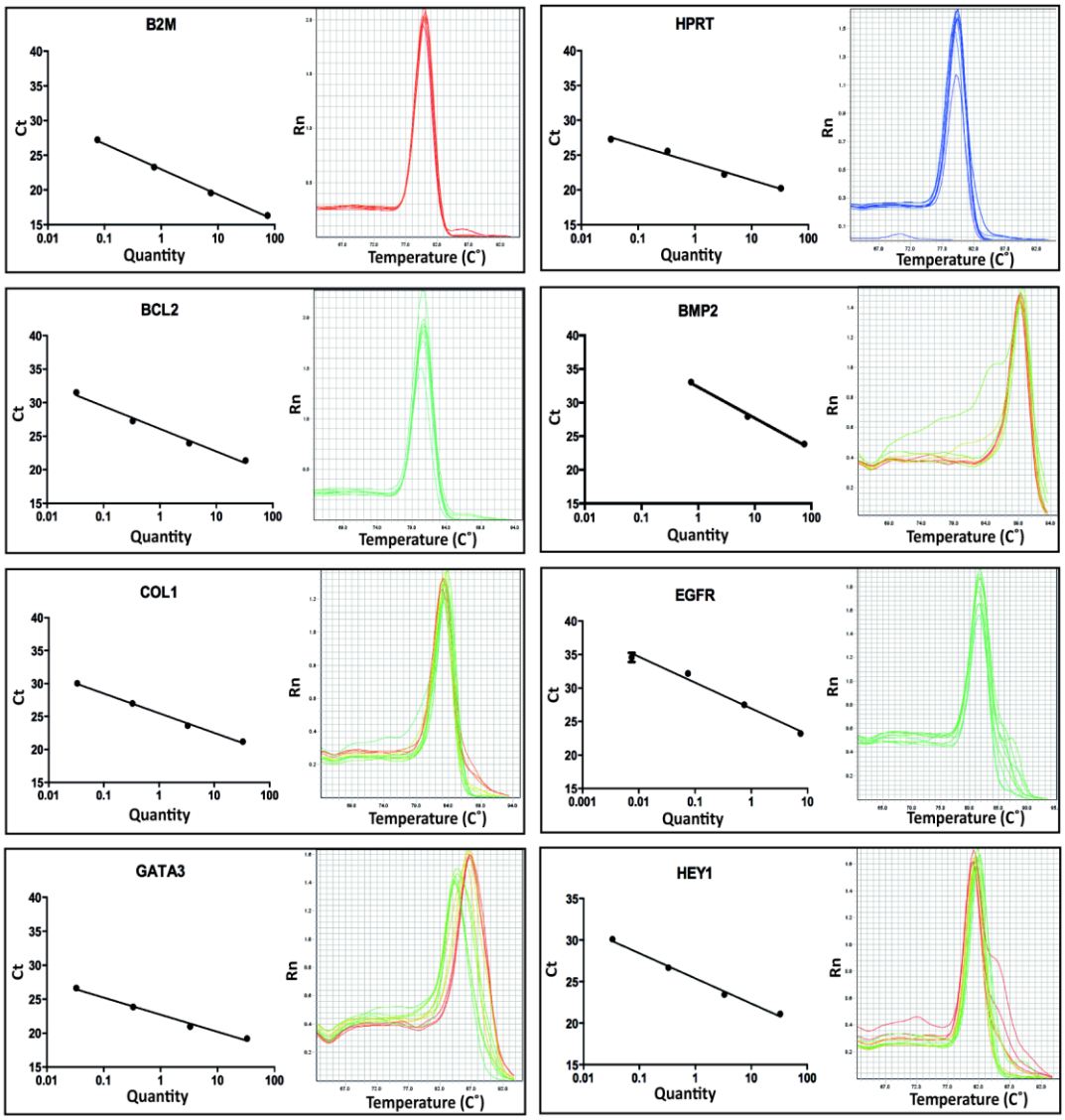

Figure 4-6A Standard curves and melting curves for each of the manually designed Real Time qPCR assays, used for validation of PCR array data.

A total of 2 reference genes and 18 GOIs (listed alphabetically, from left to right) were optimized for Real Time qPCR, by the Relative Standard Curve method. A 3 or 4-point standard curve was formed from a pooled RNA standard, and the optimal annealing/ extending temperature selected, as outlined in **section 4.2.3.1**. The variation in slopes of each assay demonstrates that they do not have a uniform level of efficiency, making this method more accurate than the $\Delta\Delta C_t$ method. Most genes showed linearity along all four standards, however BMP2 was linear only across the first three standards, possibly due to it being expressed at a lower level in the pooled RNA standard sample, compared to the rest of the genes. Melting curves for each assay were carried out during optimization steps, using the 3 or 4-point standards. The majority of these showed a single clean peak, suggesting a high level of assay accuracy. *(Figure continued on next page)*

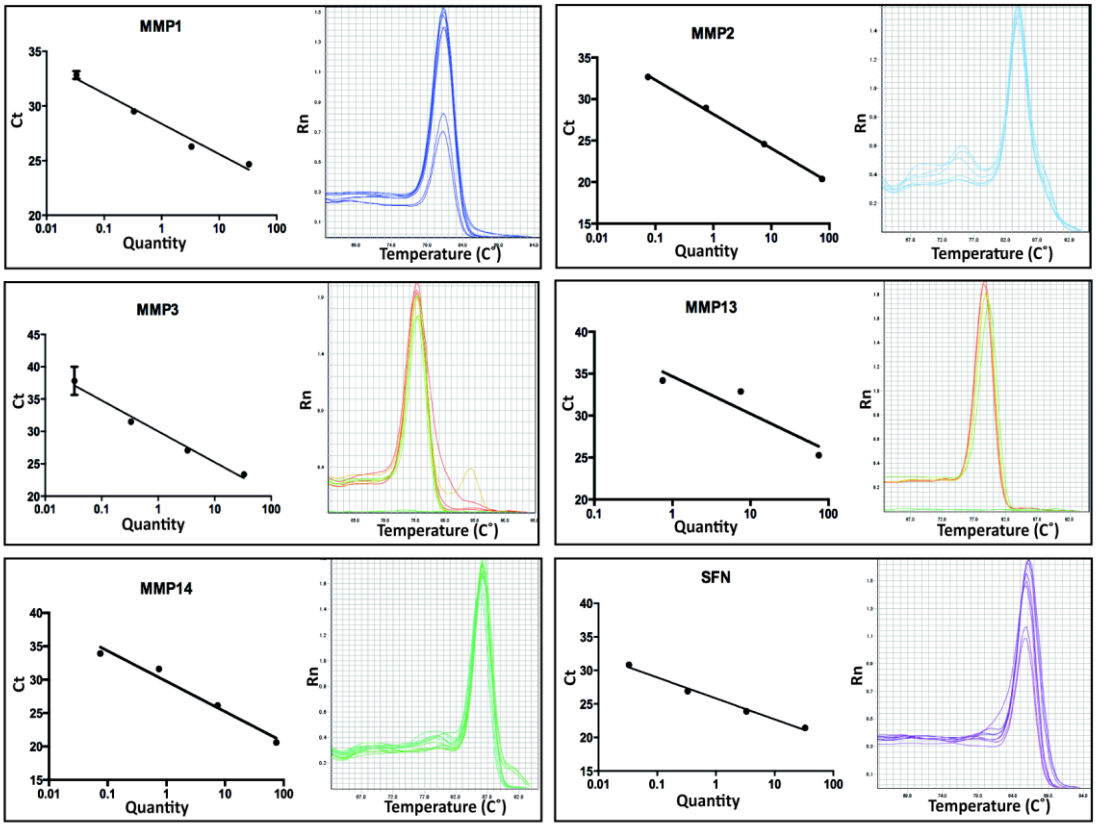

Figure 4-6B Continued from Figure 4-6A

Showing a continuation of Figure 4-6. The standard curve for MMP13 was linear only across the first three standards, possibly due it being expressed at a lower level in the pooled RNA standard sample, compared to the rest of the genes. Most genes here showed a clean single peak for their melting curve. *(Figure continued on next page)*

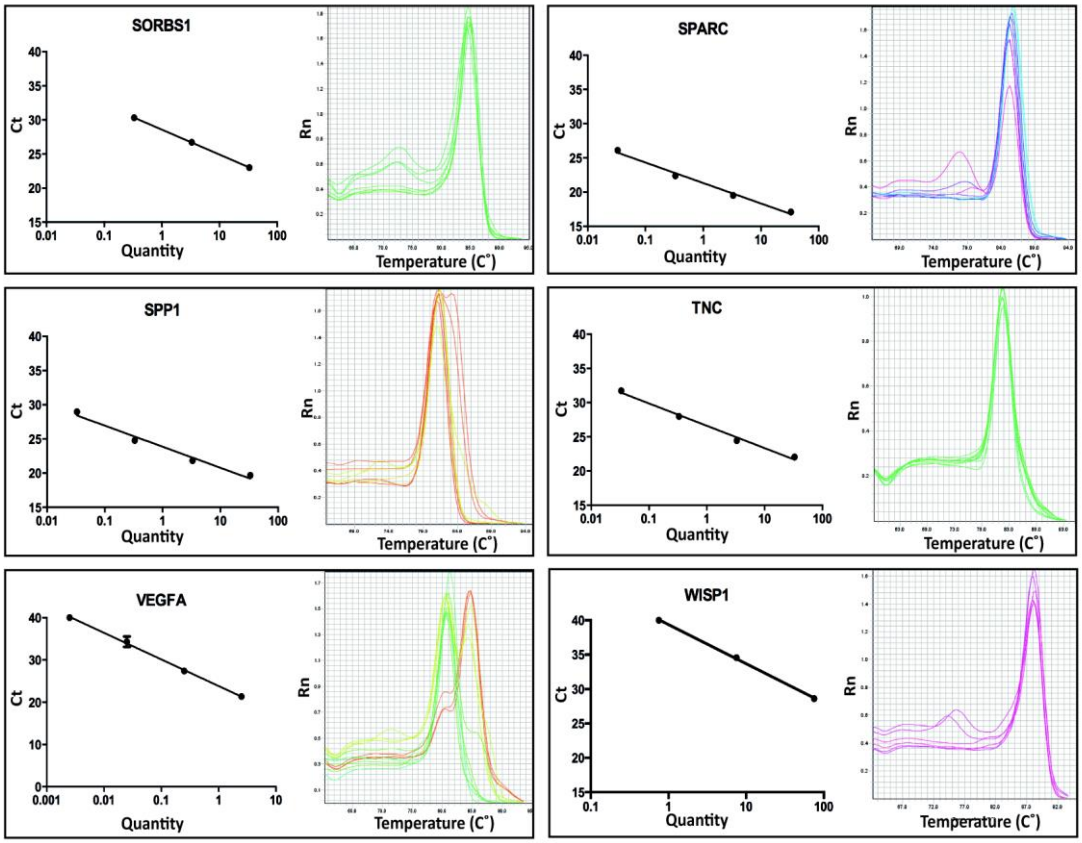

Figure 4-6C Continued from Figure 4-6B

Showing a continuation of Figure 4-6. Here, SORBS1 and WISP1 were linear only across the first three standards, possibly due to those genes being expressed at a lower level in the pooled RNA standard sample, compared to the rest of the genes. Most genes showed a clean single peak, apart from VEGFA, which consistently showed a double peak, possibly representing splice variants of the same gene. SORBS1, SPARC and WISP1 showed additional smaller peaks for the most diluted standards.

Most genes showed a clean single peak in their melting curves. For SORBS1, SPARC and WISP1, the additional smaller peaks at the lower temperatures represent the most diluted standards, where the C_t values were higher than 35. In all of these cases, the test sample C_t values appeared within the C_t values of two highest standards, and so therefore did not significantly impact on the specificity of the final results. For VEGFA, there was a consistent double peak in their melting curves, for which one reason could be the presence of transcript variants. Based on information collated on the human gene database GeneCards, VEGFA does consist of a number of variants (GeneCards, 2016). However, as I did not follow through with extensive analyses of VEGFA in my research, I did not explore this further.

4.2.3.2 Validating expression of identified altered genes by Real Time qPCR (Relative Standard Curve method)

Out of the 31 significantly different genes originally identified in the qPCR arrays, 16 of these were validated on the same range of keloid and normal tissues, using the optimized assays from section 4.2.3.1. Added to this selection was SFN (stratifin/ 14-3-3σ), which has been shown to interact with SPARC to control COL1A1 synthesis and expression in normal fibroblasts. It has been proposed that a lack of SFN and an overexpression of SPARC cause greater expression of COL1A1 via TGF-β activation, potentially explaining the development of hypertrophic scars (Chavez-Muñoz et al., 2012). Although MMP2 was less than 2-fold up-regulated in the qPCR array data, and was not significantly different to normal tissue, it was included in the validation as its protein expression levels were increased in keloids (see **section 3.2.4**, **Chapter 3**).

The fold changes in expression of the 18 selected genes are shown in **Figure 4-7** and **Table 4-4** Most of the genes revealed very little variance between samples, however genes such as SPARC, SPP1, WISP1 and HEY1 showed high inter-patient variability. When the Student's T-test was applied to see if the keloid results were statistically significantly different from the normal tissue controls, only 4 genes were deemed significantly different ($p<0.05$): BCL2, BMP2, SORBS1, and EGFR. By

contrast, all of the selected genes (except for MMP2 and SFN) had shown to be significantly different in the original qPCR arrays, using the same statistical test.

In **Figure 4-8,** the original qPCR array data is compared side by side with the validated qPCR data. Even though the same levels of change in gene expression are not directly reproduced in the validation, the fold-changes for most genes are similarly altered, i.e. both array and validation results showing an up- or down-regulation. The exception is HEY1, where the array data showed an up-regulation in keloids, whereas the validation results displayed a down-regulation.

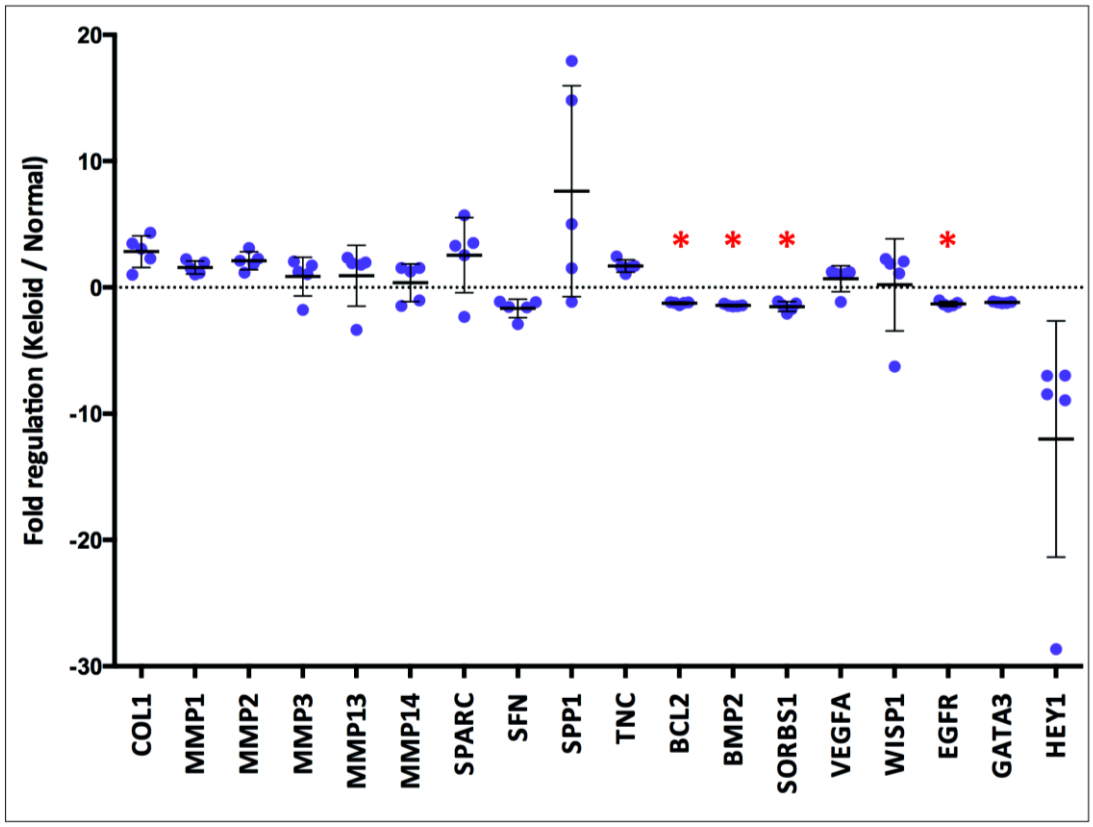

Figure 4-7 Validation of gene expression patterns identified by qPCR arrays

Expression levels of sixteen of the most altered genes from the qPCR arrays ($\Delta\Delta C_t$ method), were validated using the qPCR Relative Standard Curve method. MMP2 (matrix metalloproteinase 2) was included in the analyses, due to the increased protein expression observed in Chapter 3; SFN (stratifin) was included due to its well-published interaction with SPARC (osteonectin) affecting collagen synthesis. Gene expression changes were subtle, with only 4 genes showing statistical significance, as tested using the Student's T-test ($p<0.05$). n=5 keloids, compared against n=3 normal skin samples. Error bars represent the SD of the mean.

Table 4-4 Gene expression fold-changes from the validation qPCR assays

Data is from **Figure 4-7**. In blue are the statistically significantly altered genes ($p<0.05$), in keloids compared to normal skin. (n=5 keloids; n=3 normal controls)

Gene symbol	Mean fold-changes	St. Deviation of mean fold-changes	P value (Student's T-test)
SPP1	5.008	8.350	0.1845
SPARC	3.300	2.973	0.1207
COL1	3.069	1.260	0.0513
MMP2	2.119	0.715	0.0598
MMP13	1.917	2.412	0.2460
WISP1	1.872	3.647	0.3793
TNC	1.643	0.493	0.1085
MMP1	1.517	0.520	0.1236
MMP14	1.259	1.490	0.4132
MMP3	1.248	1.531	0.3898
VEGFA	1.083	1.026	0.3373
GATA3	-1.184	0.054	0.0538
BCL2	-1.226	0.095	0.0019
EGFR	-1.352	0.188	0.0256
SORBS1	-1.408	0.382	0.0384
BMP2	-1.452	0.090	0.0101
SFN	-1.534	0.725	0.0926
HEY1	-7.734	1.002	0.2055

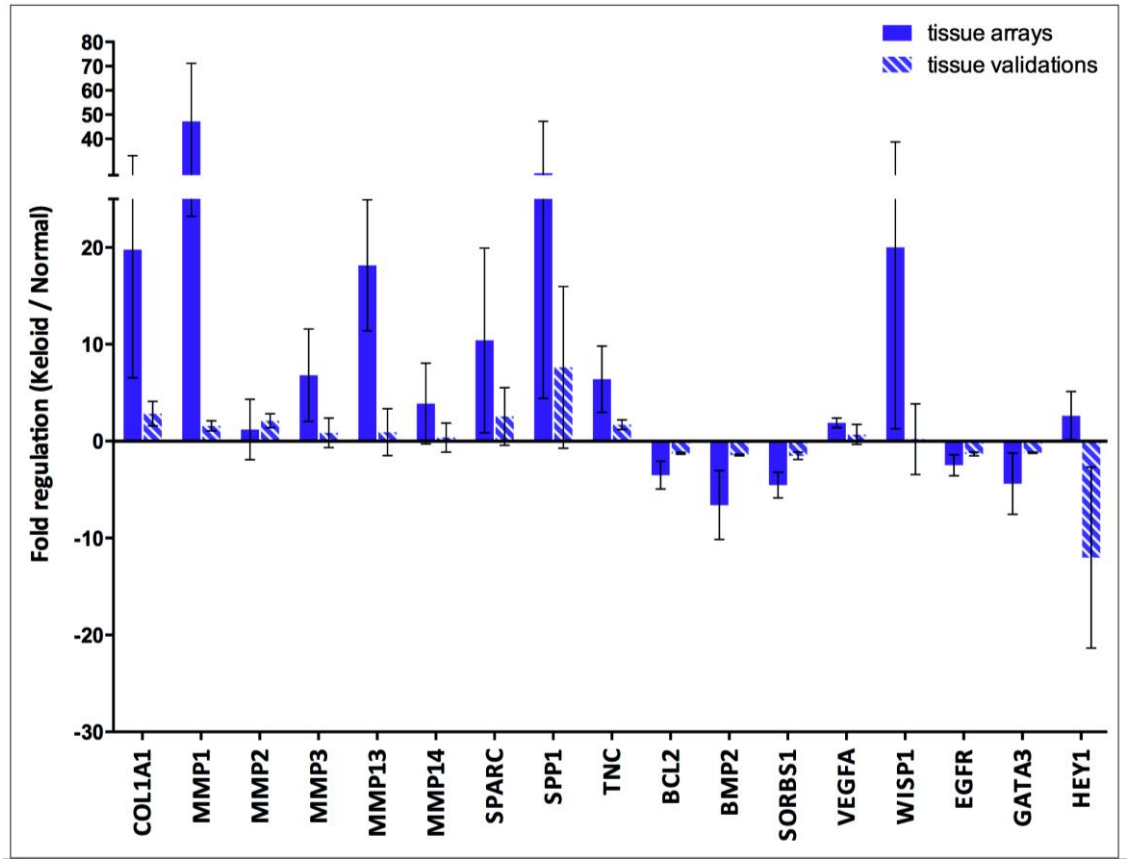

Figure 4-8 Comparison between validation and Real Time qPCR array data

The validated qPCRs showed more subtle changes in gene expression levels, as compared to the original qPCR array data. In almost all of the genes tested, the alterations were consistently in the same orientation, with the exception of HEY1, which showed opposite trends between the PCR array and validation data. Error bars represent the SD of the mean, with n=5 samples. Solid blue bars (arrays) represent data also presented in **Figures 4-2, 4-4** and **4-5**; hatched blue bars (validations) represent data also presented in **Figure 4-7**.

4.3 Discussion

In this chapter, I have identified a range of differentially expressed genes in the African-Caribbean keloids used in this study, when compared to a mixture of African-Caribbean and Caucasian normal skin samples. More specifically, the genes for structural proteins Collagens I, V, VI, XII, XIV, and XVI; fibronectin; and laminin chain alpha1, were all over-expressed in keloid scars. Similarly, the genes for secreted MMPs 1, 3, 13, as well as membrane-tethered MMPs 14 and 16 were over-expressed in keloids. By contrast, laminin chains alpha3 and beta3 were both under-expressed, as was tetranectin (CLEC3B). Interestingly, two genes linked to matrix mineralisation and ossification (Hall, 2014), SPARC (osteonectin) and SPP1 (osteopontin), were both shown to be over-expressed in keloid scar tissue. Another ECM-related gene, TNC (tenascin C), was also over-expressed in keloids, which further suggests the on-going wound healing signals are present in keloid scars (Chiquet-Ehrismann and Chiquet, 2003).

In terms of signal transduction pathway target genes, there was a down-regulation of genes linked to apoptosis, including BCL2 (Wei et al., 2008), BMP2 and BMP4 (Carreira et al., 2014). Genes related to cell survival and development, such as WISP1 (Su et al., 2002, Xu et al., 2000), HEY1 (Nakagawa et al., 2000), and ID1, were up-regulated in keloids, even though cell proliferation and survival-linked gene EGFR was shown to be under-expressed. SORBS1 was also under-regulated, suggesting an effect on signalling through the PPAR (peroxisome proliferator-activated receptor) (Chen et al., 2012) and IR (insulin receptor) (Yang et al., 2003) pathways There was also increased gene expression levels of VEGFA, suggesting a positive impact on angiogenesis (Murphy and Fitzgerald, 2001) in the keloids.

In the following sections, I discuss the differences between the two types of relative quantitation used for the qPCR analyses of this chapter, as well as the choice of statistical tests used. Then a review of the current literature on some of the most significantly altered targets identified above, and their associated factors, is presented.

4.3.1 Assessment of methodology used

4.3.1.1 Differences in PCR methods

Apart from the high inter-patient variability, the difference in qPCR methodologies used for the qPCR arrays and validation qPCR assays very likely had an impact on the final calculations. In all the qPCR data presented here, a form of relative quantitation was used, with the $\Delta\Delta C_t$ method being used in the qPCR arrays, and the relative standard curve method used for the validation qPCR assays.

The $\Delta\Delta C_t$ method is the most widely used in gene expression studies, as it is the least labour intensive, and most cost effective, since there is no space required for standard curve preparations on the qPCR plates, and the data analysis is simpler (Livak and Schmittgen, 2001). Considering the tendency for misinterpretation of qPCR data, for most researchers the $\Delta\Delta C_t$ method gives enough information for their requirements. The main disadvantage of the $\Delta\Delta C_t$ method is that it assumes the qPCR assays show equal efficiency in the samples being tested, i.e. that the amplification efficiencies of the target and reference assays are approximately equal, using the formula $[2^{-\Delta\Delta Ct}]$. Equal assay efficiency is generally more easily achieved in the case of analyzing more uniform samples such as cell lines, ensuring high RNA integrity, inhibitor-free cDNA synthesis, and when the differences between test and control samples are at least 5-fold (Larionov et al., 2005, Livak and Schmittgen, 2001). When this method is used on clinical samples, which inherently tend to have more issues with nucleic acid integrity, it is more likely that smoothing of the data will produce a higher rate of false positives (Rutledge and Côté, 2003, Larionov et al., 2005).

In the case of performing relative quantitative qPCR analysis on clinical samples, the inherent heterogeneity in the samples as well as the higher concentration of inhibitors and nucleases present, mean the final RNA integrity and cDNA quality is less consistent than for cell lines. Also, genetic variability is much higher between patient samples, meaning additional reference genes are required for the normalization steps in qPCR data analysis. Put together, it becomes less likely that the qPCR assay efficiency rates will be consistent between reference and target

genes in these sample sets, and the $\Delta\Delta C_t$ method assumptions are therefore not appropriate (Larionov et al., 2005). The use of a standard curve enables a more representative calculation of the assay efficiency rates, which can then be taken into consideration during data analysis (Larionov et al., 2005, Rutledge and Côté, 2003). The data is still processed in a relative manner, determining the difference in gene expression of the test samples against that of the control samples. This way, whether a gene has a very high or very low level of expression, the magnitude of change from "control" is more easily detected.

In terms of the quality of the samples used for analysis, other than the inherently increased risk of nuclease action normally problematic in clinical specimens, there was a time difference between the completion of the qPCR arrays and the validation qPCRs. The same RNA lysates were used for separate cDNA preparations for the qPCR arrays and qPCR validations. As the validations were performed 2-6 months after the original extractions were completed, despite following the standard procedures for long-term storage of RNA (at -80°C, with minimal freeze-thaw cycles), it is possible that the RNA integrity was reduced in the period of time between cDNA preparations. This may have further affected the validation qPCRs, and might explain why most of the genes re-analysed were not statistically significantly different.

For the qPCR validation assays, primer sequences were individually designed and therefore different to those used in the qPCR arrays, as another validation measure. Added to this, a combination of two reference genes were selected from the qPCR array data, and used for data normalization of the validation qPCR assays, to further minimise any error. The reference genes HPRT and B2M had shown the most stable level of expression across all tissue samples, making them the best choices. By making these changes to the original methodology, the aim was to add an extra level of stringency to the validation process, thereby aiming to exclude any false positives that might have occurred during the qPCR array analyses. Overall, the aim was to minimize inconsistent and inaccurate reporting of gene expression data, by following as many of the published MIQE (Minimum Information Necessary for Quantitative Real-Time PCR Experiments) guidelines as

deemed fit for purpose in this thesis (Johnson et al., 2014, Dheda et al., 2005, Bustin et al., 2010, Bustin, 2010).

4.3.1.2 Statistical analyses

Whilst assessing appropriate analysis of qPCR data, it is also important to consider the statistical analysis and any post-hoc tests used. Most small to medium-scale gene expression analyses, such as in this chapter, are subjected to a simple unpaired Student's T-test, for each gene, comparing "test" to "control" samples. For a single test, the assumption is that the data follow a normal distribution, and with a threshold set at 5%, a significant difference in gene expression between test and control would be indicated with a p value of 0.05 or less. This shows that there is a 5% or less probability that this difference would occur purely by chance, and is not related to the experimental parameters (Motulsky, 2014).

In the case of studies where multiple comparisons are being made within the same system, interpreting multiple p values becomes more complicated. With a 5% threshold, the probability that at least one comparison will be significantly different becomes much higher than 5% (Motulsky, 2014, Berry, 2007). The larger the number of tests, the easier it becomes to identify rare events ($p<0.05$), making it more likely that errors will be made. Various degrees of stringency in correcting for multiple comparisons have been developed and are applied depending on the study requirements and the number of multiplicities (Berry, 2007, Rothman, 1990, Herve, 2007). However, it is a fine balance between maximizing the possibility of identifying significant results, and making sure the more stringent corrections do not overlook real effects taking place (Herve, 2007). In my qPCR analyses, no correction for multiplicities was made, due to the relatively small number of tests being performed, in the context of gene expression studies. Additionally, one major aim of this analysis is to generate new hypotheses to test further, rather than simply prove or disprove an existing hypothesis. The overall gene expression patterns observed in this chapter were considered within the wider context of the functions of those genes, the pathways and other molecules they interact with,

rather than simply restricting research into only those specific genes (Saville, 1990).

4.3.2 Extracellular matrix and adhesion molecules

4.3.2.1 ECM structural molecules - Collagens

As described in **Chapter 1**, the collagen functions range from providing tissue structure, aiding cell adhesion and migration, to tissue repair and remodelling (Gordon and Hahn, 2010, Kadler et al., 2007, Ricard-Blum, 2011). The most abundant form of collagen in the body is fibril-forming collagen type I, which provides structure and tensile strength to tissues (Gelse et al., 2003). In keloid scarring (and fibrosis as a whole), it is well established that increased levels of collagen I make up the bulk of the fibrotic scar tissue (Jumper et al., 2015). The increased levels of collagen type I and fibronectin 1 gene expression seen in this chapter, along with the increased levels of mature collagen I protein expression discussed in **Chapter 3**, confirm the fibrotic state of the tissues (Babu et al., 1989).

Collagens V and VI have all been previously noted as overexpressed in keloid tissue and isolated cells, via microarray gene expression studies (Huang et al., 2013a). These collagens are known to interact with collagen type I, thereby affecting their gene expression levels. Collagen V filaments are often buried inside the triple helical collagen I structures (Birk, 2001, Fichard et al., 1995, Gelse et al., 2003), but have also been noted near the basement membrane in skin (Birk et al., 1986, Gay et al., 1981). Here, fine collagen V filaments may interact with collagen types IV and VI (Chanut-Delalande et al., 2004, Chanut-Delalande et al., 2001), both of which play an important role in the basement membrane, connecting the epidermis to the dermis (Gordon and Hahn, 2010, Ricard-Blum, 2011).

Out of the FACIT (fibril-associated collagens with interrupted triple helices) collagen types XII, XIV and XVI, which were significantly overexpressed in my data, collagens XII and XVI have previously been reported to be overexpressed in whole keloid tissue (Huang et al., 2013a, Chen et al., 2003). In normal skin, collagens XII and XIV crosslink with collagen I fibrils (Amenta et al., 2005, Gelse et al., 2003,

Ricard-Blum, 2011), whereas collagen XVI integrates itself into fibrillin1-containing microfibrils in the papillary dermis (Kassner et al., 2003). In a mouse model of bleomycin-induced pulmonary fibrosis, collagens XII and XIV were implicated in the fibrotic tissue development (Tzortzaki et al., 2003). Over the 12-week bleomycin treatment period, collagen XII was at its highest during weeks 4-8, whereas collagen XIV showed an increased expression from 4 to 12 weeks, suggesting distinct roles for each of these collagens during fibrosis (Tzortzaki et al., 2003). The same group confirmed this observation in pulmonary fibrosis patients, and showed that collagen XII in particular co-localised with collagen I nodules in the granulation tissue (Tzortzaki et al., 2006).

4.3.2.2 Tissue remodelling - MMPs

There is clearly a high level of ECM production taking place in keloid tissues, as demonstrated by the gene up-regulation of several collagens. As for ECM-degrading molecules, MMPs 1, 2, 3, 13, 14 and 16 gene expressions were all significantly up-regulated in keloid tissue compared to normal skin, in my PCR array findings. MMP1 in particular showed the highest gene expression level, though also had a very high standard error. This was due to the wide variance between individual keloid patients, ranging from 12-fold to 67-fold increased expression of MMP1. Protein expression patterns established in **Chapter 3** reflect the MMP13 overexpression, however the extremely high gene expression of MMP1 is not reflective of the almost no difference in protein levels observed in Chapter 3. Previous studies confirm the MMP13 overexpression in keloids, however MMP1 and MMP3 have shown to be under-expressed in keloid tissues and fibroblast cultures (Huang et al., 2013a, Smith et al., 2008). One study showed how the lack of MMP1-mediated degradation of Collagen I in keloids could be due to TIMP1 blocking MMP1 action. When TIMP1 was knocked down by siRNA in keloid fibroblasts, collagen I degradation increased, thought to be due to MMP1 and MMP2 action (Aoki et al., 2014).

MMP2 showed the highest levels of protein expression in **section 3.2.4**. of **Chapter 3**, however did not show any significant difference in gene expression

here. This is in contrast to previous studies which have found MMP2 to be overexpressed at the gene level (Huang et al., 2013a). In my findings, MMP14 gene expression was increased in keloid samples compared to normal skin, reflecting the increase in protein expression observed in **Chapter 3**. Previous microarray studies have also shown an increased MMP14 expression in both keloid and hypertrophic scars (Huang et al., 2013a). As discussed in **Chapter 3**, MMP14 enables the activation of pro-MMP2, therefore suggesting that the increased MMP14 expression could signify an increase in MMP2 activity. Other than the differences in detection methods between previous studies and the work presented in this thesis (discussed earlier), this discrepancy could be due to the differences in source material used. Added to this, it has long been debated whether *in vitro* experimentation on MMP biology is truly reflective of their actual function *in vivo* (Giannandrea and Parks, 2014, Parks et al., 2004).

4.3.2.3 ECM mineralisation-associated factors (SPARC, SPP1)

Osteogenesis- and chondrogenesis-associated genes have previously been identified as significantly increased in a keloid microarray study. These included POSTN (periostin), OGN (osteoglycin), cadherin 11, and HTRA1 (serine protease 11, IGF binding) (Naitoh et al., 2005). In hypertrophic scars, two other osteogenic factors, SPARC (osteonectin) and SPP1 (osteopontin), have been reported to be significantly overexpressed compared to normal skin (Wu et al., 2004a). In my findings, both SPARC and SPP1 were overexpressed in the keloid specimens, compared to normal tissue, despite revealing a high level of inter-patient variability in terms of the magnitude of overexpression (see **Figure 4-8**). This was especially reflected in the validation qPCRs, where one keloid even showed a small down-regulation of SPARC and another showed a small down-regulation of SPP1 (see **Figure 4-7**). Both SPARC and SPP1 are best known for their roles in bone formation, and bone ECM assembly (Sodek et al., 2000). Very little is known about the expression patterns and functions of SPARC and SPP1 in keloid scarring, however there are a number of studies reporting their effects in other types of fibrosis and in the context of wound repair (Chavez-Muñoz et al., 2012, Wu et al., 2012, Hunter et al., 2012, Goldsmith et al., 2013, Sodek et al., 2000).

SPARC is an ECM protein, known to directly affect pro-collagen processing and therefore influence collagen stability and assembly (Goldsmith et al., 2013). It has been proposed that SPARC in fact acts as a collagen molecular chaperone in the endoplasmic reticulum (ER), and together with heat-shock protein 47 (HSP47), ensures that no misfolded procollagen molecules exit from the ER (Martinek et al., 2007). An interesting study on hypertrophic scarring, showed how stratifin (SFN, also known as 14-3-3σ) interaction with SPARC may have implications for ECM regulation in dermal fibroses such as hypertrophic and keloid scars (Chavez-Muñoz et al., 2012). The SPARC/SFN complex was identified in normal keratinocyte-conditioned media (KCM), which when applied to normal fibroblasts, decreased pro-collagen type I gene expression in the fibroblasts. In human hypertrophic scar tissue SPARC was increased and SFN decreased, leading to a greater expression of collagen I. (Chavez-Muñoz et al., 2012)

In myocardial fibrosis, a lack of SPARC in myocardial fibroblasts led to an increased detection of collagen I, compared to wild-type fibroblasts, though most of the collagen was fully matured (Harris et al., 2011). The role of SPARC in collagen assembly was further elucidated *in vivo*, where a SPARC-null mouse study revealed significantly reduced collagen fibril formation and impaired collagen maturation (Schellings et al., 2009, Bradshaw et al., 2009). Taken together, these studies suggest that when SPARC is absent, the rate of collagen maturation is greatly reduced within the myocardium (Goldsmith et al., 2013). Regulating SPARC expression and action on ECM remodeling could help to attenuate excessive scar tissue growth.

SPP1 is a secreted phosphoprotein (Craig et al., 1989), which interacts with αvβ3-integrin, CD44, and other ECM molecules such as fibronectin (O'Regan and Berman, 2000, Liaw et al., 1995, Denhardt and Guo, 1993). It is functionally very diverse, and expressed in many different tissues, including bone, dentin, kidney, brain, vascular tissues, ganglia of the inner ear, the epithelia of mammary, salivary and sweat glands, distal renal tubes, activated macrophages and lymphocytes, as well as fibroblastic cells (Buback et al., 2009, Wang and Denhardt, 2008, Sodek et

al., 2000, Anborgh et al., 2011, Rittling, 2011). In fact, SPP1 is thought to be required for fibroblast differentiation into myofibroblasts (Lenga et al., 2008), as well as osteoblast differentiation (Zohar et al., 1997). SPP1 stimulates cell signalling pathway activation, via phosphorylation of a range of extracellular receptors at the cell-ECM interface (Denhardt et al., 2001, Sodek et al., 2000, Lopez et al., 1995), and has been linked to multiple processes including inflammation, cancer metastasis, apoptosis inhibition, wound healing, and ECM remodelling (particularly bone remodelling) (O'Regan and Berman, 2000, Denhardt et al., 2001, Hunter et al., 2012).

The pro-fibrotic effect of SPP1 has been shown in pulmonary fibrosis (Takahashi et al., 2001, Pardo et al., 2005), kidney fibrosis (Persy et al., 2003), and dermal fibrosis within systemic sclerosis (Wu et al., 2012, Gardner et al., 2006). In idiopathic pulmonary fibrosis patients, SPP1 gene expression was increased, and thought to promote fibroblast and epithelial cell proliferation and migration (Hunter et al., 2012, Pardo et al., 2005). In dermal wound studies, SPP1-null mice demonstrated a haphazardly organised ECM in the dermis, with collagen fibrils being reduced in size and number, compared to wild-type mice (Liaw et al., 1998). In a mouse model of bleomycin-induced dermal fibrosis, SPP1 knockouts were less fibrotic, and expressed decreased TGF-β1 levels, as compared to wild-types (Wu et al., 2012). In an equine model of wound healing, SPP1 gene expression appeared at its highest throughout the duration of wound closure, but maintained a low-level expression after wound closure was complete, and showed no expression in normal skin (Miragliotta et al., 2014). The same study found SPP1 protein expression, as tested by IHC, was increased in human keloid samples, compared to normal skin, particularly in the epidermis (Miragliotta et al., 2014).

4.3.3 Signalling pathways

Looking more closely at the significantly altered signal transduction pathway target genes in this sample group, it appears that there is no single signalling pathway apparently linked to these keloids. It is clear that TGF-β/Smad signalling is taking place, with a number of target genes from this pathway having shown

altered expression in the qPCR data of this chapter: other than collagen type I and α-SMA, ID1 (inhibitor of differentiation 1), MMP2, and Wnt target WISP1 (WNT1 inducible signalling pathway protein 1) were all overexpressed in the keloid scars. The up-regulation of HEY1 (hairy/enhancer-of-split related with YRPW motif 1), WISP1, and VEGFA (vascular endothelial growth factor A) suggests an activation of the Wnt and Notch pathways playing a role in cell survival and development (Su et al., 2002, Xu et al., 2000, Murphy and Fitzgerald, 2001). Cell proliferation and survival-linked gene EGFR was shown to be under-expressed. Although one study showed a greater growth response to EGF in keloid fibroblasts (Kikuchi et al., 1995), another study showed the opposite effect (Satish et al., 2004). Additionally, Satish et al. found that there was no real difference in EGFR expression in keloid fibroblasts (Shih and Bayat, 2010b). These genes all play a role in mediating myofibroblast activation, as well as being downstream targets of TGF-β/Smad (He and Dai, 2015, Phanish et al., 2006, Liu, 2010).

SORBS1 (sorbin and SH3 domain containing 1) is a CBL-associated protein which is linked to insulin receptor signalling (Yang et al., 2003). In keloid biology, the expression or role of SORBS1 has not been reported to date. I found SORBS1 was down-regulated in keloid tissues, suggesting an effect on signalling through the PPAR (peroxisome proliferator-activated receptor) (Chen et al., 2012) and IR (insulin receptor) (Yang et al., 2003) pathways. An under-expression of SORBS1 could suggest a reduction of insulin-stimulated glucose transport (Chen et al., 2012, Yang et al., 2003), thereby affecting cell proliferation. This could be indicative of the reported higher levels of apoptosis seen in the central keloid regions.

The down-regulation of BMP2 and BMP4 (bone morphogenetic proteins 2 and 4) could mean an inhibition of the Hedgehog pathway, which would impact parts of TGF-β and Wnt signalling. The observed downregulation of BCL2 (B-cell lymphoma 2) suggests a decrease in apoptotic pathway activity (Wei et al., 2008). SPP1 has shown to prevent apoptosis by activating NFκB (nuclear factor kappa B) in endothelial cells (Scatena et al., 1998), maintaining membrane integrity, and

preventing Bcl-x cellular redistribution (a Bcl-2 family member thought to block procaspase activation) (Sodek et al., 2000, Denhardt and Noda, 1998).

Overall, conflicting conclusions can be made from the signalling pathway target gene expression patterns observed in this chapter. It seems numerous studies looking at cell proliferation and apoptosis-related genes also show conflicting results (Shih and Bayat, 2010b). This is most likely due in large part to the source materials used, i.e. the keloid characteristics, and which lesional regions were analysed. Also, experimental design is highly variable between studies, making it difficult to deduce which targets show a true correlation to keloid pathogenesis.

In the next chapter, a first level of validation of the targets identified above, which were significantly altered in keloids, are examined in keloid-derived cell cultures. Both fibroblast and keratinocyte cultures are analysed.

5 Target validation in keloid primary cells

5.1 Introduction

A variety of cell culture systems have been used over the last three decades, to investigate the growth of keloid fibroblasts, and to define their characteristics in comparison to normal fibroblasts (Luo et al., 2001, van den Broek et al., 2014). Cell growth kinetic studies have shown keloid and normal fibroblasts do not differ significantly, when cultured in the presence of fetal calf serum (Russell and Witt, 1976, Diegelmann et al., 1979). Cell size, and density-dependent growth inhibition were similar between keloid and normal fibroblasts (Russell and Witt, 1976). However, when grown in serum-free conditions, keloid fibroblasts demonstrated a lower dependence on growth factors than normal cells (Russell et al., 1988). Additionally, keloid fibroblasts showed an increased growth response to TGF-β (Bettinger et al., 1996) and PDGF (Haisa et al., 1994) treatments, suggesting that keloid fibroblasts could have a higher growth potential than normal fibroblasts. Luo et al. showed that there were varying levels of proliferative and apoptotic fibroblasts, depending on the region of the keloid. The fibroblasts found in the deeper layers of the dermis appeared to be the least apoptotic, though all keloid fibroblast fractions (from the papillary and reticular dermis) were still at least 2-fold less apoptotic than normal control fibroblasts (Luo et al., 2001).

Keloid keratinocytes have mainly been studied in relation to fibroblasts, showing their effect on fibroblast behaviour. A variety of cell culture methods have been employed, whereby there is an interaction between keratinocytes and fibroblasts, such as: treating fibroblasts with keratinocyte conditioned media (Ghaffari et al., 2009b, Mukhopadhyay et al., 2005); co-culturing the two cell types using a trans-well system (Xia et al., 2004, Lim et al., 2002b, Lim et al., 2001); or using collagen gels for organotypic 3D cultures (Butler et al., 2008). Keloid keratinocytes have been shown to increase collagen I synthesis in both normal and keloid fibroblasts (Ghaffari et al., 2009b, Mukhopadhyay et al., 2005, Lim et al., 2002b), as well as promote fibroblast growth (Lim et al., 2001), and reduce fibroblast apoptosis (Funayama et al., 2003). Keloid keratinocytes have been shown to modulate cytokine secretion by fibroblasts, such as CTGF (connective tissue growth factor) (Khoo et al., 2006), IL6, IL8, MCP1 (monocyte chemoattractant protein-1), VEGF,

and others (Lim et al., 2009). When cultured together, both keloid keratinocytes and keloid fibroblasts displayed an increased expression of TGF-β1 and TGF-βRI, while the fibroblasts also had increased levels of TGF-β2 and Smad2 (a downstream target of the TGF-β pathway) (Xia et al., 2004). This TGF-β related overexpression was seen both in total and active forms of the proteins (Xia et al., 2004). Overall, it is clear that the epithelial-mesenchymal interaction is important for signalling processes in both cell-types, impacting on their growth, expansion and turnover.

Investigations on keloid keratinocyte monolayer cultures have not been widely documented. One gene expression profiling study compared monolayer cultured keloid fibroblasts and keratinocytes against whole keloid scar tissue (Hahn et al., 2013). Their microarray analysis found a small subset of genes with significantly altered expression in both keloid fibroblasts and keratinocytes, as well as in the original tissues, compared to their normal counterparts. Periostin (POSTN), an osteogenic factor, showed the highest gene up-regulation in tissue and fibroblasts, but not keratinocytes. Whereas transforming growth factor β receptor III (TGFβ-RIII) showed a significant down-regulation in tissue and keratinocytes, but not in fibroblasts (Hahn et al., 2013).

In terms of keloid regional differences, a small number of studies have shown differential expression of proliferative and anti-apoptotic genes being expressed in the central, marginal or adjacent normal skin of keloid biopsies. However, the same studies often failed to verify the same expression patterns in isolated fibroblasts and keratinocytes. Shih et al. found 10 genes to be significantly differentially expressed by at least 2-fold between keloid margin and adjacent normal skin, while the same 10 genes showed no statistically significant difference between fibroblast populations of the same keloid regions (Shih et al., 2010b). Despite this, the trend seen in cultured fibroblasts was the same as in the original biopsy data in 7 out of the 10 identified genes. The authors suggested that the cell culture methodology used was the most likely cause for the lack of statistical significance (Shih et al., 2010b), though the high inter-patient variability observed was potentially another contributing factor. Importantly, the related keloid

keratinocytes were not examined in this study, which might have helped to explain the difference in results between biopsies and cultured cells.

The culture system chosen for target validation of genes identified from whole tissue in **Chapter 4** was a monolayer culture of fibroblasts and keratinocytes from keloids. One of the keloids from which matching fibroblasts and keratinocytes were isolated, was also part of the analysis in both **Chapters 3** and **4**. This simple and relatively shorter protocol was selected in favour of a co-culture system, so as to be able to increase the number of patient samples being used. A more complex co-culture or organotypic culture system would restrict the sample number, due to project time constraints. Both fibroblast and keratinocyte populations were cultured from keloid and normal tissue, and expression analysis was performed on passage 3 or 4 of all cultures. Taking into account the high level of bias in defining the boundaries of each keloid margin without first looking at the histological features (discussed in **Chapter 3**), an equal proportion of keratinocytes or fibroblasts from each scar region was combined to reflect the whole scar tissue. This way, the gene expression data in keloid cells would also be comparable to the whole tissue data.

5.1.1 Aim

The primary aim of this chapter was to examine a selection of the gene targets previously validated in keloid whole tissue in **Chapter 4**, in primary cultures of fibroblasts and keratinocytes isolated from keloid and normal tissue. Both fibroblasts and keratinocytes were cultured as a single layer, and examined in isolation from each other, in order to examine the differences between keloid and normal cells. All cultures were first assessed for any difference in rate of growth, and basic morphology. Finally, a verification of the most significantly altered target was made by IHC-IF on the original patient specimens.

5.2 Results

Primary cultures from keloid and normal tissues, were established for both fibroblast and keratinocyte cell populations. **Section 2.3, Chapter 2** describes the full procedure of cell isolation and expansion. A total of six keloid patients and four normal skin donors were used for the propagation of fibroblast and keratinocyte cultures. Patient 36 was the only keloid which was analysed in full throughout this thesis in terms of the IHC in **Chapter 3**, both gene expression qPCR arrays in **Chapter 5**, and the analyses described below in both fibroblasts and keratinocytes. Patient 34 tissue was also fully characterised (**Chapter 3**), analysed in the qPCR arrays (**Chapter 4**), but only the fibroblasts were available for gene expression analysis below. Similarly, only Normal Skin 6 was fully examined throughout this thesis. Most of the remaining fibroblast and keratinocyte cultures were isolated from tissues, which were characterised in **Chapter 3**, but not analysed in the qPCR arrays of **Chapter 4**. Refer to **Tables 2-1** and **2-2** in **Chapter 2** for full information on which samples were used for which analyses.

Below, a calculation of the rate of growth of each patient's cells is presented. This is followed by an evaluation of whether the targets, previously found to be altered in whole tissue, continue to show similar gene expression patterns in cultured cells. Both cell types were grown as single layer cultures, and patient matched cells (i.e. both fibroblasts and keratinocytes from the same patient) were used wherever possible. In order to reflect the analyses thus far, where whole keloid tissues were used, inclusive of the central, edge and adjacent normal regions, the isolated fibroblasts and keratinocytes were similarly taken from all three regions of the keloid. The only difference here is that the epidermal and dermal cells were examined separately.

5.2.1 Cell morphology and growth of primary cultured cells

5.2.1.1 Primary fibroblasts

Primary fibroblast morphology was similar between normal and keloid fibroblasts. The cells had a typical elongated spindle shape, and once they reached a

confluence of higher than 50%, they began to align into parallel clusters. Both keloid and normal fibroblasts appeared very similar to each other in morphology and cell-shape. **Figure 5-1** shows representative images from primary fibroblast cultures.

The rate of growth was determined by two methods: using the Alamar Blue assay, and by population doubling. In the fibroblast population, cells were propagated from 6 keloid patients, and from 4 healthy controls. The Alamar Blue assay was carried out over 7 days, with measurements taken at days 1, 3, 5 and 7. Population doubling times were quantified over seven passages carried out over a 28 day period. There was some variation between individuals, but overall no significant difference in growth rate was found between the keloid and the normal groups, as tested by a 2-way ANOVA (**Figure 5-2**). In the first two passages the population doubling time, for all fibroblasts was between 1.5-2 population doublings per week. This rose a little to an average of 2.5-3.5 population doublings per week, at later passages.

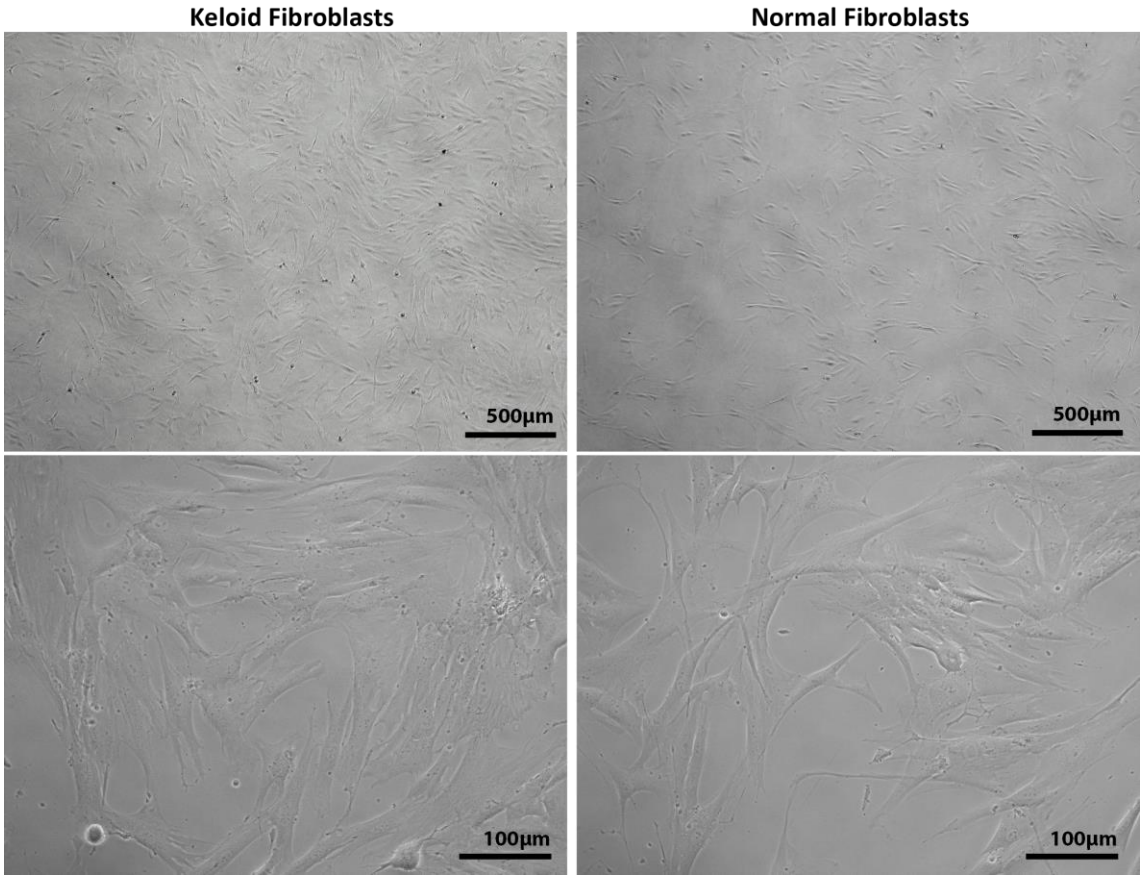

Figure 5-1 Fibroblast cell morphology

Representative images from keloid and normal fibroblast populations, imaged at approximately 70% confluence. Cells were elongated and spindle-shaped in both keloid and normal groups, with very little difference between them. Some areas of keloid fibroblast cultures showed a higher proportion of larger, more spread cells compared to normal cultures, however this was not deemed to be significant.

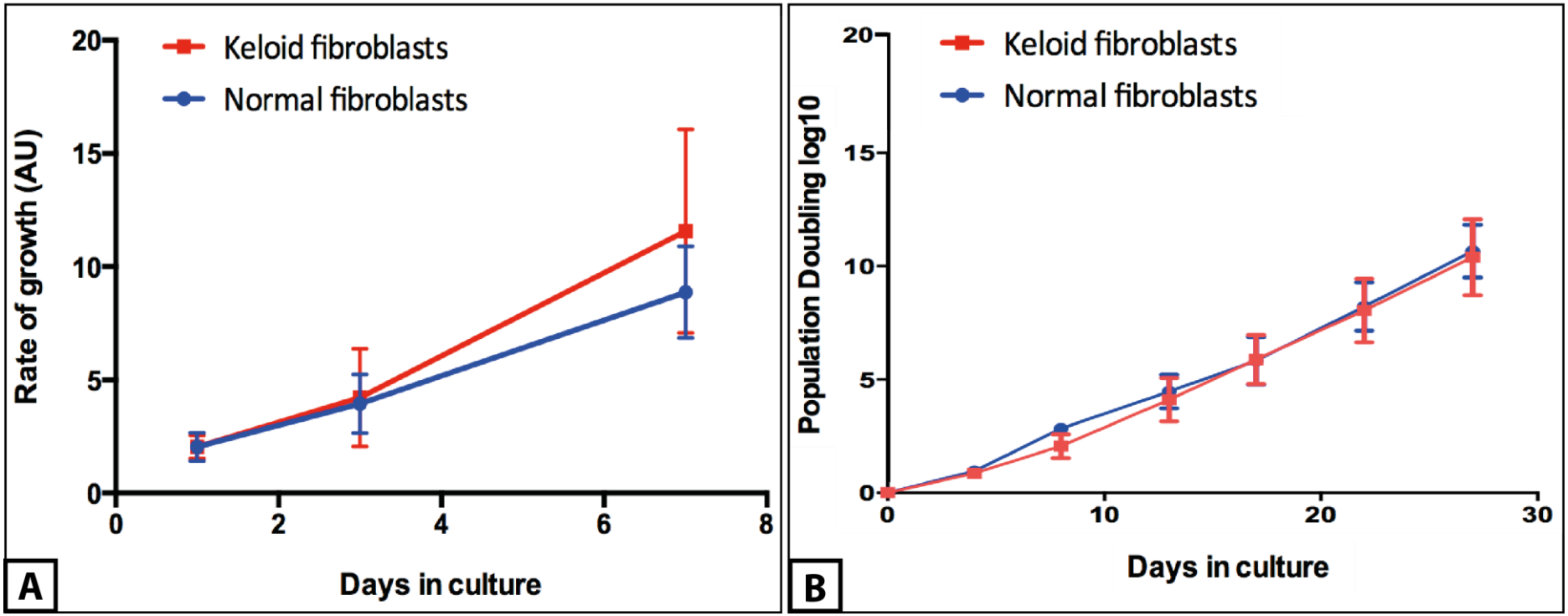

Figure 5-2 Cell growth rate of keloid and normal fibroblasts, by Alamar Blue assay and Population Doubling time calculation

Primary cultured fibroblasts were plated at passage 2 or 3, and the rate of growth measured by **Alamar Blue** assay **(A)** on days 1, 3, 5 and 7 of culture. **Population Doubling** levels **(B)** were investigated by propagating fibroblasts for 28 days through six passages, and their rate of cell doubling calculated at each passage. Fibroblasts were isolated from a total of 6 keloid patients and 4 healthy controls. No significant difference was found, as analysed using a 2-way ANOVA. Error bars represent the standard error of the mean (SEM)

5.2.1.2 Primary keratinocytes

All primary keratinocytes presented the typical "cobblestone" morphology, though there were some differences between keloid and normal cells. Primary keloid keratinocytes appeared larger, and more spread than normal keratinocytes. Both keloid and normal keratinocytes grew in colonies. However, those of normal cells were much more compact, with the individual cells looking smaller. In the keloid group, there were more cases of single cells growing outside of their colonies, compared to the normal group, particularly with increasing passage number. This would suggest that the keloid keratinocytes were undergoing differentiation at an earlier stage compared to normal keratinocytes. **Figure 5-3** shows representative images of keloid and normal keratinocytes under serum-free culture conditions.

The rate of growth was calculated by two methods: using the Alamar Blue assay, and by population doubling. In the keratinocyte population, cells were expanded from 4 keloid scars and 3 healthy controls. The Alamar Blue assay was carried out over 8 days, with measurements taken at days 1, 3, 5 and 8. Population doubling times were measured over four passages carried out over a 20 day period. There was a high level of variation in cell growth rate, particularly in the Alamar Blue assay, which showed no significant difference between keloid and normal cell cultures (as tested using a 2-way ANOVA). In the population doubling measurements however, a statistically significantly lower rate of growth was recorded for the keloid keratinocyte population (**Figure 5-4**). In the first passage of measuring population doubling time, keloid keratinocytes showed 0.2-0.5 population doublings per week. This rose a little in the next passage to 0.8-1.7 population doublings per week, but then fell down to 0.1, and even -0.6 population doublings per week in one case. This suggested that after passage 4 or 5, keloid keratinocytes were starting to differentiate and exiting the exponential growth phase. Normal keratinocytes, on the other hand, showed an initial population doubling rate of 0.5-2 per week, which went up slightly to 1-2 population doublings per week by passage 5. Overall, the total population doubling levels of the normal keratinocytes were statistically significantly higher than the keloid keratinocytes, suggesting a faster rate of growth.

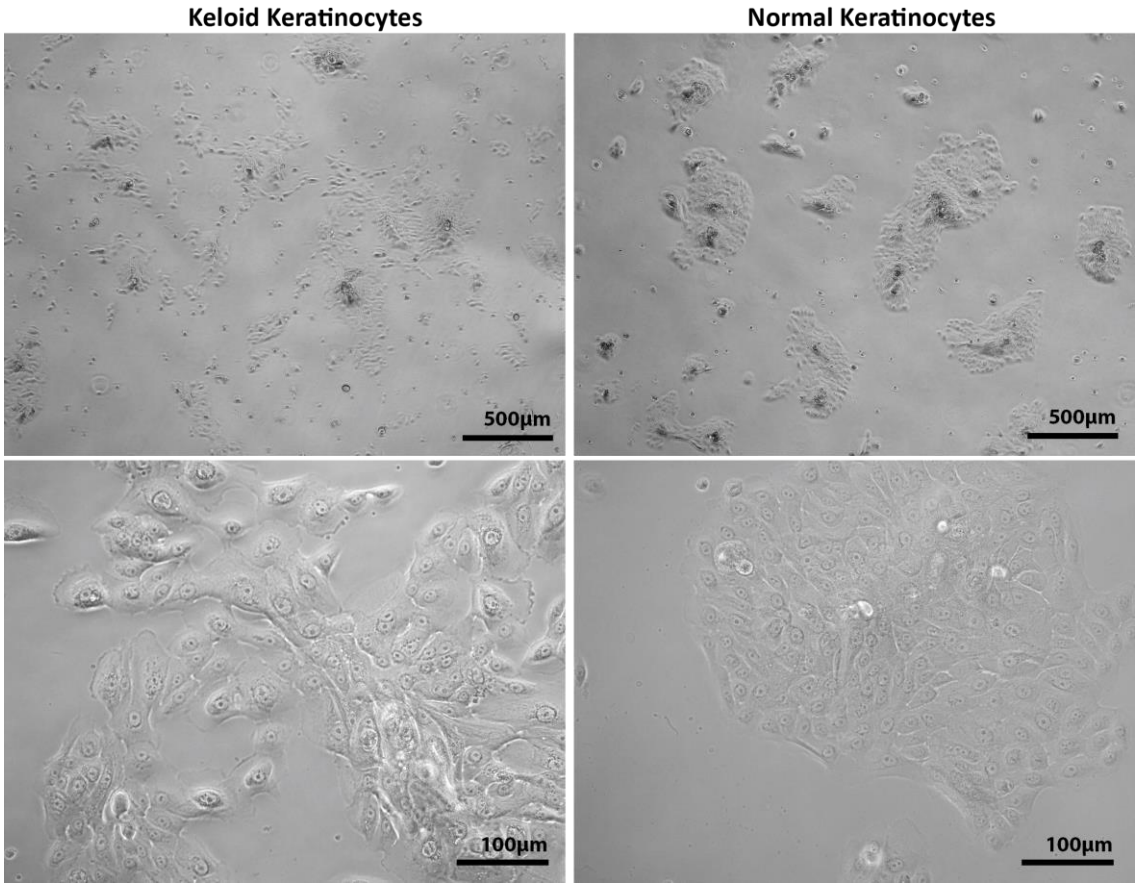

Figure 5-3 Keratinocyte cell morphology

Representative images from keloid and normal keratinocyte populations, imaged at approximately 60% confluence. Both keloid and normal keratinocytes showed a "cobblestone" morphology, though keloid cells were larger and more spread out. Also, keloid keratinocytes showed less compact colony formation, with many more single cells growing outside the colony formations, as compared to normal keratinocytes.

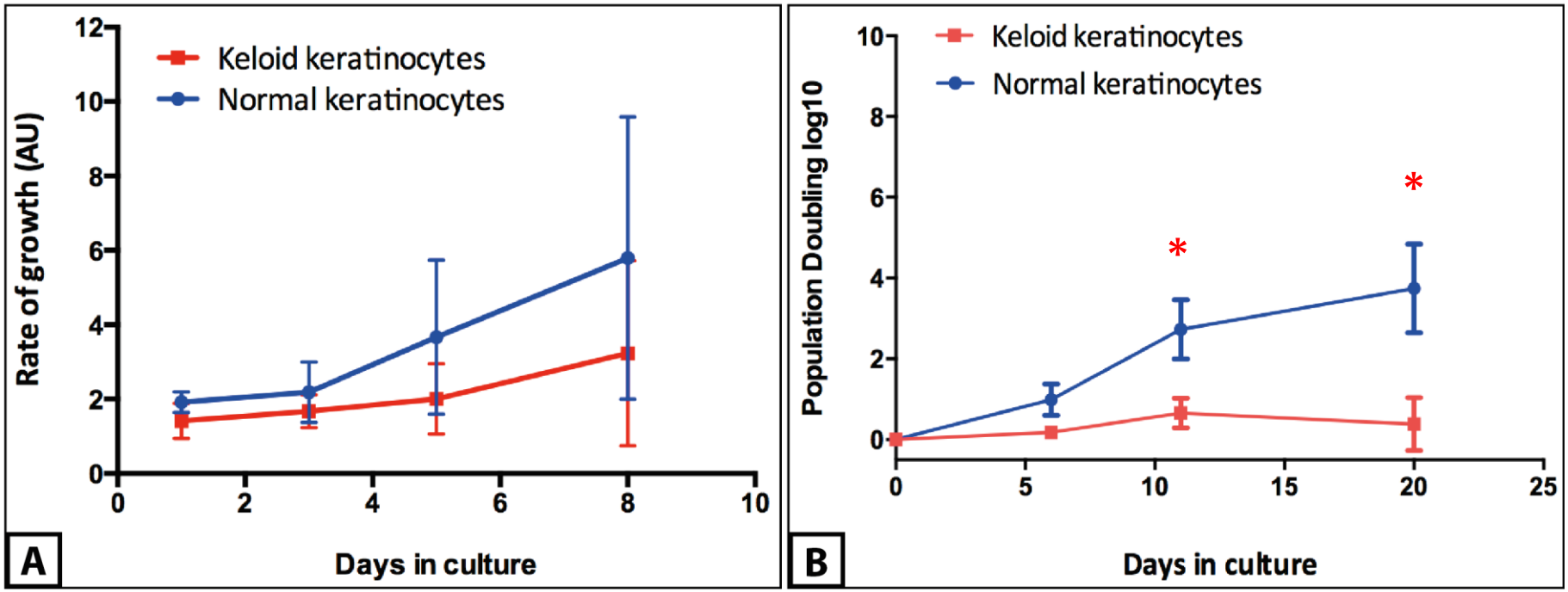

Figure 5-4 Cell growth rate of keloid and normal keratinocytes, by Alamar Blue assay and Population Doubling time calculation.

Primary cultured keratinocytes were plated at passage 2 or 3, and the rate of growth measured by **Alamar Blue** assay **(A)** at 1, 3, 5 and 8 days of culture. **Population Doubling** levels **(B)** were investigated by propagating keratinocytes for 20 days through 4 passages, and their rate of cell doubling calculated at each passage. Keratinocytes were isolated from a total of 4 keloid patients and 3 healthy controls. Keloid keratinocytes showed a statistically significantly decreased rate of growth at days 11 and 20, as measured by population doubling levels **(B)**, calculated using a 2-way ANOVA. Error bars represent the standard error of the mean (SEM)

5.2.2 Expression profiles of altered genes in primary cells

5.2.2.1 Primary fibroblasts

The 18 GOIs (genes of interest) selected from the qPCR arrays on whole tissue, and which were subsequently validated in the same tissues, using individually designed qPCR assays (relative standard curve method), were examined in the keloid and normal primary fibroblasts described so far in this chapter. Even though only four genes (EGFR, SORBS1, BCL2, and BMP2) continued to show statistically significant differences in expression between keloid and normal tissues, described in **Chapter 4**, all 18 genes were tested in the single layer cell cultures, to examine whether the cells retained the same general trends as the original tissues.

The fold-changes in expression of the 18 genes are shown in **Figure 5-5** and **Table 5-1.** Every point within each gene on the graph represents one patient's fibroblasts. Most of the genes revealed very little variance between patient cells. However MMP3, MMP13, BMP4 and GATA3 showed varying levels of expression between patients. When the Student's t-test was carried out, only SPP1 showed a statistically significant over-expression in keloid fibroblasts compared to normal fibroblasts ($p=0.026$). By contrast, all of the selected genes (except for MMP2 and SFN) had shown to be statistically significantly different in the original qPCR arrays, using the same statistical test. It was noted that SFN was almost statistically significantly different with ($p= 0.0502$) and similarly WISP1 with ($p=0.052$).

In **Figure 5-6,** the original tissue data from the qPCR validation assays is compared side by side with the fibroblast qPCR data. Even though the same levels of change in gene expression were not directly reproduced in the validation, the fold-changes for most genes were similarly altered, i.e. both array and validation results showing an up- or down-regulation. The exceptions were MMPs 1, 2 and 3, and TNC, where the whole tissue data showed an up-regulation in keloids, whereas the fibroblast culture results displayed a down-regulation. Similarly, SFN, EGFR and GATA3 all displayed a down-regulation in keloid whole tissue, though keloid fibroblasts showed an up-regulation for all three.

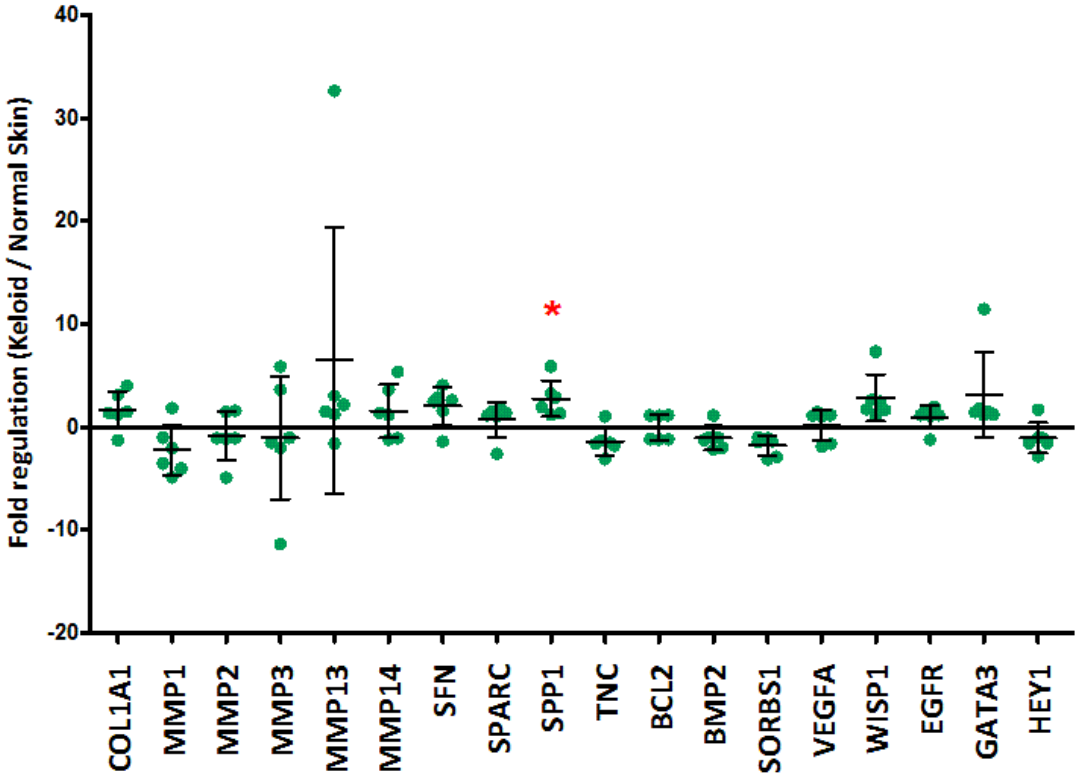

Figure 5-5 Gene expression profile in primary fibroblasts

Real Time qPCR (relative standard curve method) was performed on 18 GOIs and 2 reference genes, selected from the targets found to be differentially expressed in whole tissue (see **Chapter 4**). The majority of the genes showed a small difference between keloid and normal fibroblasts, with only SPP1 demonstrating a significant increase in keloid fibroblasts, as tested by the Student's t-test. [* = $p<0.05$]. Fibroblasts were isolated from n=6 keloid, n=4 control patients. Error bars represent the SD.

Table 5-1 Fold-changes in genes expression, in keloid primary fibroblasts. n=6 keloids; n=4 normal controls; In blue, statistically significantly altered in keloid *vs* normal ($p<0.05$). This data is plotted in Figure 5-5.

Gene symbol	Mean fold-changes	St. Deviation of mean	P value (Student's t-test)
SFN	2.558	1.865	0.0502
SPP1	2.390	1.743	0.026
WISP1	2.090	2.269	0.052
MMP13	1.842	12.895	0.178
GATA3	1.487	4.102	0.105
COL1A1	1.434	1.826	0.163
MMP14	1.280	2.584	0.181
SPARC	1.265	1.637	0.298
VEGFA	1.218	0.482	0.448
EGFR	1.167	1.119	0.335
BCL2	-0.035	1.258	0.768
MMP2	-1.082	2.366	0.569
BMP2	-1.138	1.183	0.270
MMP3	-1.261	5.947	0.752
HEY1	-1.291	1.488	0.356
SORBS1	-1.414	0.936	0.309
TNC	-1.561	1.347	0.064
MMP1	-2.775	2.453	0.129

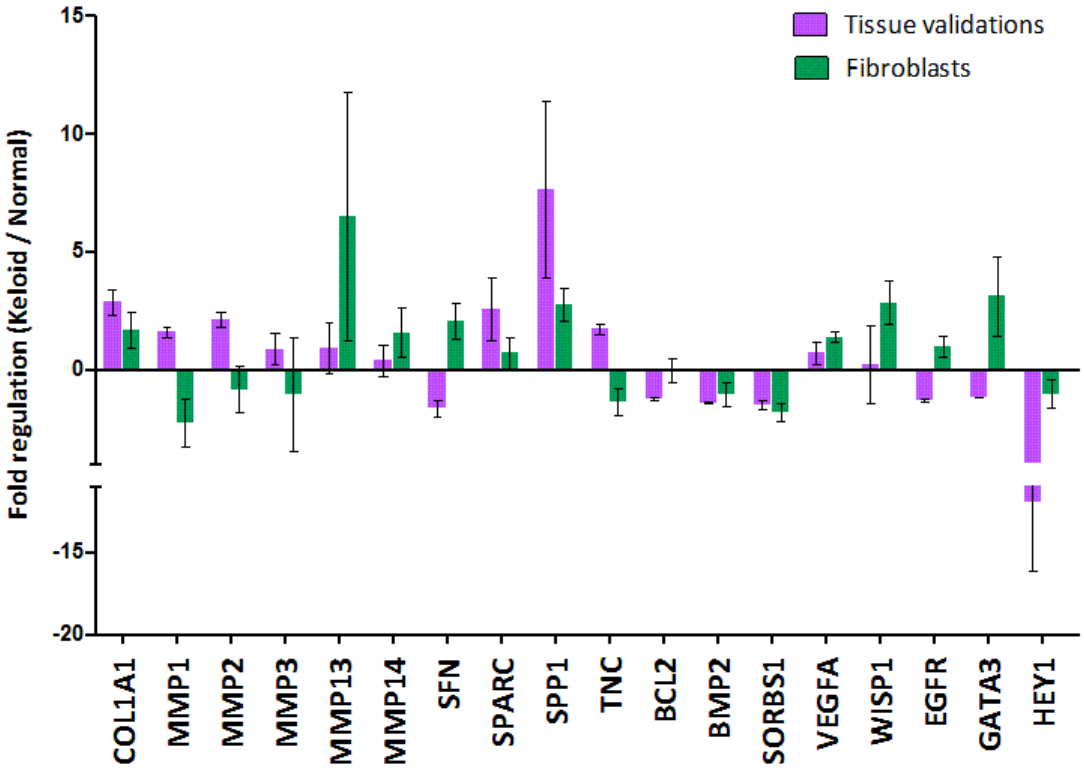

Figure 5-6 Gene expression pattern in primary fibroblasts, compared to whole tissue

The gene expression profiles in primary fibroblasts did not necessarily match the pattern of expression observed in whole tissue (tissue data represents validation qPCRs from **section 4.2.3**). MMPs 1, 2 and 3, SFN, TNC, EGFR, and GATA3 all showed opposite gene regulation, between whole tissue and isolated fibroblasts, whereas the rest of the genes showed similar gene expression trends between the two sample types. Data was taken from **Figures 4-7** (in **Chapter 4**) and **5-5,** for clearer comparison. Error bars represent the SD.

5.2.2.2 Primary keratinocytes

The fold-changes in expression of the 18 GOIs in primary keratinocytes are shown in **Figure 5-7** and **Table 5-2.** Every point within each gene on the graph represents one patient's keratinocytes. Many of the genes revealed a high level of variance between patient cells, including MMPs 1, 2, 3, 13, and 14, SPARC, SPP1, SORBS1, and WISP1. In fact, almost all of these genes showed variable expression in keloids with both up-regulation and down-regulation of expression. When the Student's t-test was carried out, no genes showed any significant difference in keloid compared to normal keratinocytes (**Table 5-2**).

In **Figure 5-8**, the original validation qPCR data is compared alongside with the keratinocyte qPCR data, as the exact same qPCR assays and statistical analyses had been used on both sets of data, making them more comparable. Even though the same levels of change in gene expression were not directly reproduced in the isolated keratinocytes, the fold-changes for most genes were similarly altered, i.e. both array and validation results showing an up- or down-regulation. The exceptions were MMPs 2, 3, 13, where the array data showed an up-regulation in keloid tissues, and a down-regulation in the keratinocyte culture results. Similarly, SFN and BCL2 showed a down-regulation in whole tissue, and an up-regulation in isolated keratinocytes.

Finally, the original validation qPCR data was compared against both the isolated fibroblast and keratinocyte data in parallel (**Figure 5-9**). A small number of genes still showed opposite effects in whole tissue to isolated keloids cells, including MMP2, MMP3, SFN and BCL2. Other genes showed consistently similar regulation between whole tissue and keloid cells, such as COL1A1, MMP14, SPARC, SPP1, BMP2, SORBS1, VEGFA, and WISP1. The remaining genes MMPs 1, 13, TNC, EGFR, and GATA3 showed an interesting pattern whereby one of the cell types linked in with the whole tissue data, and the other cell type showed the opposite. For example, MMP13 was overexpressed in both whole tissue and fibroblasts, but under-expressed in keratinocytes. By contrast, TNC showed an up-regulation in whole tissue and keratinocytes, but a down-regulation in keloid fibroblasts.

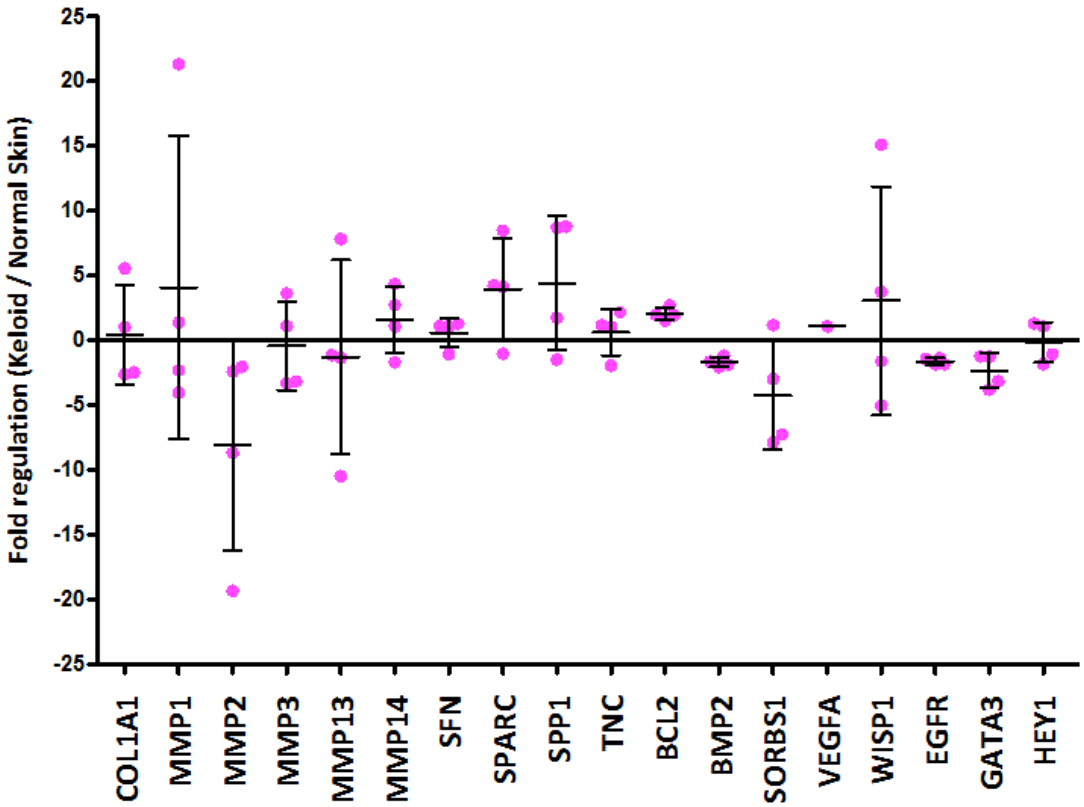

Figure 5-7 Gene expression profile in primary keratinocytes

Real Time qPCR (relative standard curve method) was performed on 18 GOIs and 2 reference genes, selected from the targets found to be differentially expressed in whole tissue (see **Chapter 4**). All genes showed a small difference between keloid and normal keratinocytes, with no genes demonstrating a statistically significant difference, as tested by the Student's t-test. Many genes including all the MMPs, SPARC, SPP1, SORBS1 and WISP1, showed varied expression levels between patients. Keratinocytes were isolated from n=4 keloid, n=3 control patients. Error bars represent the Standard Deviation (SD)

Table 5-2 Fold-changes in gene expression, in keloid primary keratinocytes. (n=6) This data is plotted in Figure 5-7

Gene symbol	Mean fold-changes	St. Deviation of mean	P value (Student's t-test)
SPP1	5.234	1.283	0.209
SPARC	4.208	1.237	0.158
BCL2	1.959	2.005	0.237
MMP14	1.914	1.454	0.428
VEGFA	1.193	1.184	0.738
TNC	1.104	1.282	0.811
SFN	1.098	1.686	0.762
WISP1	1.074	4.329	0.455
HEY1	-0.005	1.395	0.707
MMP1	-0.464	2.005	0.549
COL1A1	-0.719	2.488	0.850
MMP3	-1.017	2.029	0.804
MMP13	-1.224	1.244	0.699
EGFR	-1.630	1.359	0.129
BMP2	-1.752	1.551	0.154
GATA3	-2.181	1.337	0.052
SORBS1	-5.100	1.355	0.117
MMP2	-5.536	34.765	0.656

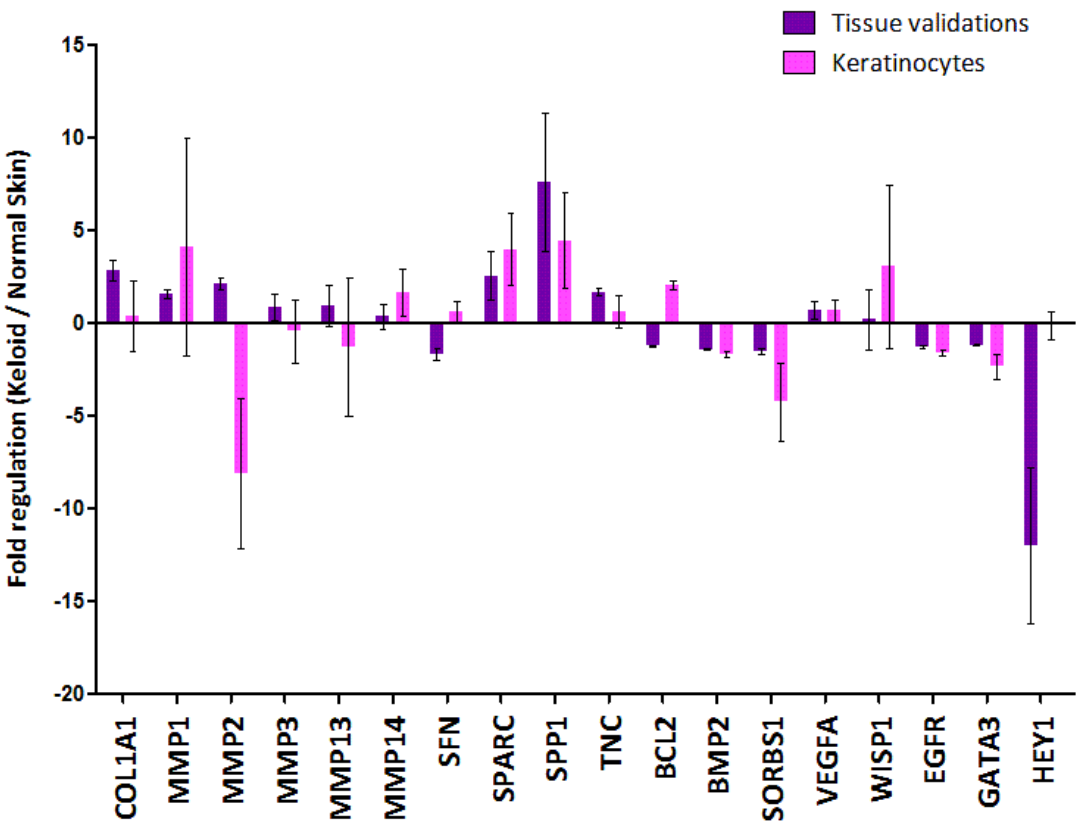

Figure 5-8 Gene expression pattern in primary keratinocytes, compared to whole tissue

The gene expression profiles in primary keratinocytes did not necessarily match the pattern of expression observed in whole tissue (tissue data represents validation qPCRs from **section 4.2.3**. in **Chapter 4**). MMPs 2, 3 and 13, SFN, and BCL2 all showed opposite gene regulation, between whole tissue and isolated fibroblasts, whereas the rest of the genes showed similar gene expression trends between the two sample types. Data was taken from **Figures 4-7 (Chapter 4)** and **5-7,** for clearer comparison. Error bars represent the SD.

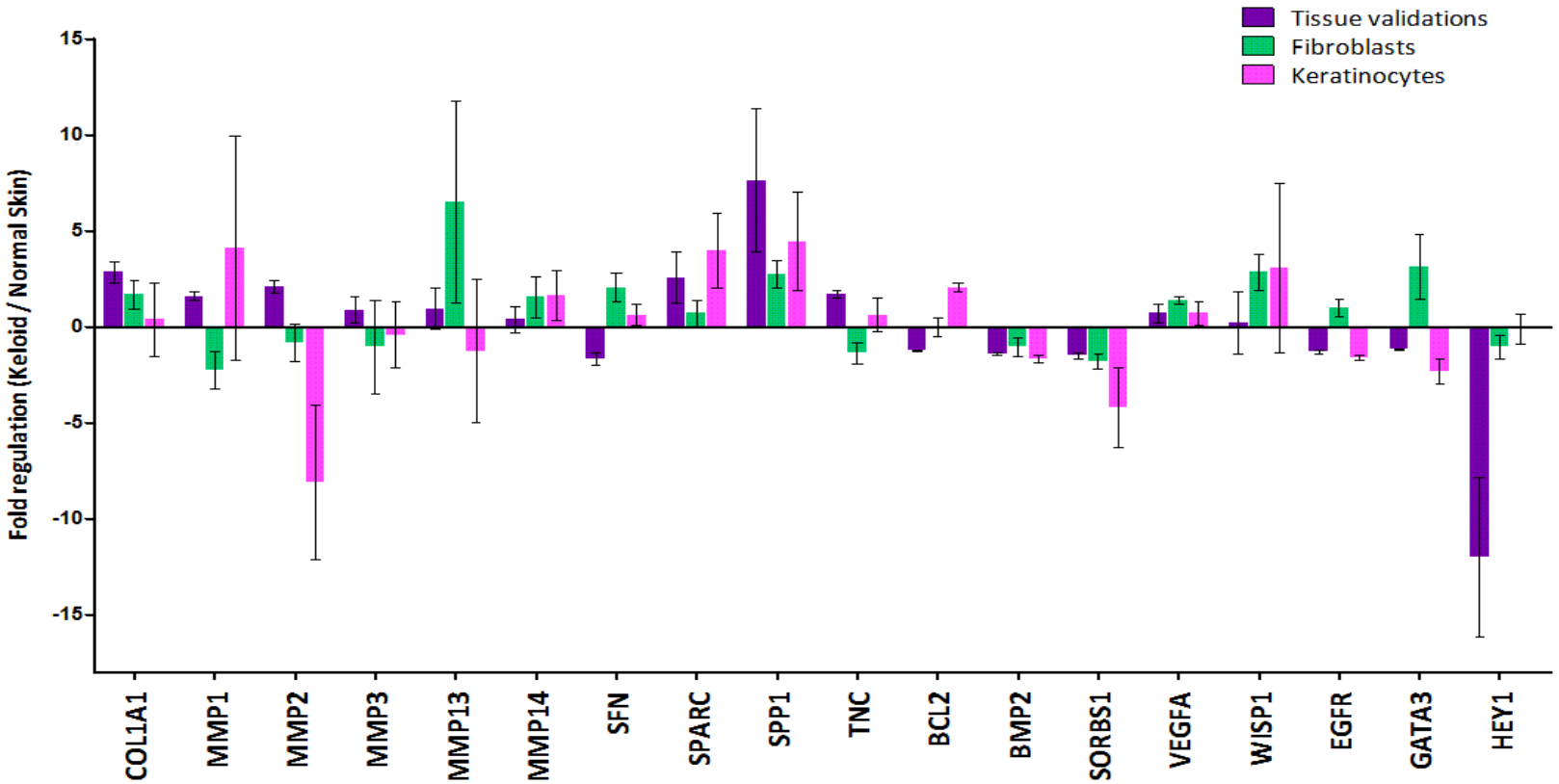

Figure 5-9 Comparing differences in gene expression patterns between whole tissue, primary fibroblasts and primary keratinocytes.

Summary of data already presented in **Figures 4-7 (in Chapter 4), 5-6** and **5-8**. For the majority of these genes, at least one cell-type reflected the gene regulation pattern in whole tissue. The exceptions were MMP2, MMP3, SFN, and BCL2, which displayed the same gene regulation pattern between fibroblasts and keratinocytes, but were in contrast to the trend seen in whole tissue. Error bars represent the SD.

5.2.3 SPP1 protein expression in tissue

As SPP1 gene expression appeared to be consistently up-regulated in whole tissue and primary keloid fibroblasts and keratinocytes, described in both the previous and current chapters, it was of interest to examine whether SPP1 protein levels were also increased in keloid scars, compared to normal tissue. For this, 3 keloid specimens, along with a hypertrophic scar and 2 control normal specimens (fully characterised in Chapter 3) were analysed by IHC-immunofluorescence. SPP1 protein expression is visible in red, and DAPI nuclear stain is in blue (**Figures 5-10, 5-11 and 5-12**).

In normal skin, there was some variability observed in the intensity of SPP1 protein expression in the dermal compartments, with patient 4 showing a higher level of SPP1 than patient 6, particularly in the reticular dermis (**Figure 5-10**). Increased expression was seen in all skin appendages such as hair follicle bulbs, sweat glands and sebaceous glands. In the epidermis, SPP1 expression was consistent across both specimens, and along the length of the entire tissues, being restricted mainly to the upper layers of the epidermis. There was very little SPP1 expression in the basal epidermis. Also, it appeared that SPP1 was present both in secreted form in amongst the ECM of the dermis, as well as intracellular form - particularly noticeable in the epidermis.

In keloid scars, there was some variability in SPP1 expression between scar regions, which appeared consistently across the 3 keloids tested here (**Figures 5-11 and 5-12**). Dermal expression of SPP1 was comparable to normal skin in the papillary dermis, though appeared increased in the deeper dermal layers. In particular, the regions containing thickened collagen nodules previously identified in Chapter 3, showed increased levels of SPP1 protein expression (**Figures 5-11 and 5-12)**. Additionally, in regions of high inflammatory invasion, notably in the edge dermal region of patients 34 (**Figure 5-11**) and 55 (**Figure 5-12**), SPP1 protein levels were at their highest. The hypertrophic scar showed a similar pattern of dermal expression to the keloid specimens. The papillary dermis had a

relatively low level of expression, though the more collagenous, myofibroblast-rich reticular dermis revealed an increased level of expression.

In the hypertrophic and keloid epidermis, SPP1 protein expression was noted across the whole length of the lesions, with the basal epidermal layer showing the most intense signal. In this case, SPP1 is mostly seen to be intracellular, in contrast to the dermis where most of the protein is in the secreted form. Overall, it is clear that these keloids and hypertrophic scar tissue show an increased SPP1 expression, compared to normal skin.

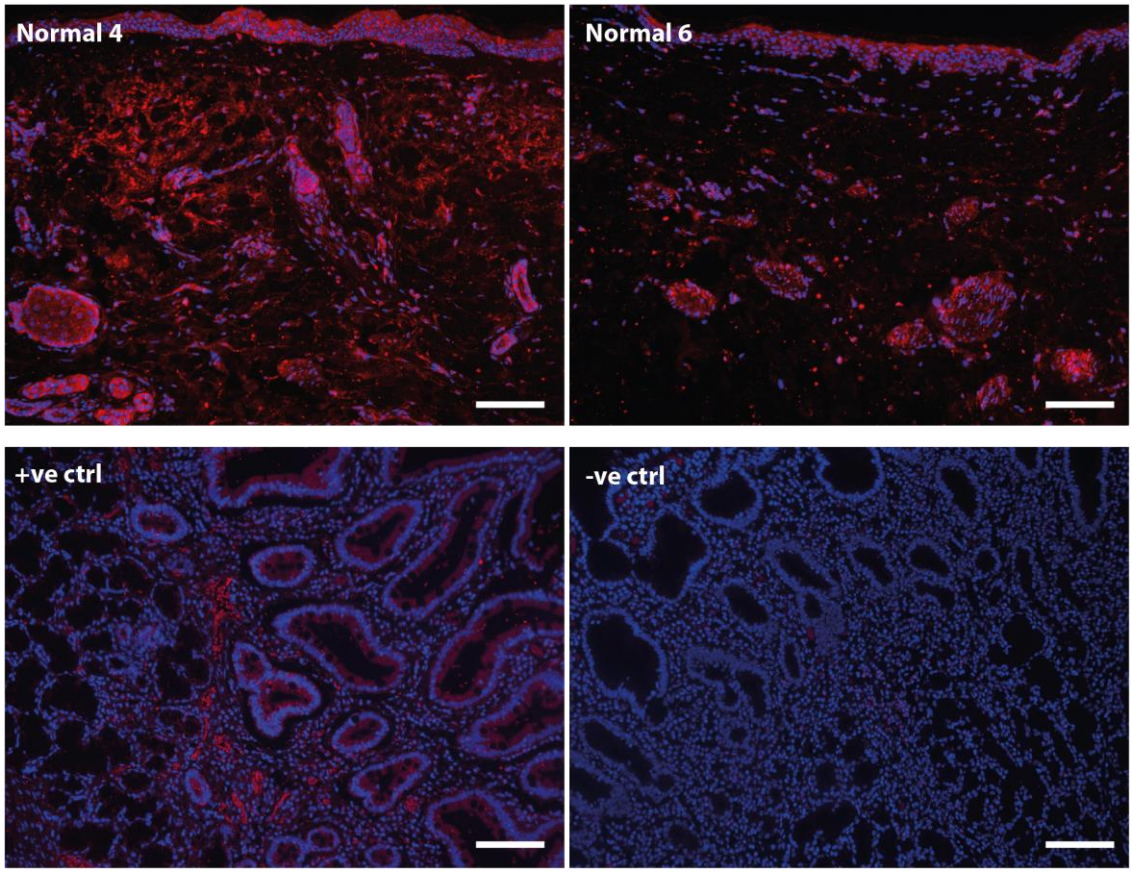

Figure 5-10 SPP1 protein expression by immunofluorescence, in normal skin and tissue controls.

SPP1 protein expression was present in the reticular dermis of normal skin, with some variability in intensity between subjects. Epidermal expression was mainly concentrated in the upper layers of the epidermis. The positive (+ve) and negative (-ve) controls were performed on human stomach cancer tissue, as directed by the antibody manufacturer. SPP1 is shown in red; DAPI nuclear stain is shown in blue. Scale bars represent 100µm. SPP1 was examined in n=3 keloids, n=1 hypertrophic scar, and n=2 normal skin in total.

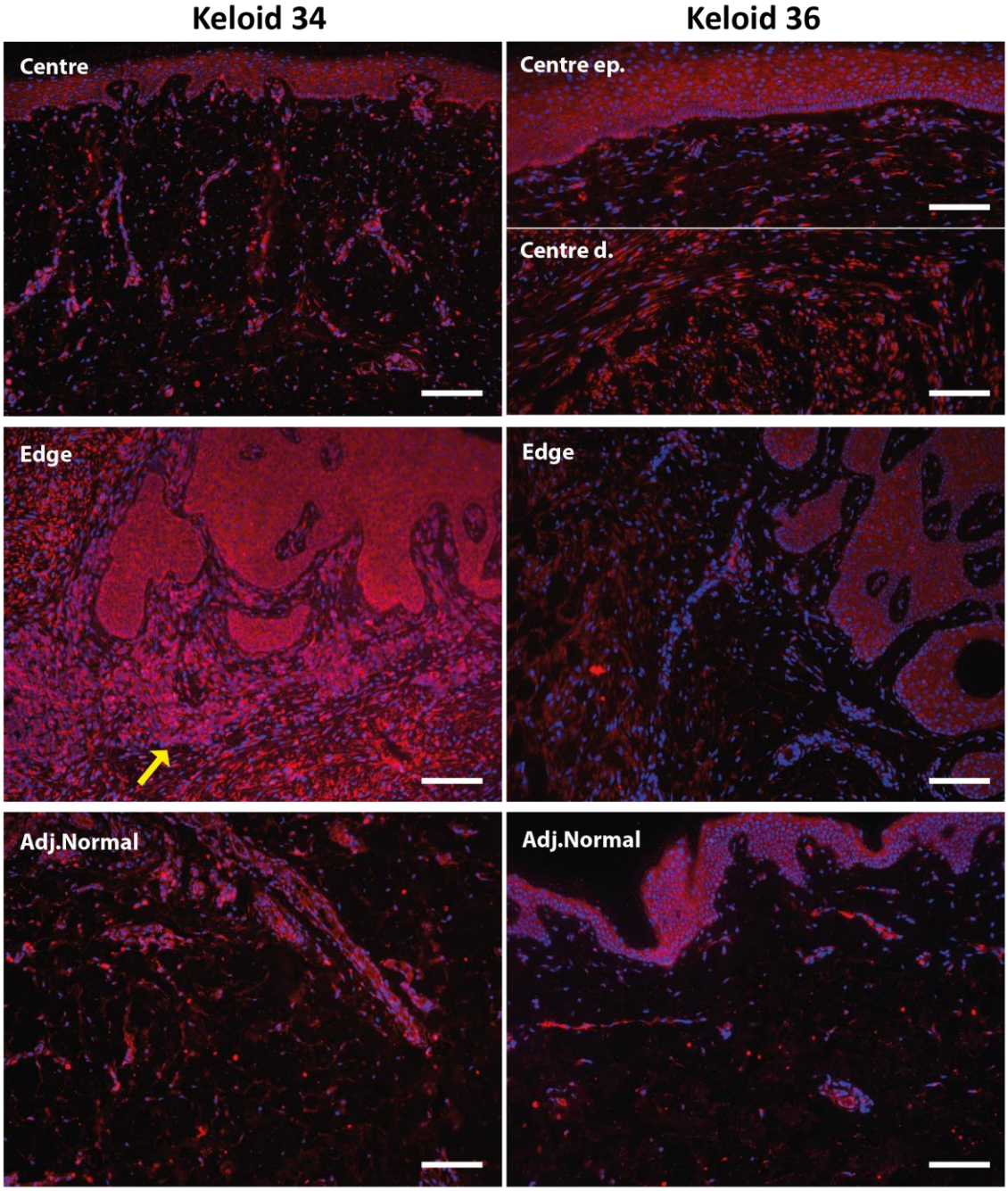

Figure 5-11 SPP1 protein expression by immunofluorescence, in keloid scars.

SPP1 protein expression was present in the papillary dermis of the central scar and adjacent normal tissue of the keloids, with increased levels noted in the collagenous nodules of the keloid centre in patient 36 (**Centre d.** = centre dermis). An intense dermal expression of SPP1 was observed in a region of inflammatory invasion, at the keloid edge of patient 34 (**yellow arrow**). Across the whole keloid scar, epidermal expression was increased in the lower layers, especially near the basement membrane, as compared to normal skin (**Figure 5-10**). SPP1 is shown in red; DAPI nuclear stain is shown in blue. Scale bars represent 100µm; **Centre ep.** = Centre epidermis. SPP1 was examined in n=3 keloids, n=1 hypertrophic scar, and n=2 normal skin in total.

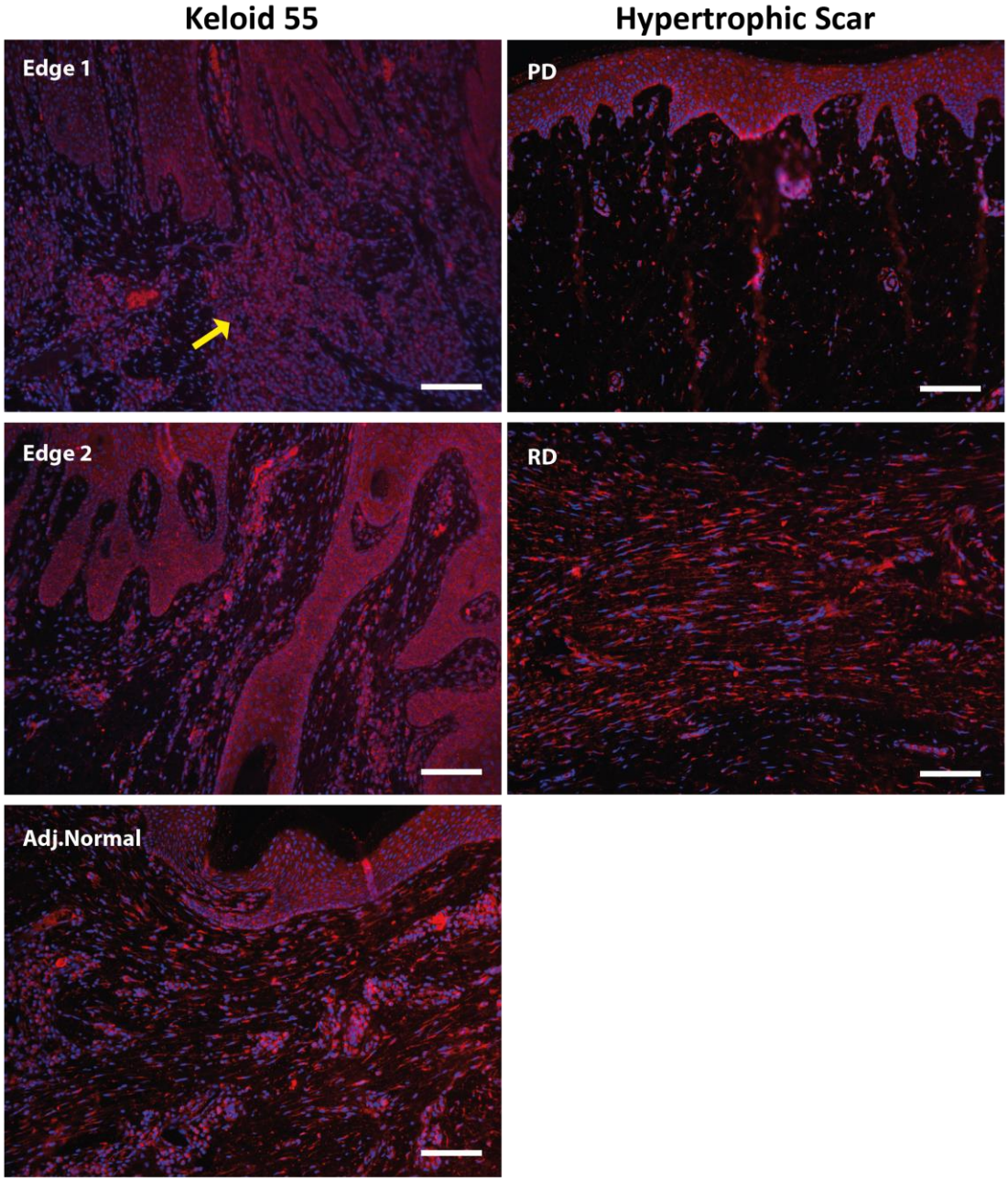

Figure 5-12 SPP1 protein expression by immunofluorescence, in keloid and hypertrophic scars

SPP1 protein expression was present across the whole dermis of patient 55, which did not have a clear central region (refer to **Figure 3- 27** and **section 3.2.3.4 in Chapter 3).** An increased level of SPP1 was noted in areas of inflammatory invasion (**yellow arrow**), and across the whole epidermis, as compared to normal skin (**Figure 5-10**). The hypertrophic scar showed a similar pattern of SPP1 expression as in keloid scars, with increased levels of in the basal epidermis and nodular collagenous region of the reticular dermis (**RD**) – also noted in patient 36 centre (**Figure 5-11**). SPP1 is shown in red; DAPI nuclear stain is shown in blue. Scale bars represent 100µm; **PD** = papillary dermis. SPP1 was examined in n=3 keloids, n=1 hypertrophic scar, and n=2 normal skin in total.

5.3 Discussion

In this chapter, I have examined the basic cell morphology and growth rate of keloid-derived fibroblasts and keratinocytes, compared against primary fibroblasts and keratinocytes from normal control skin. There was no difference in growth rate and cell morphology between keloid and normal fibroblasts. Keloid keratinocytes however showed a statistically significant decrease in growth rate, compared to normal keratinocytes. Also, keloid keratinocytes appeared larger, more spread out, and their colonies were less tight than their normal counterparts.

Out of the 18 selected and validated GOIs from **Chapter 4,** only SPP1 showed a statistically significantly different expression in keloid cells, and only within the fibroblast population. A high level of inter-patient variability was observed in the gene expression data, particularly in the keratinocyte population – a factor likely to have contributed to the lack of statistical significance found in the results. Despite this, some interesting trends were noted in the gene expression profiles, when compared against the original whole tissue data. In particular, MMPs 1, 13, TNC, EGFR, and GATA3 showed somewhat complementary gene expression profiles in the fibroblast and keratinocyte expression profiles, where only one cell type matched up with the same trend of gene expression difference as observed in whole tissue, and the other cell type showed the opposite trend.

Finally, SPP1 protein expression appeared to be increased in regions of the expanding keloid dermis, as well as in the basal epidermal layers of the whole keloid scar tissue. This may implicate osteogenic processes (Sodek et al., 2000) with keloid scarring.

5.3.1 Keloid-derived fibroblasts

As described earlier in **section 5.1**, it has been shown that cell morphology (Chipev et al., 2000) and growth rates appear to be similar between keloid and normal fibroblast cultures (Russell and Witt, 1976). Though under serum-starvation conditions, keloid fibroblasts appear not to require as many growth

factors to propagate successfully, as are required by normal fibroblasts (Russell et al., 1988). This supports my findings, where keloid and normal fibroblasts showed no differences in cell morphology or rate of growth, as tested by the Alamar Blue assay and population doubling levels. Collagen type I gene expression was not significantly altered between keloid and normal fibroblasts, even though there was a trend of increased COL1A1 expression in the keloid fibroblasts (**section 5.2.2.1**). This is most likely due to the culture system used in this chapter. It has been demonstrated that collagen type I expression is decreased in primary keloid fibroblasts grown as a monolayer, as the cell passage number increases (Syed et al., 2011). In the original tissue, regional differences in the collagen I/III ratio were also observed, with the keloid edge showing the highest level of collagen I/III. However, by passage 3 of monolayer fibroblast cultures, the differences between keloid regions were no longer significant (Syed et al., 2011). Despite this drawback to using monolayer fibroblast cultures as models to study keloid pathogenesis, multiple research groups have used them to deduce a whole range of gene (Smith et al., 2008, Seifert et al., 2010) and protein expression profiling patterns (Aoki et al., 2014, Bettinger et al., 1996, Bran et al., 2010, Chin et al., 2000), signalling pathway analysis (Chua et al., 2011, Fujiwara et al., 2005b, Satish et al., 2004), as well as to test the effectiveness of potential new keloid treatments (Wendling et al., 2003, Syed et al., 2013, Sadick et al., 2008).

During the gene expression analysis on keloid fibroblasts in this chapter SPP1 was the only gene to show a statistically significant difference. SPP1 was overexpressed by 2.4-fold in keloid compared to normal fibroblasts. The same trend was observed in both whole tissue (see **sections 4.2.1.2** in **Chapter 4**), and in keloid keratinocytes (see **section 5.2.2.2**) – though the result was not statistically significant for the keratinocyte population. The rest of the genes analysed showed no statistically significant changes, as tested by a Student's t-test for each gene.

A decreased expression of MMPs 1, 2 and 3 was noted in keloid fibroblasts, even though the opposite trend was seen in whole tissue (refer to **Figure 5-6**). In previous studies, MMPs 1 and 3 have been reported as down-regulated in keloid tissues and fibroblast cultures (Huang et al., 2013a, Smith et al., 2008).

Nevertheless, my MMP gene expression data in cultured cells was not statistically significant, and the lack of consistency in the literature on the MMP family supports the ongoing debate as to whether *in vitro* examination of MMP expression and activity is truly reflective of physiological MMP function (Giannandrea and Parks, 2014, Parks et al., 2004).

5.3.2 Keloid-derived keratinocytes

As already mentioned, the fibroblast and myofibroblast has been the main focus of research in fibrosis and keloid scarring, due to its key role in ECM synthesis. Although comparatively limited, research on the role of the epidermis and the keratinocyte cell-type in keloid pathogenesis is increasingly showing their importance in the disease (Menon et al., 2012, Xia et al., 2004). Most studies looking at the role of keloid keratinocytes are based on co-culture or 3D culture systems. In normal skin cells, simply co-culturing normal keratinocytes with normal fibroblasts significantly increases fibroblast proliferation, compared to when the fibroblasts are cultured as a monolayer (Funayama et al., 2003). The effect is increased when co-culturing keloid keratinocytes with normal fibroblasts, and even further increased when co-culturing keloid keratinocytes with keloid fibroblasts (Funayama et al., 2003, Lim et al., 2001). Furthermore, keloid keratinocytes had the strongest effect on reducing apoptosis of both normal and keloid fibroblasts (Funayama et al., 2003). These effects have been noted, regardless of whether the culture system used was inclusive (Phan et al., 2002) or not (Funayama et al., 2003) of fetal calf serum. Interestingly, keloid keratinocytes were shown to induce normal fibroblasts to secrete collagen type I in the same manner as keloid fibroblasts (Lim et al., 2002b, Phan et al., 2002). Even simply adding keratinocyte conditioned media to dermal fibroblasts increases the level of collagen production in the fibroblasts (Ghaffari et al., 2009b). This suggests that keloid keratinocytes have an important role in the mesenchymal differentiation status, and therefore in the fibrogenic nature of keloid scars (Lim et al., 2002b)(Lim et al., 2002b)(Lim et al., 2002b)(Lim et al., 2002b)(Lim et al., 2002b)(Lim et al., 2002b)(Lim et al., 2002b).

It has been shown that the microenvironment surrounding the keloid scars is often ischemic and hypoxic (Kischer and Brody, 1981), and regions within the keloid scar itself are hypoxic (Steinbrech et al., 1999, Zhang et al., 2003, Zhang et al., 2004). Increased hypoxia leads to an accumulation of HIF1α (hypoxia-inducible factor-1α) in scar tissue (Zhang et al., 2003, Wu et al., 2004b), which is thought to promote fibrogenesis through epithelial-to-mesenchymal transition (EMT), and excessive ECM production (Sun et al., 2009, Higgins et al., 2007). During EMT, epithelial cells lose their polarity and cell-cell adhesions, and acquire a migratory behavior, enabling them to transform into mesenchymal cells (Yin et al., 2013, Savagner and Arnoux, 2009, Yan et al., 2010). Ma et al. postulate that keloid keratinocytes adopt a fibroblast-like appearance through EMT, thereby enhancing their capacity to invade beyond the original wound margin, and expanding the keloid scar (Ma et al., 2015).

Keloid keratinocyte monolayer cultures appeared to form loose colonies in comparison to normal keratinocytes, and were more widely dispersed, with an increased level of motility, as tested by a scratch assay (Hahn et al., 2013). Subsequent microarray analysis revealed an up-regulation of genes related to cell adhesion, the ECM, and motility; while they showed a down-regulation of genes involved in cell differentiation, cell junctions, and EGFR signalling (Hahn et al., 2013). My findings fit in very closely with these previous studies. The keloid-derived keratinocytes showed a statistically significant decrease in growth rate, and morphologically they appeared larger and more spread than normal keratinocytes. Together with the apparent up-regulation of anti-apoptotic gene BCL2, and the down-regulation of EGFR noted in the gene expression analysis (**section 5.2.2.2**), this data tentatively supports the literature above with the notion that keloid keratinocytes are more invasive, perhaps more mesenchymal-like than their normal counterparts.

The gene expression analysis of keratinocyte cultures above revealed no significant differences between keloid and normal cells. The levels of gene expression was inconsistent between patients in almost half of the genes tested, reflecting the nature of the disorder. Overall, when comparing the three sets of

gene expression data (whole tissue, fibroblasts and keratinocytes), 4 out of 18 genes showed completely different trends in cell cultures vs tissue; 8 out of 18 genes showed consistently similar trends in all three sample groups; and 5 out 18 genes showed a mixture of trends, whereby at least one cell type was consistent with the whole tissue data (**section 5.2.2.2**). In the last group of genes, TNC and EGFR are of potential interest. TNC showed an increased expression in whole tissue and cultured keratinocytes, but a decreased expression in keloid fibroblasts (**Figure 5-9**). This hexameric glycoprotein is thought to potentially influence fibronectin activity, as it appears at the same time during the early phases of wound healing (Shrestha et al., 1996, Halper and Kjaer, 2014). TNC overexpression has previously been linked to fibrosis, including scleroderma (Lacour et al., 1992) and other hyperproliferative skin conditions (Schalkwijk et al., 1991). Little is known about TNC in relation to keloid scarring, though it has been found to be diffusely expressed in the keloid dermis, especially around the large collagen bundles of the keloid reticular dermis (Dalkowski et al., 1999, Jumper et al., 2015, Sidgwick and Bayat, 2012). TNC gene expression patterns in isolated keloid cells have not been reported, and my findings show an underexpression in the dermal cells.

5.3.3 SPP1 expression as a marker of invasiveness

SPP1 was the only target to appear as significantly altered between keloids and normal skin, shown in whole tissue as well as in isolated fibroblasts and keratinocytes, at both the gene and protein level. As discussed in **Chapter 4**, SPP1 is an osteogenic factor, which has been found to be overexpressed in hypertrophic scars (Wu et al., 2004a), and other types of fibrosis (Pardo et al., 2005, Persy et al., 2003, Gardner et al., 2006). It has been suggested that SPP1 promotes fibrosis-related signalling, through myofibroblast activation (Lenga et al., 2008). This would fit in with my findings, where SPP1 protein expression was more intense in the densely collagenous nodules of the keloid reticular dermis. By comparing the localisation of SPP1 protein expression (**Figures 5-11** and **5-12**) and the α-SMA expression (**Figures 3-10, 3-16, 3-20 and 3-28** in **Chapter 3**) in the same keloid

and hypertrophic scar tissues, it becomes plausible that SPP1 is linked with myofibroblast expression.

It is well established that SPP1 is involved in cell adhesion and cell migration. It can bind to certain integrins (mainly $\alpha_v \beta_3$), and affect cell migration via interaction with CD44 and activation of the EGFR pathway (Sodek et al., 2000). In fact, SPP1 can stimulate cell activity through a range of extracellular receptors at the cell-ECM interface, including $\alpha_v \beta_3$ integrin, EGFR, and VEGFR, affecting a range of functions, such as cytoskeletal organisation through PI3-kinase signalling, promoting cell proliferation through MAPK/Ras signalling, and preventing apoptosis by activating NFκB (Sodek et al., 2000, Lopez et al., 1995, Denhardt and Guo, 1993).

The strong epidermal expression of SPP1 in my keloid tissues is supported by Miregliotta et al., who showed a strong SPP1 expression in the epidermis of keloid lesions, though there was no clear comparison to normal healthy skin (Miragliotta et al., 2014). In psoriasis, the intensity of SPP1 expression in the lesional epidermis was associated with severity of the condition, where increased SPP1 expression was found with increased disease severity (Abdou et al., 2012). In oral squamous cell carcinoma, SPP1 expression has been proposed for use as a biomarker of disease invasion, but not as a predictive marker of progression from dysplasia to malignant transformation (Routray et al., 2013). In cancer biology in general, SPP1 has been linked to metastasis, and research into targeting this molecule as an anti-cancer therapy or as a biomarker for predicting metastasis is extensive (Jain et al., 2007, Kiss et al., 2015, Anborgh et al., 2015, Yan et al., 2015, Huang et al., 2015, Hou et al., 2015).

On this basis, further research into the feasibility of using SPP1 as a biomarker of keloid scarring, would be of interest. The current literature on SPP1 expression and its diverse functionality across tissue types and disorders, plus its established connection to promoting cell migration, would lead to the hypothesis that SPP1 might be a useful marker of keloid scar severity. Further detail on potential future work is described in the following chapter.

6 Conclusion and future work

6.1 Overall conclusions

The research presented in this thesis suggests that SPP1 could be a useful biomarker for keloid scarring. Based on the gene expression data, targets linked to the TGF-β/Smad, BMP, and Wnt pathways were altered, supporting some previous reports. Taken together, there is an indication of osteogenic and chondrogenic-related signalling taking place.

In **Chapter 3,** the keloid and control tissues used throughout the thesis were characterised in terms of whole tissue morphology, collagen fibre formation, cell proliferation, myofibroblast expression, and collagenase and gelatinase expression. I found that all the keloid scars showed an increased level of myofibroblast expression, which mainly corresponded with areas containing "keloidal collagen" in the fibrotic reticular dermis. Surrounding these regions, MMP2 and MMP14 expression in particular appeared increased, as tested by IHC. Overall, the edge scar regions showed increased levels of proliferation, increased inflammatory infiltration, and evidence of increased scar tissue formation, compared to the remaining scar regions, and unaffected normal skin. One key observation was that the degree of myofibroblast expression and amount of dense collagenous nodules present in each keloid was variable, making it challenging to define clear boundaries between central, edge and adjacent normal sites. For this reason, the ensuing gene expression investigations were carried out on whole tissue biopsies, incorporating epidermal and dermal compartments, as well as all scar regions.

In **Chapter 4**, a total of 168 genes associated with the ECM microenvironment and a selection of well-studied signalling pathways were examined in n=5 keloid n=5 control tissues. Out of these, a total of 31 genes demonstrated a statistically significant difference of expression in keloid scars compared to normal tissues. A selection of 18 genes were then validated in the same tissues, using an alternative qPCR method, which revealed only four genes (BCL-2, BMP2, SORBS1, and EGFR) remained statistically significantly altered in keloids compared to normal skin. Additional genes to take into account, despite the lack of statistical significance, were COL1, MMP2 and GATA3 as these were approximately statistically significant

at the $p<0.05$ level ($p= 0.0513$, 0.0598 and 0.0538 respectively); as well as SPP1, SPARC, and HEY1, as these genes showed the largest expression fold-change (+5.0, +3.3, and -7.7 respectively).

Based on these results, in **Chapter 5** I then investigated if these altered gene expression patterns were retained *in vitro*, in the isolated fibroblast and keratinocyte populations from the same cohort of tissues characterised in **Chapter 3**. One keloid, Patient 36, was analysed in all investigations, Patient 34 was analysed in all but the cultured keratinocyte experiments, and the rest of the keloid-derived cells used in **Chapter 5** were not matched to those used in the gene expression data of **Chapter 4**. The keloid keratinocytes showed a significantly lower rate of growth compared to normal keratinocytes, though the fibroblasts showed no difference between keloid and normal cells. In the gene expression analysis, the results were varied between patients, particularly in the keratinocyte population, leading to very little statistical significance being reached in the final analyses. SPP1 showed a strong statistically significant up-regulation in keloid fibroblasts, while SFN and WISP1 showed a near-statistically significant up-regulation in keloid fibroblasts, and GATA3 showed a near-statistically significant down-regulation in keloid keratinocytes. When comparing the gene expression analyses from this thesis to published datasets (outlined in **section 4.1.1** and **Table 4-1**, in **Chapter 4**) (Shih and Bayat, 2010b, Huang et al., 2013a), 15 genes were investigated in both cases. Ten out of these confirmed the altered gene expression in keloid material, reported in literature (**Table 6-1**). Among the 5 genes that showed a different result to the literature, were JAG-1, MMPs 1, 2 and 3, and TNC, of which the MMPs demonstrated varied gene expression patterns between whole tissue, primary fibroblasts or primary keratinocytes. The high similarity in my data compared to previous reports, taking into account the different methodologies, research teams, and patient material, provides an extra level of confidence in my research. Finally, SPP1 protein expression was increased in keloid tissue, compared to normal skin biopsies. In particular, the basal epidermal layers and "keloidal collagen" regions of the dermis within the keloid scars displayed the most intense expression.

Table 6-1 List of genes reported to be up- or down-regulated in at least two microarray studies (see Table 4-1), compared to the data presented in this thesis.

Gene code	Gene full name	Gene Up/ Down regulation:	
		Literature	Thesis
A2M	Alpha-2-macroglobulin	UP	-
ACAN	Aggrecan	UP	-
ADIPOQ	Adiponectin, C1Q and collagen domain binding	UP	-
ANXA1	Annexin-A1	UP	-
BMP6	Bone morphogenetic protein 6	UP	-
COL1A1	Collagen I alpha1	UP	UP
COL1A2	Collagen I alpha2	UP	-
COL4A2	Collagen IV alpha2	UP	UP
COL5A2	Collagen V alpha2	UP	-
COL6A1	Collagen VI alpha1	UP	UP
COL15A1	Collagen XV alpha1	UP	UP
DCN	Decorin	UP	-
EGFR	Epidermal growth factor receptor	DOWN	DOWN
FAP	Fibroblast activation protein alpha	UP	-
FN1	Fibronectin 1	UP	UP
HIF-1A	Hypoxia-inducible factor alpha subunit 1	UP	-
IGFBP7	Insulin-like growth factor binding protein 7	UP	-
JAG-1	Jagged-1	UP	DOWN
JUP	Junction plakoglobin	DOWN	-
MMP1	Matrix Metalloproteinase1 (collagenase 1	DOWN	UP (down in fibroblasts)
MMP2	Matrix Metalloproteinase2 (gelatinase A)	UP	UP (down in fibroblasts & keratinocytes
MMP3	Matrix Metalloproteinase3 (stromelysin 1)	DOWN	UP (down in fibroblasts & keratinocytes
MMP14	Matrix Metalloproteinase 14 (MT1-MMP)	UP	UP
NERP	Neuronal regeneration related protein	UP	-
NRP1	Neuropilin 1	DOWN	-
OGN	Osteoglycin	UP	-
POSTN	Periostin, osteoblast specific factor	UP	-
SERPINF1	Serpin peptidase inhibitor, clade F	DOWN	-
TGF-β1	Transforming growth factor beta 1	UP	UP
TGF-βRIII	Transforming growth factor beta receptor III	DOWN	-
THBS2	Thrombospondin 2	DOWN	UP
THBS4	Thrombospondin 4	UP	-
TNC	Tenascin C	DOWN	UP
VCAN	Versican	UP	UP

Overall, the trends identified in my research suggest involvement of more than one signalling pathway in keloid scarring. It is likely that there is cross-talk between signalling pathways. The TGF-β/BMP pathway is involved in a wide range of processes, and has shown to regulate cell proliferation, differentiation, migration, apoptosis and ECM remodelling among others (Guo and Wang, 2009). TGF-β has a particularly large number of transcriptional and non-transcriptional targets, plus multiple components, which make direct and dynamic contacts with other proteins (Guo and Wang, 2009). This gives rise to an enormous complexity, and flexibility of TGF-β/BMP functions. Interactions between the TGF-β/BMP, Wnt, Hedgehog, Notch, and MAPK pathways among others, are key to appropriate growth and tissue homeostasis (Guo and Wang, 2009). Alterations in these pathways have been identified in the development of various diseases, including in cancer development and fibrosis (Massagué, 2008, Mishra et al., 2005, Attisano and Labbé, 2004, Sumi et al., 2008). Within the MAPK pathway, RTKs (receptor tyrosine kinases) such as EGFR (epithelial growth factor receptor), FGFR (fibroblast growth factor receptor), IGFR (insulin-like growth factor receptor), PDGFR (platelet-derived growth factor receptor) and insulin receptor, can induce activation via Ras. EGFR signalling activates both the MAPK and phosphatidylinositol-3 kinase (PI3K)/Akt pathways, but also communicates with TGF-β/Smad in mammary epithelial cells, which is important in the context of breast cancer development (Siegel et al., 2003, Ueda et al., 2004, Janda et al., 2002, Wang et al., 2008, Seton-Rogers and Brugge, 2004). The contact between the EGFR/MAPK and TGF-β pathways often also leads to growth factor release, such as TGF-β and PDGF, which can lead to increased cell invasion and differentiation (Lehmann et al., 2000, Oft et al., 1996, Yue and Mulder, 2000). Cell proliferation and differentiation is also affected by TGF-β/Wnt signalling. These two pathways act synergistically at the nuclear, cytosolic and ligand binding levels, making it a truly diverse cross-talk (Guo and Wang, 2009). Another interesting signalling pathway with growing interest is the Hippo pathway, which has shown cross-talk with the TGF-β/BMP and Wnt pathways (Piccolo et al., 2014). The main transcriptional regulators of Hippo signalling are YAP/TAZ (yes-associated protein), and their activity are key for whole organ growth, and tissue renewal and

regeneration. These regulators act as sensors of cell structure, shape and polarity, as well as responding to growth factor signals being initiated by the Wnt pathway (Piccolo et al., 2014). This pathway has not been studied in relation to keloid scarring, and has minimal reports on other forms of fibrosis (Liu et al., 2015). Given the pathway interaction however, this would be another interesting cascade to study.

Finally, throughout **Chapters 4** and **5,** the consistent up-regulation of SPP1 observed in whole tissue, keloid keratinocytes and keloid fibroblasts, at both the gene and protein level has not been previously reported. This target has the potential to act as a biomarker of keloid invasiveness, especially with its increased expression noted at the keloid scar margin.

6.2 Suggested Future Research

A prevailing feature throughout the thesis was a high inter-patient variability affecting the statistical analyses of gene and protein expression patterns being examined. One disadvantage with investigating the whole scar tissue, inclusive of the different regions, means that sometimes the dynamics between the established centre and the expanding edge are not taken into consideration. For this reason, an obvious next step would be to investigate much more extensively the pathways and targets identified in this thesis, in the separate keloid regions. As the boundaries can be difficult to define, laser capture microdissection could be used to selectively isolate different regions of interest: the nodular regions of the reticular and scar margin dermis; the papillary dermis of the central scar, the dermis in the adjacent normal tissue; as well as the corresponding epidermal portions. Based on previous studies as discussed in earlier chapters, namely Bayat and his team, it is likely that the largest differences in gene regulation could be found between the expanding margin and the rest of the keloid.

As has been discussed in **Chapter 4**, previous gene expression studies on keloid whole tissue or cells have shown conflicting results. This is most likely due the use of different methodologies and source materials by different research groups. The

source materials range from whole tissue biopsies to keloid-derived primary cells; containing marginal and extralesional regions, or not; retrieved from different ethnic populations. Keloid scarring is clearly a complex, multi-faceted disorder, which is affected by much more than just two cell types and excessive collagen I production. With the aim to model a disease process *in vitro*, so that basic mechanisms can be investigated in much more detail, a simple experimental design can be very effective at elucidating which genes and proteins are constitutively dysregulated, regardless of their 3D environment or interaction with neighbouring cells. Once such biomarkers are identified, the related signalling processes and mechanisms of action can be further investigated in more complex disease models, where multiple parameters can be more effectively elaborated.

6.2.1 Characterisation of identified targets

A first line of future work would be to establish to potential use of SPP1 as a biomarker for keloid invasiveness/ aggressiveness. This would be a longer-term project, whereby a large number of keloids covering different body regions, patient ethnicities, and individual treatment histories would be examined for SPP1 protein expression. This could be compared against an equally extensive number of hypertrophic and normotrophic scar tissues, and if there is a strong link between SPP1 and scar invasiveness, this could be used to stratify patients for a more personalised treatment strategy.

Another line of further research would be to extensively characterise the pathways identified as altered in my gene expression data. The protein expression levels and phosphorylation status of key mediators within the TGF-β/Smad, BMP, and Wnt pathways, should first be analysed in the original keloid tissues, by Western Blot and IHC-IF. Alongside this, further protein expression and activity patterns of the osteogenic factors SPP1, SPARC and SFN across the keloid regions, and the differences between the epidermal and dermal compartments could be carried out. The isolated keratinocytes and fibroblasts from keloid and normal tissues could then be cultured in a transwell system or in a 3D culture system, with the aim to elucidate how the epidermal and dermal compartments influence each other. This

could be extended to examine the effect of say, the marginal keloid keratinocytes, on normal fibroblasts, and therefore investigate whether keratinocytes from different keloid regions have different fibrogenic-enhacing capabilites. The identified targets above would be analysed by Western Blot and ELISA, as well as ICC (immunocytochemistry) where appropriate.

The advantage of using these *in vitro* models over clinical samples is that the targets of interest can then be knocked down or suppressed by siRNA or drug treatment, or alternatively they can be manipulated to overexpress in the cultured cells. The effects on fibrogenesis could then be evaluated. A prolonged culture using these more comprehensive systems would also be interesting to carry out, as it is likely that the fibrogenic phenotype is enhanced over time, as the synthesised ECM accumulates, and the cells begin to differentiate and stratify. This would also help to elucidate the reason for the non appearance of statistical significance in my *in vitro* data – whether it is due to the lack of epithelial-mesechymal interaction, or whether it is due to the lack of 3D environmental cues.

6.2.2 Familial genetics

As discussed in **Chapter 1**, a small number of genome-wide studies (GWAS) have been carried out on families displaying a hereditary form of keloid scarring. These studies were performed on families of Chinese, Japanese and African-American origin, and the prevailing mode of inheritance was autosomal dominant with incomplete penetrance. Some overlap in their results has suggested potential polymorphisms to exist within the EGFR and SMAD2/3 genes (Velez Edwards et al., 2014, Nakashima et al., 2010b, Shih and Bayat, 2010b, Chen et al., 2006).

As the patient profile in our clinic has a large proportion of patients with African-Caribbean origin, we selected five families which displayed the above mode of inheritance in keloid scarring. To date, full exome sequencing has been completed on 1 to 2 family members from each family, who present keloid formation. This approach was chosen over the GWAS analysis, so as to focus on the protein-coding genes only. Based on the very small sample number of 9 individuals, 3 genes have

been initially identified as containing disease-specific polymorphisms. These results will need to first be validated by full sequencing of those genes, on a larger number of keloid samples, before the gene and associated protein functions can be investigated *in vitro* (as in **section 6.2.1**).

7 Appendices

Appendix A: Complete Gene List for ECM & Adhesion Molecule qPCR array (Chapter 2)

A total of 84 genes of interest were tested, with 5 reference genes (ACTB, B2M, GAPDH, HPRT1, and RPLP0), and 7 internal assay controls.

Plate Position	UniGene code	RefSeq code	Gene Symbol	Gene Description	Alternative Gene Names
A01	Hs.643357	NM_006988	ADAMTS1	ADAM metallopeptidase with thrombospondin type 1 motif, 1	C3-C5, KIAA1346, METH1
A02	Hs.131433	NM_139025	ADAMTS13	ADAM metallopeptidase with thrombospondin type 1 motif, 13	C9orf8, DKFZp434C2322, FLJ42993, MGC118899, MGC118900, TTP, VWFCP, vWF-CP
A03	Hs.271605	NM_007037	ADAMTS8	ADAM metallopeptidase with thrombospondin type 1 motif, 8	ADAM-TS8, FLJ41712, METH2
A04	Hs.502328	NM_000610	CD44	CD44 molecule (Indian blood group)	CDW44, CSPG8, ECMR-III, HCELL, HUTCH-I, IN, LHR, MC56, MDU2, MDU3, MGC10468, MIC4, Pgp1
A05	Hs.461086	NM_004360	CDH1	Cadherin 1, type 1, E-cadherin (epithelial)	Arc-1, CD324, CDHE, ECAD, LCAM, UVO
A06	Hs.476092	NM_003278	CLEC3B	C-type lectin domain family 3, member B	DKFZp686H17246, TN, TNA
A07	Hs.143434	NM_001843	CNTN1	Contactin 1	F3, GP135
A08	Hs.523446	NM_080629	COL11A1	Collagen, type XI, alpha 1	CO11A1, COLL6, STL2
A09	Hs.101302	NM_004370	COL12A1	Collagen, type XII, alpha 1	BA209D8.1, COL12A1L, DJ234P15.1
A10	Hs.409662	NM_021110	COL14A1	Collagen, type XIV, alpha 1	UND
A11	Hs.409034	NM_001855	COL15A1	Collagen, type XV, alpha 1	FLJ38566
A12	Hs.368921	NM_001856	COL16A1	Collagen, type XVI, alpha 1	447AA
B01	Hs.172928	NM_000088	COL1A1	Collagen, type I, alpha 1	OI4
B02	Hs.508716	NM_001846	COL4A2	Collagen, type IV, alpha 2	DKFZp686I14213, FLJ22259

B03	Hs.210283	NM_000093	COL5A1	Collagen, type V, alpha 1	-
B04	Hs.474053	NM_001848	COL6A1	Collagen, type VI, alpha 1	OPLL
B05	Hs.420269	NM_001849	COL6A2	Collagen, type VI, alpha 2	DKFZp586E1322, FLJ46862, PP3610
B06	Hs.476218	NM_000094	COL7A1	Collagen, type VII, alpha 1	EBD1, EBDCT, EBR1
B07	Hs.654548	NM_001850	COL8A1	Collagen, type VIII, alpha 1	C3orf7, MGC9568
B08	Hs.591346	NM_001901	CTGF	Connective tissue growth factor	CCN2, HCS24, IGFBP8, MGC102839, NOV2
B09	Hs.534797	NM_001903	CTNNA1	Catenin (cadherin-associated protein), alpha 1, 102kDa	CAP102, FLJ36832, FLJ52416
B10	Hs.476018	NM_001904	CTNNB1	Catenin (cadherin-associated protein), beta 1, 88kDa	CTNNB, DKFZp686D02253, FLJ25606, FLJ37923
B11	Hs.166011	NM_001331	CTNND1	Catenin (cadherin-associated protein), delta 1	CAS, CTNND, KIAA0384, P120CAS, P120CTN, p120, p120(CAS), p120(CTN)
B12	Hs.314543	NM_001332	CTNND2	Catenin (cadherin-associated protein), delta 2 (neural plakophilin-related arm-repeat protein)	GT24, NPRAP
C01	Hs.81071	NM_004425	ECM1	Extracellular matrix protein 1	-
C02	Hs.203717	NM_002026	FN1	Fibronectin 1	CIG, DKFZp686F10164, DKFZp686H0342, DKFZp686I1370, DKFZp686O13149, ED-B, FINC, FN, FNZ, GFND, GFND2, LETS, MSF
C03	Hs.57697	NM_001523	HAS1	Hyaluronan synthase 1	HAS
C04	Hs.643447	NM_000201	ICAM1	Intercellular adhesion molecule 1	BB2, CD54, P3.58
C05	Hs.644352	NM_181501	ITGA1	Integrin, alpha 1	CD49a, VLA1
C06	Hs.482077	NM_002203	ITGA2	Integrin, alpha 2 (CD49B, alpha 2 subunit of VLA-2 receptor)	BR, CD49B, GPIa, VLA-2, VLAA2
C07	Hs.265829	NM_002204	ITGA3	Integrin, alpha 3 (antigen CD49C,	CD49C, FLJ34631, FLJ34704, GAP-B3,

				alpha 3 subunit of VLA-3 receptor)	GAPB3, MSK18, VCA-2, VL3A, VLA3a
C08	Hs.694732	NM_000885	ITGA4	Integrin, alpha 4 (antigen CD49D, alpha 4 subunit of VLA-4 receptor)	CD49D, IA4, MGC90518
C09	Hs.505654	NM_002205	ITGA5	Integrin, alpha 5 (fibronectin receptor, alpha polypeptide)	CD49e, FNRA, VLA5A
C10	Hs.133397	NM_000210	ITGA6	Integrin, alpha 6	CD49f, DKFZp686J01244, FLJ18737, ITGA6B, VLA-6
C11	Hs.524484	NM_002206	ITGA7	Integrin, alpha 7	FLJ25220
C12	Hs.171311	NM_003638	ITGA8	Integrin, alpha 8	-
D01	Hs.174103	NM_002209	ITGAL	Integrin, alpha L (antigen CD11A (p180), lymphocyte function-associated antigen 1; alpha polypeptide)	CD11A, LFA-1, LFA1A
D02	Hs.172631	NM_000632	ITGAM	Integrin, alpha M (complement component 3 receptor 3 subunit)	CD11B, CR3A, MAC-1, MAC1A, MGC117044, MO1A, SLEB6
D03	Hs.436873	NM_002210	ITGAV	Integrin, alpha V (vitronectin receptor, alpha polypeptide, antigen CD51)	CD51, DKFZp686A08142, MSK8, VNRA
D04	Hs.643813	NM_002211	ITGB1	Integrin, beta 1 (fibronectin receptor, beta polypeptide, antigen CD29 includes MDF2, MSK12)	CD29, FNRB, GPIIA, MDF2, MSK12, VLA-BETA, VLAB
D05	Hs.375957	NM_000211	ITGB2	Integrin, beta 2 (complement component 3 receptor 3 and 4 subunit)	CD18, LAD, LCAMB, LFA-1, MAC-1, MF17, MFI7
D06	Hs.218040	NM_000212	ITGB3	Integrin, beta 3 (platelet glycoprotein IIIa, antigen CD61)	CD61, GP3A, GPIIIa
D07	Hs.632226	NM_000213	ITGB4	Integrin, beta 4	CD104

D08	Hs.536663	NM_002213	ITGB5	Integrin, beta 5	FLJ26658
D09	Hs.521869	NM_000216	KAL1	Kallmann syndrome 1 sequence	ADMLX, HHA, KAL, KALIG-1, KMS
D10	Hs.270364	NM_005559	LAMA1	Laminin, alpha 1	LAMA, S-LAM-alpha
D11	Hs.200841	NM_000426	LAMA2	Laminin, alpha 2	LAMM
D12	Hs.436367	NM_000227	LAMA3	Laminin, alpha 3	BM600, E170, LAMNA, LOCS, lama3a
E01	Hs.650585	NM_002291	LAMB1	Laminin, beta 1	CLM, MGC142015
E02	Hs.497636	NM_000228	LAMB3	Laminin, beta 3	BM600-125KDA, FLJ99565, LAM5, LAMNB1
E03	Hs.609663	NM_002293	LAMC1	Laminin, gamma 1 (formerly LAMB2)	LAMB2, MGC87297
E04	Hs.83169	NM_002421	MMP1	Matrix metallopeptidase 1 (interstitial collagenase)	CLG, CLGN
E05	Hs.2258	NM_002425	MMP10	Matrix metallopeptidase 10 (stromelysin 2)	SL-2, STMY2
E06	Hs.143751	NM_005940	MMP11	Matrix metallopeptidase 11 (stromelysin 3)	SL-3, ST3, STMY3
E07	Hs.1695	NM_002426	MMP12	Matrix metallopeptidase 12 (macrophage elastase)	HME, ME, MGC138506, MME, MMP-12
E08	Hs.2936	NM_002427	MMP13	Matrix metallopeptidase 13 (collagenase 3)	CLG3, MANDP1
E09	Hs.2399	NM_004995	MMP14	Matrix metallopeptidase 14 (membrane-inserted)	1, MMP-14, MMP-X1, MT-MMP, MT-MMP 1, MT1-MMP, MT1MMP, MTMMP1
E10	Hs.80343	NM_002428	MMP15	Matrix metallopeptidase 15 (membrane-inserted)	MT2-MMP, MTMMP2, SMCP-2
E11	Hs.546267	NM_005941	MMP16	Matrix metallopeptidase 16 (membrane-inserted)	C8orf57, DKFZp761D112, MMP-X2, MT-MMP2, MT-MMP3, MT3-MMP
E12	Hs.513617	NM_004530	MMP2	Matrix metallopeptidase 2	CLG4, CLG4A, MMP-II, MONA, TBE-1

				(gelatinase A, 72kDa gelatinase, 72kDa type IV collagenase)	
F01	Hs.375129	NM_002422	MMP3	Matrix metallopeptidase 3 (stromelysin 1, progelatinase)	CHDS6, MGC126102, MGC126103, MGC126104, MMP-3, SL-1, STMY, STMY1, STR1
F02	Hs.2256	NM_002423	MMP7	Matrix metallopeptidase 7 (matrilysin, uterine)	MMP-7, MPSL1, PUMP-1
F03	Hs.161839	NM_002424	MMP8	Matrix metallopeptidase 8 (neutrophil collagenase)	CLG1, HNC, MMP-8, PMNL-CL
F04	Hs.297413	NM_004994	MMP9	Matrix metallopeptidase 9 (gelatinase B, 92kDa gelatinase, 92kDa type IV collagenase)	CLG4B, GELB, MANDP2, MMP-9
F05	Hs.503878	NM_000615	NCAM1	Neural cell adhesion molecule 1	CD56, MSK39, NCAM
F06	Hs.514412	NM_000442	PECAM1	Platelet/endothelial cell adhesion molecule	CD31, FLJ34100, FLJ58394, PECAM-1
F07	Hs.89546	NM_000450	SELE	Selectin E	CD62E, ELAM, ELAM1, ESEL, LECAM2
F08	Hs.728756	NM_000655	SELL	Selectin L	CD62L, LAM1, LECAM1, LEU8, LNHR, LSEL, LYAM1, PLNHR, TQ1
F09	Hs.73800	NM_003005	SELP	Selectin P (granule membrane protein 140kDa, antigen CD62)	CD62, CD62P, FLJ45155, GMP140, GRMP, LECAM3, PADGEM, PSEL
F10	Hs.371199	NM_003919	SGCE	Sarcoglycan, epsilon	DYT11, ESG
F11	Hs.111779	NM_003118	SPARC	Secreted protein, acidic, cysteine-rich (osteonectin)	ON
F12	Hs.185597	NM_003119	SPG7	Spastic paraplegia 7 (pure and complicated autosomal recessive)	CAR, CMAR, FLJ37308, MGC126331, MGC126332, PGN, SPG5C
G01	Hs.313	NM_000582	SPP1	Secreted phosphoprotein 1	BNSP, BSPI, ETA-1, MGC110940, OPN
G02	Hs.369397	NM_000358	TGFBI	Transforming growth factor, beta-	BIGH3, CDB1, CDG2, CDGG1, CSD,

				induced, 68kDa	CSD1, CSD2, CSD3, EBMD, LCD1
G03	Hs.164226	NM_003246	THBS1	Thrombospondin 1	THBS, THBS-1, TSP, TSP-1, TSP1
G04	Hs.371147	NM_003247	THBS2	Thrombospondin 2	TSP2
G05	Hs.169875	NM_007112	THBS3	Thrombospondin 3	MGC119564, MGC119565, TSP3
G06	Hs.522632	NM_003254	TIMP1	TIMP metallopeptidase inhibitor 1	CLGI, EPA, EPO, FLJ90373, HCI, TIMP
G07	Hs.633514	NM_003255	TIMP2	TIMP metallopeptidase inhibitor 2	CSC-21K
G08	Hs.644633	NM_000362	TIMP3	TIMP metallopeptidase inhibitor 3	HSMRK222, K222, K222TA2, SFD
G09	Hs.143250	NM_002160	TNC	Tenascin C	150-225, GMEM, GP, HXB, JI, MGC167029, TN, TN-C
G10	Hs.109225	NM_001078	VCAM1	Vascular cell adhesion molecule 1	CD106, DKFZp779G2333, INCAM-100, MGC99561
G11	Hs.643801	NM_004385	VCAN	Versican	CSPG2, DKFZp686K06110, ERVR, GHAP, PG-M, WGN, WGN1
G12	Hs.2257	NM_000638	VTN	Vitronectin	V75, VN, VNT
H01	Hs.520640	NM_001101	ACTB	Actin, beta	PS1TP5BP1
H02	Hs.534255	NM_004048	B2M	Beta-2-microglobulin	-
H03	Hs.592355	NM_002046	GAPDH	Glyceraldehyde-3-phosphate dehydrogenase	G3PD, GAPD, MGC88685
H04	Hs.412707	NM_000194	HPRT1	Hypoxanthine phosphoribosyltransferase 1	HGPRT, HPRT
H05	Hs.546285	NM_001002	RPLP0	Ribosomal protein, large, P0	L10E, LP0, MGC111226, MGC88175, P0, PRLP0, RPP0
H06	N/A	SA_00105	HGDC	Human Genomic DNA Contamination	HIGX1A
H07	N/A	SA_00104	RTC	Reverse Transcription Control	RTC
H08	N/A	SA_00104	RTC	Reverse Transcription Control	RTC

H09	N/A	SA_00104	RTC	Reverse Transcription Control	RTC
H10	N/A	SA_00103	PPC	Positive PCR Control	PPC
H11	N/A	SA_00103	PPC	Positive PCR Control	PPC
H12	N/A	SA_00103	PPC	Positive PCR Control	PPC

Appendix B: Complete Gene List for Signal Transduction PathwayFinder qPCR array (Chapter 2)

A total of 84 genes of interest were tested, with 5 reference genes (ACTB, B2M, GAPDH, HPRT1, and RPLP0), and 7 internal assay controls.

Plate Position	UniGene code	RefSeq code	Gene Symbol	Gene Description	Alternative Gene Names
A01	Hs.655772	NM_004457	ACSL3	Acyl-CoA synthetase long-chain family member 3	ACS3, FACL3, PRO2194
A02	Hs.268785	NM_004458	ACSL4	Acyl-CoA synthetase long-chain family member 4	ACS4, FACL4, LACS4, MRX63, MRX68
A03	Hs.11638	NM_016234	ACSL5	Acyl-CoA synthetase long-chain family member 5	ACS2, ACS5, FACL5
A04	Hs.441047	NM_001124	ADM	Adrenomedullin	AM
A05	Hs.632446	NM_001668	ARNT	Aryl hydrocarbon receptor nuclear translocator	HIF-1-beta, HIF-1beta, HIF1-beta, HIF1B, HIF1BETA, TANGO, bHLHe2
A06	Hs.496487	NM_001675	ATF4	Activating transcription factor 4 (tax-responsive enhancer element B67)	CREB-2, CREB2, TAXREB67, TXREB
A07	Hs.156527	NM_004655	AXIN2	Axin 2	AXIL, DKFZp781B0869, MGC10366, MGC126582
A08	Hs.624291	NM_004324	BAX	BCL2-associated X protein	BCL2L4
A09	Hs.467020	NM_014417	BBC3	BCL2 binding component 3	FLJ42994, JFY1, PUMA
A10	Hs.150749	NM_000633	BCL2	B-cell CLL/lymphoma 2	Bcl-2
A11	Hs.227817	NM_004049	BCL2A1	BCL2-related protein A1	ACC-1, ACC-2, BCL2L5, BFL1, GRS, HBPA1
A12	Hs.516966	NM_138578	BCL2L1	BCL2-like 1	BCL-XL, S, BCL2L, BCLX, BCLXL, BCLXS, Bcl-X, DKFZp781P2092, bcl-xL, bcl-xS
B01	Hs.127799	NM_001165	BIRC3	Baculoviral IAP repeat containing 3	AIP1, API2, CIAP2, HAIP1, HIAP1, MALT2, MIHC, RNF49, c-IAP2
B02	Hs.73853	NM_001200	BMP2	Bone morphogenetic protein 2	BMP2A

B03	Hs.68879	NM_130851	BMP4	Bone morphogenetic protein 4	BMP2B, BMP2B1, MCOPS6, OFC11, ZYME
B04	Hs.519162	NM_006763	BTG2	BTG family, member 2	MGC126063, MGC126064, PC3, TIS21
B05	Hs.63287	NM_001216	CA9	Carbonic anhydrase IX	CAIX, MN
B06	Hs.514821	NM_002985	CCL5	Chemokine (C-C motif) ligand 5	D17S136E, MGC17164, RANTES, SCYA5, SISd, TCP228
B07	Hs.523852	NM_053056	CCND1	Cyclin D1	BCL1, D11S287E, PRAD1, U21B31
B08	Hs.376071	NM_001759	CCND2	Cyclin D2	KIAK0002, MGC102758
B09	Hs.370771	NM_000389	CDKN1A	Cyclin-dependent kinase inhibitor 1A (p21, Cip1)	CAP20, CDKN1, CIP1, MDA-6, P21, SDI1, WAF1, p21CIP1
B10	Hs.238990	NM_004064	CDKN1B	Cyclin-dependent kinase inhibitor 1B (p27, Kip1)	CDKN4, KIP1, MEN1B, MEN4, P27KIP1
B11	Hs.440829	NM_005195	CEBPD	CCAAT/enhancer binding protein (C/EBP), delta	C, EBP-delta, CELF, CRP3, NF-IL6-beta
B12	Hs.705379	NM_000098	CPT2	Carnitine palmitoyltransferase 2	CPT1, CPTASE
C01	Hs.591402	NM_000757	CSF1	Colony stimulating factor 1 (macrophage)	MCSF, MGC31930
C02	Hs.481980	NM_001343	DAB2	Disabled homolog 2, mitogen-responsive phosphoprotein (Drosophila)	DOC-2, DOC2, FLJ26626
C03	Hs.488293	NM_005228	EGFR	Epidermal growth factor receptor	ERBB, ERBB1, HER1, PIG61, mENA
C04	Hs.707901	NM_001423	EMP1	Epithelial membrane protein 1	CL-20, EMP-1, TMP
C05	Hs.2303	NM_000799	EPO	Erythropoietin	EP, MGC138142, MVCD2
C06	Hs.380135	NM_001443	FABP1	Fatty acid binding protein 1, liver	FABPL, L-FABP
C07	Hs.244139	NM_000043	FAS	Fas (TNF receptor superfamily, member 6)	ALPS1A, APO-1, APT1, CD95, FAS1, FASTM, TNFRSF6
C08	Hs.465778	NM_002002	FCER2	Fc fragment of IgE, low affinity II,	CD23, CD23A, CLEC4J, FCE2, IGEBF

				receptor for (CD23)	
C09	Hs.283565	NM_005438	FOSL1	FOS-like antigen 1	FRA, FRA1, fra-1
C10	Hs.645560	NM_002032	FTH1	Ferritin, heavy polypeptide 1	FHC, FTH, FTHL6, MGC104426, PIG15, PLIF
C11	Hs.80409	NM_001924	GADD45A	Growth arrest and DNA-damage-inducible, alpha	DDIT1, GADD45
C12	Hs.110571	NM_015675	GADD45B	Growth arrest and DNA-damage-inducible, beta	DKFZp566B133, GADD45BETA, MYD118
D01	Hs.524134	NM_002051	GATA3	GATA binding protein 3	HDR, MGC2346, MGC5199, MGC5445
D02	Hs.654465	NM_001498	GCLC	Glutamate-cysteine ligase, catalytic subunit	GCL, GCS, GLCL, GLCLC
D03	Hs.315562	NM_002061	GCLM	Glutamate-cysteine ligase, modifier subunit	GLCLR
D04	Hs.271510	NM_000637	GSR	Glutathione reductase	MGC78522
D05	Hs.146393	NM_014685	HERPUD1	Homocysteine-inducible, endoplasmic reticulum stress-inducible, ubiquitin-like domain member 1	HERP, KIAA0025, Mif1, SUP
D06	Hs.250666	NM_005524	HES1	Hairy and enhancer of split 1, (Drosophila)	FLJ20408, HES-1, HHL, HRY, bHLHb39
D07	Hs.57971	NM_001010926	HES5	Hairy and enhancer of split 5 (Drosophila)	bHLHb38
D08	Hs.234434	NM_012258	HEY1	Hairy/enhancer-of-split related with YRPW motif 1	BHLHb31, CHF2, HERP2, HESR1, HRT-1, MGC1274, OAF1
D09	Hs.144287	NM_012259	HEY2	Hairy/enhancer-of-split related with YRPW motif 2	CHF1, GRIDLOCK, GRL, HERP1, HESR2, HRT2, MGC10720, bHLHb32
D10	Hs.472566	NM_014571	HEYL	Hairy/enhancer-of-split related with YRPW motif-like	HEY3, HRT3, MGC12623, bHLHb33

D11	Hs.517581	NM_002133	HMOX1	Heme oxygenase (decycling) 1	HO-1, HSP32, bK286B10
D12	Hs.643447	NM_000201	ICAM1	Intercellular adhesion molecule 1	BB2, CD54, P3.58
E01	Hs.504609	NM_002165	ID1	Inhibitor of DNA binding 1, dominant negative helix-loop-helix protein	ID, bHLHb24
E02	Hs.856	NM_000619	IFNG	Interferon, gamma	IFG, IFI
E03	Hs.7879	NM_001550	IFRD1	Interferon-related developmental regulator 1	PC4, TIS7
E04	Hs.436061	NM_002198	IRF1	Interferon regulatory factor 1	IRF-1, MAR
E05	Hs.728907	NM_000214	JAG1	Jagged 1	AGS, AHD, AWS, CD339, HJ1, JAGL1, MGC104644
E06	Hs.2795	NM_005566	LDHA	Lactate dehydrogenase A	GSD11, LDH1, LDHM
E07	Hs.159142	NM_001040167	LFNG	LFNG O-fucosylpeptide 3-beta-N-acetylglucosaminyltransferase	SCDO3
E08	Hs.655559	NM_052972	LRG1	Leucine-rich alpha-2-glycoprotein 1	FLJ45787, HMFT1766, LRG
E09	Hs.632486	NM_021960	MCL1	Myeloid cell leukemia sequence 1 (BCL2-related)	BCL2L3, EAT, MCL1-ES, MCL1L, MCL1S, MGC104264, MGC1839, Mcl-1, TM, bcl2-L-3, mcl1, EAT
E10	Hs.2256	NM_002423	MMP7	Matrix metallopeptidase 7 (matrilysin, uterine)	MMP-7, MPSL1, PUMP-1
E11	Hs.202453	NM_002467	MYC	V-myc myelocytomatosis viral oncogene homolog (avian)	MRTL, bHLHe39, c-Myc
E12	Hs.495473	NM_017617	NOTCH1	Notch 1	TAN1, hN1
F01	Hs.406515	NM_000903	NQO1	NAD(P)H dehydrogenase, quinone 1	DHQU, DIA4, DTD, NMOR1, NMORI, QR1
F02	Hs.412484	NM_002543	OLR1	Oxidized low density lipoprotein (lectin-like) receptor 1	CLEC8A, LOX1, LOXIN, SCARE1, SLOX1
F03	Hs.728886	NM_182649	PCNA	Proliferating cell nuclear antigen	MGC8367

F04	Hs.696032	NM_006238	PPARD	Peroxisome proliferator-activated receptor delta	FAAR, MGC3931, NR1C2, NUC1, NUCI, NUCII, PPARB
F05	Hs.494538	NM_000264	PTCH1	Patched 1	BCNS, FLJ26746, FLJ42602, HPE7, NBCCS, PTC, PTC1, PTCH, PTCH11
F06	Hs.408528	NM_000321	RB1	Retinoblastoma 1	OSRC, RB, p105-Rb, pRb, pp110
F07	Hs.414795	NM_000602	SERPINE1	Serpin peptidase inhibitor, clade E (nexin, plasminogen activator inhibitor type 1), member 1	PAI, PAI-1, PAI1, PLANH1
F08	Hs.656699	NM_005094	SLC27A4	Solute carrier family 27 (fatty acid transporter), member 4	ACSVL4, FATP4, IPS
F09	Hs.473721	NM_006516	SLC2A1	Solute carrier family 2 (facilitated glucose transporter), member 1	DYT17, DYT18, GLUT, GLUT1, GLUT1DS, MGC141895, MGC141896, PED
F10	Hs.527973	NM_003955	SOCS3	Suppressor of cytokine signalling 3	ATOD4, CIS3, Cish3, MGC71791, SOCS-3, SSI-3, SSI3
F11	Hs.38621	NM_006434	SORBS1	Sorbin and SH3 domain containing 1	CAP, DKFZp451C066, DKFZp586P1422, FLAF2, FLJ12406, KIAA1296, R85FL, SH3D5, SH3P12, SORB1
F12	Hs.437277	NM_003900	SQSTM1	Sequestosome 1	A170, OSIL, PDB3, ZIP3, p60, p62, p62B
G01	Hs.642990	NM_007315	STAT1	Signal transducer and activator of transcription 1, 91kDa	DKFZp686B04100, ISGF-3, STAT91
G02	Hs.241570	NM_000594	TNF	Tumor necrosis factor	DIF, TNF-alpha, TNFA, TNFSF2
G03	Hs.478275	NM_003810	TNFSF10	Tumor necrosis factor (ligand) superfamily, member 10	APO2L, Apo-2L, CD253, TL2, TRAIL
G04	Hs.435136	NM_003329	TXN	Thioredoxin	DKFZp686B1993, MGC61975, TRX, TRX1
G05	Hs.728817	NM_003330	TXNRD1	Thioredoxin reductase 1	GRIM-12, MGC9145, TR, TR1, TRXR1, TXNR
G06	Hs.73793	NM_003376	VEGFA	Vascular endothelial growth factor A	MGC70609, MVCD1, VEGF, VPF
G07	Hs.492974	NM_003882	WISP1	WNT1 inducible signalling pathway	CCN4, FLJ14388, WISP1c, WISP1i, WISP1tc

				protein 1	
G08	Hs.248164	NM_005430	WNT1	Wingless-type MMTV integration site family, member 1	INT1
G09	Hs.258575	NM_004185	WNT2B	Wingless-type MMTV integration site family, member 2B	WNT13, XWNT2
G10	Hs.336930	NM_033131	WNT3A	Wingless-type MMTV integration site family, member 3A	MGC119418, MGC119419, MGC119420
G11	Hs.696364	NM_003392	WNT5A	Wingless-type MMTV integration site family, member 5A	hWNT5A
G12	Hs.29764	NM_006522	WNT6	Wingless-type MMTV integration site family, member 6	-
H01	Hs.520640	NM_001101	ACTB	Actin, beta	PS1TP5BP1
H02	Hs.534255	NM_004048	B2M	Beta-2-microglobulin	-
H03	Hs.592355	NM_002046	GAPDH	Glyceraldehyde-3-phosphate dehydrogenase	G3PD, GAPD, MGC88685
H04	Hs.412707	NM_000194	HPRT1	Hypoxanthine phosphoribosyltransferase 1	HGPRT, HPRT
H05	Hs.546285	NM_001002	RPLP0	Ribosomal protein, large, P0	L10E, LP0, MGC111226, MGC88175, P0, PRLP0, RPP0
H06	N/A	SA_00105	HGDC	Human Genomic DNA Contamination	HIGX1A
H07	N/A	SA_00104	RTC	Reverse Transcription Control	RTC
H08	N/A	SA_00104	RTC	Reverse Transcription Control	RTC
H09	N/A	SA_00104	RTC	Reverse Transcription Control	RTC
H10	N/A	SA_00103	PPC	Positive PCR Control	PPC
H11	N/A	SA_00103	PPC	Positive PCR Control	PPC
H12	N/A	SA_00103	PPC	Positive PCR Control	PPC

Appendix C: Full data for ECM and Adhesion Molecule qPCR array (Chapter 4)

The results above were estimated with the data analysis template provided by Qiagen (http://www.sabiosciences.com/PCRArrayPlate.php)

Full description of the genes are in **Appendix A**.

Gene Symbol	Well	Average ΔC_t (Ct(GOI) - Avg Ct (REF))		$2^{(-\Delta Ct)}$		Fold Change (KEL / NS)	Fold Up- or Down-Regulation	P value (Student's T-test)
		KELOID	NORMAL	KELOID	NORMAL			
ADAMTS1	A01	7.18	5.08	6.9E-03	2.9E-02	0.23	-4.28	0.391261
ADAMTS13	A02	12.29	11.90	2.0E-04	2.6E-04	0.76	-1.31	0.869222
ADAMTS8	A03	10.80	10.22	5.6E-04	8.4E-04	0.67	-1.50	0.743437
CD44	A04	1.90	1.29	2.7E-01	4.1E-01	0.66	-1.52	0.077257
CDH1	A05	2.22	2.64	2.2E-01	1.6E-01	1.34	1.34	0.230413
CLEC3B	A06	5.25	2.87	2.6E-02	1.4E-01	0.19	-5.20	0.007131
CNTN1	A07	3.80	5.72	7.2E-02	1.9E-02	3.78	3.78	0.056307
COL11A1	A08	3.14	9.79	1.1E-01	1.1E-03	100.50	100.50	0.152714
COL12A1	A09	3.91	7.43	6.7E-02	5.8E-03	11.44	11.44	0.041628
COL14A1	A10	0.96	3.08	5.1E-01	1.2E-01	4.33	4.33	0.032894
COL15A1	A11	3.17	3.98	1.1E-01	6.3E-02	1.76	1.76	0.063871
COL16A1	A12	2.42	4.88	1.9E-01	3.4E-02	5.50	5.50	0.019857
COL1A1	B01	-3.39	1.24	1.1E+01	4.2E-01	24.84	24.84	0.013361
COL4A2	B02	3.61	4.79	8.2E-02	3.6E-02	2.27	2.27	0.030212
COL5A1	B03	2.39	6.58	1.9E-01	1.0E-02	18.26	18.26	0.013699
COL6A1	B04	0.84	3.08	5.6E-01	1.2E-01	4.73	4.73	0.026889
COL6A2	B05	1.20	3.38	4.3E-01	9.6E-02	4.52	4.52	0.036823
COL7A1	B06	4.71	4.95	3.8E-02	3.2E-02	1.18	1.18	0.737516
COL8A1	B07	9.28	12.75	1.6E-03	1.4E-04	11.09	11.09	0.155489

CTGF	B08	1.47	1.12	3.6E-01	4.6E-01	0.79	-1.27	0.969107
CTNNA1	B09	2.86	2.77	1.4E-01	1.5E-01	0.94	-1.06	0.723164
CTNNB1	B10	4.39	5.72	4.8E-02	1.9E-02	2.53	2.53	0.049249
CTNND1	B11	4.06	3.79	6.0E-02	7.2E-02	0.83	-1.20	0.338003
CTNND2	B12	11.58	10.78	3.3E-04	5.7E-04	0.57	-1.74	0.533543
ECM1	C01	1.96	2.60	2.6E-01	1.7E-01	1.55	1.55	0.269241
FN1	C02	-1.12	2.09	2.2E+00	2.3E-01	9.28	9.28	0.018301
HAS1	C03	12.62	9.53	1.6E-04	1.4E-03	0.12	-8.51	0.188207
ICAM1	C04	5.53	4.95	2.2E-02	3.2E-02	0.67	-1.50	0.222020
ITGA1	C05	4.64	5.38	4.0E-02	2.4E-02	1.66	1.66	0.086869
ITGA2	C06	4.11	3.91	5.8E-02	6.6E-02	0.87	-1.14	0.410996
ITGA3	C07	4.97	4.55	3.2E-02	4.3E-02	0.75	-1.34	0.175365
ITGA4	C08	6.02	7.60	1.5E-02	5.1E-03	3.01	3.01	0.050691
ITGA5	C09	4.97	5.42	3.2E-02	2.3E-02	1.37	1.37	0.309134
ITGA6	C10	3.66	3.57	7.9E-02	8.4E-02	0.94	-1.06	0.640923
ITGA7	C11	7.70	7.51	4.8E-03	5.5E-03	0.88	-1.14	0.787563
ITGA8	C12	7.51	6.70	5.5E-03	9.6E-03	0.57	-1.75	0.376324
ITGAL	D01	10.02	9.89	9.6E-04	1.1E-03	0.92	-1.09	0.626094
ITGAM	D02	8.30	7.67	3.2E-03	4.9E-03	0.65	-1.54	0.281092
ITGAV	D03	2.59	3.48	1.7E-01	9.0E-02	1.85	1.85	0.061350
ITGB1	D04	0.77	2.09	5.9E-01	2.4E-01	2.50	2.50	0.049593
ITGB2	D05	6.33	6.31	1.2E-02	1.3E-02	0.99	-1.01	0.932733
ITGB3	D06	6.47	6.70	1.1E-02	9.6E-03	1.17	1.17	0.798189
ITGB4	D07	5.67	5.03	2.0E-02	3.1E-02	0.64	-1.56	0.064969
ITGB5	D08	4.04	4.74	6.1E-02	3.8E-02	1.62	1.62	0.140738
KAL1	D09	4.36	6.42	4.9E-02	1.2E-02	4.16	4.16	0.091676
LAMA1	D10	10.85	13.12	5.4E-04	1.1E-04	4.81	4.81	0.008354

LAMA2	D11	4.92	5.24	3.3E-02	2.6E-02	1.25	1.25	0.372134
LAMA3	D12	5.52	4.03	2.2E-02	6.1E-02	0.36	-2.80	0.010269
LAMB1	E01	2.71	3.83	1.5E-01	7.0E-02	2.16	2.16	0.052244
LAMB3	E02	6.51	5.48	1.1E-02	2.2E-02	0.49	-2.04	0.041922
LAMC1	E03	1.95	2.15	2.6E-01	2.3E-01	1.15	1.15	0.371435
MMP1	E04	7.59	13.28	5.2E-03	1.0E-04	51.78	51.78	0.002595
MMP10	E05	11.13	12.53	4.5E-04	1.7E-04	2.64	2.64	0.289883
MMP11	E06	5.64	9.57	2.0E-02	1.3E-03	15.25	15.25	0.079780
MMP12	E07	8.57	8.43	2.6E-03	2.9E-03	0.90	-1.11	0.700688
MMP13	E08	7.91	12.52	4.2E-03	1.7E-04	24.34	24.34	0.000502
MMP14	E09	4.92	6.86	3.3E-02	8.6E-03	3.85	3.85	0.046886
MMP15	E10	12.50	13.01	1.7E-04	1.2E-04	1.43	1.43	0.439033
MMP16	E11	5.60	7.97	2.1E-02	4.0E-03	5.18	5.18	0.049611
MMP2	E12	1.02	1.75	4.9E-01	3.0E-01	1.66	1.66	0.182191
MMP3	F01	8.08	11.29	3.7E-03	4.0E-04	9.22	9.22	0.029302
MMP7	F02	6.54	6.19	1.1E-02	1.4E-02	0.78	-1.28	0.280388
MMP8	F03	12.69	11.53	1.5E-04	3.4E-04	0.45	-2.23	0.453450
MMP9	F04	7.75	7.19	4.6E-03	6.9E-03	0.68	-1.48	0.778497
NCAM1	F05	9.96	9.52	1.0E-03	1.4E-03	0.74	-1.35	0.458615
PECAM1	F06	3.58	4.71	8.4E-02	3.8E-02	2.20	2.20	0.346497
SELE	F07	7.38	7.82	6.0E-03	4.4E-03	1.35	1.35	0.767086
SELL	F08	8.92	10.44	2.1E-03	7.2E-04	2.86	2.86	0.278719
SELP	F09	7.29	8.42	6.4E-03	2.9E-03	2.18	2.18	0.072656
SGCE	F10	3.90	4.30	6.7E-02	5.1E-02	1.32	1.32	0.744538
SPARC	F11	-1.58	1.63	3.0E+00	3.2E-01	9.24	9.24	0.033400
SPG7	F12	7.16	7.17	7.0E-03	6.9E-03	1.00	1.00	0.923552
SPP1	G01	6.27	11.15	1.3E-02	4.4E-04	29.59	29.59	0.032033

TGFBI	G02	0.69	1.88	6.2E-01	2.7E-01	2.28	2.28	0.042894
THBS1	G03	3.54	4.81	8.6E-02	3.6E-02	2.40	2.40	0.142607
THBS2	G04	1.02	3.21	4.9E-01	1.1E-01	4.58	4.58	0.016805
THBS3	G05	10.10	10.44	9.1E-04	7.2E-04	1.27	1.27	0.252470
TIMP1	G06	4.97	5.89	3.2E-02	1.7E-02	1.89	1.89	0.048601
TIMP2	G07	1.89	2.30	2.7E-01	2.0E-01	1.34	1.34	0.278459
TIMP3	G08	2.16	0.91	2.2E-01	5.3E-01	0.42	-2.39	0.132625
TNC	G09	0.94	3.48	5.2E-01	8.9E-02	5.85	5.85	0.007962
VCAM1	G10	3.40	4.25	9.5E-02	5.3E-02	1.81	1.81	0.085035
VCAN	G11	1.73	4.12	3.0E-01	5.8E-02	5.23	5.23	0.051174
VTN	G12	12.87	11.85	1.3E-04	2.7E-04	0.49	-2.03	0.115585
ACTB	H01	0.26	0.64	8.3E-01	6.4E-01	1.30	1.30	0.681253
B2M	H02	-2.00	-2.41	4.0E+00	5.3E+00	0.75	-1.33	0.162935
GAPDH	H03	0.87	1.52	5.5E-01	3.5E-01	1.57	1.57	0.176600
HPRT1	H04	4.98	4.98	3.2E-02	3.2E-02	1.00	1.00	0.959250
RPLP0	H05	-3.85	-4.10	1.4E+01	1.7E+01	0.84	-1.19	0.383135

Appendix D: Full data for Signal Transduction PathwayFinder qPCR array (Chapter 4)

The results above were estimated with the data analysis template provided by Qiagen (http://www.sabiosciences.com/PCRArrayPlate.php)

Full description of the genes are in **Appendix B**

Gene Symbol	Well	Average ΔC_t (Ct(GOI) - Avg Ct (REF))		$2^{(-\Delta Ct)}$		Fold Change KEL / NS	Fold Up- or Down-Regulation	P value (Student's T-test)
		KELOID	NORMAL	KELOID	NORMAL			
ACSL3	A01	2.97	3.35	1.3E-01	9.8E-02	1.30	1.30	0.216806
ACSL4	A02	4.12	4.24	5.7E-02	5.3E-02	1.08	1.08	0.764788
ACSL5	A03	5.48	6.30	2.2E-02	1.3E-02	1.77	1.77	0.217011
ADM	A04	5.74	4.59	1.9E-02	4.1E-02	0.45	-2.22	0.083592
ARNT	A05	7.36	7.07	6.1E-03	7.4E-03	0.82	-1.22	0.372955
ATF4	A06	1.38	1.52	3.9E-01	3.5E-01	1.10	1.10	0.574682
AXIN2	A07	5.11	4.50	2.9E-02	4.4E-02	0.66	-1.52	0.068553
BAX	A08	4.11	4.41	5.8E-02	4.7E-02	1.23	1.23	0.188123
BBC3	A09	7.90	7.78	4.2E-03	4.6E-03	0.92	-1.09	0.997460
BCL2	A10	6.57	4.93	1.1E-02	3.3E-02	0.32	-3.12	0.002738
BCL2A1	A11	7.86	8.93	4.3E-03	2.1E-03	2.10	2.10	0.257681
BCL2L1	A12	5.88	5.37	1.7E-02	2.4E-02	0.70	-1.43	0.046001
BIRC3	B01	5.96	5.28	1.6E-02	2.6E-02	0.63	-1.60	0.119844
BMP2	B02	9.20	6.86	1.7E-03	8.6E-03	0.20	-5.04	0.019109
BMP4	B03	7.21	5.33	6.8E-03	2.5E-02	0.27	-3.67	0.010352
BTG2	B04	7.41	7.10	5.9E-03	7.3E-03	0.81	-1.24	0.930445
CA9	B05	9.71	8.34	1.2E-03	3.1E-03	0.39	-2.58	0.646662
CCL5	B06	4.97	5.86	3.2E-02	1.7E-02	1.85	1.85	0.088517
CCND1	B07	3.95	2.62	6.4E-02	1.6E-01	0.40	-2.52	0.064827

CCND2	B08	3.03	3.58	1.2E-01	8.4E-02	1.46	1.46	0.135709
CDKN1A	B09	2.21	2.53	2.2E-01	1.7E-01	1.25	1.25	0.554369
CDKN1B	B10	4.60	4.03	4.1E-02	6.1E-02	0.67	-1.48	0.183205
CEBPD	B11	6.28	5.17	1.3E-02	2.8E-02	0.46	-2.16	0.319870
CPT2	B12	6.67	6.86	9.8E-03	8.6E-03	1.14	1.14	0.602308
CSF1	C01	5.86	5.46	1.7E-02	2.3E-02	0.76	-1.32	0.088254
DAB2	C02	5.11	5.84	2.9E-02	1.7E-02	1.66	1.66	0.168331
EGFR	C03	3.43	2.27	9.3E-02	2.1E-01	0.45	-2.23	0.009781
EMP1	C04	0.44	0.26	7.3E-01	8.3E-01	0.88	-1.13	0.275246
EPO	C05	12.47	12.41	1.8E-04	1.8E-04	0.96	-1.04	0.505581
FABP1	C06	12.05	11.62	2.4E-04	3.2E-04	0.74	-1.35	0.382597
FAS	C07	3.08	3.12	1.2E-01	1.2E-01	1.03	1.03	0.898058
FCER2	C08	12.76	12.03	1.4E-04	2.4E-04	0.61	-1.65	0.413576
FOSL1	C09	7.42	8.32	5.8E-03	3.1E-03	1.86	1.86	0.816903
FTH1	C10	-2.06	-1.73	4.2E+00	3.3E+00	1.25	1.25	0.219272
GADD45A	C11	8.80	8.40	2.2E-03	3.0E-03	0.76	-1.31	0.689107
GADD45B	C12	3.34	4.14	9.9E-02	5.7E-02	1.74	1.74	0.064647
GATA3	D01	8.36	6.70	3.1E-03	9.6E-03	0.32	-3.15	0.023721
GCLC	D02	4.06	3.61	6.0E-02	8.2E-02	0.73	-1.36	0.166876
GCLM	D03	5.08	5.84	3.0E-02	1.7E-02	1.70	1.70	0.139488
GSR	D04	9.20	8.16	1.7E-03	3.5E-03	0.48	-2.06	0.192992
HERPUD1	D05	4.04	4.37	6.1E-02	4.8E-02	1.26	1.26	0.361058
HES1	D06	4.79	4.55	3.6E-02	4.3E-02	0.85	-1.18	0.900575
HES5	D07	9.33	7.71	1.6E-03	4.8E-03	0.33	-3.06	0.075277
HEY1	D08	5.30	6.69	2.5E-02	9.7E-03	2.62	2.62	0.032749
HEY2	D09	4.82	7.35	3.5E-02	6.1E-03	5.78	5.78	0.079819
HEYL	D10	9.29	9.84	1.6E-03	1.1E-03	1.47	1.47	0.203567

HMOX1	D11	5.06	5.25	3.0E-02	2.6E-02	1.14	1.14	0.526496
ICAM1	D12	5.49	5.92	2.2E-02	1.6E-02	1.35	1.35	0.097339
ID1	E01	2.44	3.95	1.8E-01	6.5E-02	2.84	2.84	0.032846
IFNG	E02	10.20	10.91	8.5E-04	5.2E-04	1.64	1.64	0.344414
IFRD1	E03	4.56	4.55	4.2E-02	4.3E-02	0.99	-1.01	0.872188
IRF1	E04	5.27	5.10	2.6E-02	2.9E-02	0.89	-1.12	0.562025
JAG1	E05	1.36	0.92	3.9E-01	5.3E-01	0.74	-1.36	0.251756
LDHA	E06	0.24	0.30	8.5E-01	8.1E-01	1.05	1.05	0.766327
LFNG	E07	5.63	4.40	2.0E-02	4.7E-02	0.42	-2.35	0.120184
LRG1	E08	6.37	6.71	1.2E-02	9.5E-03	1.27	1.27	0.867053
MCL1	E09	0.72	0.45	6.1E-01	7.3E-01	0.83	-1.21	0.453196
MMP7	E10	6.68	6.39	9.7E-03	1.2E-02	0.82	-1.23	0.684311
MYC	E11	1.96	1.11	2.6E-01	4.6E-01	0.55	-1.81	0.179182
NOTCH1	E12	7.51	7.41	5.5E-03	5.9E-03	0.93	-1.08	0.847396
NQO1	F01	5.59	5.70	2.1E-02	1.9E-02	1.08	1.08	0.631394
OLR1	F02	11.25	12.50	4.1E-04	1.7E-04	2.37	2.37	0.171092
PCNA	F03	3.27	3.49	1.0E-01	8.9E-02	1.16	1.16	0.251301
PPARD	F04	6.29	6.11	1.3E-02	1.5E-02	0.88	-1.13	0.837181
PTCH1	F05	11.52	10.30	3.4E-04	8.0E-04	0.43	-2.33	0.080442
RB1	F06	3.92	3.80	6.6E-02	7.2E-02	0.92	-1.09	0.410839
SERPINE1	F07	6.31	6.65	1.3E-02	9.9E-03	1.27	1.27	0.267068
SLC27A4	F08	4.90	5.36	3.4E-02	2.4E-02	1.37	1.37	0.315273
SLC2A1	F09	3.50	3.85	8.8E-02	6.9E-02	1.27	1.27	0.271907
SOCS3	F10	5.94	6.94	1.6E-02	8.1E-03	2.01	2.01	0.327575
SORBS1	F11	5.78	3.79	1.8E-02	7.2E-02	0.25	-3.97	0.016236
SQSTM1	F12	2.70	2.49	1.5E-01	1.8E-01	0.86	-1.16	0.771592
STAT1	G01	3.50	3.84	8.9E-02	7.0E-02	1.27	1.27	0.154955

TNF	G02	8.12	9.25	3.6E-03	1.6E-03	2.20	2.20	0.576176
TNFSF10	G03	2.84	3.31	1.4E-01	1.0E-01	1.38	1.38	0.383086
TXN	G04	0.32	-0.19	8.0E-01	1.1E+00	0.71	-1.42	0.385635
TXNRD1	G05	4.87	4.75	3.4E-02	3.7E-02	0.92	-1.09	0.450042
VEGFA	G06	4.51	5.55	4.4E-02	2.1E-02	2.06	2.06	0.019082
WISP1	G07	4.38	7.72	4.8E-02	4.7E-03	10.10	10.10	0.043855
WNT1	G08	12.90	12.72	1.3E-04	1.5E-04	0.88	-1.13	0.786171
WNT2B	G09	4.91	4.12	3.3E-02	5.8E-02	0.58	-1.74	0.316136
WNT3A	G10	11.79	10.51	2.8E-04	6.8E-04	0.41	-2.42	0.333833
WNT5A	G11	5.45	7.77	2.3E-02	4.6E-03	5.00	5.00	0.107835
WNT6	G12	11.33	10.30	3.9E-04	8.0E-04	0.49	-2.05	0.191243
ACTB	H01	-0.75	-0.63	1.7E+00	1.6E+00	1.09	1.09	0.497115
B2M	H02	-2.24	-2.69	4.7E+00	6.5E+00	0.73	-1.37	0.051859
GAPDH	H03	0.81	1.11	5.7E-01	4.6E-01	1.23	1.23	0.336504
HPRT1	H04	4.88	4.89	3.4E-02	3.4E-02	1.01	1.01	0.979106
RPLP0	H05	-3.45	-3.32	1.1E+01	1.0E+01	1.10	1.10	0.480909

Bibliography

AARABI, S., DRAPER, L., GRAYSON, B. & GURTNER, G. C. 2008. Bisphosphonate-associated osteonecrosis of the jaw: successful treatment at 2-year follow-up. *Plastic and Reconstructive Surgery,* 122**,** 57e-9e.

ABDOU, A. G., EL FARARGY, S., SELEIT, I., ANTAR, A. G., ELHEFNY, M. & ELNAIDANY, N. F. 2012. Osteopontin expression in chronic plaque psoriasis: an association with the severity of disease. *Anal Quant Cytol Histol,* 34**,** 79-85.

ABERGEL, R. P., PIZZURRO, D., MEEKER, C. A., LASK, G., MATSUOKA, L. Y., MINOR, R. R., CHU, M. L. & UITTO, J. 1985. Biochemical composition of the connective tissue in keloids and analysis of collagen metabolism in keloid fibroblast cultures. *J Invest Dermatol,* 84**,** 384-90.

ABREU, J. G., KETPURA, N. I., REVERSADE, B. & DE ROBERTIS, E. M. 2002. Connective-tissue growth factor (CTGF) modulates cell signalling by BMP and TGF-beta. *Nat Cell Biol,* 4**,** 599-604.

ADELMANN-GRILL, B. C., HEIN, R., WACH, F. & KRIEG, T. 1987. Inhibition of fibroblast chemotaxis by recombinant human interferon gamma and interferon alpha. *J Cell Physiol,* 130**,** 270-5.

AIBA, S., TABATA, N., ISHII, H., OOTANI, H. & TAGAMI, H. 1992. Dermatofibrosarcoma protuberans is a unique fibrohistiocytic tumour expressing CD34. *Br J Dermatol,* 127**,** 79-84.

AKASAKA, Y., FUJITA, K., ISHIKAWA, Y., ASUWA, N., INUZUKA, K., ISHIHARA, M., ITO, M., MASUDA, T., AKISHIMA, Y., ZHANG, L., ITO, K. & ISHII, T. 2001. Detection of apoptosis in keloids and a comparative study on apoptosis between keloids, hypertrophic scars, normal healed flat scars, and dermatofibroma. *Wound Repair Regen,* 9**,** 501-6.

ALA-AHO, R. & KÄHÄRI, V. M. 2005. Collagenases in cancer. *Biochimie,* 87**,** 273-86.

ALAISH, S. M., YAGER, D. R., DIEGELMANN, R. F. & COHEN, I. K. 1995. Hyaluronic acid metabolism in keloid fibroblasts. *J Pediatr Surg,* 30**,** 949-52.

ALBERTS, B. 2008. *Molecular biology of the cell,* New York, Garland Science ; [London : Taylor & Francis, distributor].

ALTMAN, D. A., NICKOLOFF, B. J. & FIVENSON, D. P. 1993. Differential expression of factor XIIIa and CD34 in cutaneous mesenchymal tumors. *J Cutan Pathol,* 20**,** 154-8.

ALVES, J. V., MATOS, D. M., BARREIROS, H. F. & BÁRTOLO, E. A. 2014. Variants of dermatofibroma--a histopathological study. *An Bras Dermatol,* 89**,** 472-7.

AMADEU, T. P., BRAUNE, A. S., PORTO, L. C., DESMOULIÈRE, A. & COSTA, A. M. 2004. Fibrillin-1 and elastin are differentially expressed in hypertrophic scars and keloids. *Wound Repair Regen,* 12**,** 169-74.

AMENTA, P. S., SCIVOLETTI, N. A., NEWMAN, M. D., SCIANCALEPORE, J. P., LI, D. & MYERS, J. C. 2005. Proteoglycan-collagen XV in human tissues is seen linking banded collagen fibers subjacent to the basement membrane. *J Histochem Cytochem,* 53**,** 165-76.

ANBORGH, P. H., CARIA, L. B., CHAMBERS, A. F., TUCK, A. B., STITT, L. W. & BRACKSTONE, M. 2015. Role of plasma osteopontin as a biomarker in locally advanced breast cancer. *Am J Transl Res,* 7**,** 723-32.

ANBORGH, P. H., MUTRIE, J. C., TUCK, A. B. & CHAMBERS, A. F. 2011. Pre- and post-translational regulation of osteopontin in cancer. *J Cell Commun Signal,* 5**,** 111-22.

AOKI, M., MIYAKE, K., OGAWA, R., DOHI, T., AKAISHI, S., HYAKUSOKU, H. & SHIMADA, T. 2014. siRNA knockdown of tissue inhibitor of metalloproteinase-1 in keloid fibroblasts leads to degradation of collagen type I. *J Invest Dermatol,* 134**,** 818-26.

ASHCROFT, G. S., DODSWORTH, J., VAN BOXTEL, E., TARNUZZER, R. W., HORAN, M. A., SCHULTZ, G. S. & FERGUSON, M. W. 1997a. Estrogen accelerates cutaneous wound healing associated with an increase in TGF-beta1 levels. *Nat Med,* 3**,** 1209-15.

ASHCROFT, G. S., HORAN, M. A. & FERGUSON, M. W. 1997b. Aging is associated with reduced deposition of specific extracellular matrix components, an upregulation of angiogenesis, and an altered inflammatory response in a murine incisional wound healing model. *J Invest Dermatol,* 108**,** 430-7.

ATIYEH, B. S., COSTAGLIOLA, M. & HAYEK, S. N. 2005. Keloid or hypertrophic scar: the controversy: review of the literature. *Ann Plast Surg,* 54**,** 676-80.

ATKINSON, J. J., TOENNIES, H. M., HOLMBECK, K. & SENIOR, R. M. 2007. Membrane type 1 matrix metalloproteinase is necessary for distal airway epithelial repair and keratinocyte growth factor receptor expression after acute injury. *Am J Physiol Lung Cell Mol Physiol,* 293**,** L600-10.

ATTISANO, L. & LABBÉ, E. 2004. TGFbeta and Wnt pathway cross-talk. *Cancer Metastasis Rev,* 23**,** 53-61.

BABU, M., DIEGELMANN, R. & OLIVER, N. 1989. Fibronectin is overproduced by keloid fibroblasts during abnormal wound healing. *Mol Cell Biol,* 9**,** 1642-50.

BAGABIR, R., SYED, F., PAUS, R. & BAYAT, A. 2012. Long-term organ culture of keloid disease tissue. *Experimental Dermatology,* 21**,** 376-381.

BARR, R. J., YOUNG, E. M. & KING, D. F. 1986. Non-polarizable collagen in dermatofibrosarcoma protuberans: a useful diagnostic aid. *J Cutan Pathol,* 13**,** 339-46.

BAUM, C. L. & ARPEY, C. J. 2005. Normal cutaneous wound healing: clinical correlation with cellular and molecular events. *Dermatol Surg,* 31**,** 674-86; discussion 686.

BAUR, P. S., LARSON, D. L. & STACEY, T. R. 1975. The observation of myofibroblasts in hypertrophic scars. *Surg Gynecol Obstet,* 141**,** 22-6.

BAYAT, A., BOCK, O., MROWIETZ, U., OLLIER, W. E. & FERGUSON, M. W. 2004. Genetic susceptibility to keloid disease: transforming growth factor beta receptor gene polymorphisms are not associated with keloid disease. *Exp Dermatol,* 13**,** 120-4.

BAYAT, A., WALTER, J. M., BOCK, O., MROWIETZ, U., OLLIER, W. E. & FERGUSON, M. W. 2005. Genetic susceptibility to keloid disease: mutation screening of the TGFbeta3 gene. *Br J Plast Surg,* 58**,** 914-21.

BEER, T. W. 2005. Keloids are not angiogenic lesions. *J Am Acad Dermatol,* 53**,** 1097; author reply 1097-8.

BEER, T. W., BALDWIN, H. C., GODDARD, J. R., GALLAGHER, P. J. & WRIGHT, D. H. 1998. Angiogenesis in pathological and surgical scars. *Hum Pathol,* 29**,** 1273-8.

BELLA, H., HEISE, M., YAGI, K. I., BLACK, G., MCGROUTHER, D. A. & BAYAT, A. 2011. A clinical characterization of familial keloid disease in unique African tribes reveals distinct keloid phenotypes. *Plastic and Reconstructive Surgery,* 127**,** 689-702.

BERRY, D. A. 2007. The difficult and ubiquitous problems of multiplicities. *Pharm Stat,* 6**,** 155-60.

BETTINGER, D. A., YAGER, D. R., DIEGELMANN, R. F. & COHEN, I. K. 1996. The effect of TGF-beta on keloid fibroblast proliferation and collagen synthesis. *Plast Reconstr Surg,* 98**,** 827-33.

BIERIE, B. & MOSES, H. L. 2006. Tumour microenvironment: TGFbeta: the molecular Jekyll and Hyde of cancer. *Nature reviews. Cancer,* 6**,** 506-20.

BIRK, D. E. 2001. Type V collagen: heterotypic type I/V collagen interactions in the regulation of fibril assembly. *Micron,* 32**,** 223-37.

BIRK, D. E., FITCH, J. M. & LINSENMAYER, T. F. 1986. Organization of collagen types I and V in the embryonic chicken cornea. *Invest Ophthalmol Vis Sci,* 27**,** 1470-7.

BLACKBURN, W. R. & COSMAN, B. 1966. Histologic basis of keloid and hypertrophic scar differentiation. Clinicopathologic correlation. *Arch Pathol,* 82**,** 65-71.

BLANPAIN, C. & FUCHS, E. 2006. Epidermal stem cells of the skin. *Annual review of cell and developmental biology,* 22**,** 339-73.

BLOOR, B. K., TIDMAN, N., LEIGH, I. M., ODELL, E., DOGAN, B., WOLLINA, U., GHALI, L. & WASEEM, A. 2003. Expression of keratin K2e in cutaneous and oral lesions: association with keratinocyte activation, proliferation, and keratinization. *Am J Pathol,* 162**,** 963-75.

BODE, W., GOMIS-RÜTH, F. X. & STÖCKLER, W. 1993. Astacins, serralysins, snake venom and matrix metalloproteinases exhibit identical zinc-binding environments (HEXXHXXGXXH and Met-turn) and topologies and should be grouped into a common family, the 'metzincins'. *FEBS Lett,* 331**,** 134-40.

BOYCE, S. T., SUPP, A. P., SWOPE, V. B. & WARDEN, G. D. 2002. Vitamin C Regulates Keratinocyte Viability, Epidermal Barrier, and Basement Membrane In Vitro, and Reduces Wound Contraction After Grafting of Cultured Skin Substitutes. 118**,** 565-572.

BRADSHAW, A. D., BAICU, C. F., RENTZ, T. J., VAN LAER, A. O., BOGGS, J., LACY, J. M. & ZILE, M. R. 2009. Pressure overload-induced alterations in fibrillar collagen content and myocardial diastolic function: role of secreted protein acidic and rich in cysteine (SPARC) in post-synthetic procollagen processing. *Circulation,* 119**,** 269-80.

BRAN, G. M., GOESSLER, U. R., BAFTIRI, A., HORMANN, K., RIEDEL, F. & SADICK, H. 2010. Effect of transforming growth factor-beta1 antisense oligonucleotides on matrix metalloproteinases and their inhibitors in keloid fibroblasts. *Otolaryngol Head Neck Surg,* 143**,** 66-71.

BREMNES, R. M., DONNEM, T., AL-SAAD, S., AL-SHIBLI, K., ANDERSEN, S., SIRERA, R., CAMPS, C., MARINEZ, I. & BUSUND, L. T. 2011. The role of tumor stroma in cancer progression and prognosis: emphasis on carcinoma-associated fibroblasts and non-small cell lung cancer. *Journal of thoracic oncology : official publication of the International Association for the Study of Lung Cancer,* 6**,** 209-17.

BROUGHTON, G., 2ND, JANIS, J. E. & ATTINGER, C. E. 2006a. The basic science of wound healing. *Plastic and Reconstructive Surgery,* 117**,** 12S-34S.

BROUGHTON, G., 2ND, JANIS, J. E. & ATTINGER, C. E. 2006b. Wound healing: an overview. *Plastic and Reconstructive Surgery,* 117**,** 1e-S-32e-S.

BROWN, B. C., MCKENNA, S. P., SIDDHI, K., MCGROUTHER, D. A. & BAYAT, A. 2008a. The hidden cost of skin scars: quality of life after skin scarring. *J Plast Reconstr Aesthet Surg,* 61**,** 1049-58.

BROWN, J. J., OLLIER, W., ARSCOTT, G., KE, X., LAMB, J., DAY, P. & BAYAT, A. 2008b. Genetic susceptibility to keloid scarring: SMAD gene SNP frequencies in Afro-Caribbeans. *Exp Dermatol,* 17**,** 610-3.

BRUCKNER, P. 2010. Suprastructures of extracellular matrices: paradigms of functions controlled by aggregates rather than molecules. *Cell Tissue Res,* 339**,** 7-18.

BUBACK, F., RENKL, A. C., SCHULZ, G. & WEISS, J. M. 2009. Osteopontin and the skin: multiple emerging roles in cutaneous biology and pathology. *Exp Dermatol,* 18**,** 750-9.

BUECHNER, S. A., WINKELMANN, R. K., LAUTENSCHLAGER, S., GILLI, L. & RUFLI, T. 1993. Localized scleroderma associated with Borrelia burgdorferi infection. Clinical, histologic, and immunohistochemical observations. *J Am Acad Dermatol,* 29**,** 190-6.

BUSTIN, S. A. 2010. Why the need for qPCR publication guidelines?--The case for MIQE. *Methods,* 50**,** 217-26.

BUSTIN, S. A., BEAULIEU, J. F., HUGGETT, J., JAGGI, R., KIBENGE, F. S., OLSVIK, P. A., PENNING, L. C. & TOEGEL, S. 2010. MIQE précis: Practical implementation of minimum standard guidelines for fluorescence-based quantitative real-time PCR experiments. *BMC Mol Biol,* 11**,** 74.

BUTLER, P. D., LY, D. P., LONGAKER, M. T. & YANG, G. P. 2008. Use of organotypic coculture to study keloid biology. *Am J Surg,* 195**,** 144-8.

CAMPOS, A. C., GROTH, A. K. & BRANCO, A. B. 2008. Assessment and nutritional aspects of wound healing. *Curr Opin Clin Nutr Metab Care,* 11**,** 281-8.

CARREIRA, A. C., ALVES, G. G., ZAMBUZZI, W. F., SOGAYAR, M. C. & GRANJEIRO, J. M. 2014. Bone Morphogenetic Proteins: structure, biological function and therapeutic applications. *Arch Biochem Biophys,* 561**,** 64-73.

CATHERINO, W. H., LEPPERT, P. C., STENMARK, M. H., PAYSON, M., POTLOG-NAHARI, C., NIEMAN, L. K. & SEGARS, J. H. 2004. Reduced dermatopontin expression is a molecular link between uterine leiomyomas and keloids. *Genes Chromosomes Cancer,* 40**,** 204-17.

CHANG, E. I., BONILLAS, R. G., EL-FTESI, S., CERADINI, D. J., VIAL, I. N., CHAN, D. A., MICHAELS, J. T. & GURTNER, G. C. 2009. Tissue engineering using autologous microcirculatory beds as vascularized bioscaffolds. *FASEB J,* 23**,** 906-15.

CHANG, H. Y., CHI, J. T., DUDOIT, S., BONDRE, C., VAN DE RIJN, M., BOTSTEIN, D. & BROWN, P. O. 2002. Diversity, topographic differentiation, and positional memory in human fibroblasts. *Proc Natl Acad Sci U S A,* 99**,** 12877-82.

CHANUT-DELALANDE, H., BONOD-BIDAUD, C., COGNE, S., MALBOUYRES, M., RAMIREZ, F., FICHARD, A. & RUGGIERO, F. 2004. Development of a functional skin matrix requires deposition of collagen V heterotrimers. *Mol Cell Biol,* 24**,** 6049-57.

CHANUT-DELALANDE, H., FICHARD, A., BERNOCCO, S., GARRONE, R., HULMES, D. J. & RUGGIERO, F. 2001. Control of heterotypic fibril formation by collagen V is determined by chain stoichiometry. *J Biol Chem,* 276**,** 24352-9.

CHAR, F. 1971. Ehlers-Danlos syndrome. *Birth Defects Orig Artic Ser,* 7**,** 300-2.

CHAVEZ-MUÑOZ, C., HARTWELL, R., JALILI, R. B., JAFARNEJAD, S. M., LAI, A., NABAI, L., GHAFFARI, A., HOJABRPOUR, P., KANAAN, N., DURONIO, V., GUNS, E., CHERKASOV, A. & GHAHARY, A. 2012. SPARC/SFN interaction, suppresses type I collagen in dermal fibroblasts. *Journal of Cellular Biochemistry,* 113**,** 2622-2632.

CHEN, W., FU, X., SUN, X., SUN, T., ZHAO, Z. & SHENG, Z. 2003. Analysis of differentially expressed genes in keloids and normal skin with cDNA microarray. *J Surg Res,* 113**,** 208-16.

CHEN, Y., GAO, J. H., LIU, X. J., YAN, X. & SONG, M. 2006. Characteristics of occurrence for Han Chinese familial keloids. *Burns,* 32**,** 1052-9.

CHEN, Y. Z., XUE, J. Y., CHEN, C. M., YANG, B. L., XU, Q. H., WU, F., LIU, F., YE, X., MENG, X., LIU, G. Y., SHEN, Z. Z., SHAO, Z. M. & WU, J. 2012. PPAR signaling pathway may be an important predictor of breast cancer response to neoadjuvant chemotherapy. *Cancer Chemother Pharmacol,* 70**,** 637-44.

CHIN, G. S., LIU, W., STEINBRECH, D., HSU, M., LEVINSON, H. & LONGAKER, M. T. 2000. Cellular signaling by tyrosine phosphorylation in keloid and normal human dermal fibroblasts. *Plast Reconstr Surg,* 106**,** 1532-40.

CHIPEV, C. C., SIMMAN, R., HATCH, G., KATZ, A. E., SIEGEL, D. M. & SIMON, M. 2000. Myofibroblast phenotype and apoptosis in keloid and palmar fibroblasts in vitro. *Cell Death Differ,* 7**,** 166-76.

CHIPEV, C. C. & SIMON, M. 2002. Phenotypic differences between dermal fibroblasts from different body sites determine their responses to tension and TGFbeta1. *BMC Dermatol,* 2**,** 13.

CHIQUET-EHRISMANN, R. & CHIQUET, M. 2003. Tenascins: regulation and putative functions during pathological stress. *J Pathol,* 200**,** 488-99.

CHONG, Y., PARK, T. H., SEO, S. & CHANG, C. H. 2015. Histomorphometric analysis of collagen architecture of auricular keloids in an Asian population. *Dermatol Surg,* 41**,** 415-22.

CHUA, A. W., GAN, S. U., TING, Y., FU, Z., LIM, C. K., SONG, C., SABAPATHY, K. & PHAN, T. T. 2011. Keloid fibroblasts are more sensitive to Wnt3a treatment in terms of elevated cellular growth and fibronectin expression. *J Dermatol Sci,* 64**,** 199-209.

CHUNG, M. J., LIU, T., ULLENBRUCH, M. & PHAN, S. H. 2007. Antiapoptotic effect of found in inflammatory zone (FIZZ)1 on mouse lung fibroblasts. *J Pathol,* 212**,** 180-7.

CLARK, J. A., TURNER, M. L., HOWARD, L., STANESCU, H., KLETA, R. & KOPP, J. B. 2009. Description of familial keloids in five pedigrees: evidence for autosomal dominant inheritance and phenotypic heterogeneity. *BMC Dermatol,* 9**,** 8.

COLE, R. & HERRON, B. 2010. Imaging of angiogenesis: past, present and future. *In:* MENDEZ-VILAS, A. & DIAZ, J. (eds.) *Microscopy: Science, Technology, Applications and Education.* Formatex.

CONNOLLY, K. L., CHAFFINS, M. & OZOG, D. 2014. Vascular patterns in mature hypertrophic burn scars treated with fractional CO2 laser. *Lasers Surg Med,* 46**,** 597-600.

CRAIG, A. M., SMITH, J. H. & DENHARDT, D. T. 1989. Osteopontin, a transformation-associated cell adhesion phosphoprotein, is induced by 12-O-tetradecanoylphorbol 13-acetate in mouse epidermis. *J Biol Chem,* 264**,** 9682-9.

CRAWFORD, J., NYGARD, K., GAN, B. S. & O'GORMAN, D. B. 2015. Periostin induces fibroblast proliferation and myofibroblast persistence in hypertrophic scarring. *Exp Dermatol,* 24**,** 120-6.

CRISCIONE, V. D. & WEINSTOCK, M. A. 2007. Descriptive epidemiology of dermatofibrosarcoma protuberans in the United States, 1973 to 2002. *J Am Acad Dermatol,* 56**,** 968-73.

CURRY, T. E. & OSTEEN, K. G. 2003. The Matrix Metalloproteinase System: Changes, Regulation, and Impact throughout the Ovarian and Uterine Reproductive Cycle. *Endocrine Reviews,* 24**,** 428-465.

DA COSTA, V., WEI, R., LIM, R., SUN, C. H., BROWN, J. J. & WONG, B. J. 2008. Nondestructive imaging of live human keloid and facial tissue using multiphoton microscopy. *Arch Facial Plast Surg,* 10**,** 38-43.

DALKOWSKI, A., SCHUPPAN, D., ORFANOS, C. E. & ZOUBOULIS, C. C. 1999. Increased expression of tenascin C by keloids in vivo and in vitro. *Br J Dermatol,* 141**,** 50-6.

DARBY, I., SKALLI, O. & GABBIANI, G. 1990. Alpha-smooth muscle actin is transiently expressed by myofibroblasts during experimental wound healing. *Lab Invest,* 63**,** 21-9.

DARBY, I. A. & HEWITSON, T. D. 2007. Fibroblast Differentiation in Wound Healing and Fibrosis. *In:* KWANG, W. J. (ed.) *International Review of Cytology.* Academic Press.

DARBY, I. A., LAVERDET, B., BONTÉ, F. & DESMOULIÈRE, A. 2014. Fibroblasts and myofibroblasts in wound healing. *Clin Cosmet Investig Dermatol,* 7**,** 301-11.

DEES, C., TOMCIK, M., ZERR, P., AKHMETSHINA, A., HORN, A., PALUMBO, K., BEYER, C., ZWERINA, J., DISTLER, O., SCHETT, G. & DISTLER, J. H. 2011. Notch signalling regulates fibroblast activation and collagen release in systemic sclerosis. *Ann Rheum Dis,* 70**,** 1304-10.

DENHARDT, D. T. & GUO, X. 1993. Osteopontin: a protein with diverse functions. *FASEB J,* 7**,** 1475-82.

DENHARDT, D. T. & NODA, M. 1998. Osteopontin expression and function: role in bone remodeling. *J Cell Biochem Suppl,* 30-31**,** 92-102.

DENHARDT, D. T., NODA, M., O'REGAN, A. W., PAVLIN, D. & BERMAN, J. S. 2001. Osteopontin as a means to cope with environmental insults: regulation of inflammation, tissue remodeling, and cell survival. *J Clin Invest,* 107**,** 1055-61.

DERYNCK, R. & ZHANG, Y. E. 2003. Smad-dependent and Smad-independent pathways in TGF-beta family signalling. *Nature,* 425**,** 577-84.

DESMOULIÈRE, A., REDARD, M., DARBY, I. & GABBIANI, G. 1995. Apoptosis mediates the decrease in cellularity during the transition between granulation tissue and scar. *Am J Pathol,* 146**,** 56-66.

DHEDA, K., HUGGETT, J. F., CHANG, J. S., KIM, L. U., BUSTIN, S. A., JOHNSON, M. A., ROOK, G. A. & ZUMLA, A. 2005. The implications of using an inappropriate reference gene

for real-time reverse transcription PCR data normalization. *Anal Biochem,* 344**,** 141-3.

DIEGELMANN, R. F., COHEN, I. K. & MCCOY, B. J. 1979. Growth kinetics and collagen synthesis of normal skin, normal scar and keloid fibroblasts in vitro. *J Cell Physiol,* 98**,** 341-6.

EDDY, R. J., PETRO, J. A. & TOMASEK, J. J. 1988. Evidence for the nonmuscle nature of the "myofibroblast" of granulation tissue and hypertropic scar. An immunofluorescence study. *Am J Pathol,* 130**,** 252-60.

EGEBLAD, M. & WERB, Z. 2002. New functions for the matrix metalloproteinases in cancer progression. *Nat Rev Cancer,* 2**,** 161-74.

EHRLICH, H. P., DESMOULIERE, A., DIEGELMANN, R. F., COHEN, I. K., COMPTON, C. C., GARNER, W. L., KAPANCI, Y. & GABBIANI, G. 1994. Morphological and immunochemical differences between keloid and hypertrophic scar. *Am J Pathol,* 145**,** 105-13.

ENDO, H., NIIOKA, M., SUGIOKA, Y., ITOH, J., KAMEYAMA, K., OKAZAKI, I., ALA-AHO, R., KÄHÄRI, V. M. & WATANABE, T. 2011. Matrix metalloproteinase-13 promotes recovery from experimental liver cirrhosis in rats. *Pathobiology,* 78**,** 239-52.

FALLOWFIELD, J. A., MIZUNO, M., KENDALL, T. J., CONSTANDINOU, C. M., BENYON, R. C., DUFFIELD, J. S. & IREDALE, J. P. 2007. Scar-associated macrophages are a major source of hepatic matrix metalloproteinase-13 and facilitate the resolution of murine hepatic fibrosis. *J Immunol,* 178**,** 5288-95.

FARAGE, M. A., MILLER, K. W. & MAIBACH, H. I. 2010. Degenerative Changes in Aging Skin. *Textbook of Aging Skin.* Springer.

FESSLER, J. H., SHIGAKI, N. & FESSLER, L. I. 1985. Biosynthesis and properties of procollagens V. *Ann N Y Acad Sci,* 460**,** 181-6.

FICHARD, A., KLEMAN, J. P. & RUGGIERO, F. 1995. Another look at collagen V and XI molecules. *Matrix Biol,* 14**,** 515-31.

FLEISCHMAJER, R., MACDONALD, E. D., PERLISH, J. S., BURGESON, R. E. & FISHER, L. W. 1990. Dermal collagen fibrils are hybrids of type I and type III collagen molecules. *J Struct Biol,* 105**,** 162-9.

FORONJY, R. F., SUN, J., LEMAITRE, V. & D'ARMIENTO, J. M. 2008. Transgenic expression of matrix metalloproteinase-1 inhibits myocardial fibrosis and prevents the transition to heart failure in a pressure overload mouse model. *Hypertens Res,* 31**,** 725-35.

FRENEAUX, P., NOS, C., CHARVOLIN, J. Y., VINCENT-SALOMON, A., ZAFRANI, B., SALMON, R. J., CLOUGH, K. B. & SASTRE-GARAU, X. 2000. [Value of macroscopic analysis for authentification of axillary sentinel nodes detected by Patent Blue dye alone during breast cancer surgery]. *Ann Pathol,* 20**,** 545-8.

FRIEDMAN, D. W., BOYD, C. D., MACKENZIE, J. W., NORTON, P., OLSON, R. M. & DEAK, S. B. 1993. Regulation of collagen gene expression in keloids and hypertrophic scars. *J Surg Res,* 55**,** 214-22.

FUCHS, E. 1990. Epidermal differentiation: the bare essentials. *The Journal of cell biology,* 111**,** 2807-14.

FUJIWARA, M., MURAGAKI, Y. & OOSHIMA, A. 2005a. Keloid-derived fibroblasts show increased secretion of factors involved in collagen turnover and depend on matrix metalloproteinase for migration. *Br J Dermatol,* 153**,** 295-300.

FUJIWARA, M., MURAGAKI, Y. & OOSHIMA, A. 2005b. Upregulation of transforming growth factor-beta1 and vascular endothelial growth factor in cultured keloid fibroblasts: relevance to angiogenic activity. *Arch Dermatol Res,* 297**,** 161-9.

FUNAYAMA, E., CHODON, T., OYAMA, A. & SUGIHARA, T. 2003. Keratinocytes promote proliferation and inhibit apoptosis of the underlying fibroblasts: an important role in the pathogenesis of keloid. *J Invest Dermatol,* 121**,** 1326-31.

FURUKAWA, F., MATSUZAKI, K., MORI, S., TAHASHI, Y., YOSHIDA, K., SUGANO, Y., YAMAGATA, H., MATSUSHITA, M., SEKI, T., INAGAKI, Y., NISHIZAWA, M.,

FUJISAWA, J. & INOUE, K. 2003. p38 MAPK mediates fibrogenic signal through Smad3 phosphorylation in rat myofibroblasts. *Hepatology,* 38**,** 879-89.
GABBIANI, G. & MAJNO, G. 1972. Dupuytren's contracture: fibroblast contraction? An ultrastructural study. *Am J Pathol,* 66**,** 131-46.
GABBIANI, G., SCHMID, E., WINTER, S., CHAPONNIER, C., DE CKHASTONAY, C., VANDEKERCKHOVE, J., WEBER, K. & FRANKE, W. W. 1981. Vascular smooth muscle cells differ from other smooth muscle cells: predominance of vimentin filaments and a specific alpha-type actin. *Proc Natl Acad Sci U S A,* 78**,** 298-302.
GARDNER, H., SHEARSTONE, J. R., BANDARU, R., CROWELL, T., LYNES, M., TROJANOWSKA, M., PANNU, J., SMITH, E., JABLONSKA, S., BLASZCZYK, M., TAN, F. K. & MAYES, M. D. 2006. Gene profiling of scleroderma skin reveals robust signatures of disease that are imperfectly reflected in the transcript profiles of explanted fibroblasts. *Arthritis Rheum,* 54**,** 1961-73.
GARNER, W. L. 1998. Epidermal regulation of dermal fibroblast activity. *Plast Reconstr Surg,* 102**,** 135-9.
GAY, S., MARTINEZ-HERNANDEZ, A., RHODES, R. K. & MILLER, E. J. 1981. The collagenous exocytoskeleton of smooth muscle cells. *Coll Relat Res,* 1**,** 377-84.
GELSE, K., PÖSCHL, E. & AIGNER, T. 2003. Collagens--structure, function, and biosynthesis. *Adv Drug Deliv Rev,* 55**,** 1531-46.
GENECARDS, H. G. D. 2016. *VEGFA gene (Protein Coding), Vascular Endothelial Growth Factor A* [Online]. Weizmann Institute of Science. [Accessed 20th January 2016].
GHAFFARI, A., KILANI, R. T. & GHAHARY, A. 2009a. Keratinocyte-conditioned media regulate collagen expression in dermal fibroblasts. *The Journal of investigative dermatology,* 129**,** 340-7.
GHAFFARI, A., KILANI, R. T. & GHAHARY, A. 2009b. Keratinocyte-conditioned media regulate collagen expression in dermal fibroblasts. *J Invest Dermatol,* 129**,** 340-7.
GIANNANDREA, M. & PARKS, W. C. 2014. Diverse functions of matrix metalloproteinases during fibrosis. *Dis Model Mech,* 7**,** 193-203.
GILL, S. E. & PARKS, W. C. 2008. Metalloproteinases and their inhibitors: regulators of wound healing. *Int J Biochem Cell Biol,* 40**,** 1334-47.
GILLARD, J. A., REED, M. W., BUTTLE, D., CROSS, S. S. & BROWN, N. J. 2004. Matrix metalloproteinase activity and immunohistochemical profile of matrix metalloproteinase-2 and -9 and tissue inhibitor of metalloproteinase-1 during human dermal wound healing. *Wound Repair Regen,* 12**,** 295-304.
GIRA, A. K., BROWN, L. F., WASHINGTON, C. V., COHEN, C. & ARBISER, J. L. 2004. Keloids demonstrate high-level epidermal expression of vascular endothelial growth factor. *J Am Acad Dermatol,* 50**,** 850-3.
GOLDSMITH, E. C., BRADSHAW, A. D. & SPINALE, F. G. 2013. Cellular mechanisms of tissue fibrosis. 2. Contributory pathways leading to myocardial fibrosis: moving beyond collagen expression. *Am J Physiol Cell Physiol,* 304**,** C393-402.
GONZÁLEZ-MARTÍNEZ, R., MARÍN-BERTOLÍN, S. & AMORRORTU-VELAYOS, J. 1995. Association between keloids and Dupuytren's disease: case report. *Br J Plast Surg,* 48**,** 47-8.
GORDON, M. K. & HAHN, R. A. 2010. Collagens. *Cell Tissue Res,* 339**,** 247-57.
GOSAIN, A. & DIPIETRO, L. A. 2004. Aging and wound healing. *World J Surg,* 28**,** 321-6.
GROTENDORST, G. R., SOMA, Y., TAKEHARA, K. & CHARETTE, M. 1989. EGF and TGF-alpha are potent chemoattractants for endothelial cells and EGF-like peptides are present at sites of tissue regeneration. *J Cell Physiol,* 139**,** 617-23.
GUO, S. & DIPIETRO, L. A. 2010. Factors affecting wound healing. *J Dent Res,* 89**,** 219-29.
GUO, X. & WANG, X. F. 2009. Signaling cross-talk between TGF-beta/BMP and other pathways. *Cell Res,* 19**,** 71-88.
GURTNER, A., FUSCHI, P., MAGI, F., COLUSSI, C., GAETANO, C., DOBBELSTEIN, M., SACCHI, A. & PIAGGIO, G. 2008a. NF-Y dependent epigenetic modifications discriminate between proliferating and postmitotic tissue. *Plos One,* 3**,** e2047.

GURTNER, G. C., WERNER, S., BARRANDON, Y. & LONGAKER, M. T. 2008b. Wound repair and regeneration. *Nature,* 453**,** 314-21.

HADLER-OLSEN, E., FADNES, B., SYLTE, I., UHLIN-HANSEN, L. & WINBERG, J. O. 2011. Regulation of matrix metalloproteinase activity in health and disease. *FEBS J,* 278**,** 28-45.

HAHN, J. M., GLASER, K., MCFARLAND, K. L., ARONOW, B. J., BOYCE, S. T. & SUPP, D. M. 2013. Keloid-derived keratinocytes exhibit an abnormal gene expression profile consistent with a distinct causal role in keloid pathology. *Wound Repair Regen,* 21**,** 530-44.

HAISA, M., OKOCHI, H. & GROTENDORST, G. R. 1994. Elevated levels of PDGF alpha receptors in keloid fibroblasts contribute to an enhanced response to PDGF. *J Invest Dermatol,* 103**,** 560-3.

HALL, B. 2014. *Bones and Cartilage: Developmental and Evolutionary Skeletal Biology,* Oxford, UK, Academic Press.

HALPER, J. & KJAER, M. 2014. Basic components of connective tissues and extracellular matrix: elastin, fibrillin, fibulins, fibrinogen, fibronectin, laminin, tenascins and thrombospondins. *Adv Exp Med Biol,* 802**,** 31-47.

HAMBRICK, G. W. & CARTER, D. M. 1966. Pachydermoperiostosis. Touraine-Solente-Golé syndrome. *Arch Dermatol,* 94**,** 594-607.

HARPER, R. A. 1989. Keloid fibroblasts in culture: abnormal growth behaviour and altered response to the epidermal growth factor. *Cell Biol Int Rep,* 13**,** 325-35.

HARRIS, B. S., ZHANG, Y., CARD, L., RIVERA, L. B., BREKKEN, R. A. & BRADSHAW, A. D. 2011. SPARC regulates collagen interaction with cardiac fibroblast cell surfaces. *Am J Physiol Heart Circ Physiol,* 301**,** H841-7.

HE, S., LIU, X., YANG, Y., HUANG, W., XU, S., YANG, S., ZHANG, X. & ROBERTS, M. S. 2010. Mechanisms of transforming growth factor beta(1)/Smad signalling mediated by mitogen-activated protein kinase pathways in keloid fibroblasts. *Br J Dermatol,* 162**,** 538-46.

HE, W. & DAI, C. 2015. Key Fibrogenic Signaling. *Curr Pathobiol Rep,* 3**,** 183-192.

HELLSTRÖM, M., HELLSTRÖM, S., ENGSTRÖM-LAURENT, A. & BERTHEIM, U. 2014. The structure of the basement membrane zone differs between keloids, hypertrophic scars and normal skin: a possible background to an impaired function. *J Plast Reconstr Aesthet Surg,* 67**,** 1564-72.

HENRY, G. & GARNER, W. L. 2003. Inflammatory mediators in wound healing. *Surg Clin North Am,* 83**,** 483-507.

HERNÁNDEZ-PÉREZ, M. & MAHALINGAM, M. 2012. Matrix metalloproteinases in health and disease: insights from dermatopathology. *Am J Dermatopathol,* 34**,** 565-79.

HEROVICI, C. 1963. A polychrome stain for differentiating procollagen from collagen. *Stain Technology* [Online], 38.

HERVE, A. 2007. The Bonferonni and Sidak Corrections for Multiple Comparisons. *Encyclopedia of Measurement and Statistics.* Thousand Oaks.

HIGGINS, D. F., KIMURA, K., BERNHARDT, W. M., SHRIMANKER, N., AKAI, Y., HOHENSTEIN, B., SAITO, Y., JOHNSON, R. S., KRETZLER, M., COHEN, C. D., ECKARDT, K. U., IWANO, M. & HAASE, V. H. 2007. Hypoxia promotes fibrogenesis in vivo via HIF-1 stimulation of epithelial-to-mesenchymal transition. *J Clin Invest,* 117**,** 3810-20.

HINZ, B. 2007. Formation and function of the myofibroblast during tissue repair. *J Invest Dermatol,* 127**,** 526-37.

HINZ, B. & GABBIANI, G. 2003. Cell-matrix and cell-cell contacts of myofibroblasts: role in connective tissue remodeling. *Thromb Haemost,* 90**,** 993-1002.

HOU, X., WU, X., HUANG, P., ZHAN, J., ZHOU, T., MA, Y., QIN, T., LUO, R., FENG, Y., XU, Y., CHEN, L. & ZHANG, L. 2015. Osteopontin is a useful predictor of bone metastasis and survival in patients with locally advanced nasopharyngeal carcinoma. *Int J Cancer,* 137**,** 1672-8.

HU, Z. F., GAO, J. H., LI, W., SONG, Y. B. & LI, C. L. 2006. [Differential gene expression profile of keloids: a study with cDNA microarray]. *Nan Fang Yi Ke Da Xue Xue Bao,* 26**,** 308-12.

HUANG, C., NIE, F., QIN, Z., LI, B. & ZHAO, X. 2013a. A snapshot of gene expression signatures generated using microarray datasets associated with excessive scarring. *Am J Dermatopathol,* 35**,** 64-73.

HUANG, L., CAI, Y. J., LUNG, I., LEUNG, B. C. & BURD, A. 2013b. A study of the combination of triamcinolone and 5-fluorouracil in modulating keloid fibroblasts in vitro. *J Plast Reconstr Aesthet Surg,* 66**,** e251-9.

HUANG, X., QIAN, Y., WU, H., XIE, X., ZHOU, Q., WANG, Y., KUANG, W., SHEN, L., LI, K., SU, J. & CHEN, X. 2015. Aberrant expression of osteopontin and E-cadherin indicates radiation resistance and poor prognosis for patients with cervical carcinoma. *J Histochem Cytochem,* 63**,** 88-98.

HUNASGI, S., KONERU, A., VANISHREE, M. & SHAMALA, R. 2013. Keloid: A case report and review of pathophysiology and differences between keloid and hypertrophic scars. *J Oral Maxillofac Pathol,* 17**,** 116-20.

HUNTER, C., BOND, J., KUO, P. C., SELIM, M. A. & LEVINSON, H. 2012. The role of osteopontin and osteopontin aptamer (OPN-R3) in fibroblast activity. *J Surg Res,* 176**,** 348-58.

HUXLEY-JONES, J., CLARKE, T. K., BECK, C., TOUBARIS, G., ROBERTSON, D. L. & BOOT-HANDFORD, R. P. 2007. The evolution of the vertebrate metzincins; insights from Ciona intestinalis and Danio rerio. *BMC Evol Biol,* 7**,** 63.

IGOTA, S., TOSA, M., MURAKAMI, M., EGAWA, S., SHIMIZU, H., HYAKUSOKU, H. & GHAZIZADEH, M. 2013. Identification and characterization of Wnt signaling pathway in keloid pathogenesis. *Int J Med Sci,* 10**,** 344-54.

IIMURO, Y., NISHIO, T., MORIMOTO, T., NITTA, T., STEFANOVIC, B., CHOI, S. K., BRENNER, D. A. & YAMAOKA, Y. 2003. Delivery of matrix metalloproteinase-1 attenuates established liver fibrosis in the rat. *Gastroenterology,* 124**,** 445-58.

IMAIZUMI, R., AKASAKA, Y., INOMATA, N., OKADA, E., ITO, K., ISHIKAWA, Y. & MARUYAMA, Y. 2009. Promoted activation of matrix metalloproteinase (MMP)-2 in keloid fibroblasts and increased expression of MMP-2 in collagen bundle regions: implications for mechanisms of keloid progression. *Histopathology,* 54**,** 722-30.

IQBAL, S. A., SIDGWICK, G. P. & BAYAT, A. 2012. Identification of fibrocytes from mesenchymal stem cells in keloid tissue: a potential source of abnormal fibroblasts in keloid scarring. *Archives of Dermatological Research,* 304**,** 665-671.

ISHIHARA, H., YOSHIMOTO, H., FUJIOKA, M., MURAKAMI, R., HIRANO, A., FUJII, T., OHTSURU, A., NAMBA, H. & YAMASHITA, S. 2000. Keloid fibroblasts resist ceramide-induced apoptosis by overexpression of insulin-like growth factor I receptor. *J Invest Dermatol,* 115**,** 1065-71.

ITOH, Y. & SEIKI, M. 2006. MT1-MMP: a potent modifier of pericellular microenvironment. *J Cell Physiol,* 206**,** 1-8.

JAGADEESAN, J. & BAYAT, A. 2007. Transforming growth factor beta (TGFbeta) and keloid disease. *Int J Surg,* 5**,** 278-85.

JAHODA, C. A., WHITEHOUSE, J., REYNOLDS, A. J. & HOLE, N. 2003. Hair follicle dermal cells differentiate into adipogenic and osteogenic lineages. *Exp Dermatol,* 12**,** 849-59.

JAIN, S., CHAKRABORTY, G., BULBULE, A., KAUR, R. & KUNDU, G. C. 2007. Osteopontin: an emerging therapeutic target for anticancer therapy. *Expert Opin Ther Targets,* 11**,** 81-90.

JANDA, E., LEHMANN, K., KILLISCH, I., JECHLINGER, M., HERZIG, M., DOWNWARD, J., BEUG, H. & GRÜNERT, S. 2002. Ras and TGF[beta] cooperatively regulate epithelial cell plasticity and metastasis: dissection of Ras signaling pathways. *J Cell Biol,* 156**,** 299-313.

JIMENEZ, S. A., FREUNDLICH, B. & ROSENBLOOM, J. 1984. Selective inhibition of human diploid fibroblast collagen synthesis by interferons. *J Clin Invest,* 74**,** 1112-6.

JIN, S.-E., KIM, C.-K. & KIM, Y.-B. Cellular delivery of cationic lipid nanoparticle-based SMAD3 antisense oligonucleotides for the inhibition of collagen production in keloid fibroblasts. *European Journal of Pharmaceutics and Biopharmaceutics*.

JOHNSON, G., NOUR, A. A., NOLAN, T., HUGGETT, J. & BUSTIN, S. 2014. Minimum information necessary for quantitative real-time PCR experiments. *Methods Mol Biol,* 1160**,** 5-17.

JUMPER, N., PAUS, R. & BAYAT, A. 2015. Functional histopathology of keloid disease. *Histol Histopathol***,** 11624.

KAAR, J. L., LI, Y., BLAIR, H. C., ASCHE, G., KOEPSEL, R. R., HUARD, J. & RUSSELL, A. J. 2008. Matrix metalloproteinase-1 treatment of muscle fibrosis. *Acta Biomater,* 4**,** 1411-20.

KADLER, K. E., BALDOCK, C., BELLA, J. & BOOT-HANDFORD, R. P. 2007. Collagens at a glance. *J Cell Sci,* 120**,** 1955-8.

KALAMAJSKI, S. & OLDBERG, A. 2010. The role of small leucine-rich proteoglycans in collagen fibrillogenesis. *Matrix Biol,* 29**,** 248-53.

KALLURI, R. & ZEISBERG, M. 2006. Fibroblasts in cancer. *Nature reviews. Cancer,* 6**,** 392-401.

KASSNER, A., HANSEN, U., MIOSGE, N., REINHARDT, D. P., AIGNER, T., BRUCKNER-TUDERMAN, L., BRUCKNER, P. & GRÄSSEL, S. 2003. Discrete integration of collagen XVI into tissue-specific collagen fibrils or beaded microfibrils. *Matrix Biol,* 22**,** 131-43.

KERKELÄ, E. & SAARIALHO-KERE, U. 2003. Matrix metalloproteinases in tumor progression: focus on basal and squamous cell skin cancer. *Exp Dermatol,* 12**,** 109-25.

KHOO, Y. T., ONG, C. T., MUKHOPADHYAY, A., HAN, H. C., DO, D. V., LIM, I. J. & PHAN, T. T. 2006. Upregulation of secretory connective tissue growth factor (CTGF) in keratinocyte-fibroblast coculture contributes to keloid pathogenesis. *J Cell Physiol,* 208**,** 336-43.

KIKUCHI, K., KADONO, T. & TAKEHARA, K. 1995. Effects of various growth factors and histamine on cultured keloid fibroblasts. *Dermatology,* 190**,** 4-8.

KISCHER, C. W. & BRODY, G. S. 1981. Structure of the collagen nodule from hypertrophic scars and keloids. *Scan Electron Microsc***,** 371-6.

KISCHER, C. W. & HENDRIX, M. J. 1983. Fibronectin (FN) in hypertrophic scars and keloids. *Cell Tissue Res,* 231**,** 29-37.

KISS, T., ECSEDI, S., VIZKELETI, L., KOROKNAI, V., EMRI, G., KOVÁCS, N., ADANY, R. & BALAZS, M. 2015. The role of osteopontin expression in melanoma progression. *Tumour Biol*.

KNAPP, T. R., DANIELS, R. J. & KAPLAN, E. N. 1977. Pathologic scar formation. Morphologic and biochemical correlates. *Am J Pathol,* 86**,** 47-70.

KOPP, J., PREIS, E., SAID, H., HAFEMANN, B., WICKERT, L., GRESSNER, A. M., PALLUA, N. & DOOLEY, S. 2005. Abrogation of transforming growth factor-beta signaling by SMAD7 inhibits collagen gel contraction of human dermal fibroblasts. *J Biol Chem,* 280**,** 21570-6.

KRTOLICA, A. & CAMPISI, J. 2002. Cancer and aging: a model for the cancer promoting effects of the aging stroma. *The international journal of biochemistry & cell biology,* 34**,** 1401-14.

KUO, Y. R., JENG, S. F., WANG, F. S., CHEN, T. H., HUANG, H. C., CHANG, P. R. & YANG, K. D. 2004. Flashlamp pulsed dye laser (PDL) suppression of keloid proliferation through down-regulation of TGF-beta1 expression and extracellular matrix expression. *Lasers Surg Med,* 34**,** 104-8.

KUO, Y. R., WU, W. S., JENG, S. F., WANG, F. S., HUANG, H. C., LIN, C. Z. & YANG, K. D. 2005. Suppressed TGF-beta1 expression is correlated with up-regulation of matrix metalloproteinase-13 in keloid regression after flashlamp pulsed-dye laser treatment. *Lasers Surg Med,* 36**,** 38-42.

KURKINEN, M., VAHERI, A., ROBERTS, P. J. & STENMAN, S. 1980. Sequential appearance of fibronectin and collagen in experimental granulation tissue. *Lab Invest,* 43**,** 47-51.
KUROKAWA, N., UEDA, K. & TSUJI, M. 2010. Study of microvascular structure in keloid and hypertrophic scars: density of microvessels and the efficacy of three-dimensional vascular imaging. *J Plast Surg Hand Surg,* 44**,** 272-7.
KÖSE, O. & WASEEM, A. 2008. Keloids and hypertrophic scars: are they two different sides of the same coin? *Dermatol Surg,* 34**,** 336-46.
LACOUR, J. P., VITETTA, A., CHIQUET-EHRISMANN, R., PISANI, A. & ORTONNE, J. P. 1992. Increased expression of tenascin in the dermis in scleroderma. *Br J Dermatol,* 127**,** 328-34.
LADIN, D. A., HOU, Z., PATEL, D., MCPHAIL, M., OLSON, J. C., SAED, G. M. & FIVENSON, D. P. 1998. p53 and apoptosis alterations in keloids and keloid fibroblasts. *Wound Repair Regen,* 6**,** 28-37.
LAMETSCHWANDTNER, A. & STAINDL, O. 1990. [Angioarchitecture of keloids. A scanning electron microscopy study of a corrosion specimen]. *HNO,* 38**,** 202-7.
LARIONOV, A., KRAUSE, A. & MILLER, W. 2005. A standard curve based method for relative real time PCR data processing. *BMC Bioinformatics,* 6**,** 62.
LAWRENCE, W. T. & DIEGELMANN, R. F. 1994. Growth factors in wound healing. *Clin Dermatol,* 12**,** 157-69.
LE, H., KLEINERMAN, R., LERMAN, O. Z., BROWN, D., GALIANO, R., GURTNER, G. C., WARREN, S. M., LEVINE, J. P. & SAADEH, P. B. 2008. Hedgehog signaling is essential for normal wound healing. *Wound Repair Regen,* 16**,** 768-73.
LEAKE, D., DOERR, T. D. & SCOTT, G. 2003. Expression of urokinase-type plasminogen activator and its receptor in keloids. *Arch Otolaryngol Head Neck Surg,* 129**,** 1334-8.
LEASK, A. & ABRAHAM, D. J. 2004. TGF-beta signaling and the fibrotic response. *FASEB J,* 18**,** 816-27.
LEE, C. H., HONG, C. H., CHEN, Y. T., CHEN, Y. C. & SHEN, M. R. 2012. TGF-beta1 increases cell rigidity by enhancing expression of smooth muscle actin: keloid-derived fibroblasts as a model for cellular mechanics. *J Dermatol Sci,* 67**,** 173-80.
LEE, J. Y., YANG, C. C., CHAO, S. C. & WONG, T. W. 2004. Histopathological differential diagnosis of keloid and hypertrophic scar. *Am J Dermatopathol,* 26**,** 379-84.
LEE, W. J., CHOI, I. K., LEE, J. H., KIM, Y. O. & YUN, C. O. 2013. A novel three-dimensional model system for keloid study: organotypic multicellular scar model. *Wound Repair Regen,* 21**,** 155-65.
LEEMING, D., HE, Y., VEIDAL, S., NGUYEN, Q., LARSEN, D., KOIZUMI, M., SEGOVIA-SILVESTRE, T., ZHANG, C., ZHENG, Q., SUN, S., CAO, Y., BARKHOLT, V., HÄGGLUND, P., BAY-JENSEN, A., QVIST, P. & KARSDAL, M. 2011. A novel marker for assessment of liver matrix remodeling: an enzyme-linked immunosorbent assay (ELISA) detecting a MMP generated type I collagen neo-epitope (C1M). *Biomarkers,* 16**,** 616-28.
LEHMANN, K., JANDA, E., PIERREUX, C. E., RYTÖMAA, M., SCHULZE, A., MCMAHON, M., HILL, C. S., BEUG, H. & DOWNWARD, J. 2000. Raf induces TGFbeta production while blocking its apoptotic but not invasive responses: a mechanism leading to increased malignancy in epithelial cells. *Genes Dev,* 14**,** 2610-22.
LEIGH, I. M., PURKIS, P. E., MARKEY, A., COLLINS, P., NEILL, S., PROBY, C., GLOVER, M. & LANE, E. B. 1993. Keratinocyte alterations in skin tumour development. *Recent results in cancer research. Fortschritte der Krebsforschung. Progres dans les recherches sur le cancer,* 128**,** 179-91.
LENGA, Y., KOH, A., PERERA, A. S., MCCULLOCH, C. A., SODEK, J. & ZOHAR, R. 2008. Osteopontin expression is required for myofibroblast differentiation. *Circ Res,* 102**,** 319-27.
LEVAME, M. & MEYER, F. 1987. [Herovici's picropolychromium. Application to the identification of type I and III collagens]. *Pathol Biol (Paris),* 35**,** 1183-8.

LI, H., NAHAS, Z., FENG, F., ELISSEEFF, J. H. & BOAHENE, K. 2013. Tissue engineering for in vitro analysis of matrix metalloproteinases in the pathogenesis of keloid lesions. *JAMA Facial Plast Surg,* 15**,** 448-56.

LI, J., ZHENG, H., WANG, J., YU, F., MORRIS, R. J., WANG, T. C., HUANG, S. & AI, W. 2012a. Expression of Kruppel-Like Factor KLF4 in Mouse Hair Follicle Stem Cells Contributes to Cutaneous Wound Healing. *Plos One,* 7**,** e39663.

LI, Q., GAO, Y., JIA, Z., MISHRA, L., GUO, K., LI, Z., LE, X., WEI, D., HUANG, S. & XIE, K. 2012b. Dysregulated KLF4 and Vitamin D Receptor Signaling Promotes Hepatocellular Carcinoma Progression. *Gastroenterology*.

LIAW, L., BIRK, D. E., BALLAS, C. B., WHITSITT, J. S., DAVIDSON, J. M. & HOGAN, B. L. 1998. Altered wound healing in mice lacking a functional osteopontin gene (spp1). *J Clin Invest,* 101**,** 1468-78.

LIAW, L., SKINNER, M. P., RAINES, E. W., ROSS, R., CHERESH, D. A., SCHWARTZ, S. M. & GIACHELLI, C. M. 1995. The adhesive and migratory effects of osteopontin are mediated via distinct cell surface integrins. Role of alpha v beta 3 in smooth muscle cell migration to osteopontin in vitro. *J Clin Invest,* 95**,** 713-24.

LILLIE, R. D., TRACY, R. E., PIZZOLATO, P., DONALDSON, P. T. & REYNOLDS, C. 1980. Differential staining of collagen types in paraffin sections: a color change in degraded forms. *Virchows Arch A Pathol Anat Histol,* 386**,** 153-9.

LIM, C. P., PHAN, T. T., LIM, I. J. & CAO, X. 2009. Cytokine profiling and Stat3 phosphorylation in epithelial-mesenchymal interactions between keloid keratinocytes and fibroblasts. *J Invest Dermatol,* 129**,** 851-61.

LIM, I. J., PHAN, T.-T., BAY, B.-H., QI, R., HUYNH, H., TAN, W. T.-L., LEE, S.-T. & LONGAKER, M. T. 2002a. Fibroblasts cocultured with keloid keratinocytes: normal fibroblasts secrete collagen in a keloidlike manner. *American Journal of Physiology - Cell Physiology,* 283**,** C212-C222.

LIM, I. J., PHAN, T. T., BAY, B. H., QI, R., HUYNH, H., TAN, W. T., LEE, S. T. & LONGAKER, M. T. 2002b. Fibroblasts cocultured with keloid keratinocytes: normal fibroblasts secrete collagen in a keloidlike manner. *Am J Physiol Cell Physiol,* 283**,** C212-22.

LIM, I. J., PHAN, T. T., SONG, C., TAN, W. T. & LONGAKER, M. T. 2001. Investigation of the influence of keloid-derived keratinocytes on fibroblast growth and proliferation in vitro. *Plast Reconstr Surg,* 107**,** 797-808.

LIU, F., LAGARES, D., CHOI, K. M., STOPFER, L., MARINKOVIĆ, A., VRBANAC, V., PROBST, C. K., HIEMER, S. E., SISSON, T. H., HOROWITZ, J. C., ROSAS, I. O., FREDENBURGH, L. E., FEGHALI-BOSTWICK, C., VARELAS, X., TAGER, A. M. & TSCHUMPERLIN, D. J. 2015. Mechanosignaling through YAP and TAZ drives fibroblast activation and fibrosis. *Am J Physiol Lung Cell Mol Physiol,* 308**,** L344-57.

LIU, Y. 2010. New insights into epithelial-mesenchymal transition in kidney fibrosis. *J Am Soc Nephrol,* 21**,** 212-22.

LIVAK, K. J. & SCHMITTGEN, T. D. 2001. Analysis of relative gene expression data using real-time quantitative PCR and the 2(-Delta Delta C(T)) Method. *Methods,* 25**,** 402-8.

LOPEZ, C. A., DAVIS, R. L., MOU, K. & DENHARDT, D. T. 1995. Activation of a signal transduction pathway by osteopontin. *Ann N Y Acad Sci,* 760**,** 324-6.

LUO, S., BENATHAN, M., RAFFOUL, W., PANIZZON, R. G. & EGLOFF, D. V. 2001. Abnormal balance between proliferation and apoptotic cell death in fibroblasts derived from keloid lesions. *Plastic and Reconstructive Surgery,* 107**,** 87-96.

LUZAR, B. & CALONJE, E. 2010. Cutaneous fibrohistiocytic tumours - an update. *Histopathology,* 56**,** 148-65.

MA, X., CHEN, J., XU, B., LONG, X., QIN, H., ZHAO, R. C. & WANG, X. 2015. Keloid-derived keratinocytes acquire a fibroblast-like appearance and an enhanced invasive capacity in a hypoxic microenvironment in vitro. *Int J Mol Med,* 35**,** 1246-56.

MACHESNEY, M., TIDMAN, N., WASEEM, A., KIRBY, L. & LEIGH, I. 1998. Activated keratinocytes in the epidermis of hypertrophic scars. *Am J Pathol,* 152**,** 1133-41.

MANICONE, A. M. & MCGUIRE, J. K. 2008. Matrix metalloproteinases as modulators of inflammation. *Semin Cell Dev Biol,* 19**,** 34-41.
MARKEY, A. C., LANE, E. B., MACDONALD, D. M. & LEIGH, I. M. 1992. Keratin expression in basal cell carcinomas. *The British journal of dermatology,* 126**,** 154-60.
MARNEROS, A. G., NORRIS, J. E., OLSEN, B. R. & REICHENBERGER, E. 2001. Clinical genetics of familial keloids. *Arch Dermatol,* 137**,** 1429-34.
MARNEROS, A. G., NORRIS, J. E., WATANABE, S., REICHENBERGER, E. & OLSEN, B. R. 2004a. Genome scans provide evidence for keloid susceptibility loci on chromosomes 2q23 and 7p11. *J Invest Dermatol,* 122**,** 1126-32.
MARNEROS, A. G., NORRIS, J. E. C., WATANABE, S., REICHENBERGER, E. & OLSEN, B. R. 2004b. Genome Scans Provide Evidence for Keloid Susceptibility Loci on Chromosomes 2q23 and 7p11. *J Investig Dermatol,* 122**,** 1126-1132.
MARTINEK, N., SHAHAB, J., SODEK, J. & RINGUETTE, M. 2007. Is SPARC an evolutionarily conserved collagen chaperone? *J Dent Res,* 86**,** 296-305.
MARTINO, M. M., TORTELLI, F., MOCHIZUKI, M., TRAUB, S., BEN-DAVID, D., KUHN, G. A., MÜLLER, R., LIVNE, E., EMING, S. A. & HUBBELL, J. A. 2011. Engineering the growth factor microenvironment with fibronectin domains to promote wound and bone tissue healing. *Sci Transl Med,* 3**,** 100ra89.
MASSAGUÉ, J. 2008. TGFbeta in Cancer. *Cell,* 134**,** 215-30.
MATHIEU, D., J-C., L. & F., W. 2006. Non-healing wounds. *In:* MATHIEU, D. (ed.) *Handbook on hyperbaric medicine.* Netherlands: Springer.
MATSUOKA, L. Y., UITTO, J., WORTSMAN, J., ABERGEL, R. P. & DIETRICH, J. 1988. Ultrastructural characteristics of keloid fibroblasts. *Am J Dermatopathol,* 10**,** 505-8.
MATSUZAKI, K. & OKAZAKI, K. 2006. Transforming growth factor-beta during carcinogenesis: the shift from epithelial to mesenchymal signaling. *J Gastroenterol,* 41**,** 295-303.
MCCAULEY, R. L., CHOPRA, V., LI, Y. Y., HERNDON, D. N. & ROBSON, M. C. 1992. Altered cytokine production in black patients with keloids. *J Clin Immunol,* 12**,** 300-8.
MCCAWLEY, L. J. & MATRISIAN, L. M. 2001. Matrix metalloproteinases: they're not just for matrix anymore! *Curr Opin Cell Biol,* 13**,** 534-40.
MCGRATH, J. A., EADY, E. A. J. & POPE, F. M. 2004. Anatomy and Organisation of Human Skin. *Rook's Textbook of Dermatology.*
MCQUIBBAN, G. A., GONG, J. H., TAM, E. M., MCCULLOCH, C. A., CLARK-LEWIS, I. & OVERALL, C. M. 2000. Inflammation dampened by gelatinase A cleavage of monocyte chemoattractant protein-3. *Science,* 289**,** 1202-6.
MENON, S. N., FLEGG, J. A., MCCUE, S. W., SCHUGART, R. C., DAWSON, R. A. & MCELWAIN, D. L. S. 2012. Modelling the interaction of keratinocytes and fibroblasts during normal and abnormal wound healing processes. *Proceedings of the Royal Society B: Biological Sciences*.
MESSADI, D. V., LE, A., BERG, S., HUANG, G., ZHUANG, W. & BERTOLAMI, C. N. 1998. Effect of TGF-beta 1 on PDGF receptors expression in human scar fibroblasts. *Front Biosci,* 3**,** a16-22.
MEYER, L. J., RUSSELL, S. B., RUSSELL, J. D., TRUPIN, J. S., EGBERT, B. M., SHUSTER, S. & STERN, R. 2000. Reduced hyaluronan in keloid tissue and cultured keloid fibroblasts. *J Invest Dermatol,* 114**,** 953-9.
MIRAGLIOTTA, V., PIRONE, A., DONADIO, E., ABRAMO, F., RICCIARDI, M. P. & THEORET, C. L. 2014. Osteopontin expression in healing wounds of horses and in human keloids. *Equine Vet J*.
MISHRA, L., SHETTY, K., TANG, Y., STUART, A. & BYERS, S. W. 2005. The role of TGF-beta and Wnt signaling in gastrointestinal stem cells and cancer. *Oncogene,* 24**,** 5775-89.
MISHRA, S., AGARWALLA, S. K., POTPALLE, D. R. & DASH, N. N. 2015. Rubinstein-Taybi syndrome with agenesis of corpus callosum. *J Pediatr Neurosci,* 10**,** 175-7.

MOGILI, N. S., KRISHNASWAMY, V. R., JAYARAMAN, M., RAJARAM, R., VENKATRAMAN, A. & KORRAPATI, P. S. 2012. Altered angiogenic balance in keloids: a key to therapeutic intervention. *Transl Res,* 159**,** 182-9.

MOINZADEH, P., AGARWAL, P., BLOCH, W., ORTEU, C., HUNZELMANN, N., ECKES, B. & KRIEG, T. 2013. Systemic sclerosis with multiple nodules: characterization of the extracellular matrix. *Arch Dermatol Res,* 305**,** 645-52.

MOTT, J. D. & WERB, Z. 2004. Regulation of matrix biology by matrix metalloproteinases. *Curr Opin Cell Biol,* 16**,** 558-64.

MOTULSKY, H. 2014. *Intuitive Biostatistics*, Oxford University Press.

MUKHOPADHYAY, A., TAN, E. K. J., KHOO, Y. T. A., CHAN, S. Y., LIM, I. J. & PHAN, T. T. 2005. Conditioned medium from keloid keratinocyte/keloid fibroblast coculture induces contraction of fibroblast-populated collagen lattices. *British Journal of Dermatology,* 152**,** 639-645.

MURPHY, J. F. & FITZGERALD, D. J. 2001. Vascular endothelial growth factor induces cyclooxygenase-dependent proliferation of endothelial cells via the VEGF-2 receptor. *FASEB J,* 15**,** 1667-9.

MUSTOE, T. A., COOTER, R. D., GOLD, M. H., HOBBS, F. D., RAMELET, A. A., SHAKESPEARE, P. G., STELLA, M., TÉOT, L., WOOD, F. M., ZIEGLER, U. E. & MANAGEMENT, I. A. P. O. S. 2002. International clinical recommendations on scar management. *Plast Reconstr Surg,* 110**,** 560-71.

NA, G. Y., SEO, S. K., LEE, S. J., KIM, D. W., KIM, M. K. & KIM, J. C. 2004. Upregulation of the NNP-1 (novel nuclear protein-1, D21S2056E) gene in keloid tissue determined by cDNA microarray and in situ hybridization. *Br J Dermatol,* 151**,** 1143-9.

NAITOH, M., KUBOTA, H., IKEDA, M., TANAKA, T., SHIRANE, H., SUZUKI, S. & NAGATA, K. 2005. Gene expression in human keloids is altered from dermal to chondrocytic and osteogenic lineage. *Genes Cells,* 10**,** 1081-91.

NAKAGAWA, O., MCFADDEN, D. G., NAKAGAWA, M., YANAGISAWA, H., HU, T., SRIVASTAVA, D. & OLSON, E. N. 2000. Members of the HRT family of basic helix-loop-helix proteins act as transcriptional repressors downstream of Notch signaling. *Proc Natl Acad Sci U S A,* 97**,** 13655-60.

NAKAMURA, M. & TOKURA, Y. 2011. Epithelial-mesenchymal transition in the skin. *J Dermatol Sci,* 61**,** 7-13.

NAKAO, A., AFRAKHTE, M., MOREN, A., NAKAYAMA, T., CHRISTIAN, J. L., HEUCHEL, R., ITOH, S., KAWABATA, M., HELDIN, N. E., HELDIN, C. H. & TEN DIJKE, P. 1997. Identification of Smad7, a TGFbeta-inducible antagonist of TGF-beta signalling. *Nature,* 389**,** 631-5.

NAKASHIMA, M., CHUNG, S., TAKAHASHI, A., KAMATANI, N., KAWAGUCHI, T., TSUNODA, T., HOSONO, N., KUBO, M., NAKAMURA, Y. & ZEMBUTSU, H. 2010a. A genome-wide association study identifies four susceptibility loci for keloid in the Japanese population. *Nat Genet,* 42**,** 768-771.

NAKASHIMA, M., CHUNG, S., TAKAHASHI, A., KAMATANI, N., KAWAGUCHI, T., TSUNODA, T., HOSONO, N., KUBO, M., NAKAMURA, Y. & ZEMBUTSU, H. 2010b. A genome-wide association study identifies four susceptibility loci for keloid in the Japanese population. *Nat Genet,* 42**,** 768-71.

NANODROP. 2007. *260/280 and 260/230 ratios* [Online]. http://www.bio.davidson.edu/projects/gcat/protocols/NanoDrop_tip.pdf: Nanodrop Technologies. [Accessed 28th April 2015].

NANODROP. 2012. *Interpretation of Nucleic Acid 260/280 ratios* [Online]. http://www.nanodrop.com/Library/T123-NanoDrop-Lite-Interpretation-of-Nucleic-Acid-260-280-Ratios.pdf: Thermo Scientific. Available: http://www.nanodrop.com/Library/T123-NanoDrop-Lite-Interpretation-of-Nucleic-Acid-260-280-Ratios.pdf [Accessed 29th April 2015].

NEELY, A. N., CLENDENING, C. E., GARDNER, J., GREENHALGH, D. G. & WARDEN, G. D. 1999. Gelatinase activity in keloids and hypertrophic scars. *Wound Repair Regen,* 7**,** 166-71.

NIEHRS, C. 2012. The complex world of WNT receptor signalling. *Nat Rev Mol Cell Biol,* 13**,** 767-79.

NIESSEN, F. B., SPAUWEN, P. H., SCHALKWIJK, J. & KON, M. 1999. On the nature of hypertrophic scars and keloids: a review. *Plastic and Reconstructive Surgery,* 104**,** 1435-58.

NIYIBIZI, C. & EYRE, D. R. 1989. Bone type V collagen: chain composition and location of a trypsin cleavage site. *Connect Tissue Res,* 20**,** 247-50.

O'KANE, S. & FERGUSON, M. W. 1997. Transforming growth factor beta s and wound healing. *Int J Biochem Cell Biol,* 29**,** 63-78.

O'REGAN, A. & BERMAN, J. S. 2000. Osteopontin: a key cytokine in cell-mediated and granulomatous inflammation. *Int J Exp Pathol,* 81**,** 373-90.

OFT, M., PELI, J., RUDAZ, C., SCHWARZ, H., BEUG, H. & REICHMANN, E. 1996. TGF-beta1 and Ha-Ras collaborate in modulating the phenotypic plasticity and invasiveness of epithelial tumor cells. *Genes Dev,* 10**,** 2462-77.

OLSEN, B. R. 1997. Collagen IX. *Int J Biochem Cell Biol,* 29**,** 555-8.

OMO-DARE, P. 1975. Genetic studies on keloid. *J Natl Med Assoc,* 67**,** 428-32.

ONG, C. T., KHOO, Y. T., MUKHOPADHYAY, A., MASILAMANI, J., DO, D. V., LIM, I. J. & PHAN, T. T. 2010. Comparative proteomic analysis between normal skin and keloid scar. *Br J Dermatol,* 162**,** 1302-15.

OPALENIK, S. R. & DAVIDSON, J. M. 2005. Fibroblast differentiation of bone marrow-derived cells during wound repair. *FASEB J,* 19**,** 1561-3.

ORIENTE, A., FEDARKO, N. S., PACOCHA, S. E., HUANG, S. K., LICHTENSTEIN, L. M. & ESSAYAN, D. M. 2000. Interleukin-13 modulates collagen homeostasis in human skin and keloid fibroblasts. *J Pharmacol Exp Ther,* 292**,** 988-94.

OWENS, D. M. & WATT, F. M. 2003. Contribution of stem cells and differentiated cells to epidermal tumours. *Nature reviews. Cancer,* 3**,** 444-51.

PARDO, A., GIBSON, K., CISNEROS, J., RICHARDS, T. J., YANG, Y., BECERRIL, C., YOUSEM, S., HERRERA, I., RUIZ, V., SELMAN, M. & KAMINSKI, N. 2005. Up-regulation and profibrotic role of osteopontin in human idiopathic pulmonary fibrosis. *PLoS Med,* 2**,** e251.

PARKS, W. C. 1999. Matrix metalloproteinases in repair. *Wound Repair and Regeneration,* 7**,** 423-432.

PARKS, W. C., WILSON, C. L. & LÓPEZ-BOADO, Y. S. 2004. Matrix metalloproteinases as modulators of inflammation and innate immunity. *Nat Rev Immunol,* 4**,** 617-29.

PASPARAKIS, M., HAASE, I. & NESTLE, F. O. 2014. Mechanisms regulating skin immunity and inflammation. *Nat Rev Immunol,* 14**,** 289-301.

PELTONEN, J., HSIAO, L. L., JAAKKOLA, S., SOLLBERG, S., AUMAILLEY, M., TIMPL, R., CHU, M. L. & UITTO, J. 1991. Activation of collagen gene expression in keloids: co-localization of type I and VI collagen and transforming growth factor-beta 1 mRNA. *J Invest Dermatol,* 97**,** 240-8.

PERSY, V. P., VERHULST, A., YSEBAERT, D. K., DE GREEF, K. E. & DE BROE, M. E. 2003. Reduced postischemic macrophage infiltration and interstitial fibrosis in osteopontin knockout mice. *Kidney Int,* 63**,** 543-53.

PETRATOS, P. B., FELSEN, D., TRIERWEILER, G., PRATT, B., MCPHERSON, J. M. & POPPAS, D. P. 2002. Transforming growth factor-beta2 (TGF-beta2) reverses the inhibitory effects of fibrin sealant on cutaneous wound repair in the pig. *Wound Repair Regen,* 10**,** 252-8.

PHAN, T. T., LIM, I. J., AALAMI, O., LORGET, F., KHOO, A., TAN, E. K., MUKHOPADHYAY, A. & LONGAKER, M. T. 2005. Smad3 signalling plays an important role in keloid pathogenesis via epithelial-mesenchymal interactions. *J Pathol,* 207**,** 232-42.

PHAN, T. T., LIM, I. J., BAY, B. H., QI, R., HUYNH, H. T., LEE, S. T. & LONGAKER, M. T. 2002. Differences in collagen production between normal and keloid-derived fibroblasts in serum-media co-culture with keloid-derived keratinocytes. *J Dermatol Sci,* 29**,** 26-34.

PHAN, T. T., LIM, I. J., BAY, B. H., QI, R., LONGAKER, M. T., LEE, S. T. & HUYNH, H. 2003. Role of IGF system of mitogens in the induction of fibroblast proliferation by keloid-derived keratinocytes in vitro. *Am J Physiol Cell Physiol,* 284**,** C860-9.

PHANISH, M. K., WAHAB, N. A., COLVILLE-NASH, P., HENDRY, B. M. & DOCKRELL, M. E. 2006. The differential role of Smad2 and Smad3 in the regulation of pro-fibrotic TGFbeta1 responses in human proximal-tubule epithelial cells. *Biochem J,* 393**,** 601-7.

PHILANDRIANOS, C., ANDRAC-MEYER, L., MORDON, S., FEUERSTEIN, J.-M., SABATIER, F., VERAN, J., MAGALON, G. & CASANOVA, D. Comparison of five dermal substitutes in full-thickness skin wound healing in a porcine model. *Burns*.

PICCOLO, S., DUPONT, S. & CORDENONSI, M. 2014. The biology of YAP/TAZ: hippo signaling and beyond. *Physiol Rev,* 94**,** 1287-312.

PITTENGER, M. F., MACKAY, A. M., BECK, S. C., JAISWAL, R. K., DOUGLAS, R., MOSCA, J. D., MOORMAN, M. A., SIMONETTI, D. W., CRAIG, S. & MARSHAK, D. R. 1999. Multilineage potential of adult human mesenchymal stem cells. *Science,* 284**,** 143-7.

POPE, F. M., MARTIN, G. R., LICHTENSTEIN, J. R., PENTTINEN, R., GERSON, B., ROWE, D. W. & MCKUSICK, V. A. 1975. Patients with Ehlers-Danlos syndrome type IV lack type III collagen. *Proc Natl Acad Sci U S A,* 72**,** 1314-6.

POPE, F. M., MARTIN, G. R. & MCKUSICK, V. A. 1977. Inheritance of Ehlers-Danlos type IV syndrome. *J Med Genet,* 14**,** 200-4.

PROCKOP, D. J. & FERTALA, A. 1998. Inhibition of the self-assembly of collagen I into fibrils with synthetic peptides. Demonstration that assembly is driven by specific binding sites on the monomers. *J Biol Chem,* 273**,** 15598-604.

RASP, G., HOCHSTRASSER, K., WACHTER, E. & REISINGER, P. W. 1987. The amino-acid sequence of the trypsin-released inhibitor from sheep inter-alpha-trypsin inhibitor. *Biol Chem Hoppe Seyler,* 368**,** 727-31.

RAWLINS, J. M., LAM, W. L., KAROO, R. O., NAYLOR, I. L. & SHARPE, D. T. 2006. Quantifying collagen type in mature burn scars: a novel approach using histology and digital image analysis. *J Burn Care Res,* 27**,** 60-5.

RENCIC, A., BRINSTER, N. & NOUSARI, C. H. 2003. Keloid morphea and nodular scleroderma: two distinct clinical variants of scleroderma? *J Cutan Med Surg,* 7**,** 20-4.

REYNOLDS, J. J. 1996. Collagenases and tissue inhibitors of metalloproteinases: a functional balance in tissue degradation. *Oral Dis,* 2**,** 70-6.

RHEINWALD, J. G. & GREEN, H. 1975. Serial cultivation of strains of human epidermal keratinocytes: the formation of keratinizing colonies from single cells. *Cell,* 6**,** 331-43.

RHEINWALD, J. G. & GREEN, H. 1977. Epidermal growth factor and the multiplication of cultured human epidermal keratinocytes. *Nature,* 265**,** 421-4.

RICARD-BLUM, S. 2011. The collagen family. *Cold Spring Harb Perspect Biol,* 3**,** a004978.

RINN, J. L., BONDRE, C., GLADSTONE, H. B., BROWN, P. O. & CHANG, H. Y. 2006. Anatomic demarcation by positional variation in fibroblast gene expression programs. *PLoS Genet,* 2**,** e119.

RITTLING, S. R. 2011. Osteopontin in macrophage function. *Expert Rev Mol Med,* 13**,** e15.

ROHDE, C., HOWELL, B. W., BUNCKE, G. M., GURTNER, G. C., LEVIN, L. S., PU, L. L. & LEVINE, J. P. 2009. A recommended protocol for the immediate postoperative care of lower extremity free-flap reconstructions. *J Reconstr Microsurg,* 25**,** 15-9.

ROSAS, I. O., RICHARDS, T. J., KONISHI, K., ZHANG, Y., GIBSON, K., LOKSHIN, A. E., LINDELL, K. O., CISNEROS, J., MACDONALD, S. D., PARDO, A., SCIURBA, F., DAUBER, J.,

SELMAN, M., GOCHUICO, B. R. & KAMINSKI, N. 2008. MMP1 and MMP7 as potential peripheral blood biomarkers in idiopathic pulmonary fibrosis. *PLoS Med,* 5**,** e93.
ROTHMAN, K. J. 1990. No adjustments are needed for multiple comparisons. *Epidemiology,* 1**,** 43-6.
ROUTRAY, S., KHEUR, S. M. & KHEUR, M. 2013. Osteopontin: a marker for invasive oral squamous cell carcinoma but not for potentially malignant epithelial dysplasias. *Ann Diagn Pathol,* 17**,** 421-4.
RUDOLPH, R. 1987. Wide spread scars, hypertrophic scars, and keloids. *Clin Plast Surg,* 14**,** 253-60.
RUSSELL, J. D. & WITT, W. S. 1976. Cell size and growth characteristics of cultured fibroblasts isolated from normal and keloid tissue. *Plast Reconstr Surg,* 57**,** 207-12.
RUSSELL, S. B., RUSSELL, J. D., TRUPIN, K. M., GAYDEN, A. E., OPALENIK, S. R., NANNEY, L. B., BROQUIST, A. H., RAJU, L. & WILLIAMS, S. M. 2010. Epigenetically altered wound healing in keloid fibroblasts. *J Invest Dermatol,* 130**,** 2489-96.
RUSSELL, S. B., TRUPIN, K. M., RODRÍGUEZ-EATON, S., RUSSELL, J. D. & TRUPIN, J. S. 1988. Reduced growth-factor requirement of keloid-derived fibroblasts may account for tumor growth. *Proc Natl Acad Sci U S A,* 85**,** 587-91.
RUTLEDGE, R. G. & CÔTÉ, C. 2003. Mathematics of quantitative kinetic PCR and the application of standard curves. *Nucleic Acids Res,* 31**,** e93.
SABATER-MARCO, V., PÉREZ-VALLÉS, A., BERZAL-CANTALEJO, F., RODRIGUEZ-SERNA, M., MARTINEZ-DIAZ, F. & MARTORELL-CEBOLLADA, M. 2006. Sclerosing dermatofibrosarcoma protuberans (DFSP): an unusual variant with focus on the histopathologic differential diagnosis. *Int J Dermatol,* 45**,** 59-62.
SADICK, H., HERBERGER, A., RIEDEL, K., BRAN, G., GOESSLER, U., HOERMANN, K. & RIEDEL, F. 2008. TGF-beta1 antisense therapy modulates expression of matrix metalloproteinases in keloid-derived fibroblasts. *Int J Mol Med,* 22**,** 55-60.
SAED, G. M., LADIN, D., OLSON, J., HAN, X., HOU, Z. & FIVENSON, D. 1998. Analysis of p53 gene mutations in keloids using polymerase chain reaction-based single-strand conformational polymorphism and DNA sequencing. *Arch Dermatol,* 134**,** 963-7.
SANDBO, N. & DULIN, N. 2011. Actin cytoskeleton in myofibroblast differentiation: ultrastructure defining form and driving function. *Transl Res,* 158**,** 181-96.
SANTIBAÑEZ, J. F., QUINTANILLA, M. & BERNABEU, C. 2011. TGF-β/TGF-β receptor system and its role in physiological and pathological conditions. *Clinical Science,* 121**,** 233-251.
SANTUCCI, M., BORGOGNONI, L., REALI, U. M. & GABBIANI, G. 2001. Keloids and hypertrophic scars of Caucasians show distinctive morphologic and immunophenotypic profiles. *Virchows Arch,* 438**,** 457-63.
SARRAZY, V., BILLET, F., MICALLEF, L., COULOMB, B. & DESMOULIÈRE, A. 2011. Mechanisms of pathological scarring: role of myofibroblasts and current developments. *Wound Repair Regen,* 19 Suppl 1**,** s10-5.
SATISH, L., BABU, M., TRAN, K. T., HEBDA, P. A. & WELLS, A. 2004. Keloid fibroblast responsiveness to epidermal growth factor and activation of downstream intracellular signaling pathways. *Wound Repair Regen,* 12**,** 183-92.
SATO, M. 2006. Upregulation of the Wnt/beta-catenin pathway induced by transforming growth factor-beta in hypertrophic scars and keloids. *Acta Derm Venereol,* 86**,** 300-7.
SAVAGNER, P. & ARNOUX, V. 2009. [Epithelio-mesenchymal transition and cutaneous wound healing]. *Bull Acad Natl Med,* 193**,** 1981-91; discussion 1992.
SAVILLE, D. 1990. Multiple Comparison Procedures: The Practical Solution. *American Statistical Association* [Online], 44.
SAWICKI, G., MARCOUX, Y., SARKHOSH, K., TREDGET, E. E. & GHAHARY, A. 2005. Interaction of keratinocytes and fibroblasts modulates the expression of matrix metalloproteinases-2 and -9 and their inhibitors. *Mol Cell Biochem,* 269**,** 209-16.

SCATENA, M., ALMEIDA, M., CHAISSON, M. L., FAUSTO, N., NICOSIA, R. F. & GIACHELLI, C. M. 1998. NF-kappaB mediates alphavbeta3 integrin-induced endothelial cell survival. *J Cell Biol,* 141**,** 1083-93.

SCHALKWIJK, J., VAN VLIJMEN, I., OOSTERLING, B., PERRET, C., KOOPMAN, R., VAN DEN BORN, J. & MACKIE, E. J. 1991. Tenascin expression in hyperproliferative skin diseases. *Br J Dermatol,* 124**,** 13-20.

SCHELLINGS, M. W., VANHOUTTE, D., SWINNEN, M., CLEUTJENS, J. P., DEBETS, J., VAN LEEUWEN, R. E., D'HOOGE, J., VAN DE WERF, F., CARMELIET, P., PINTO, Y. M., SAGE, E. H. & HEYMANS, S. 2009. Absence of SPARC results in increased cardiac rupture and dysfunction after acute myocardial infarction. *J Exp Med,* 206**,** 113-23.

SCHOLZEN, T. & GERDES, J. 2000. The Ki-67 protein: from the known and the unknown. *J Cell Physiol,* 182**,** 311-22.

SEBASTIAN, A., SYED, F., PERRY, D., BALAMURUGAN, V., COLTHURST, J., CHAUDHRY, I. H. & BAYAT, A. 2011. Acceleration of cutaneous healing by electrical stimulation: degenerate electrical waveform down-regulates inflammation, up-regulates angiogenesis and advances remodeling in temporal punch biopsies in a human volunteer study. *Wound Repair Regen,* 19**,** 693-708.

SEIFERT, O., BAYAT, A., GEFFERS, R., DIENUS, K., BUER, J., LOFGREN, S. & MATUSSEK, A. 2008. Identification of unique gene expression patterns within different lesional sites of keloids. *Wound Repair Regen,* 16**,** 254-65.

SEIFERT, O., DIENUS, K., BAYAT, A. & GILMORE, B. F. 2010. Increased expression of fibroblast activation protein-alpha in keloid fibroblasts: implications for development of a novel treatment option. *Archives of Dermatological Research,* 302**,** 725-731.

SETON-ROGERS, S. E. & BRUGGE, J. S. 2004. ErbB2 and TGF-beta: a cooperative role in mammary tumor progression? *Cell Cycle,* 3**,** 597-600.

SHI, Y. & MASSAGUE, J. 2003. Mechanisms of TGF-beta signaling from cell membrane to the nucleus. *Cell,* 113**,** 685-700.

SHIH, B. & BAYAT, A. Comparative genomic hybridisation analysis of keloid tissue in Caucasians suggests possible involvement of HLA-DRB5 in disease pathogenesis. *Archives of Dermatological Research***,** 1-9.

SHIH, B. & BAYAT, A. 2010a. Genetics of keloid scarring. *Archives of Dermatological Research,* 302**,** 319-339.

SHIH, B. & BAYAT, A. 2010b. Genetics of keloid scarring. *Arch Dermatol Res,* 302**,** 319-39.

SHIH, B., GARSIDE, E., MCGROUTHER, D. A. & BAYAT, A. 2010a. Molecular dissection of abnormal wound healing processes resulting in keloid disease. *Wound Repair Regen,* 18**,** 139-53.

SHIH, B., MCGROUTHER, D. A. & BAYAT, A. 2010b. Identification of novel keloid biomarkers through profiling of tissue biopsies versus cell cultures in keloid margin specimens compared to adjacent normal skin. *Eplasty,* 10**,** e24.

SHRESTHA, P., SUMITOMO, S., LEE, C. H., NAGAHARA, K., KAMEGAI, A., YAMANAKA, T., TAKEUCHI, H., KUSAKABE, M. & MORI, M. 1996. Tenascin: growth and adhesion modulation--extracellular matrix degrading function: an in vitro study. *Eur J Cancer B Oral Oncol,* 32B**,** 106-13.

SIBLE, J. C., ERIKSSON, E., SMITH, S. P. & SMITH, N. 1994. Fibronectin gene expression differs in normal and abnormal human wound healing. *Wound Repair Regen,* 2**,** 3-19.

SIDGWICK, G. P. & BAYAT, A. 2012. Extracellular matrix molecules implicated in hypertrophic and keloid scarring. *Journal of the European Academy of Dermatology and Venereology,* 26**,** 141-152.

SIEGEL, P. M., SHU, W., CARDIFF, R. D., MULLER, W. J. & MASSAGUÉ, J. 2003. Transforming growth factor beta signaling impairs Neu-induced mammary tumorigenesis while promoting pulmonary metastasis. *Proc Natl Acad Sci U S A,* 100**,** 8430-5.

SIMPSON, C. L., PATEL, D. M. & GREEN, K. J. 2011. Deconstructing the skin: cytoarchitectural determinants of epidermal morphogenesis. *Nat Rev Mol Cell Biol,* 12**,** 565-80.

SINGER, A. J. & CLARK, R. A. 1999. Cutaneous wound healing. *N Engl J Med,* 341**,** 738-46.

SIRAGANIAN, P. A., RUBINSTEIN, J. H. & MILLER, R. W. 1989. Keloids and neoplasms in the Rubinstein-Taybi syndrome. *Med Pediatr Oncol,* 17**,** 485-91.

SKALLI, O., ROPRAZ, P., TRZECIAK, A., BENZONANA, G., GILLESSEN, D. & GABBIANI, G. 1986. A monoclonal antibody against alpha-smooth muscle actin: a new probe for smooth muscle differentiation. *J Cell Biol,* 103**,** 2787-96.

SKALLI, O., SCHÜRCH, W., SEEMAYER, T., LAGACÉ, R., MONTANDON, D., PITTET, B. & GABBIANI, G. 1989. Myofibroblasts from diverse pathologic settings are heterogeneous in their content of actin isoforms and intermediate filament proteins. *Lab Invest,* 60**,** 275-85.

SMILEY, A. K., KLINGENBERG, J. M., ARONOW, B. J., BOYCE, S. T., KITZMILLER, W. & SUPP, D. M. 2005. Microarray Analysis of Gene Expression in Cultured Skin Substitutes Compared with Native Human Skin. *J Investig Dermatol,* 125**,** 1286-1301.

SMITH, J. C., BOONE, B. E., OPALENIK, S. R., WILLIAMS, S. M. & RUSSELL, S. B. 2008. Gene profiling of keloid fibroblasts shows altered expression in multiple fibrosis-associated pathways. *J Invest Dermatol,* 128**,** 1298-310.

SMOLA, H., THIEKÖTTER, G. & FUSENIG, N. E. 1993. Mutual induction of growth factor gene expression by epidermal-dermal cell interaction. *J Cell Biol,* 122**,** 417-29.

SODEK, J., GANSS, B. & MCKEE, M. D. 2000. Osteopontin. *Crit Rev Oral Biol Med,* 11**,** 279-303.

SPINALE, F. G., MUKHERJEE, R., ZAVADZKAS, J. A., KOVAL, C. N., BOUGES, S., STROUD, R. E., DOBRUCKI, L. W. & SINUSAS, A. J. 2010. Cardiac restricted overexpression of membrane type-1 matrix metalloproteinase causes adverse myocardial remodeling following myocardial infarction. *J Biol Chem,* 285**,** 30316-27.

STEINBRECH, D. S., MEHRARA, B. J., CHAU, D., ROWE, N. M., CHIN, G., LEE, T., SAADEH, P. B., GITTES, G. K. & LONGAKER, M. T. 1999. Hypoxia upregulates VEGF production in keloid fibroblasts. *Ann Plast Surg,* 42**,** 514-9; discussion 519-20.

STUCKER, F. J. & SHAW, G. Y. 1992. An approach to management of keloids. *Arch Otolaryngol Head Neck Surg,* 118**,** 63-7.

SU, F., OVERHOLTZER, M., BESSER, D. & LEVINE, A. J. 2002. WISP-1 attenuates p53-mediated apoptosis in response to DNA damage through activation of the Akt kinase. *Genes Dev,* 16**,** 46-57.

SUMI, T., TSUNEYOSHI, N., NAKATSUJI, N. & SUEMORI, H. 2008. Defining early lineage specification of human embryonic stem cells by the orchestrated balance of canonical Wnt/beta-catenin, Activin/Nodal and BMP signaling. *Development,* 135**,** 2969-79.

SUN, S., NING, X., ZHANG, Y., LU, Y., NIE, Y., HAN, S., LIU, L., DU, R., XIA, L., HE, L. & FAN, D. 2009. Hypoxia-inducible factor-1alpha induces Twist expression in tubular epithelial cells subjected to hypoxia, leading to epithelial-to-mesenchymal transition. *Kidney Int,* 75**,** 1278-87.

SYED, F., AHMADI, E., IQBAL, S. A., SINGH, S., MCGROUTHER, D. A. & BAYAT, A. 2011. Fibroblasts from the growing margin of keloid scars produce higher levels of collagen I and III compared with intralesional and extralesional sites: clinical implications for lesional site-directed therapy. *Br J Dermatol,* 164**,** 83-96.

SYED, F. & BAYAT, A. 2012. Notch signaling pathway in keloid disease: enhanced fibroblast activity in a Jagged-1 peptide-dependent manner in lesional vs. extralesional fibroblasts. *Wound Repair Regen,* 20**,** 688-706.

SYED, F., SANGANEE, H. J., BAHL, A. & BAYAT, A. 2013. Potent dual inhibitors of TORC1 and TORC2 complexes (KU-0063794 and KU-0068650) demonstrate in vitro and ex vivo anti-keloid scar activity. *J Invest Dermatol,* 133**,** 1340-50.

SÖDERHÄLL, C., MARENHOLZ, I., KERSCHER, T., RÜSCHENDORF, F., ESPARZA-GORDILLO, J., WORM, M., GRUBER, C., MAYR, G., ALBRECHT, M., ROHDE, K., SCHULZ, H., WAHN, U., HUBNER, N. & LEE, Y. A. 2007. Variants in a novel epidermal collagen gene (COL29A1) are associated with atopic dermatitis. *PLoS Biol,* 5**,** e242.

TAKAHASHI, F., TAKAHASHI, K., OKAZAKI, T., MAEDA, K., IENAGA, H., MAEDA, M., KON, S., UEDE, T. & FUKUCHI, Y. 2001. Role of osteopontin in the pathogenesis of bleomycin-induced pulmonary fibrosis. *Am J Respir Cell Mol Biol,* 24**,** 264-71.

TAN, K. T., MCGROUTHER, D. A., DAY, A. J., MILNER, C. M. & BAYAT, A. 2011. Characterization of hyaluronan and TSG-6 in skin scarring: differential distribution in keloid scars, normal scars and unscarred skin. *J Eur Acad Dermatol Venereol,* 25**,** 317-27.

TAN, K. T., SHAH, N., PRITCHARD, S. A., MCGROUTHER, D. A. & BAYAT, A. 2010. The influence of surgical excision margins on keloid prognosis. *Ann Plast Surg,* 64**,** 55-8.

TANRIVERDI-AKHISAROGLU, S., MENDERES, A. & OKTAY, G. 2009. Matrix metalloproteinase-2 and -9 activities in human keloids, hypertrophic and atrophic scars: a pilot study. *Cell Biochem Funct,* 27**,** 81-7.

TATTI, O., VEHVILÄINEN, P., LEHTI, K. & KESKI-OJA, J. 2008. MT1-MMP releases latent TGF-beta1 from endothelial cell extracellular matrix via proteolytic processing of LTBP-1. *Exp Cell Res,* 314**,** 2501-14.

TOMASEK, J. J., GABBIANI, G., HINZ, B., CHAPONNIER, C. & BROWN, R. A. 2002. Myofibroblasts and mechano-regulation of connective tissue remodelling. *Nat Rev Mol Cell Biol,* 3**,** 349-63.

TORISEVA, M. & KAHARI, V. M. 2009. Proteinases in cutaneous wound healing. *Cell Mol Life Sci,* 66**,** 203-24.

TOSA, M., GHAZIZADEH, M., SHIMIZU, H., HIRAI, T., HYAKUSOKU, H. & KAWANAMI, O. 2005. Global gene expression analysis of keloid fibroblasts in response to electron beam irradiation reveals the involvement of interleukin-6 pathway. *J Invest Dermatol,* 124**,** 704-13.

TROMPEZINSKI, S., PERNET, I., MAYOUX, C., SCHMITT, D. & VIAC, J. 2000. Transforming growth factor-beta1 and ultraviolet A1 radiation increase production of vascular endothelial growth factor but not endothelin-1 in human dermal fibroblasts. *Br J Dermatol,* 143**,** 539-45.

TSUKADA, T., MCNUTT, M. A., ROSS, R. & GOWN, A. M. 1987. HHF35, a muscle actin-specific monoclonal antibody. II. Reactivity in normal, reactive, and neoplastic human tissues. *Am J Pathol,* 127**,** 389-402.

TUAN, T. L. & NICHTER, L. S. 1998. The molecular basis of keloid and hypertrophic scar formation. *Mol Med Today,* 4**,** 19-24.

TUAN, T. L., WU, H., HUANG, E. Y., CHONG, S. S., LAUG, W., MESSADI, D., KELLY, P. & LE, A. 2003. Increased plasminogen activator inhibitor-1 in keloid fibroblasts may account for their elevated collagen accumulation in fibrin gel cultures. *Am J Pathol,* 162**,** 1579-89.

TUAN, T. L., ZHU, J. Y., SUN, B., NICHTER, L. S., NIMNI, M. E. & LAUG, W. E. 1996. Elevated levels of plasminogen activator inhibitor-1 may account for the altered fibrinolysis by keloid fibroblasts. *J Invest Dermatol,* 106**,** 1007-11.

TZORTZAKI, E. G., KOUTSOPOULOS, A. V., DAMBAKI, K. I., LAMBIRI, I., PLATAKI, M., GORDON, M. K., GERECKE, D. R. & SIAFAKAS, N. M. 2006. Active remodeling in idiopathic interstitial pneumonias: evaluation of collagen types XII and XIV. *J Histochem Cytochem,* 54**,** 693-700.

TZORTZAKI, E. G., TISCHFIELD, J. A., SAHOTA, A., SIAFAKAS, N. M., GORDON, M. K. & GERECKE, D. R. 2003. Expression of FACIT collagens XII and XIV during bleomycin-induced pulmonary fibrosis in mice. *Anat Rec A Discov Mol Cell Evol Biol,* 275**,** 1073-80.

UCHIDA, G., YOSHIMURA, K., KITANO, Y., OKAZAKI, M. & HARII, K. 2003. Tretinoin reverses upregulation of matrix metalloproteinase-13 in human keloid-derived fibroblasts. *Exp Dermatol,* 12 Suppl 2**,** 35-42.

UCHINAMI, H., SEKI, E., BRENNER, D. A. & D'ARMIENTO, J. 2006. Loss of MMP 13 attenuates murine hepatic injury and fibrosis during cholestasis. *Hepatology,* 44**,** 420-9.

UEDA, Y., WANG, S., DUMONT, N., YI, J. Y., KOH, Y. & ARTEAGA, C. L. 2004. Overexpression of HER2 (erbB2) in human breast epithelial cells unmasks transforming growth factor beta-induced cell motility. *J Biol Chem,* 279**,** 24505-13.

UITTO, J., PEREJDA, A. J., ABERGEL, R. P., CHU, M. L. & RAMIREZ, F. 1985. Altered steady-state ratio of type I/III procollagen mRNAs correlates with selectively increased type I procollagen biosynthesis in cultured keloid fibroblasts. *Proc Natl Acad Sci U S A,* 82**,** 5935-9.

ULRICH, D., ULRICH, F., UNGLAUB, F., PIATKOWSKI, A. & PALLUA, N. 2010. Matrix metalloproteinases and tissue inhibitors of metalloproteinases in patients with different types of scars and keloids. *J Plast Reconstr Aesthet Surg,* 63**,** 1015-21.

VAN DEN BROEK, L. J., LIMANDJAJA, G. C., NIESSEN, F. B. & GIBBS, S. 2014. Human hypertrophic and keloid scar models: principles, limitations and future challenges from a tissue engineering perspective. *Exp Dermatol,* 23**,** 382-6.

VARGA, J. & PASCHE, B. 2008. Antitransforming growth factor-beta therapy in fibrosis: recent progress and implications for systemic sclerosis. *Curr Opin Rheumatol,* 20**,** 720-8.

VEIDAL, S. S., KARSDAL, M. A., NAWROCKI, A., LARSEN, M. R., DAI, Y., ZHENG, Q., HÄGGLUND, P., VAINER, B., SKJØT-ARKIL, H. & LEEMING, D. J. 2011. Assessment of proteolytic degradation of the basement membrane: a fragment of type IV collagen as a biochemical marker for liver fibrosis. *Fibrogenesis Tissue Repair,* 4**,** 22.

VELEIRINHO, B., COELHO, D. S., DIAS, P. F., MARASCHIN, M., RIBEIRO-DO-VALLE, R. M. & LOPES-DA-SILVA, J. A. Nanofibrous poly(3-hydroxybutyrate-co-3-hydroxyvalerate)/chitosan scaffolds for skin regeneration. *International Journal of Biological Macromolecules*.

VELEZ EDWARDS, D. R., TSOSIE, K. S., WILLIAMS, S. M., EDWARDS, T. L. & RUSSELL, S. B. 2014. Admixture mapping identifies a locus at 15q21.2-22.3 associated with keloid formation in African Americans. *Hum Genet,* 133**,** 1513-23.

VISSE, R. & NAGASE, H. 2003. Matrix metalloproteinases and tissue inhibitors of metalloproteinases: structure, function, and biochemistry. *Circ Res,* 92**,** 827-39.

WACHSSTOCK, D. H., WILKINS, J. A. & LIN, S. 1987. Specific interaction of vinculin with alpha-actinin. *Biochem Biophys Res Commun,* 146**,** 554-60.

WANG, K. X. & DENHARDT, D. T. 2008. Osteopontin: role in immune regulation and stress responses. *Cytokine Growth Factor Rev,* 19**,** 333-45.

WANG, S. E., XIANG, B., GUIX, M., OLIVARES, M. G., PARKER, J., CHUNG, C. H., PANDIELLA, A. & ARTEAGA, C. L. 2008. Transforming growth factor beta engages TACE and ErbB3 to activate phosphatidylinositol-3 kinase/Akt in ErbB2-overexpressing breast cancer and desensitizes cells to trastuzumab. *Mol Cell Biol,* 28**,** 5605-20.

WANG, Z., LIU, X., ZHANG, D., WANG, X., ZHAO, F., SHI, P. & PANG, X. 2015. Co- culture with human fetal epidermal keratinocytes promotes proliferation and migration of human fetal and adult dermal fibroblasts. *Mol Med Rep,* 11**,** 1105-10.

WEI, Y., PATTINGRE, S., SINHA, S., BASSIK, M. & LEVINE, B. 2008. JNK1-mediated phosphorylation of Bcl-2 regulates starvation-induced autophagy. *Mol Cell,* 30**,** 678-88.

WELCH, M. P., ODLAND, G. F. & CLARK, R. A. 1990. Temporal relationships of F-actin bundle formation, collagen and fibronectin matrix assembly, and fibronectin receptor expression to wound contraction. *J Cell Biol,* 110**,** 133-45.

WENDLING, J., MARCHAND, A., MAUVIEL, A. & VERRECCHIA, F. 2003. 5-fluorouracil blocks transforming growth factor-beta-induced alpha 2 type I collagen gene (COL1A2)

expression in human fibroblasts via c-Jun NH2-terminal kinase/activator protein-1 activation. *Mol Pharmacol,* 64**,** 707-13.

WENSTRUP, R. J., FLORER, J. B., BRUNSKILL, E. W., BELL, S. M., CHERVONEVA, I. & BIRK, D. E. 2004. Type V collagen controls the initiation of collagen fibril assembly. *J Biol Chem,* 279**,** 53331-7.

WERNER, S., KRIEG, T. & SMOLA, H. 2007. Keratinocyte-fibroblast interactions in wound healing. *J Invest Dermatol,* 127**,** 998-1008.

WITTE, M. B. & BARBUL, A. 1997. General principles of wound healing. *Surg Clin North Am,* 77**,** 509-28.

WITTE, M. B. & BARBUL, A. 2002. Role of nitric oxide in wound repair. *Am J Surg,* 183**,** 406-12.

WOLFRAM, D., TZANKOV, A., PULZL, P. & PIZA-KATZER, H. 2009. Hypertrophic scars and keloids--a review of their pathophysiology, risk factors, and therapeutic management. *Dermatol Surg,* 35**,** 171-81.

WU, J., MA, B., YI, S., WANG, Z., HE, W., LUO, G., CHEN, X., WANG, X., CHEN, A. & BARISONI, D. 2004a. Gene expression of early hypertrophic scar tissue screened by means of cDNA microarrays. *J Trauma,* 57**,** 1276-86.

WU, J. J., WEIS, M. A., KIM, L. S. & EYRE, D. R. 2010. Type III collagen, a fibril network modifier in articular cartilage. *J Biol Chem,* 285**,** 18537-44.

WU, M., SCHNEIDER, D. J., MAYES, M. D., ASSASSI, S., ARNETT, F. C., TAN, F. K., BLACKBURN, M. R. & AGARWAL, S. K. 2012. Osteopontin in systemic sclerosis and its role in dermal fibrosis. *J Invest Dermatol,* 132**,** 1605-14.

WU, Y., ZHANG, Q., ANN, D. K., AKHONDZADEH, A., DUONG, H. S., MESSADI, D. V. & LE, A. D. 2004b. Increased vascular endothelial growth factor may account for elevated level of plasminogen activator inhibitor-1 via activating ERK1/2 in keloid fibroblasts. *Am J Physiol Cell Physiol,* 286**,** C905-12.

XIA, W., PHAN, T. T., LIM, I. J., LONGAKER, M. T. & YANG, G. P. 2004. Complex epithelial-mesenchymal interactions modulate transforming growth factor-beta expression in keloid-derived cells. *Wound Repair Regen,* 12**,** 546-56.

XIA, Y. P., ZHAO, Y., MARCUS, J., JIMENEZ, P. A., RUBEN, S. M., MOORE, P. A., KHAN, F. & MUSTOE, T. A. 1999. Effects of keratinocyte growth factor-2 (KGF-2) on wound healing in an ischaemia-impaired rabbit ear model and on scar formation. *J Pathol,* 188**,** 431-8.

XU, L., CORCORAN, R. B., WELSH, J. W., PENNICA, D. & LEVINE, A. J. 2000. WISP-1 is a Wnt-1- and beta-catenin-responsive oncogene. *Genes Dev,* 14**,** 585-95.

YAN, C., GRIMM, W. A., GARNER, W. L., QIN, L., TRAVIS, T., TAN, N. & HAN, Y. P. 2010. Epithelial to mesenchymal transition in human skin wound healing is induced by tumor necrosis factor-alpha through bone morphogenic protein-2. *Am J Pathol,* 176**,** 2247-58.

YAN, C. H., LV, M., LI, H., SONG, X., YAN, F., CAO, S. & REN, X. 2015. Osteopontin is a novel prognostic biomarker in early-stage non-small cell lung cancer after surgical resection. *J Cancer Res Clin Oncol,* 141**,** 1371-8.

YAN, X., GAO, J. H., CHEN, Y., SONG, M. & LIU, X. J. 2007. [Preliminary linkage analysis and mapping of keloid susceptibility locus in a Chinese pedigree]. *Zhonghua Zheng Xing Wai Ke Za Zhi,* 23**,** 32-5.

YANG, W. S., LEE, W. J., HUANG, K. C., LEE, K. C., CHAO, C. L., CHEN, C. L., TAI, T. Y. & CHUANG, L. M. 2003. mRNA levels of the insulin-signaling molecule SORBS1 in the adipose depots of nondiabetic women. *Obes Res,* 11**,** 586-90.

YANG, Y., YANG, S., CHEN, M., ZHANG, X., ZOU, Y. & ZHANG, X. 2008. Compound Astragalus and Salvia miltiorrhiza Extract exerts anti-fibrosis by mediating TGF-beta/Smad signaling in myofibroblasts. *J Ethnopharmacol,* 118**,** 264-70.

YIN, S. Y., PENG, A. P., HUANG, L. T., WANG, Y. T., LAN, C. W. & YANG, N. S. 2013. The Phytochemical Shikonin Stimulates Epithelial-Mesenchymal Transition (EMT) in Skin Wound Healing. *Evid Based Complement Alternat Med,* 2013**,** 262796.

YOUNG, P., FISHER, M., SEGEL, J., STUCKER, F., BECKER, A. & CHEN, A. 2013. Treatment of Large Keloids With Secondary-Intention Healing. *American Journal of Cosmetic Surgery,* 30**,** 193-199.

YOUSSEF, K. K., VAN KEYMEULEN, A., LAPOUGE, G., BECK, B., MICHAUX, C., ACHOURI, Y., SOTIROPOULOU, P. A. & BLANPAIN, C. 2010. Identification of the cell lineage at the origin of basal cell carcinoma. *Nature cell biology,* 12**,** 299-305.

YU, H., BOCK, O., BAYAT, A., FERGUSON, M. W. & MROWIETZ, U. 2006. Decreased expression of inhibitory SMAD6 and SMAD7 in keloid scarring. *J Plast Reconstr Aesthet Surg,* 59**,** 221-9.

YUE, J. & MULDER, K. M. 2000. Requirement of Ras/MAPK pathway activation by transforming growth factor beta for transforming growth factor beta 1 production in a smad-dependent pathway. *J Biol Chem,* 275**,** 35656.

ZHANG, G., JIANG, J. J., LUO, S. J., TANG, S. M., LIANG, J. & YU, Q. 2008. [The relationship between RUNX3 gene mutation and keloid]. *Zhonghua Zheng Xing Wai Ke Za Zhi,* 24**,** 224-7.

ZHANG, Q., WU, Y., ANN, D. K., MESSADI, D. V., TUAN, T. L., KELLY, A. P., BERTOLAMI, C. N. & LE, A. D. 2003. Mechanisms of hypoxic regulation of plasminogen activator inhibitor-1 gene expression in keloid fibroblasts. *J Invest Dermatol,* 121**,** 1005-12.

ZHANG, Q., WU, Y., CHAU, C. H., ANN, D. K., BERTOLAMI, C. N. & LE, A. D. 2004. Crosstalk of hypoxia-mediated signaling pathways in upregulating plasminogen activator inhibitor-1 expression in keloid fibroblasts. *J Cell Physiol,* 199**,** 89-97.

ZHANG, Z., NIE, F., CHEN, X., QIN, Z., KANG, C., CHEN, B., MA, J., PAN, B. & MA, Y. 2015. Upregulated periostin promotes angiogenesis in keloids through activation of the ERK 1/2 and focal adhesion kinase pathways, as well as the upregulated expression of VEGF and angiopoietin- 1. *Mol Med Rep,* 11**,** 857-64.

ZIGRINO, P., AYACHI, O., SCHILD, A., KALTENBERG, J., ZAMEK, J., NISCHT, R., KOCH, M. & MAUCH, C. Loss of epidermal MMP-14 expression interferes with angiogenesis but not with re-epithelialization. *European Journal of Cell Biology*.

ZILE, M. R., BAICU, C. F., STROUD, R. E., VAN LAER, A., ARROYO, J., MUKHERJEE, R., JONES, J. A. & SPINALE, F. G. 2012. Pressure overload-dependent membrane type 1-matrix metalloproteinase induction: relationship to LV remodeling and fibrosis. *Am J Physiol Heart Circ Physiol,* 302**,** H1429-37.

ZIPS, D., KRAUSE, M., YAROMINA, A., DORFLER, A., EICHELER, W., SCHUTZE, C., GURTNER, K. & BAUMANN, M. 2008. Epidermal growth factor receptor inhibitors for radiotherapy: biological rationale and preclinical results. *J Pharm Pharmacol,* 60**,** 1019-28.

ZOHAR, R., LEE, W., ARORA, P., CHEIFETZ, S., MCCULLOCH, C. & SODEK, J. 1997. Single cell analysis of intracellular osteopontin in osteogenic cultures of fetal rat calvarial cells. *J Cell Physiol,* 170**,** 88-100.